2020

# Molecular and phenotypic characterization of doubled haploid lines derived from different cycles of the Iowa Stiff Stalk Synthetic maize population

Alejandro Ledesma M
*Iowa State University*

**Molecular and phenotypic characterization of doubled haploid lines derived from different cycles of the Iowa Stiff Stalk Synthetic maize population**

by

**Alejandro Ledesma M**

A dissertation submitted to the graduate faculty

in partial fulfillment of the requirements for the degree of

DOCTOR OF PHILOSOPHY

Major: Plant Breeding

Program of Study Committee:
Thomas Lübberstedt, Major Professor
Jode W. Edwards
Matthew B. Hufford
Willian D. Beavis
Paul M. Scott

The student author, whose presentation of the scholarship herein was approved by the program of study committee, is solely responsible for the content of this dissertation. The Graduate College will ensure this dissertation is globally accessible and will not permit alterations after a degree is conferred.

Iowa State University

Ames, Iowa

2020

## DEDICATION

Special dedication to the loving memory of my father Arturo Ledesma† and my father in law Javier Casillas† which we lost them during my Ph.D. studies.

To my family Ledesma-Casillas: Jessica, Matias, and Zara. To my mother, Lucy Miramontes, and siblings: Adriana, Leonardo, and Carolina, for your love, support, and encouragement to follow my dreams.

To Casillas-Gonzalez, family for your love and your support.

# TABLE OF CONTENTS

Page

## LIST OF FIGURES

Page

## LIST OF TABLES

Page

## ACKNOWLEDGMENTS

I would like to thank Dr. Lübberstedt for the patience and the opportunity to work on his lab and research project. Thank you to my committee members, Dr. Edwards, Dr. Hufford, Dr. Beavis, and Dr. Scott, for their continuing guidance and support throughout this research, which was essential to the success of this research. Also, thanks to Dr. Sarah Hearne for your collaboration and support.

I would like to thank my wife Jessica Casillas, parents Arturo Ledesma† and Lucy Miramontes, and my entire family for their continued support.

Special thanks to Dr. Jose Luis Ramirez (INIFAP-Mexico) for being my mentor and introducing me to the Plant Breeding world and encouraging me to continue growing in this field.

I would also like to thank Lübberstedt lab members, friends, faculty, and staff for making my time at Iowa State University a great experience.

Finally, I would like to acknowledge the National Council for Science and Technology (CONACYT), International Maize and Wheat Improvement Center (CIMMYT), and the National Institute for Agricultural, Livestock, and Forestry Research (INIFAP) from Mexico for the scholarship 2016 for Ph.D. studies. Without your financial support, my Ph.D. program would not have been achieved.

## ABSTRACT

Molecular characterization of a given set of maize germplasm could be useful for understanding the use of the assembled germplasm for further improvement in a breeding program, such as analyzing genetic diversity, selecting a parental line, assigning heterotic groups, creating a core set of germplasm and performing association analysis for traits of interest. In this study, we used single nucleotide polymorphism (SNP) markers to assess the genetic diversity in a set of doubled haploid (DH) lines derived from "C0" (BSSS(R)C0), "C17" (BSSS(R)C17) and the cross "C0/C17" (BSSS(R)C0/BSSS(R)C17) of the Iowa Stiff Stalk Synthetic (BSSS) maize population. With the aim to explore if we have potentially lost diversity from C0 to C17 derived DH lines and to observe whether useful genetic variation in C0 was left behind during the selection process since C0 could be a reservoir of genetic diversity that could be untapped using DH technology. Assessing the genetic relationship and genetic divergence within and among the evaluated cycles of selection will allow us to explore the BSSS DH lines' breeding potential for broadening the genetic base of the Stiff Stalk (SS) heterotic pool. Additionally, we quantify the BSSS progenitors' contribution in each set of DH lines using a high-resolution detection of identity by descend (IBD) segments. The DH lines developed plus the 16 progenitors were evaluated in a *per se* evaluation trial and phenotypic data were collected on an individual plot basis for male flowering, female flowering, anthesis-silking interval, plant height, ear height, flag leaf angle, tassel length, and the number of primary tassel branches to compare C0, C17, and C0/C17 derived DH lines for plant architecture traits and identify DH lines with both significant C0 background and in addition modern plant architecture traits conferring adaptation to high plant density, that could be used as genetic resources. Using the genotypic and phenotypic information of the BSSS DH lines, we performed Genome-Wide

Association Studies (GWAS) to identify regions in the genome associated with these plant architecture changes. The molecular characterization analysis confirmed the apparent separation and the loss of genetic variability from C0 to C17 through the recurrent selection process. The progenitors had a higher genetic contribution in C0 compared with C0/C17 and C17 derived DH lines. Although genetic drift can explain most of the genetic structure genome-wide, phenotypic data provide evidence that selection has altered favorable alleles frequencies in the BSSS maize population. Descriptive statistical analysis confirmed trait variability in the different groups of DH lines. Considerable variation between populations was observed for all traits except for plant height. As expected, phenotypic differences ($P \leq 0.001$) were found between different groups of DH lines, indicating a wide range of variability present. DH lines within the C0_DHL group had the highest mean values for flowering time, ear height, flag leaf angle, and the number of primary tassel branches and were statistically different ($P \leq 0.001$) between the groups of DH lines. Using GWAS analysis, significant SNP markers-trait associations were found in flowering and plant architecture traits using different GWAS analysis models. 38 SNP markers were found associated with different evaluated traits across more than one method tested and among the groups of DH lines. The genome regions with the highest significance were found on chromosomes 2 and 7 for the traits number of primary tassel branches and flag leaf angles. By searching for candidate genes up and downstream of the 38 in common significant SNP markers, 55 candidate genes were associated with flowering time and different plant architecture traits. Molecular characterization information provided by this research will help maize breeders better understand how to utilize the current set of DH lines developed from the BSSS maize population. Additionally, identifying candidate genes for plant architecture traits in this study may help to elucidate the genetic basis of these plant architecture traits.

# CHAPTER 1. GENERAL INTRODUCTION

Maize (*Zea mays*) is an important cereal crop in the world. It is a staple food in many countries, and it is also used for animal feed, ethanol production, and chemical production. It is estimated that the demand for maize in the developing world will continue to increase. Maize yields have risen continually wherever hybrid maize has been adopted, starting in the U.S. corn belt in the early 1930s, where plant breeding and improved management practices have produced this gain jointly (Duvick 2005).

Maize breeding has been impacted by rapid technological advances in genotyping technologies, genetic transformation, data science progress, and novel breeding approach like doubled haploid (DH) technology (Andorf et al. 2019). DH technology has become an important tool in plant breeding programs because it shortens the breeding cycle by the rapid development of completely homozygous lines accelerating the breeding process (Chaikam et al. 2019; Forster and Thomas 2010; Geiger and Gordillo, 2009; Strigens et al. 2013). Another advantage of using DH technology is the unmasking of detrimental recessive alleles after haploidization, promoting the elimination of the genetic load in one step. Alleles present in a heterogeneous population of heterozygous individuals can be fixed in homozygous and homogenous doubled haploid lines, and the entire genetic variance within a population can be made available to unlock untapped genetic diversity (Böhm et al. 2017; Chaikam et al. 2019; Smelser et al. 2016).

Genetic diversity is essential in plant breeding programs. Plant breeders typically focus on short-term breeding goals, mainly because of the need to deliver new varieties. This may result in a narrow genetic base of elite maize germplasm (Andorf et al. 2019; Smith 1988) and could lead to a yield plateau, increasing vulnerability to pests, and make it difficult to meet new market demands (Pollak 2003). There is evidence that genetic variation is present for agronomic

traits associated with the present elite germplasm. However, it represents a small portion of the total available genetic diversity in maize. Assessment of the genetic variability that exists in available germplasm is fundamental for crop improvement. Genetic improvement of important agronomic traits while maintaining genetic variability long-term is desirable in maize breeding programs (Hallauer and Darrah 1985). Genetic variability will be preserved if an adequate number of lines are intermated for the synthesis of the next cycle of selection. Recurrent selection procedures in maize have proven to be an effective way of increasing the frequency of superior lines for grain yield and other agronomic traits while maintaining genetic variability (Hallauer and Darrah 1985).

Recurrent selection is the systematic selection of desirable individuals from a population followed by the selected individuals' recombination to form a new cycle of the population. It was suggested by (Jenkins 1940) as a method of intrapopulation improvement and later described for population improvement using a tester (Hull 1945). The most significant advantage of this method is the increase in populations' mean performance for one or more characters by increasing the frequency of favorable alleles while maintaining genetic variability for continued genetic improvement (Hull 1945; Jenkins 1940).

The Iowa Stiff Stalk Synthetic (BSSS) maize population (Sprague 1946) has undergone recurrent selection since 1939. This population was developed by intermating 16 inbred lines selected by various corn breeders for superior stalk quality (Sprague 1946). Of these progenitors, 10 were derived from multiple strains of the 'Reid Yellow Dent' open-pollinated population, 4 had miscellaneous origins, and the genetic background of 2 is unknown (Sprague 1946). The base population cycle 0 (BSSS(R)C0) was submitted to multiple recurrent selection cycles. Currently, cycle 19 is available. The BSSS maize population has been under recurrent selection

for increasing grain yield, low grain moisture at harvest, and increased resistance to root and stalk lodging. Several inbreeds lines have been developed from the BSSS population (B14, B37, B73, and B84). They have made significant contributions to the maize industry in the U.S., especially B73 (Coffman et al. 2019), one of the most successful maize inbred lines developed in the public sector and benefited industry and farmers substantially.

The BSSS maize population has been under recurrent selection for increased grain yield, low grain moisture at harvest, and increased resistance to root and stalk lodging. However, phenotypic and genotypic (Edwards, 2011; Gerke et al. 2015; Hagdorn et al. 2003; Labate et al. 1999; Messmer et al. 1991) changes have been observed in this population, suggesting an apparent separation from C0 to more advanced selection cycles. Most of the phenotypic changes that have been observed in this population are based on plant architecture traits: plant height, anthesis-silking interval (ASI), leaf angle, number of tassel branches, and yield have experienced changes (Brekke et al. 2011). For grain production, a short-statured plant is preferable (Peiffer et al. 2014), upright upper leaves are the desired trait since it permits more light to penetrate the canopy (Edwards 2011). Large tassels block sunlight and reduce photosynthesis by 19 %. Thus, a short tassel size is a desirable trait (Duncan et al. 1967). Modern hybrids have a shorter anthesis-silking interval (ASI), and researchers have demonstrated that a large ASI can result in mild to extreme yield losses. Therefore, a short ASI is a desirable trait for grain yield (Bolaños and Edmeades 1996). Yield has increased in most selection cycles, with an average of 2.6% per cycle in the first 11 cycles of selection, and after 11 cycles of selection, grain yield improved 77 % over the C0 interpopulation mean (Holthaus and Lamkey 1995). Brekke et al. (2011), when evaluating population per se yield, found a 2 % increase in grain yield per cycle between BSSS and the seventeenth cycle of a reciprocal recurrent selection program.

In the BSSS maize population, yield increases could be interpreted as an increase in adaptation to high plant density (Edwards 2011). Thus, exploring early BSSS cycles using DH technology may reveal useful genetic diversity left behind in the recurrent selection process. Selection in the BSSS maize population for high yield, grain moisture, and root and stalk lodging has indirectly modified plant architecture traits that are important for adaptation to high plant density (Edwards 2011).

Applying genetic information to identifying alleles, map regions, and candidate genes that confer adaptation to high plant density and selecting traits related to adaptation to high plant density could speed up the plant breeding process. Genome-wide association studies (GWAS) are an effective approach for analyzing allelic diversity to identify superior alleles and dissect the genetic architecture related to plant architecture traits, furthering genetic improvement in crops (Atwell et al. 2010). The increasingly wide application of association mapping is due to the rapid development of genotyping techniques, which has produced effective high-throughput molecular technology (Li et al. 2018).

In this study, we used a panel of DH lines, representing different cycles of the BSSS maize population (BSSS, BSSS(R)17 and BSSS/BSSS(R)17) to investigate traits that have been modified in the recurrent selection program and are likely associated with adaptation to high plant density: flowering time, plant and ear height, flag leaf angle, tassel size and the number of primary tassel branches to aid in the understanding of adapting germplasm to high plant density.

The overall objective of this study was to use DH technology to characterize the genetic variation present in different cycles of BSSS, represented by DH lines. Thus, the first set of objectives (Chapter 2) were to i) assess the genetic diversity in a set of doubled haploid (DH) lines derived from the Iowa Stiff Stalk Synthetic (BSSS) maize population in different cycles of

selection, ii) explore if genetic diversity was lost from “cycle 0” to “cycle 17”, iii) assess the genetic relationships and genetic divergence within and among the cycles of selection and iv) perform a haplotype analysis based on IBD segments to quantify the contribution of the progenitors in each set of DH lines. The second set of objectives (Chapter 3) were to v) compare C0 and C17 derived DH lines for plant architecture traits, vi) identify DH lines with both significant C0 background and in addition modern plant architecture traits conferring adaptation to high plant density, that could be used as genetic resources, vii) evaluate how to best use DH lines from the three subpopulations (C0, C17, C0/C17) to identify regions affecting plant architecture traits, and viii) determine the inheritance of those regions, particularly whether major genes are involved that may facilitate the introgression of other genetic resources

## References

Andorf, C., Beavis, W. D., Hufford, M., Smith, S., Suza, W. P., Wang, K., … Lübberstedt, T. (2019). Technological advances in maize breeding: past, present and future. Theoretical and Applied Genetics. https://doi.org/10.1007/s00122-019-03306-3

Atwell, S., Huang, Y. S., Vilhjálmsson, B. J., Willems, G., Horton, M., Li, Y., … Nordborg, M. (2010). Genome-wide association study of 107 phenotypes in Arabidopsis thaliana inbred lines. Nature, 465(7298), 627–631. https://doi.org/10.1038/nature08800

Böhm, J., Schipprack, W., Utz, H. F., & Melchinger, A. E. (2017). Tapping the genetic diversity of landraces in allogamous crops with doubled haploid lines: a case study from European flint maize. Theoretical and Applied Genetics, 130(5), 861–873. https://doi.org/10.1007/s00122-017-2856-x

Bolaños, J., & Edmeades, G. O. (1996). The importance of the anthesis-silking interval in breeding for drought tolerance in tropical maize. Field Crops Research, 48(1), 65–80. https://doi.org/10.1016/0378-4290(96)00036-6

Brekke, B., Edwards, J., & Knapp, A. (2011). Selection and adaptation to high plant density in the Iowa StiffStalk Synthetic maize (Zea mays L.) population: II. plant morphology. Crop Science, 51(6), 2344–2351. https://doi.org/10.2135/cropsci2010.09.0562

Chaikam, V., Molenaar, W., Melchinger, A. E., & Boddupalli, P. M. (2019). Doubled haploid technology for line development in maize: technical advances and prospects. Theoretical and Applied Genetics, 132(12), 3227–3243. https://doi.org/10.1007/s00122-019-03433-x

Coffman, S. M., Hufford, M. B., Andorf, C. M., & Lübberstedt, T. (2019). Haplotype structure in commercial maize breeding programs in relation to key founder lines. Theoretical and Applied Genetics. https://doi.org/10.1007/s00122-019-03486-y

Duncan, W. G., Loomis, R. S., Williams, W. A., & Hanau, R. (1967). A model for simulating photosynthesis in plant communities. Hilgardia, 38(4), 181–205. https://doi.org/10.3733/hilg.v38n04p181

Duvick, D. N. (2005). The Contribution of Breeding to Yield Advances in maize (Zea mays L.). Advances in Agronomy. https://doi.org/10.1016/S0065-2113(05)86002-X

Edwards, J. (2011). Changes in plant morphology in response to recurrent selection in the Iowa StiffStalk Synthetic maize population. Crop Science, 51(6), 2352–2361. https://doi.org/10.2135/cropsci2010.09.0564

Forster, B. P., & Thomas, W. T. B. (2010). Doubled Haploids in Genetics and Plant Breeding. In Plant Breeding Reviews (pp. 57–88). Oxford, UK: John Wiley & Sons, Inc. https://doi.org/10.1002/9780470650301.ch3

Geiger H. H., & G.A. Gordillo. (2009). Doubled Haploids in Hybrid Maize Breeding. Maydica, 54(485–499), 485–499. Retrieved from http://www.maydica.org/articles/54_485.pdf

Gerke, J. P., Edwards, J. W., Guill, K. E., Ross-Ibarra, J., & McMullen, M. D. (2015). The genomic impacts of drift and selection for hybrid performance in maize. Genetics, 201(3), 1201–1211. https://doi.org/10.1534/genetics.115.182410

Hagdorn, S., Lamkey, K. R., Frisch, M., Guimara, P. E. O., Melchinger, A. E., Corn, I., … Reid, P. (2003). Molecular Genetic Diversity among Progenitors and Derived Elite Lines of BSSS and BSCB1 Maize Populations. Crop Science, 43(1), 474–482.

Hallauer, A. R., and Darrah, L. L. (1985). Compendium of recurrent selection methods and their application. Critical Reviews in Plant Sciences, 3(1), 1–33. https://doi.org/10.1080/07352688509382202

Holthaus, J., & Lamkey, K. (1995). Response to selection and changes in genetic parameters for 13 plant and ear traits in two maize recurrent selection programs. Maydica, 40(4), 357–370.

Hull, F. H. (1945). Recurrent Selection for Specific Combining Ability in Corn 1. Agronomy Journal, 37(2), 134–145. https://doi.org/10.2134/agronj1945.00021962003700020006x

Jenkins, M. T. (1940). The Segregation of Genes Affecting Yield of Grain in Maize 1. Agronomy Journal, 32(1), 55–63. https://doi.org/10.2134/agronj1940.00021962003200010008x

Labate, J. A., Lamkey, K. R., Lee, M., & Woodman, W. L. (1999). Temporal changes in allele frequencies in two reciprocally selected maize populations. Theoretical and Applied Genetics, 99(7–8), 1166–1178. https://doi.org/10.1007/s001220051321

Li, H., Rasheed, A., Hickey, L. T., & He, Z. (2018). Fast-Forwarding Genetic Gain. Trends in Plant Science, 23(3), 184–186. https://doi.org/10.1016/j.tplants.2018.01.007

Messmer, M. M., Melchinger, A. E., Lee, M., Woodman, W. L., Lee, E. A., & Lamkey, K. R. (1991). Genetic diversity among progenitors and elite lines from the Iowa Stiff Stalk Synthetic (BSSS) maize population: comparison of allozyme and RFLP data. Theoretical and Applied Genetics, 83(1), 97–107. https://doi.org/10.1007/BF00229231

Peiffer, J. A., Romay, M. C., Gore, M. A., Flint-Garcia, S. A., Zhang, Z., Millard, M. J., … Buckler, E. S. (2014). The genetic architecture of maize height. Genetics, 196(4), 1337–1356. https://doi.org/10.1534/genetics.113.159152

Pollak, L. M. (2003). The History and Success of the public-private project on germplasm enhancement of maize (GEM) (pp. 45–87). https://doi.org/10.1016/S0065-2113(02)78002-4

Smelser, A., Gardner, C., Blanco, M., Lübberstedt, T., & Frei, U. (2016). Germplasm enhancement of maize: a look into haploid induction and chromosomal doubling of haploids from temperate-adapted tropical sources. Plant Breeding, 135(5), 593–597. https://doi.org/10.1111/pbr.12397

Smith, J. S. C. (1988). Diversity of United States Hybrid Maize Germplasm; Isozymic and Chromatographic Evidence. Crop Science, 28(1), 63–69. https://doi.org/10.2135/cropsci1988.0011183x002800010016x

Sprague, G. F. (1946). Early Testing of Inbred Lines of Corn. Journal of the American Society of Agronomy.

Strigens, A., Schipprack, W., Reif, J. C., & Melchinger, A. E. (2013). Unlocking the Genetic Diversity of Maize Landraces with Doubled Haploids Opens New Avenues for Breeding. PLoS ONE, 8(2), 7–9. https://doi.org/10.1371/journal.pone.0057234

# CHAPTER 2. MOLECULAR CHARACTERIZATION OF DOUBLED HAPLOID LINES DERIVED FROM DIFFERENT CYCLES OF THE IOWA STIFF STALK SYNTHETIC (BSSS) MAIZE POPULATION

Alejandro Ledesma M.[1], Fernando S. Aguilar[1], Sarah Hearne[2], Ursula Frei[1], Jode Edwards[3], and Thomas Lübberstedt[1]

[1]Department of Agronomy, Iowa State University, Ames, IA 50011, USA.

[2]Molecular Geneticist, Seed of Discovery - Maize lead, CIMMYT, Texcoco, México.

[3]USDA-ARS Corn Insects and Crop Genetics Research Unit, Ames, IA 50011, USA.

Modified from a manuscript to be submitted to *Theoretical and Applied Genetics*

## Abstract

Molecular characterization of a given set of maize germplasm could be useful for understanding the use of the assembled germplasm for further improvement in a breeding program, such as analyzing genetic diversity, selecting a parental line, assigning heterotic groups, creating a core set of germplasm and performing association analysis for traits of interest. In this study, we used single nucleotide polymorphism (SNP) markers to assess the genetic diversity in a set of doubled haploid (DH) lines derived from "C0" (BSSS(R)C0), "C17" (BSSS(R)C17) and the cross "C0/C17" (BSSS(R)C0/BSSS(R)C17) of the Iowa Stiff Stalk Synthetic (BSSS) maize population. With the aim to explore if we have potentially lost diversity from C0 to C17 derived DH lines and to observe whether useful genetic variation in C0 was left behind during the selection process since C0 could be a reservoir of genetic diversity that could be untapped using DH technology. Additionally, we quantify the contribution of the BSSS progenitors in each set of DH lines. The molecular characterization analysis confirmed the apparent separation and the loss of genetic variability from C0 to C17 through the recurrent selection process. The progenitors had a higher genetic contribution in C0 compared with

C0/C17 and C17 derived DH lines. Although genetic drift can explain most of the genetic structure genome-wide, phenotypic data provide evidence that selection has altered favorable alleles frequencies in the BSSS maize population. Molecular characterization information provided by this research will help maize breeders better understand how to utilize the current set of DH lines developed from the BSSS maize population.

Keywords: Diversity, genetic resources, homozygous lines, *Zea mays*

## Introduction

The maize Iowa Stiff Stalk Synthetic (BSSS) population has undergone recurrent selection since 1939. This population was developed by intermating 16 inbred lines selected by various corn breeders for superior stalk quality (Sprague and Jenkins 1943). The "C0" base population was subjected to multiple cycles of recurrent selection. Currently, cycle 19 is available. The BSSS maize population has been under recurrent selection for increased grain yield, low grain moisture at harvest, and increased resistance to root and stalk lodging. However, phenotypic and genotypic changes have been observed in this population (Edwards 2011; Gerke et al. 2015; Hagdorn et al. 2003; Labate et al. 1999; Messmer et al. 1991), suggesting loss of genetic variability from C0 to more advanced cycles of selection. To better understand the level of diversity present at the genome and phenotypic level in different cycles of the BSSS population, Doubled Haploid (DH) lines have been developed. Alleles present in a heterogeneous population of heterozygous individuals can be fixed in homozygous and homogenous DH lines. The entire genetic variance within a population can thus be made available to unlock untapped genetic diversity (Böhm et al. 2017). The combination of DH technology with high-throughput genotyping drives progress in major maize breeding programs today (Andorf et al. 2019) and has been applied in this study to understand the evolution and genotypic composition of different cycles of BSSS.

Molecular markers like single nucleotide polymorphism (SNP) markers have proven to be valuable for the characterization of maize germplasm and become even more feasible over the past two decades because of the availability of new sequencing technologies resulting in the reduction of costs per data point. Characterizing and understanding the genetic diversity and genetic relationships of lines within a breeding program is essential for germplasm improvement. Molecular markers have been used to estimate the relative strengths of evolutionary forces (mutation, natural selection, migration, and genetic drift) (Ouborg et al. 1999) and a possible loss of genetic diversity in specific populations, including BSSS (Gerke et al. 2015). Gerke et al. (2015), when evaluating different cycles of selection in two recurrent selection programs, found that the populations steadily decrease in genetic diversity within populations and increase in genetic differentiation between populations mainly due to genetic drift and selection. The BSSS C0 population has drifted away from the BSSS founders, despite the absence of intentional selection during the creation and maintenance of C0 (Gerke et al. 2015). In our study, we similarly examine the loss of genetic diversity and the degree of genetic differentiation. However, we used different methods proposed as genetic diversity and genetic differentiation measures using genotypic information. Additionally, we used developed DH lines instead of individual plants representing the original populations.

It is expected that different cycles of selection in the BSSS maize population resulted in population stratification. Population structure is referred to as any form of relatedness among subgroups within the overall sample, including ancestry differences or cryptic relatedness (Sul et al. 2018). The population structure analysis involves a similar grouping of individuals into subpopulations based on shared genetic variants and can be assessed through principal component analysis (PCA). PCA has been a useful tool for analyzing genotypic data. It can

identify differences in ancestry among populations and individuals, regardless of the historical patterns underlying population structure (Price et al. 2006), since PCA clusters individuals based on the number of markers that are identical by state between them.

Plant breeders have used knowledge about the relationship between and within families to reduce inbreeding within their breeding programs, avoiding the negative consequences of mating closely related individuals. For instance, kinship coefficients have been used to estimate the genetic relationships within populations and to estimate the genetic contribution of a set of parents to its descendants. Therefore, the estimation of kinship coefficients represents a way to utilize breeding resources better as they can help breeders understand the genetic background of the germplasm and identify close genetic relatives (Beckett et al. 2017).

An identity by descend (IBD) segment refers to DNA segments descended from common ancestors and could be useful to estimate the genetic diversity and genetic contribution in a population. IBD occurs when identical alleles are inherited from a common ancestor and constitutes a measure of the degree of relationship between individuals (Wright 1922). The estimation of the degree of the relationship depends on the description of an ancestral population, which by definition, is assumed to be the base from where past ancestry is no longer accounted (Wright 1922). With the advent of high-throughput genotyping technologies, IBD segments can be estimated at a molecular scale. The identification of shared segments in the genome and haplotype information has been used for a range of purposes, including the quantification of inbreeding (Keller et al. 2011), identification of patterns of inheritance (Kirin et al. 2010), genotype imputation and haplotype inference (Browning and Browning 2007), genetic characterization and diversity analysis (Nelson et al. 2008), the genetic contribution of a set of founder lines in commercial maize breeding programs (Coffman et al. 2019), improve the

accuracy on genome-wide association analysis (GWAS) (Maldonado et al. 2019) and genomic prediction (Won et al. 2020).

In addition, in our study of the BSSS at the genomic level, we intended to observe whether useful genetic variation in C0 was left behind during the selection process since C0 could be a reservoir of genetic diversity that could be untapped using DH technology since genetic heterogeneity and high genetic load presented in C0 could be overcome by the production of DH lines (Böhm et al. 2017). Thus, producing DH lines from initial selection cycles could be used to unlocking their untapped genetic diversity.

Assessing the genetic relationship and genetic divergence within and among the evaluated cycles of selection will allow us to explore the BSSS DH lines' breeding potential for broadening the genetic base of the Stiff Stalk (SS) heterotic pool, providing additional relevance because lines derived from the BSSS maize population (B73, B14, and B37) have had a significant impact on the development of commercial hybrids (Coffman et al. 2019).

Useful measures of the quality of genetic markers' polymorphisms are the gene diversity or expected heterozygosity ($H_{exp}$) and the polymorphic information content (PIC). Expected heterozygosity ($H_e$) is defined as the probability that any two alleles at a single locus, chosen randomly from the population, are different from each other (Nei 1978). The PIC value is commonly used in genetics as a measure of informativeness of a marker locus (Shete et al. 2000), and it ranges from zero (no allelic variation) to 1 (balanced frequencies of multiple alleles per locus).

The genetic relationship based on genetic distance was first defined by Nei (1973) as the difference between two samples that can be described by allelic variation, meaning that genotypes with many similar genes have a smaller genetic distance between them. The degree of

genetic differentiation using the fixation index ($F_{ST}$) (Wright 1951) is a standard measure for the degree of genetic differentiation among subpopulations. $F_{ST}$ provides important insights into the evolutionary processes that influence the structure of genetic variation within and among populations (Holsinger and Weir 2009). $F_{ST}$ estimates can identify regions of the genome that have been targeted for selection. The comparisons of $F_{ST}$ from different genome regions can provide insights into populations' demographic history (Holsinger and Weir 2009).

Our overall question was whether potentially useful genetic diversity was left behind in the recurrent selection process. We used SNP markers to i) assess the genetic diversity in a set of doubled haploid (DH) lines derived from the Iowa Stiff Stalk Synthetic (BSSS) maize population in different cycles of selection, ii) explore if genetic diversity was lost from "C0" to "C17", iii) assess the genetic relationships and genetic divergence within and among the cycles of selection and iv) perform a haplotype analysis based on IBD segments to quantify the contribution of the progenitors in each set of DH lines.

## Materials and Methods

### Breeding Populations

Three synthetic populations BSSS(R)C0, BSSS(R)C17, and BSSS(R)C0/BSSS(R)C17 representing different stages of cycle advancement in the recurrent selection program of the Iowa Stiff Stalk maize population [BSSS(R)] were used to develop DH lines. The synthetic BSSS(R)C0 corresponds to the unselected base population (C0) formed by intermating 16 inbred lines selected for above average stalk quality in 1934 (Sprague 1946). The C0 seed used came from subsequent cycles of seed multiplication in C0 for maintenance over time. The BSSS(R)C17 population corresponds to the most advanced cycle (C17) available of the reciprocal recurrent selection program. Finally, the BSSS(R)C0/BSSS(R)17 population was created by intermating plants from BSSS(R)C0 and BSSS(R)C17 to create the BSSS(R)C0/C17

population (C0/C17). The 16 known progenitors of the BSSS maize population (A3G-3-3-1-3, CI 540, Fe (Parent of F1B1), I-159, IL12E, B2 (Parent of F1B1), Oh 3167B, Os 420, Tr 9-1-1-6, WD 456, I224, LE 23, 461, Hy, AH83, CI 187-2) were also included in this study.

**DH Line Development**

Randomly selected individuals within each population were pollinated with a maternal haploid inducer BHI301 (Almeida et al. 2020) in an isolation field to generate the haploid seed. Seed produced from these plants was screened and kernels expressing the *R-nj* marker gene in the endosperm but not in the embryo were classified as haploid kernels. The haploid seed was then germinated in plug trays in a greenhouse at the Department of Agronomy, Iowa State University (ISU). Once seedlings developed 2-3 leaves, a colchicine treatment was applied following the protocol used by the DH Facility at ISU (Vanous et al. 2017). Two days after the colchicine treatment, haploid seedlings were transplanted in the field at the Agricultural Engineering and Agronomy Research Farm, Boone, IA. At the flowering stage, putative $DH_0$ plants shedding pollen were self-pollinated to produce $DH_1$ seed. Seed multiplication was performed during subsequent generations, and lines were screened for uniformity and discarded if segregating or variable. In total, 132 DH lines from BSSS(R)C0 (C0_DHL), 185 DH lines from BSSS(R)17 (C17_ DHL), and 170 DH lines from BSSS(R)C0/BSSS(R)17 (C0C17_DHL) plus the 16 progenitors of the BSSS maize population were included. The DH lines were developed by the DH Facility at ISU (http://www.plantbreeding.iastate.edu/DHF/DHF.htm).

**Genotyping and Quality Control**

Genomic DNA was extracted from DH line seedlings established in the greenhouse at Agronomy Department at Iowa State University. Leaf tissue samples from three plants per DH line were collected at the 3-4 leaf developmental stage. DNA extraction was done using the standard CIMMYT laboratory protocol (CIMMYT 2005). Genotyping was carried out using the

Diversity Arrays Technology sequencing (DArT-seq) method (Kilian et al. 2012) provided by the Genetic Analysis Service for Agriculture (SAGA) laboratory at CIMMYT. DArT-seq is a high-throughput, robust, reproducible, and cost-effective marker system based on genome complexity reduction using a combination of restriction enzymes, followed by hybridization to microarrays to simultaneously assay hundreds to thousands of markers across the genome (Kilian et al. 2012). A total of 51,418 SNP markers were generated, but only 32,929 SNP markers were successfully called within the B73 RefGen_v4 (Jiao et al. 2017). Monomorphic, multi-allelic, and duplicate SNP markers were removed using the conditional formatting highlight in Excel. Un-imputed data without filtering for minor allele frequency (MAF) were used for further characterization analyses.

The inbred line B73 was used as technical control and was repeated in seven separate plates to verify assay reproducibility. The resulting SNP core set was 24,885 SNP markers corresponding to 487 DH lines (132 C0_DHLs, 170 C0C17_DHLs, 185 C17_ DHLs) and 15 progenitors). The progenitor CI 187-2 was omitted because of heterozygosity greater than 8.8 % (not expected in inbred lines) and was removed from further analyses.

**Genotypic Data Analysis**

Minor allele frequency analysis for each locus across the genotypes was calculated using the 24,885 SNP markers with the function ‘Geno summary’ analysis tool in the software TASSEL v.5.2.64 (Bradbury et al. 2007). The polymorphic information content (PIC) values, described by Botstein et al. (1980) for referring to the relative value of each marker with the amount of polymorphism was calculated according to the following formula in Microsoft Excel:

$$PIC = 1 - \sum_{i=l}^{l} P_i^2 - \sum_{i=1}^{l-1} \sum_{j=i+1}^{l} 2 P_i^2 P_j^2$$

Where: *Pi* and *Pj* are the population frequency of the $i^{th}$ and $j^{th}$ allele for SNP *i* evaluated, respectively; the summation extends over *n* alleles (Nagy et al. 2012).

Gene diversity or expected heterozygosity ($H_{exp}$) was calculated to quantify the genetic variation in the maize lines sampled. The gene diversity is defined as the probability that two alleles randomly chosen from the test sample are different (Nei 1978). Gene diversity was calculated using the R Poppr package (Kamvar et al. 2014), where the calculation of $H_{exp}$ is $(\frac{n}{n-1})\ 1\ -\ \sum_{i=1}^{k} p_i^2$ where p is the allele frequency at a given locus and n is the number of observed alleles for each locus (Nei 1978).

The computation of dissimilarity coefficients or Euclidean genetic distance (Gower and Legendre 1986) between DH lines and progenitor groups was performed with the 24,885 SNP markers using the R Poppr package (Kamvar et al. 2014). The genetic distance between the progenitors, C0_DHL, C0C17_DHL, and C17_DHL groups, respectively, was calculated based on the average genetic distance of all lines within each other group. A cluster analysis was performed to subdivide the three sets of DH lines and the progenitor group into genetic subgroups using the unweighted pair group method with arithmetic mean (UPGMA). Finally, a dendrogram was constructed based on genetic distances using the visualization software Interactive Tree of Life (iTOL) (Letunic and Bork 2019).

To assess the degree of genetic differentiation between the groups of DH lines and the progenitors, we used the Wright's F-statistics ($F_{ST}$) on a per locus basis using the methodology described by Weir and Cockerham (1984), which accounts for unequal population sizes and sampling variances since the heterozygous loci are weighted by the number of alleles observed in each population. The R package Hierfstat (Goudet 2005) was used to obtain estimates of $F_{ST}$.

The $F_{ST}$ values can range from zero to one, where high $F_{ST}$ values rely on a considerable degree of differentiation in the overall population.

The pairwise relative kinship for all 487 DH lines and the 15 progenitors was estimated based on the 24,885 SNP markers using the software TASSEL v.5.2.64 (Bradbury et al. 2007) using the centered_IBS method (Endelman and Jannink 2012). The relative kinship reflects the approximate degree of identity between two given individuals over the average probability of identity between two random individuals (Yu et al. 2006). The pairwise relative kinship is used to measure the genetic resemblance between individuals. A relative kinship close to zero indicates no relationship, and values close to one indicate a close relationship. Marker-based kinship coefficients show the relationship between lines based on genotypic information and rely on the marker allele frequencies in the reference population, which in practice is not known (Wang 2014). However, 15 of the 16 progenitors of BSSS are known. These estimates commonly use the sample of genotyped individuals as the reference population, resulting in estimates that two homologous genes within or between individuals are shared by descent (Wang 2014). Marker-based estimation of kinship coefficients can result in negative values. Wang (2014) states that the kinship coefficient's negative values could be interpreted as a lower probability that two homologous alleles are shared by descent compared to the probability that two alleles are taken at random from the reference population.

The selected 487 DH lines and the progenitors were known to belong to the four subpopulations BSSS(R)C0, BSSS(R)C17, BSSS(R)C0/C17 and the progenitor groups, respectively. However, to examine the overall population structure across all lines, we performed a principal component analysis (PCA). PCA analysis allows the classification of individuals into genetically similar groups. PCA relies on reducing dimensionality by using principal components

to maximize genetic variability (Price et al. 2006). Under this analysis, each principal component will account for a percentage of the total genetic variance by grouping the individuals into clusters with similar genetic information. After reducing dimensionality, a linear regression model is fitted to each of the axes of variation, and the residuals are extracted to compute associations (Price et al. 2006). PCA avoids any prior information about individual ancestries, the population of origin, and assumptions about the data, handling genome-wide data for thousands of individuals (Paschou et al. 2007). PCA was performed using the software GAPIT v.3 (Lipka et al. 2012). Bayesian Information Criterion (BIC) (Schwarz 1978) was used to identify the optimal number of principal components by selecting the lowest BIC model. The principal components results were used to display the first two principal components in R software (R Core Team 2019).

The average linkage disequilibrium (LD) decay between SNP markers for each chromosome was determined in each group of DH lines using the squared Pearson correlation coefficient ($r^2$) between alleles at two loci, for all possible combinations of alleles, and then weighting them according to the allele frequency. P-values are determined by a two-sided Fishers Exact test (Bradbury et al. 2007). The option “Full Matrix LD” on TASSEL v.5.2.64 was used to calculate LD for every combination of sites in the alignment (Bradbury et al. 2007). The resulting data were imported into R (R Core Team 2019) to create LD decay plots and fit a smooth line using Hill and Weir expectations of $r^2$ between adjacent sites (Hill and Weir 1988).

To quantify the progenitor's genetic contribution in the different sets of DH lines, we used a high-resolution detection of identity by descend (IBD) segments. An IBD segment refers to DNA segments descended from common ancestors. IBD occurs when identical alleles are inherited from a common ancestor and could be used to estimate the genetic contribution.

Estimation of IBD segments with genotypic data allows the quantification of the proportion of the covered genome descended from each progenitor. For the genetic contribution and the average LD decay between SNP marker analysis, a different filtering process of the genotypic data was conducted to have the most reliable SNP markers and ensure genotype concordance. From the 32,929 SNP markers successfully called within the B73 RefGen_v4 (Jiao et al. 2017). Monomorphic, multi-allelic, and duplicate SNP markers were removed using the conditional formatting in Excel. Then, SNP markers with missing information rate above 10 % (calling rate 90 %) were removed in TASSEL v.5.2.64 (Bradbury et al. 2007). Genotypes were phased and imputed using the LDkNNi (linkage disequilibrium k-nearest neighbors imputation) method (Money et al. 2016) on TASSEL v.5.2.52 (Bradbury et al. 2007). LDkNNi process considers the linkage disequilibrium (LD) between SNPs when choosing the nearest neighbors. It exploits the fact that markers useful for imputation are often not physically close to the missing genotype rather distributed throughout the genome (Money et al. 2016).

Physical distance for each marker was converted to genetic distance using a dense 0.2 cM resolution map (Ogut et al. 2015), with a genetic distance of 1385.6 Kb per cM. After completing the data's filtering and quality control, the genotypic data file contains 10344 sites for each of the 502 genotypes (487 DH lines and 15 progenitors) with coverage of 2102.7Mb (1517.5 cM) of the genome and with a marker every 203.2 Kb on average. The SNP markers not included in an IBD segment were referred to as non-IBD markers, while those within the IBD segment were labeled with the progenitor sharing the segment. The proportion of the genome descended from the progenitor was calculated by dividing the total number of SNP markers classified as IBD by the total number of polymorphic SNPs used. Regions in the genome (IBD segments) that have been inherited from the progenitor were identified with the identity by

descent linkage disequilibrium (IBDLD) program v.3.38 (Han and Abney 2011, 2013). IBDLD program uses a probabilistic approach with a hidden Markov model to estimate IBD segments in individuals' pairs. IBDLD program further expresses the emission probability conditioned on the actual genotype of *n* previous loci to account for linkage disequilibrium (Han and Abney 2011). IBD segments were constrained for each pair of individuals to have a minimum length of 350 Kb, have more than 10 SNP markers and SNP markers with an IBD probability above 70 %. These parameters force the segment to be a long IBD section, avoiding segments formed by an occasional genotyping error or missing genotype occurring in otherwise-unbroken segments that could underestimate IBD segments for each pair of individuals (McQuillan et al. 2008).

## Results

### Genotypic Data Analysis

The initial number of SNP markers in the DArT-seq data set were 51,418. A total of 32,929 SNP markers were successfully called within the B73 RefGen_v4 (Jiao et al. 2017). After removing monomorphic, multi-allelic, and duplicated markers, the final SNP marker data set included 24,885 SNPs distributed across the ten chromosomes. The number of SNP markers on each chromosome ranged from 3976 on chromosome 1 to 1688 on chromosome 10. The missing marker data rate across the ten chromosomes ranged from 18.6 % on chromosome 4 to 22 % on chromosome 9, with a mean value of 20.5 %. The heterozygosity rate varied from 1.2 % on chromosomes 2 and 7 to 1.6 % on chromosome 9, with a mean value of 1.3 % across the ten chromosomes (Table 2.1).

The 24,885 SNP markers were polymorphic with a MAF greater than zero (Figure 2.1). The average MAF was 0.13, with continuous distribution classes from 0.0 to 0.50 at intervals of 0.05. When analyzing the differences in MAF among the groups of DH lines and the progenitors,

we found that the average MAF was 0.193, 0.157, 0.134, and 0.065 in the progenitor, C0_DHL, C0/C17_DHL, and C17_DHL groups, respectively (Table 2.2).

The PIC values of the three sets of DH lines were slightly different. In the C17_DHL group, the PIC value was the lowest at 0.072, and the progenitor group had the highest PIC value with 0.211. Moreover, the C0_DHL and C0/C17_DHL the PIC values were similar with 0.167 and 0.149, respectively (Table 2.2).

The highest gene diversity was in the progenitor's group (0.276), followed by the C0_DHL group with 0.211. The lowest gene diversity value was observed in the C17_DHL group as expected. In comparison, the group C0C17_DHL had a gene diversity value of 0.185 (Table 2.2). The estimates of MAF, PIC, and gene diversity allows comparing diversity across populations.

The computation of dissimilarity coefficients or Euclidean genetic distance between the different groups of DH lines was broader between the progenitors and the C17_DHL group (0.175) as expected, and a lower genetic distance was observed between C17_DHLs and C0/C17_DHL (0.108) (Table 2.3). The cluster analysis based on the computation of dissimilarity coefficients using the unweighted pair group method with arithmetic mean (UPGMA) method separates the different groups of DH lines and the progenitors (Figure 2.2, 2.3 and 2.4).

The lowest $F_{st}$ among the DH lines was observed between the progenitors and the C0_DHL group, with 0.148. The highest value was observed between progenitors and C17_DHL, with 0.496 (Table 2.3). Manhattan plots in Figures 2.5 and 2.6 show the genetic differentiation among the different comparisons performed between the progenitors and the different groups of DH lines across the ten chromosomes, with similar patterns across chromosomes (Figures 2.5 and 2.6). $F_{ST}$ values of 1 and closer to 1 were observed between the

progenitor group and the C17_DH lines group across the genome as expected, demonstrating a considerable differentiation degree.

The pairwise relative kinship distribution for the entire set of 487 maize DH lines and 15 progenitors estimated with 24,885 SNP markers is shown in Figure 2.7. 53.2 % of the kinship coefficient in the entire panel was equal to 0, 46.0% ranged between 0 and 0.4, and only 0.8 % were greater than 0.5 (Figure 2.7). Thus, most of the entire panel lines were either not related or distantly related to each other according to the pairwise relative kinship.

Based on PCA, population structure analysis suggested that the DH lines developed from BSSS can be divided into three subgroups. The principal components, plotted in a two-dimensional plot using discriminant analysis of principal components (DAPC), showed a clear grouping of the DH lines into the C0_DHL, C17_DHL, C0C17_DHL (Figure 2.8). The progenitor lines are grouped within the C0_DHL cluster as expected since the combination of these 16 progenitor lines formed this population (Figure 2.8). The first two principal components explained 12.5 % of the total SNP variation in the entire panel. The C0C17_DH lines group was also scattered over a broader range, similar to the C0_DHL group (Figure 2.8).

LD decay varied across the ten chromosomes and different genetic regions within chromosomes. The C17_DHL group showed the most extended LD decay distance ranging from 1229 to 2709 Kb on chromosomes 3 and 1, respectively. In contrast, the C0/C17_DHL group displayed the shortest LD decay distance (384 kb on chromosome 5 to 1024Kb on chromosome 3). For C0_DHL, the LD decay varied from 486 Kb to 1322Kb for chromosomes 7 and 3, respectively. The LD within the C17_DHL group is more extensive than in C0_DHL and C0/C17_DHL (Figure 2.9).

For the progenitors' genetic contribution to each set of DH lines, a total of 10,344 polymorphic SNP markers distributed across the whole genome were used to estimate IBD segments among the 15 progenitors and 487 DH lines. The mean genetic contribution of the progenitors to each DH line is listed in Appendix: Supplemental Table S2.1. In general, the progenitor A3G-3-3-1-3 had a lower genetic contribution to the different sets of DH lines with 0.91, 0.87, and 0.63 % in the C0, C0/C17, and C17_DH line groups, respectively (Figure 2.10). In comparison, the progenitor line WD 456 had a higher genetic contribution to the different sets of DH lines with 5.76, 4.90, and 4.14 % in the C0_DHL, C0/C17, and C17_DH line groups, respectively. The progenitors CI 540 and Os 420 had a similar contribution to the different groups of DH lines (Figure 2.10). In general, the 15 progenitors evaluated had a higher genetic contribution in C0_DHLs, ranging from 0.91 % to 5.87 % for individual progenitors, compared with C0/C17 (0.87 to 4.90 %) and C17 (0.63 to 4.62 %). The progenitor with the highest genetic contribution in C0 (Oh 3167B with 5.87 %) had a lower contribution in C0/C17 and C17 with 4.78 and 3.71 %, respectively (Figure 2.10). On average, progenitor lines had 60.07 % of the genome classified as identical by descent with C0_DHLs, 50.03 % within the C0/C17, and 41.61% with C17. The remaining 39.93 %, 49.97 %, and 58.39 % in C0, C0/C17, and C17, respectively, correspond to SNP markers not included within the IBD segment between DH group lines and progenitors.

## Discussion

The final SNP marker data set included 24,885 SNPs distributed across the ten chromosomes and 502 genotypes corresponding to DHL derived from different recurrent selection cycles (132 C0_DHL, 185 C17_ DHL, and 170 C0C17_DHL) plus 15 progenitors of the BSSS maize population. The rationale of using un-imputed data without filtering for MAF was that the BSSS maize population came from 16 founder genotypes. For some SNP markers,

an allele was provided by only one founder; the expected frequency would be ~6.2 %. If by chance, genetic drift has occurred, the actual frequency in C0 can be even lower. We do not know exactly how much reduction in allele frequency drift can account for. It Will likely require that we know how many individuals were used to create C0 and how it was done in some detail. The C0 seed used in this research came from subsequent cycles of seed multiplication for maintenance, giving more genetic drift chances to occur.

The heterozygosity rate of 1.3 % is normal for a maize inbred line collection. However, since we analyzed DH lines in this study, we expected values close to zero. The heterozygosity rate of B73 used as technical control of the genotyping process was, on average, 2.0 %, ranging from 1.1 to 4.5 % (data not shown). The heterozygosity rate found in this data set could be due to genotyping errors or the inclusion of the progenitors (inbred lines). The progenitor line CI 187-2 had 8.8 % of heterozygosity, which was suspicious for an inbred line and was removed for the characterization analysis.

**Changes in Genetic Diversity in Different Cycles of Selection**

The application of molecular markers has led to new insights into the patterns of genetic diversity. Next-generation sequencing and high-throughput genotyping platforms promise to further our understanding of genetic diversity, effective identification, and use of novel alleles and haplotypes and designing strategies to utilize the genomic information for maize improvement. Using genotypic information, we identified highly heterozygous individuals that were not true DH lines (data not shown). One cause of a high level of heterozygosity (> 3.5 %) found was likely the cross-pollination of DH plants or a physical mix up of seed from different DH lines during seed multiplication. Additionally, we found some DH lines with a low level of heterozygosity, which could be due to genotyping errors or heterozygous markers that may

reflect true genetic heterozygosity caused by an unknown mechanism during the DH process (Brenner et al. 2012).

Closer MAF, PIC, and gene diversity values of C0_DHLs and the progenitor group (Table 2.2) were expected, even though the progenitors were randomly mated during five to six generations to form the BSSS maize population with adequate population size. However, there has been much more recombination than that because of population maintenance. Unfortunately, we do not have adequate records indicating how the seed has been maintained since 1939 when the population was created. However, a reduction in MAF, PIC, and gene diversity was observed when we compared C0_DHL versus C17_DHL. The reduction in MAF between these groups was expected due to the recurrent selection process and genetic drift. The PIC assesses the diversity in a population. Lower PIC values found in the C17_DHL could be due to the low genetic diversity found in this group since values close to zero indicates no allelic variation in the population. PIC values can reach a max of 1 if a genotype has only a new allele. The highest PIC values found in the progenitor group could be due to the higher genetic diversity of this group since the progenitors were selected with different genetic backgrounds.

Additionally, the highest gene diversity values found in the C0_DHL group could be an indication of the presence of more rare alleles, which could be an important source to find new functional alleles of desirable traits that could be lost during the recurrent selection program and can be used to broaden the genetic base of maize breeding populations. These results gave us an indication of potential losses in genetic diversity when advancing to more advanced cycles and were consistent with previous studies in the BSSS maize population in different eras of the recurrent selection program (Gerke et al. 2015; Hagdorn et al. 2003; Hinze et al. 2005; Labate et

al. 1997; Messmer et al. 1991) where genome-wide genetic diversity has decreased across cycles of selection.

Additionally, Gerke et al. (2015), when analyzing the progenitors and individuals from different selection cycles in the BSSS maize population, found a clear separation in the BSSS when advancing cycles of selection to BSSS(R)16 even when there has been nothing new genetic material intentionally introduced into BSSS maize population, so the substantial increase in genetic distance from C0_DHL versus C17_DHL could only arise from the loss of genetic diversity within the population due to selection and genetic drift.

Improvement of plant architecture traits like flowering time, flag leaf angle, and yield has been observed when advancing cycles in the BSSS recurrent selection program (Brekke et al. 2011; Edwards 2011). These changes may suggest some positive fixation of favorable alleles during the recurrent selection program. Thus, exploring early BSSS cycles using DH technology may reveal natural and useful genetic diversity left behind in the recurrent selection process and could be an important resource to help drive future genetic gains in maize breeding program.

**Genetic Differentiation of BSSS Maize Population**

The Wright's F-statistics ($F_{ST}$) used to measure population substructure, and the overall genetic divergence among the different groups showed that the degree of differentiation is higher between the progenitor inbred lines and the C17_DHL group (Table 2.3) as expected since the two groups share fewer alleles between them. Lower $F_{ST}$ values indicate limited differentiation between groups of DH lines. These results can be confirmed with the wider genetic distance found between them (Table 2.3), reflecting the uniqueness of most lines between these groups. Similar results were found by (Gerke et al. 2015) when evaluating the progenitors and samples from different cycles of the BSSS maize population (C0, C4, C8, C12, and C16), indicating a

clear differentiation between the founder lines and the population at cycle 16 caused by the loss of different alleles within BSSS maize population.

The pairwise relative kinship distribution indicates that most of the lines in the entire panel are distantly related to each other according to the measure of the genetic resemblance between individuals (Figures 2.7). Low or negative kinship coefficients among pairs of DH lines reflect the uniqueness of most lines, mainly in the C17_DHL group. The estimation of the degree of the relationship depends on the description of an ancestral population, which by definition, is assumed to be the base from where the past ancestry is no longer accounted (Wright 1922). Thus, the lower the number of common ancestors or the lower the number of generations separating the ancestral with the current population, the higher the kinship coefficient between individuals because of a reduced number of possible recombination events (Wang 2014).

Population structure based on principal component analysis (PCA) is used to reveal genetic divergence between populations (Price et al. 2006). In this study, the results suggest a clear separation into three significant subgroups among all the BSSS DH lines and the progenitors (Figure 2.8). Also, we observed that the C0/C17_DHL group was more scattered over a wide range, similar to C0_DHL, indicating a broader genetic divergence within the lines than C17_DHL (Figure 2.8).

**Linkage Disequilibrium in BSSS DH Lines**

Linkage disequilibrium (LD) refers to the non-random co-segregation of alleles at two loci. Recombination shuffles genetic material during meiosis between homologous chromosomes and causes LD to decay with increasing distance. Multiple factors are affecting LD in crops. Generally, LD decays faster in cross-pollinated crops, diverse populations, but also, different genes and genomic regions in the same crop can exhibit different rates of LD decay. It is expected in maize, genome regions to decay at distances around 1kb for exotic landraces, as

described by (Romay et al. 2013). In the Ames panel subset corresponding to 384 lines, (Pace et al. 2015) found that the LD decay rate was similar across chromosomes with an average distance of 10 kb throughout the genome. However, it has been observed that LD decay over higher distances in DH germplasm. Sanchez et al. (2018) found that in the GEM-DH panel, the LD decay was slower with the threshold ($r^2$=0.20). The LD decay was not reached even after 100 Mb. Vanous et al. (2018) also found that the LD decayed ($r^2$ = 0.2 threshold) over a distance greater than 500 kb for all chromosomes when evaluated a diverse panel of exotic derived DH lines. In this study, we found a more considerable LD decay distance in the C17_DH lines compare with C0_DHL and C0C17_DHL groups. The larger LD decay distance in C17_DHL was expected. It could be due to the narrow genetic diversity found in this group confirmed with the average MAF, PIC, and gene diversity results (Table 2.2). In a population under selection, the number of homozygotes tends to increase for many favorable alleles. In consequence, the LD between these selected alleles tend to increase in the C17_DH lines group. Additionally, the rate of effective recombination is declining over selection cycles due to the occurrence of bottlenecks or due to fixation for favorable alleles over time, since 17 cycles of recurrent selection may lead to a lower genetic diversity available in the C17_DHL group, since LD distance decay more rapid in pools with higher genetic diversity (Romay et al. 2013; Wu et al. 2016). The C17_DH lines come from a population that was gone through 17 cycles of recurrent selection, which probably have caused some genetic drift, or a small effective population size, resulting in the more considerable decay distances

**Progenitors Genetic Contribution in Different Groups of DH Lines**

On average, the mean genetic contribution of the BSSS progenitors lines estimated using high-resolution detection of IBD segments changed in the different groups of DH lines. The progenitors had the highest genetic contribution in the C0_DHL group with 60.07 %, followed

by C0/C17_DHL with 50.03 %, and C17_DHL had the lowest genetic contribution of the progenitors with 41.61 %, suggesting that relationships caused by more recent ancestry have the most significant contribution in the IBD segments between individuals. Additionally, 17 cycles of recurrent selection have changed the allele frequencies in the C17_DHL because only individuals with superior performance for the selected trait will contribute with alleles to the next generation (Albrechtsen et al. 2010). However, if an allele affects a trait under selection, the selection will increase the probability that multiple individuals inherit identical alleles.

In the identification of regions in the genome inherited from the progenitors, we found in overall the prevalence of small to medium segments where 50.4 % of the segments were between 2.43 to 4.06 Mb, and 28.2 % of the segments ranged from 4.06 to 8.1 Mb inherited from the progenitor inbred lines with a trend of decreasing the number of segments as the length of the segment increases (Data not shown). Large preserved regions in the genome could be associated with selection processes, resulting in long DNA segments inherited as a block from the parents. Therefore, under positive selection favoring a phenotype, a slight increase in LD surrounding the favored alleles will be produced. In these cases, the length of the IBD segment surrounding the alleles subject to selection will increase, experiencing less recombination at the population level (Albrechtsen et al. 2010). Albrechtsen et al. (2010) state that a reduced recombination rate in the genome, leading to significant LD, could be explained as a function of the effective population size. An increase in random genetic drift could partially explain these results because of the population size, which will increase the length of DNA that will be shared between individuals in the population similar to what could happened in the C17_DHL with the 17 cycles of the recurrent selection process. The detection of long IBD segments in populations could be used as evidence for strong and recent selection processes because these segments have not suffered

from recombination. However, even though the progenitors were randomly mated during five to six generations to form the BSSS C0 maize population with adequate population size, there has been much more recombination than that because of subsequent cycles of seed multiplication and population maintenance. Unfortunately, we do not have adequate records indicating how the seed has been maintained since 1939 when the population was created, giving more chances for genetic drift to occur. In cases where alleles within long IBD segments are in linkage disequilibrium, specifically in a repulsion phase, unfavorable alleles will persist in the population, inducing the hitch-hiking effect and reducing the genetic diversity (Hospital and Chevalet 1993). This hitch-hiking will increase genetic drift and significantly decrease the effective population size (Smith and Haigh 1974). IBD segments shared between different groups of DH lines and the 15 progenitor lines will allow the estimation of genetic diversity and progenitors genetic contribution to newly released lines.

The selection process and the effective population size applied to the BSSS maize population have reduced the genetic variability from C0 to C17, even when more recombination events have been created in C17, reducing the IBS segments' length. However, distant relatedness with the progenitors was found. Additionally, there was a higher genetic contribution of the progenitors to the C0_DHL group compared to the genetic contribution of the C0/C17 and C17_DHL groups. Using IBD segments, we found that few progenitors (Os 420, WD 456, and Hy) have contributed larger proportions of the genome to the C17_DHL group with more extended regions in the genome inherited from these progenitors.

Using DH lines, these molecular characterization analyses confirm the separation from BSSS(R)C0 to BSSS(R)C17 through the recurrent selection process. Consistent with previous studies (Gerke et al. 2015; Hagdorn et al. 2003; Hinze et al. 2005; Labate et al. 1997; Messmer et

al. 1991). Although genetic drift can explain most of the genetic structure genome-wide, phenotypic data provide evidence that selection has altered favorable alleles' frequencies in the BSSS maize population. Different experiments have shown that the BSSS maize population and the hybrids formed from them exhibit genetic gain for hybrid yield, plant architecture traits, and tolerance to high plant density (Brekke et al. 2011; Edwards 2011; Holthaus and Lamkey 1995; Keeratinijakal and Lamkey, 1993). Complete homozygous lines offer a higher phenotype to genotype correlation. Thus, the DH lines developed from the BSSS maize population can be evaluated in replicated trials. Genomic selection can be applied to estimate the breeding value for each DH line from genotypic data.

Additionally, DH lines derived from the BSSS maize population could be ideal for association mapping due to the low population structure. Thus, we could identify genes or regions in the genome associated with a particular trait. Using genome-based data and DH technology is a powerful tool for access to the genetic diversity available in C0_DHL or C0/C17_DHL groups, which would be beneficial to incorporate in BSSS(R)17 to broaden its genetic variation while minimizing yield or other penalties.

## Tables and Figures

Table 2.1 Genotypic data summary on the 24,885 SNP markers and the entire panel of DH lines and progenitors.

| Chromosome number | Number of SNP markers | Missing rate (%) | Heterozygosity rate (%) |
|---|---|---|---|
| 1 | 3976 | 20.1 | 1.3 |
| 2 | 2978 | 21.0 | 1.3 |
| 3 | 2721 | 18.9 | 1.2 |
| 4 | 2453 | 18.6 | 1.5 |
| 5 | 2798 | 20.9 | 1.3 |
| 6 | 1929 | 22.0 | 1.4 |
| 7 | 2203 | 21.1 | 1.2 |
| 8 | 2105 | 20.5 | 1.5 |
| 9 | 2034 | 22.0 | 1.6 |
| 10 | 1688 | 21.5 | 1.4 |
| Genome-wide | 24885 | 20.5 | 1.3 |

Table 2.2 Average Minor Allele Frequency (MAF), Polymorphic Information Content (PIC), and gene diversity within each group of DH lines and progenitors.

| Group | Genotypes | MAF | PIC | Gene diversity |
|---|---|---|---|---|
| Progenitors | 15 | 0.193 ± 0.001 | 0.211 ± 0.001 | 0.276 ± 0.001 |
| C0_DHL | 132 | 0.157 ± 0.001 | 0.167 ± 0.001 | 0.211 ± 0.001 |
| C0/C17_DHL | 170 | 0.134 ± 0.001 | 0.149 ± 0.001 | 0.185 ± 0.001 |
| C17_DHL | 185 | 0.065 ± 0.001 | 0.072 ± 0.001 | 0.089 ± 0.001 |

Table 2.3 Pairwise genetic distance and degree of genetic differentiation ($F_{ST}$) between different groups of DH lines and the progenitors of the BSSS maize population.

| Group | Progenitors | C0_DHL | C0/C17_DHL | C17_DHL |
|---|---|---|---|---|
| Progenitors | | 0.168 | 0.170 | 0.175 |
| C0_DHL | 0.148 | | 0.141 | 0.147 |
| C0/C17_DHL | 0.220 | 0.092 | | 0.108 |
| C17_DHL | 0.496 | 0.340 | 0.131 | |

* Lower diagonal shows pairwise $F_{ST}$ estimates, whereas the upper diagonal shows pairwise genetic distance between different groups of DH lines and the progenitors.

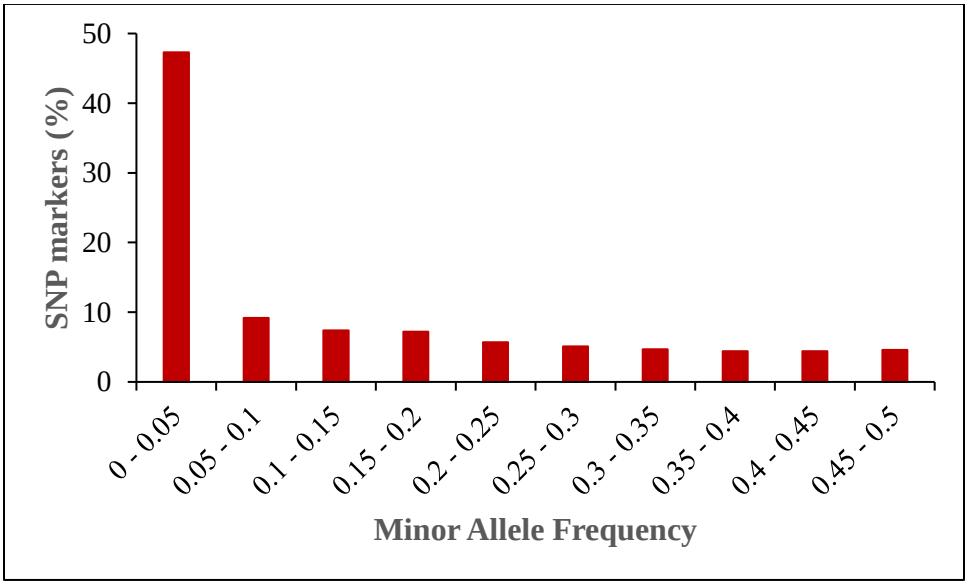


Figure 2.1 Frequency distribution of minor alleles in the entire panel of 487 BSSS DH lines and the 15 progenitors based on 24,885 SNP markers.

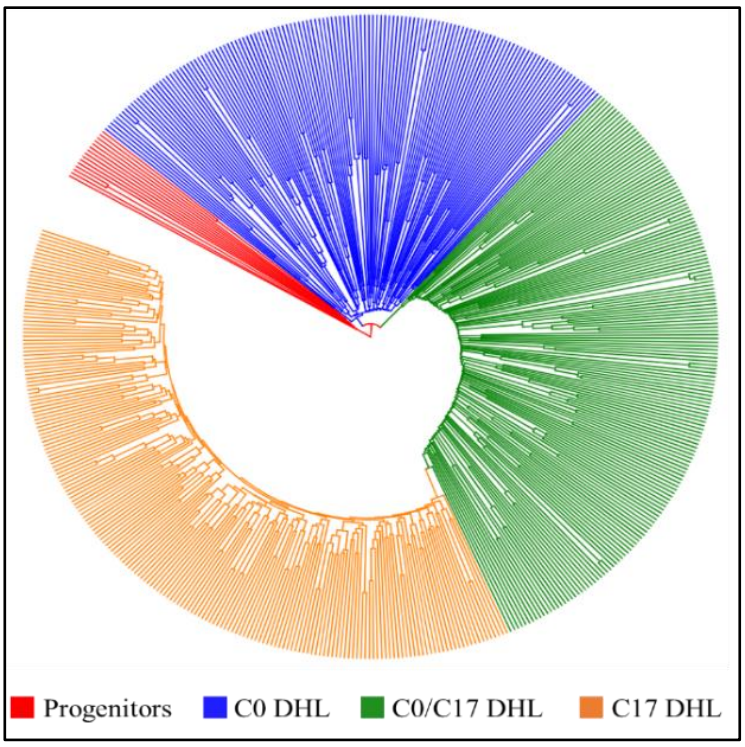


Figure 2.2 Dendrogram constructed from Euclidean genetic distance based on the UPGMA tree method for a panel of 15 progenitors and 495 DH lines derived from the BSSS maize population.

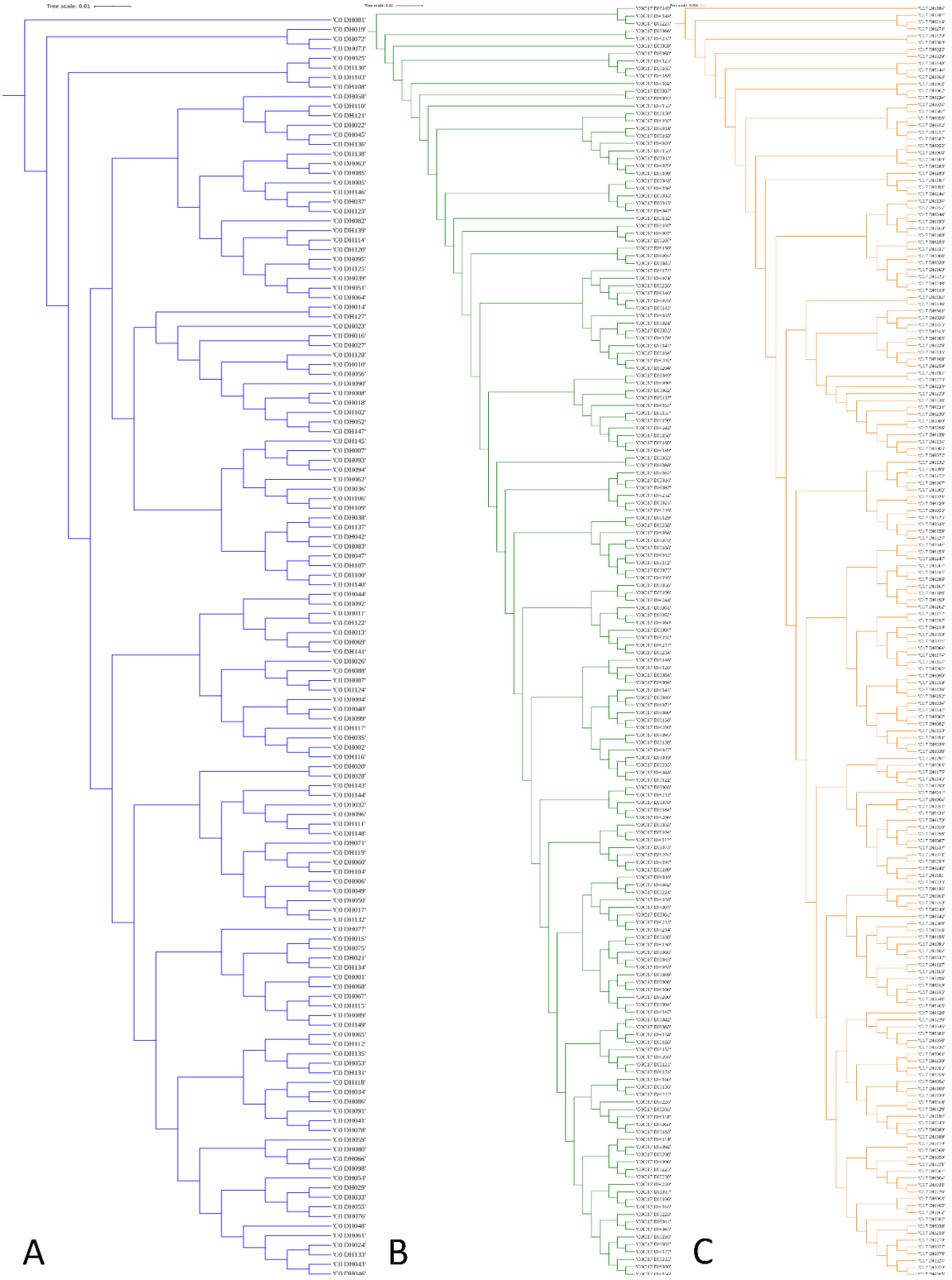


Figure 2.3 Dendrogram constructed from Euclidean genetic distance based on the UPGMA tree method. A) C0_DH lines, B) C0/C17_DH lines, C) C17_DH lines developed from the BSSS maize population.

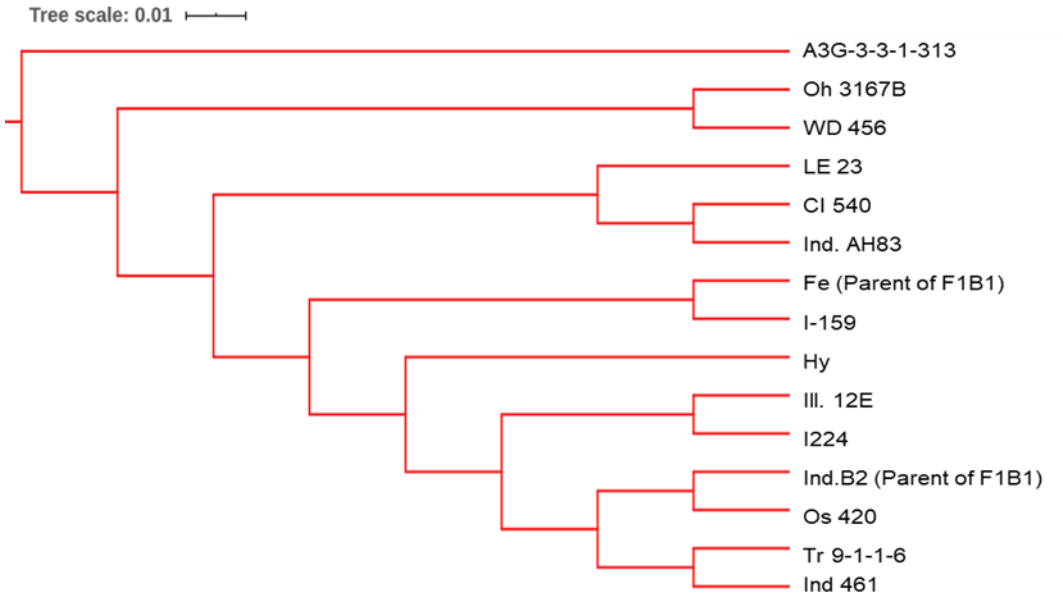


Figure 2.4 Dendrogram constructed from Euclidean genetic distance based on the UPGMA tree method in the progenitors of the BSSS maize population.

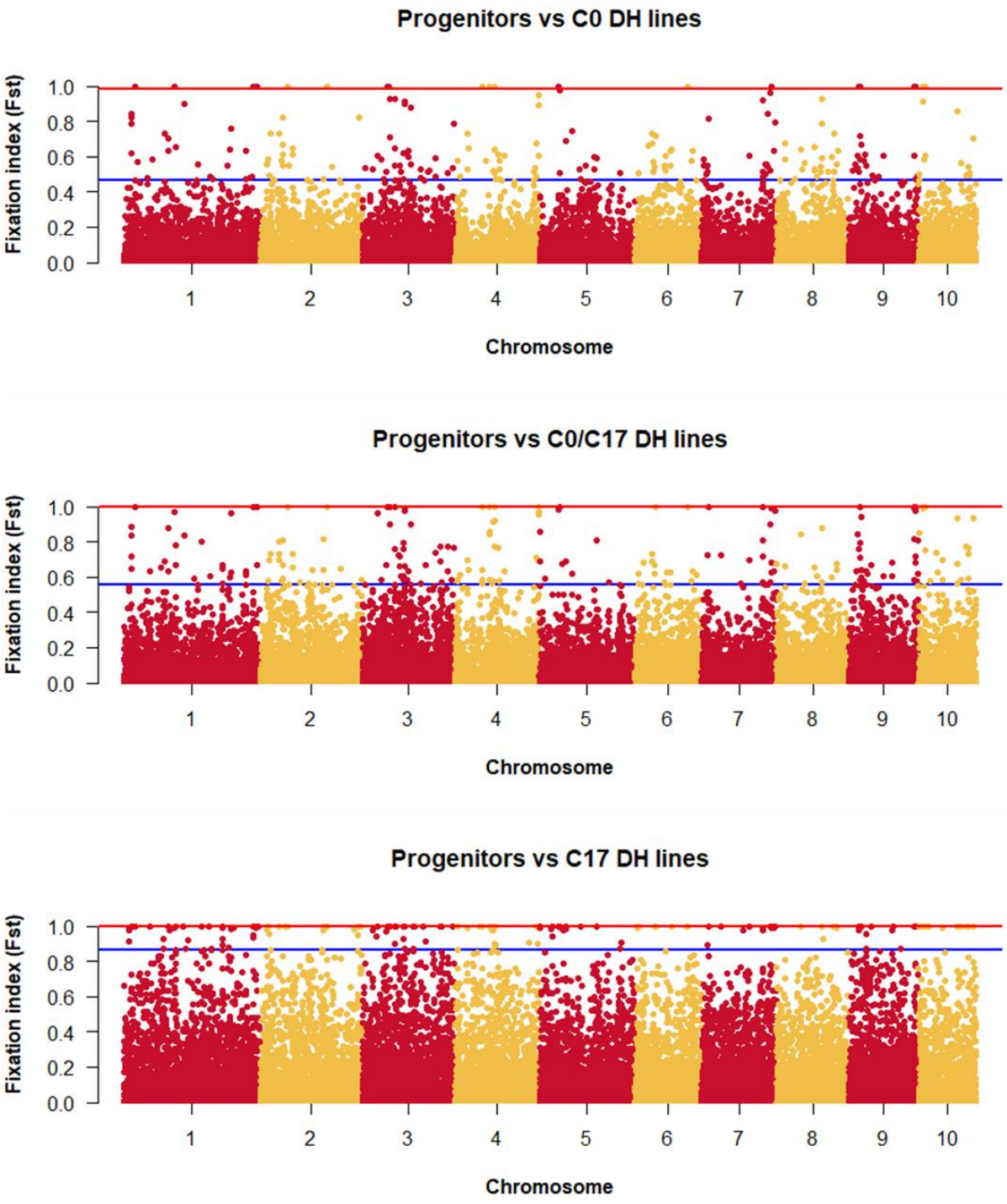


Figure 2.5 Genetic differentiation comparing the progenitor group and the different groups of DH lines across chromosomes (x-axis) with the $F_{ST}$ value (y-axis). Dots between the red and the blue lines represent the highest 1 % of the $F_{ST}$ values.

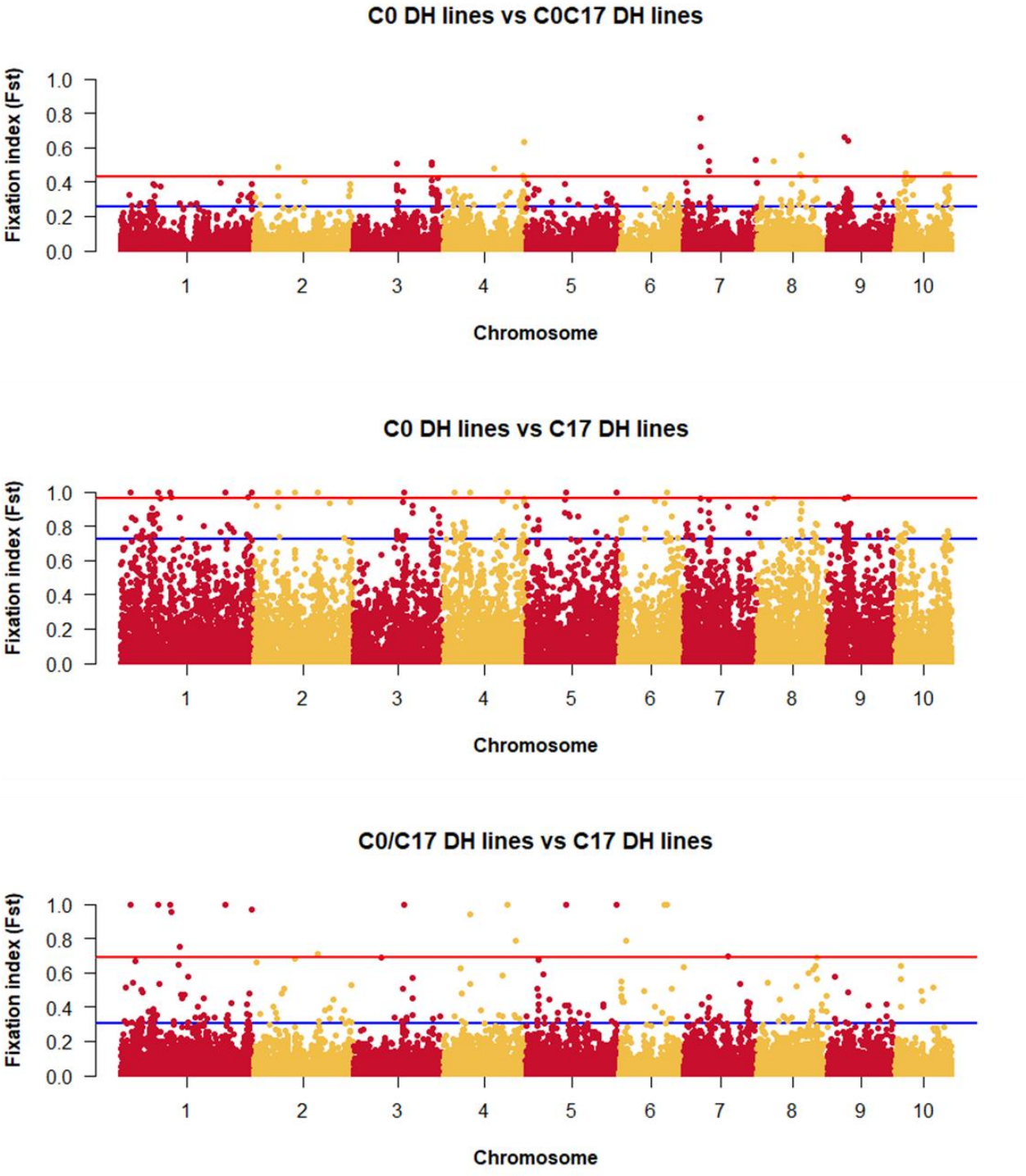


Figure 2.6 Genetic differentiation comparing the different groups of DH lines across chromosomes (x-axis) with the $F_{ST}$ value (y-axis). Dots between the rad and the blue lines represent the highest 1 % of the $F_{ST}$ values.

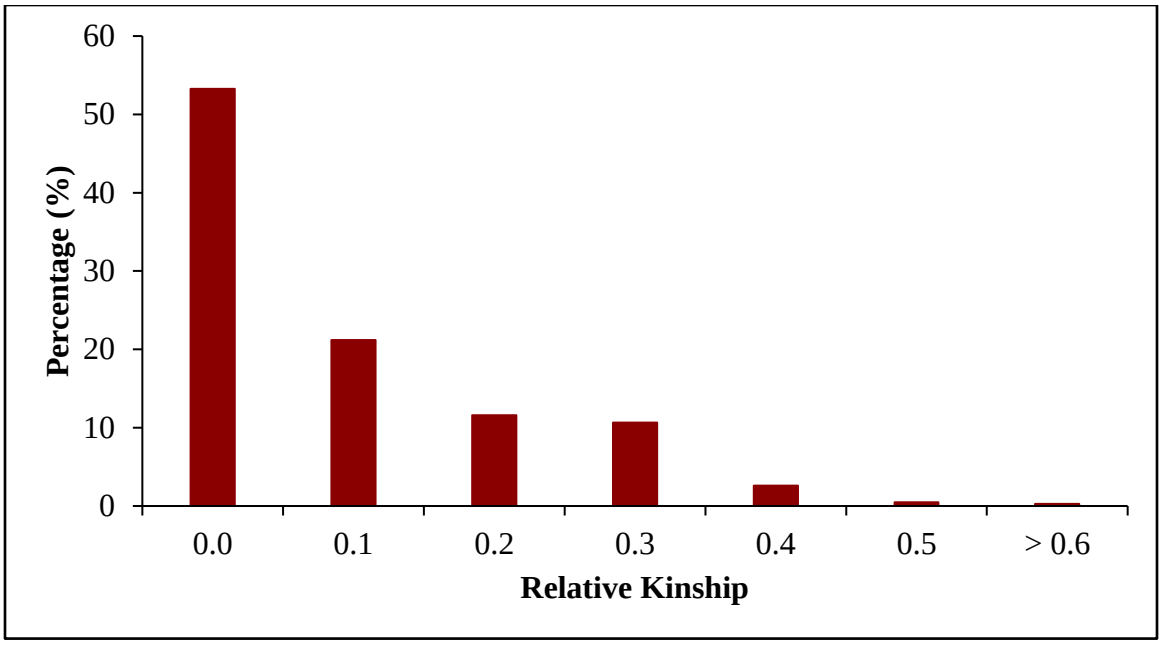


Figure 2.7 Distribution of pairwise relative kinship for 487 maize DH lines and 15 progenitors lines of the BSSS maize population calculated using 24,885 SNP markers.

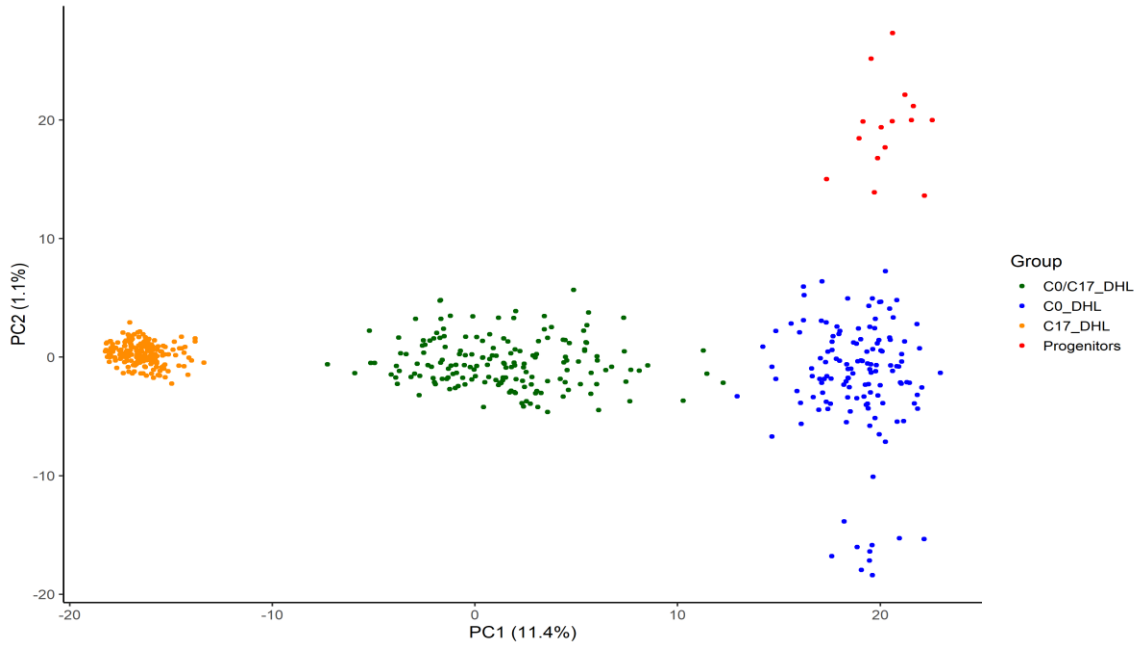


Figure 2.8 Scatter plot of the discriminant analysis of principal components based on 487 DH lines and 15 progenitors of the BSSS maize population. The dots represent each of the DH lines within their respective population. The axes represent the first two discriminant functions, respectively.

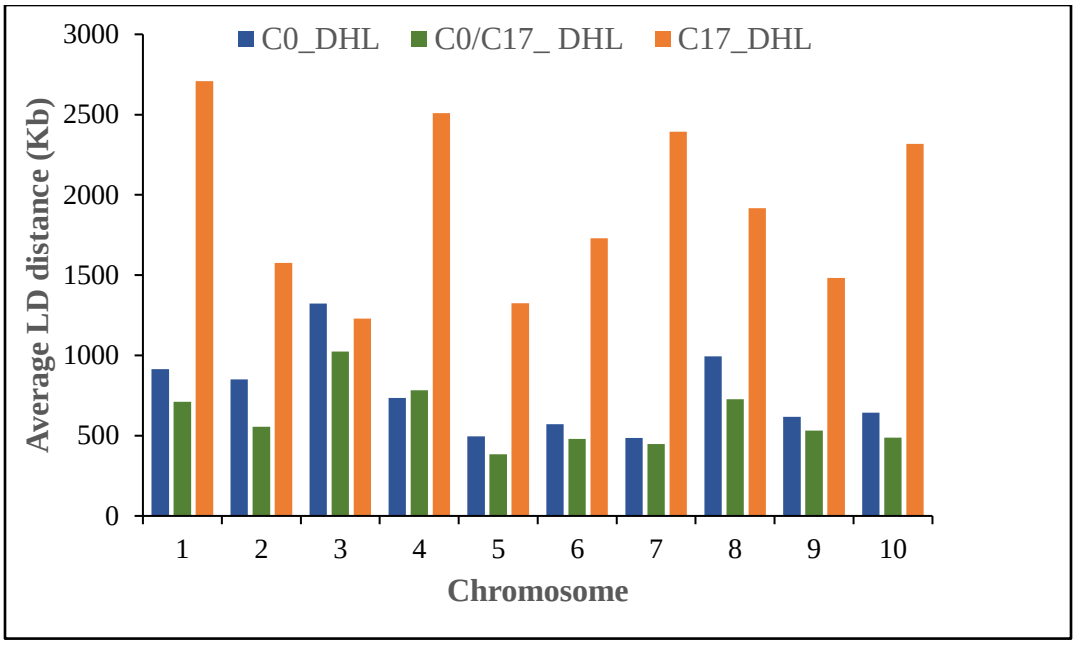


Figure 2.9 Linkage Disequilibrium (LD) decay distance per chromosome in the different groups of DH lines.

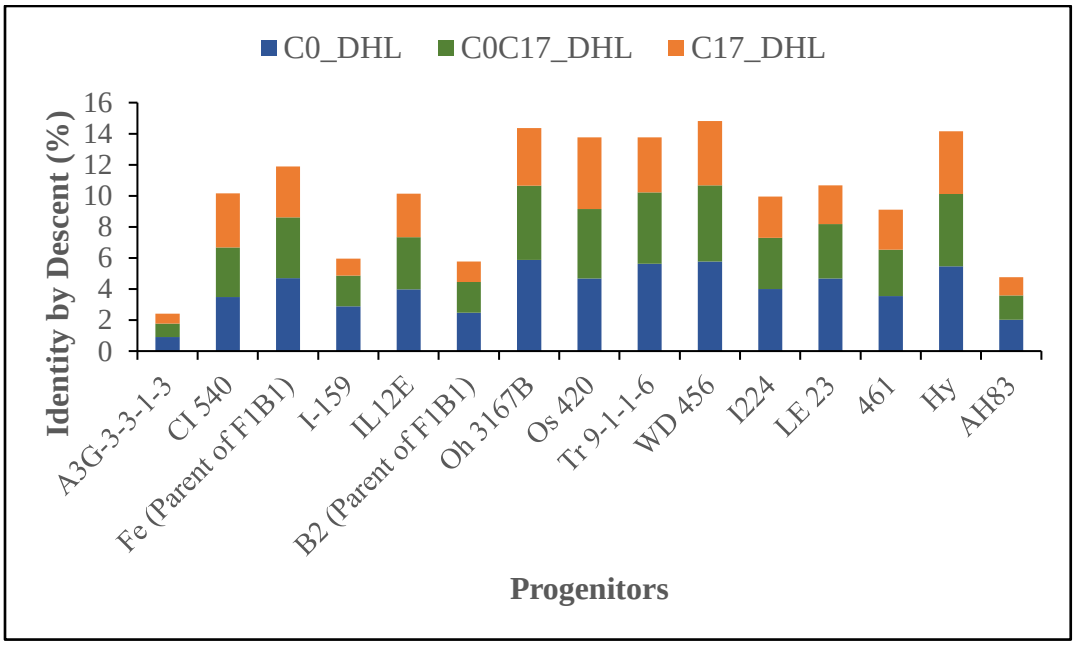


Figure 2.10 The genome's proportion classified as IBD between the BSSS progenitors inbred lines for each group of DH lines evaluated (C0_DH, C0/C17_DH, and C17_DH lines) identified with marker-based dissimilarity values.

## References

Albrechtsen, A., Moltke, I., & Nielsen, R. (2010). Natural Selection and the Distribution of Identity-by-Descent in the Human Genome. Genetics, 186(1), 295–308. https://doi.org/10.1534/genetics.110.113977

Almeida, V. C., Trentin, H. U., Frei, U. K., & Lübberstedt, T. (2020). Genomic prediction of maternal haploid induction rate in maize. Plant Genome, 13(1). https://doi.org/10.1002/tpg2.20014

Andorf, C., Beavis, W. D., Hufford, M., Smith, S., Suza, W. P., Wang, K., … Lübberstedt, T. (2019). Technological advances in maize breeding: past, present and future. Theoretical and Applied Genetics. https://doi.org/10.1007/s00122-019-03306-3

Beckett, T. J., Morales, A. J., Koehler, K. L., & Rocheford, T. R. (2017). Genetic relatedness of previously Plant-Variety-Protected commercial maize inbreds. PLoS ONE, 12(12), 1–23. https://doi.org/10.1371/journal.pone.0189277

Böhm, J., Schipprack, W., Utz, H. F., & Melchinger, A. E. (2017). Tapping the genetic diversity of landraces in allogamous crops with doubled haploid lines: a case study from European flint maize. Theoretical and Applied Genetics, 130(5), 861–873. https://doi.org/10.1007/s00122-017-2856-x

Botstein, D., White, R. L., Skolnick, M., & Davis, R. W. (1980). 1980 Botstein. American Journal of Human Genetics, 32, 314–331. Retrieved from papers2://publication/uuid/0BCEC67F-8A97-4A0A-9B37-6B8450CE68AA

Bradbury, P. J., Zhang, Z., Kroon, D. E., Casstevens, T. M., Ramdoss, Y., & Buckler, E. S. (2007). TASSEL: Software for association mapping of complex traits in diverse samples. Bioinformatics, 23(19), 2633–2635. https://doi.org/10.1093/bioinformatics/btm308

Brekke, B., Edwards, J., & Knapp, A. (2011). Selection and adaptation to high plant density in the Iowa StiffStalk Synthetic maize (Zea mays L.) population: II. plant morphology. Crop Science, 51(6), 2344–2351. https://doi.org/10.2135/cropsci2010.09.0562

Brenner, E. A., Blanco, M., Gardner, C., & Lübberstedt, T. (2012). Genotypic and phenotypic characterization of isogenic doubled haploid exotic introgression lines in maize. Molecular Breeding, 30(2), 1001–1016. https://doi.org/10.1007/s11032-011-9684-5

Browning, S. R., & Browning, B. L. (2007). Rapid and accurate haplotype phasing and missing-data inference for whole-genome association studies by use of localized haplotype clustering. American Journal of Human Genetics, 81(5), 1084–1097. https://doi.org/10.1086/521987

CIMMYT. (2005). Laboratory Protocols: CIMMYT Applied Molecular Genetics Laboratory (Third Edit). Mexico, D.F: CIMMYT. Retrieved from papers2://publication/uuid/B00DBE67-68B3-4845-BA5F-F687141F2DF7

Coffman, S. M., Hufford, M. B., Andorf, C. M., & Lübberstedt, T. (2019). Haplotype structure in commercial maize breeding programs in relation to key founder lines. Theoretical and Applied Genetics. https://doi.org/10.1007/s00122-019-03486-y

Edwards, J. (2011). Changes in plant morphology in response to recurrent selection in the Iowa StiffStalk Synthetic maize population. Crop Science, 51(6), 2352–2361. https://doi.org/10.2135/cropsci2010.09.0564

Endelman, J. B., & Jannink, J.-L. (2012). Shrinkage Estimation of the Realized Relationship Matrix. G3: Genes|Genomes|Genetics, 2(11), 1405–1413. https://doi.org/10.1534/g3.112.004259

Gerke, J. P., Edwards, J. W., Guill, K. E., Ross-Ibarra, J., & McMullen, M. D. (2015). The genomic impacts of drift and selection for hybrid performance in maize. Genetics, 201(3), 1201–1211. https://doi.org/10.1534/genetics.115.182410

Goudet, J. (2005). HIERFSTAT, a Package for R to compute and test hierarchical F-statistics. Molecular Ecology Notes, 2(5), 184–186. https://doi.org/10.1111/j.1471-8278

Gower, J. C., & Legendre, P. (1986). Metric and Euclidean properties of dissimilarity coefficients. Journal of Classification, 3(1), 5–48. https://doi.org/10.1007/BF01896809

Hagdorn, S., Lamkey, K. R., Frisch, M., Guimara, P. E. O., Melchinger, A. E., Corn, I., … Reid, P. (2003). Molecular Genetic Diversity among Progenitors and Derived Elite Lines of BSSS and BSCB1 Maize Populations. Crop Science, 43(1), 474–482.

Han, L., & Abney, M. (2013). Using identity by descent estimation with dense genotype data to detect positive selection. European Journal of Human Genetics, 21(2), 205–211. https://doi.org/10.1038/ejhg.2012.148

Han, L. and A. M. (2011). Identity by Descent Estimation With Dense Genome-Wide Genotype Data. Genetic Epidemiology, 2335(6), 557–567. https://doi.org/10.1002/gepi.20606.

Hill, W. G., & Weir, B. S. (1988). Variances and covariances of squared linkage disequilibria in finite populations. Theoretical Population Biology, 33(1), 54–78. https://doi.org/10.1016/0040-5809(88)90004-4

Hinze, L. L., Kresovich, S., Nason, J. D., & Lamkey, K. R. (2005). Population Genetic Diversity in a Maize Reciprocal Recurrent Selection Program, 1, 2435–2442. https://doi.org/10.2135/cropsci2004.0662

Holsinger, K. E., & Weir, B. S. (2009). Genetics in geographically structured populations: defining, estimating and interpreting F(ST). Nature Reviews. Genetics, 10(9), 639–650. https://doi.org/10.1038/nrg2611

Holthaus, J., & Lamkey, K. (1995). Response to selection and changes in genetic parameters for 13 plant and ear traits in two maize recurrent selection programs. Maydica, 40(4), 357–370.

Hospital, F., & Chevalet, C. (1993). Effects of population size and linkage on optimal selection intensity. Theoretical and Applied Genetics, 86(6), 775–780. https://doi.org/10.1007/BF00222669

Jiao, Y., Peluso, P., Shi, J., Liang, T., Stitzer, M. C., Wang, B., … Ware, D. (2017). Improved maize reference genome with single-molecule technologies. Nature, 546(7659), 524–527. https://doi.org/10.1038/nature22971

Kamvar, Z. N., Tabima, J. F., & Gŕunwald, N. J. (2014). Poppr: An R package for genetic analysis of populations with clonal, partially clonal, and/or sexual reproduction. PeerJ, 2013(1), 1–14. https://doi.org/10.7717/peerj.281

Keeratinijakal, V., & Lamkey, K. R. (1993). Responses to Reciprocal Recurrent Selection in BSSS and BSCB1 Maize Populations. Crop Science, 33(1), 73–77. https://doi.org/10.2135/cropsci1993.0011183x003300010012x

Keller, M. C., Visscher, P. M., & Goddard, M. E. (2011). Quantification of Inbreeding Due to Distant Ancestors and Its Detection Using Dense Single Nucleotide Polymorphism Data. Genetics, 189(1), 237–249. https://doi.org/10.1534/genetics.111.130922

Kilian, A., Wenzl, P., Huttner, E., Carling, J., Xia, L., Blois, H., … Uszynski, G. (2012). Diversity Arrays Technology: A Generic Genome Profiling Technology on Open Platforms (pp. 67–89). https://doi.org/10.1007/978-1-61779-870-2_5

Kirin, M., McQuillan, R., Franklin, C. S., Campbell, H., Mckeigue, P. M., & Wilson, J. F. (2010). Genomic runs of homozygosity record population history and consanguinity. PLoS ONE, 5(11), 1–7. https://doi.org/10.1371/journal.pone.0013996

Labate, J. A., Lamkey, K. R., Lee, M., & Woodman, W. L. (1999). Temporal changes in allele frequencies in two reciprocally selected maize populations. Theoretical and Applied Genetics, 99(7–8), 1166–1178. https://doi.org/10.1007/s001220051321

Labate, Joanne A, Lamkey, R., Lee, M., & Woodman, W. L. (1997). Molecular Genetic Diversity after Reciprocal Recurrent Selection in BSSS and BSCBI Maize Populations. Crop Science, (37), 416–423.

Letunic, I., & Bork, P. (2019). Interactive Tree Of Life (iTOL) v4: recent updates and new developments. Nucleic Acids Research, 47(W1), W256–W259. https://doi.org/10.1093/nar/gkz239

Lipka, A. E., Tian, F., Wang, Q., Peiffer, J., Li, M., Bradbury, P. J., … Zhang, Z. (2012). GAPIT: genome association and prediction integrated tool. Bioinformatics, 28(18), 2397–2399. https://doi.org/10.1093/bioinformatics/bts444

Maldonado, C., Mora, F., Scapim, C. A., & Coan, M. (2019). Genome-wide haplotype-based association analysis of key traits of plant lodging and architecture of maize identifies major determinants for leaf angle: hapLA4. PLOS ONE, 14(3), e0212925. https://doi.org/10.1371/journal.pone.0212925

McQuillan, R., Leutenegger, A. L., Abdel-Rahman, R., Franklin, C. S., Pericic, M., Barac-Lauc, L., … Wilson, J. F. (2008). Runs of Homozygosity in European Populations. American Journal of Human Genetics, 83(3), 359–372. https://doi.org/10.1016/j.ajhg.2008.08.007

Messmer, M. M., Melchinger, A. E., Lee, M., Woodman, W. L., Lee, E. A., & Lamkey, K. R. (1991). Genetic diversity among progenitors and elite lines from the Iowa Stiff Stalk Synthetic (BSSS) maize population: comparison of allozyme and RFLP data. Theoretical and Applied Genetics, 83(1), 97–107. https://doi.org/10.1007/BF00229231

Money, D., Gardner, K., Migicovsky, Z., Schwaninger, H., Zhong, G., & Myles, S. (2016). LinkImpute : Fast and Accurate Genotype Imputation for Non-Model LinkImpute : Fast and Accurate Genotype Imputation for Nonmodel Organisms, (January). https://doi.org/10.1534/g3.115.021667

Nagy, S., Poczai, P., Cernák, I., Gorji, A. M., Hegedűs, G., & Taller, J. (2012). PICcalc: An online program to calculate polymorphic information content for molecular genetic studies. Biochemical Genetics, 50(9–10), 670–672. https://doi.org/10.1007/s10528-012-9509-1

Nei, M. (1973). Analysis of gene diversity in subdivided populations. Proceedings of the National Academy of Sciences of the United States of America, 70(12), 3321–3323. https://doi.org/10.1073/pnas.70.12.3321

Nei, M. (1978). Estimation of average heterozygosity and genetic distance from a small number of individuals. Genetics, 89(3), 583–590.

Nelson, P. T., Coles, N. D., Holland, J. B., Bubeck, D. M., Smith, S., & Goodman, M. M. (2008). Molecular Characterization of Maize Inbreds with Expired U.S. Plant Variety Protection. Crop Science, 48(5), 1673–1685. https://doi.org/10.2135/cropsci2008.02.0092

Ogut, F., Bian, Y., Bradbury, P. J., & Holland, J. B. (2015). Joint-multiple family linkage analysis predicts within-family variation better than single-family analysis of the maize nested association mapping population. Heredity, 114(6), 552–563. https://doi.org/10.1038/hdy.2014.123

Ouborg, N. J., Piquot, Y., & Van Groenendael, J. M. (1999). Population genetics, molecular markers and the study of dispersal in plants. Journal of Ecology, 87(4), 551–568. https://doi.org/10.1046/j.1365-2745.1999.00389.x

Pace, J., Gardner, C., Romay, C., Ganapathysubramanian, B., & Lübberstedt, T. (2015). Genome-wide association analysis of seedling root development in maize (Zea mays L.). BMC Genomics, 16(1). https://doi.org/10.1186/s12864-015-1226-9

Paschou, P., Ziv, E., Burchard, E. G., Choudhry, S., Rodriguez-Cintron, W., Mahoney, M. W., & Drineas, P. (2007). PCA-correlated SNPs for structure identification in worldwide human populations. PLoS Genetics, 3(9), 1672–1686. https://doi.org/10.1371/journal.pgen.0030160

Price, A. L., Patterson, N. J., Plenge, R. M., Weinblatt, M. E., Shadick, N. A., & Reich, D. (2006). Principal components analysis corrects for stratification in genome-wide association studies. Nature Genetics, 38(8), 904–909. https://doi.org/10.1038/ng1847

R Core Team. (2019). R: A language and environment for statistical computing. R Foundation for Statistical Computing.

Romay, M. C., Flint-Garcia, S. A., Casstevens, T. M., Glaubitz, J. C., McMullen, M. D., Holland, J. B., … Buckler, E. S. (2013). Comprehensive genotyping of the USA national maize inbred seed bank. Genome Biology, 14(6). https://doi.org/10.1186/gb-2013-14-6-r55

Sanchez, D. L., Liu, S., Ibrahim, R., Blanco, M., & Lübberstedt, T. (2018). Genome-wide association studies of doubled haploid exotic introgression lines for root system architecture traits in maize (Zea mays L.). Plant Science. https://doi.org/10.1016/j.plantsci.2017.12.004

Schwarz, G. (1978). Estimating the Dimension of a Model. *The Annals of Statistics*, *6*(2), 461–464.

Shete, S., Tiwari, H., & Elston, R. C. (2000). On Estimating the Heterozygosity and Polymorphism Information Content Value. Theoretical Population Biology, 57(3), 265–271. https://doi.org/10.1006/tpbi.2000.1452

Smith, M., J., & Haigh, J. (1974). The hitch-hiking effect of a favourable gene. Genetics Research, 23, 23–35. https://doi.org/10.1017/S0016672308009579

Sprague, G. F. (1946). Early Testing of Inbred Lines of Corn. Journal of the American Society of Agronomy.

Sprague, G. F., & Jenkins, M. T. (1943). A Comparison of Synthetic Varieties, Multiple Crosses, and Double Crosses in Corn1. Agronomy Journal, 35(2), 137. https://doi.org/10.2134/agronj1943.00021962003500020007x

Sul, J. H., Martin, L. S., & Eskin, E. (2018). Population structure in genetic studies: Confounding factors and mixed models. PLoS Genetics, 14(12), 1–22. https://doi.org/10.1371/journal.pgen.1007309

Vanous, A., Gardner, C., Blanco, M., Martin-Schwarze, A., Lipka, A. E., Flint-Garcia, S., … Lübberstedt, T. (2018). Association Mapping of Flowering and Height Traits in Germplasm Enhancement of Maize Doubled Haploid (GEM-DH) Lines. The Plant Genome, 11(2), 0. https://doi.org/10.3835/plantgenome2017.09.0083

Vanous, K., Vanous, A., Frei, U. K., & Lübberstedt, T. (2017). Generation of Maize ( Zea mays ) Doubled Haploids via Traditional Methods. Current Protocols in Plant Biology, 147–157. https://doi.org/10.1002/cppb.20050

Wang, J. (2014). Marker-based estimates of relatedness and inbreeding coefficients: an assessment of current methods. Journal of Evolutionary Biology, 27(3), 518–530. https://doi.org/10.1111/jeb.12315

Weir, B. S., & Cockerham, C. C. (1984). Estimating F-Statistics for the Analysis of Population Structure. Evolution, 38(6), 1358. https://doi.org/10.2307/2408641

Won, S., Park, J.-E., Son, J.-H., Lee, S.-H., Park, B. H., Park, M., … Lim, D. (2020). Genomic Prediction Accuracy Using Haplotypes Defined by Size and Hierarchical Clustering Based on Linkage Disequilibrium. Frontiers in Genetics, 11. https://doi.org/10.3389/fgene.2020.00134

Wright, S. (1922). Coefficients of inbreeding and relationship. The American Naturalist, (56), 330–338.

Wright, S. (1951). The genetical structure of populations. Annals of Eugenics, 15, 323–354.

Wu, Y., San Vicente, F., Huang, K., Dhliwayo, T., Costich, D. E., Semagn, K., … Babu, R. (2016). Molecular characterization of CIMMYT maize inbred lines with genotyping-by-sequencing SNPs. Theoretical and Applied Genetics, 129(4), 753–765. https://doi.org/10.1007/s00122-016-2664-8

Yu, J., Pressoir, G., Briggs, W. H., Bi, I. V., Yamasaki, M., Doebley, J. F., … Buckler, E. S. (2006). A unified mixed-model method for association mapping that accounts for multiple levels of relatedness. Nature Genetics, 38(2), 203–208. https://doi.org/10.1038/ng1702

## Appendix: Supplemental Table

**Supplemental Table S2.1**. Mean genetic contribution of the BSSS progenitors to each DH lines estimated using high-resolution detection of IBD segments.

| DH Line | A3G-3-3-1-3 | CI 540 | Fe (Parent of F1B1) | I-159 | IL1 2E | B2 (Parent of F1B1) | Oh 3167 B | Os 420 | Tr 9-1-1-6 | WD 456 | I224 | LE 23 | 461 | Hy | AH 83 | Non-IBD |
|---|---|---|---|---|---|---|---|---|---|---|---|---|---|---|---|---|
| C0_DH001 | 0.98 | 4.58 | 5.22 | 3.45 | 3.69 | 4.00 | 5.00 | 3.54 | 3.34 | 5.35 | 3.13 | 3.35 | 2.80 | 5.61 | 1.74 | 44.23 |
| C0_DH002 | 1.05 | 2.54 | 4.32 | 1.79 | 4.88 | 2.04 | 5.82 | 4.27 | 3.57 | 4.37 | 4.41 | 4.88 | 2.46 | 3.00 | 1.48 | 49.13 |
| C0_DH004 | 0.43 | 4.67 | 3.06 | 2.14 | 3.56 | 2.26 | 4.98 | 3.84 | 5.41 | 7.48 | 4.07 | 3.58 | 3.07 | 6.74 | 3.07 | 41.63 |
| C0_DH005 | 0.83 | 2.48 | 5.18 | 2.67 | 4.16 | 1.90 | 9.76 | 5.80 | 7.94 | 4.58 | 4.33 | 3.82 | 3.32 | 5.35 | 2.11 | 35.78 |
| C0_DH006 | 0.90 | 4.77 | 3.72 | 3.49 | 5.00 | 1.99 | 6.82 | 4.39 | 5.57 | 3.95 | 5.49 | 5.36 | 3.56 | 4.28 | 2.68 | 38.02 |
| C0_DH007 | 0.62 | 2.55 | 7.72 | 2.75 | 3.57 | 2.43 | 7.69 | 4.20 | 6.99 | 4.57 | 3.73 | 2.75 | 4.28 | 4.58 | 1.37 | 40.20 |
| C0_DH008 | 1.14 | 3.36 | 4.44 | 2.30 | 4.25 | 2.35 | 5.23 | 8.59 | 4.47 | 5.20 | 3.85 | 3.32 | 2.66 | 5.47 | 1.96 | 41.42 |
| C0_DH010 | 0.94 | 2.71 | 6.19 | 2.25 | 3.87 | 2.21 | 5.82 | 5.27 | 6.29 | 3.54 | 3.88 | 4.60 | 3.34 | 3.80 | 1.96 | 43.31 |
| C0_DH011 | 1.04 | 2.48 | 4.58 | 3.23 | 4.70 | 3.45 | 6.25 | 3.80 | 4.84 | 4.94 | 4.95 | 4.37 | 2.49 | 6.81 | 2.29 | 39.79 |
| C0_DH013 | 1.14 | 1.89 | 3.84 | 1.83 | 4.12 | 2.35 | 8.94 | 3.66 | 3.35 | 3.75 | 4.09 | 2.00 | 3.26 | 9.30 | 1.95 | 44.54 |
| C0_DH014 | 0.99 | 2.67 | 3.96 | 2.46 | 3.73 | 2.19 | 5.96 | 6.58 | 5.55 | 5.50 | 3.98 | 5.12 | 3.15 | 7.97 | 2.07 | 38.12 |
| C0_DH015 | 1.05 | 2.47 | 5.03 | 3.52 | 4.97 | 3.21 | 6.95 | 4.46 | 6.19 | 7.02 | 5.12 | 3.30 | 2.77 | 5.79 | 1.75 | 36.41 |
| C0_DH016 | 1.22 | 4.86 | 4.68 | 2.72 | 4.03 | 1.73 | 7.23 | 4.86 | 5.50 | 4.96 | 4.30 | 5.09 | 2.90 | 6.77 | 2.59 | 36.57 |
| C0_DH017 | 0.64 | 2.92 | 2.02 | 2.32 | 6.75 | 2.94 | 6.58 | 4.47 | 5.20 | 6.00 | 5.59 | 8.14 | 3.23 | 4.75 | 2.39 | 36.05 |
| C0_DH018 | 1.02 | 2.21 | 4.00 | 2.55 | 4.64 | 2.04 | 8.15 | 6.59 | 4.86 | 6.22 | 4.12 | 3.54 | 2.37 | 5.57 | 1.97 | 40.16 |
| C0_DH019 | 0.87 | 2.08 | 1.74 | 2.73 | 5.37 | 3.00 | 5.27 | 4.95 | 5.63 | 5.28 | 6.06 | 5.64 | 3.04 | 4.87 | 2.36 | 41.11 |
| C0_DH020 | 0.96 | 4.49 | 3.22 | 2.92 | 3.95 | 2.78 | 5.72 | 3.31 | 7.57 | 7.34 | 4.03 | 3.90 | 4.03 | 5.96 | 2.45 | 37.39 |
| C0_DH021 | 1.34 | 3.58 | 5.11 | 2.89 | 4.12 | 2.82 | 7.40 | 3.80 | 7.68 | 4.64 | 4.10 | 2.45 | 3.24 | 5.29 | 2.03 | 39.52 |
| C0_DH022 | 0.80 | 4.87 | 5.78 | 3.76 | 3.64 | 2.46 | 4.82 | 4.39 | 6.17 | 7.53 | 3.93 | 3.84 | 3.22 | 3.59 | 2.31 | 38.90 |
| C0_DH023 | 1.06 | 5.10 | 6.77 | 2.74 | 4.23 | 2.93 | 4.94 | 4.81 | 2.47 | 4.86 | 4.17 | 3.30 | 4.35 | 3.18 | 1.98 | 43.12 |
| C0_DH024 | 0.66 | 2.67 | 5.58 | 3.41 | 3.61 | 2.71 | 3.70 | 2.41 | 6.03 | 7.74 | 3.55 | 5.80 | 4.34 | 5.73 | 2.18 | 39.88 |
| C0_DH025 | 1.11 | 2.31 | 4.52 | 3.19 | 4.35 | 3.03 | 3.06 | 5.84 | 5.00 | 6.02 | 3.98 | 5.51 | 2.88 | 7.46 | 2.23 | 39.50 |
| C0_DH026 | 0.90 | 3.31 | 3.41 | 2.18 | 3.25 | 3.88 | 5.47 | 3.12 | 5.09 | 4.43 | 2.82 | 7.53 | 3.48 | 8.75 | 1.60 | 40.78 |
| C0_DH027 | 1.21 | 4.14 | 4.72 | 2.48 | 4.14 | 1.58 | 6.97 | 4.65 | 6.19 | 4.88 | 4.34 | 4.73 | 2.64 | 6.82 | 2.75 | 37.75 |
| C0_DH028 | 0.92 | 4.45 | 3.25 | 2.74 | 3.89 | 2.56 | 5.42 | 3.33 | 7.59 | 7.28 | 4.36 | 4.12 | 3.91 | 5.52 | 2.47 | 38.20 |
| C0_DH029 | 1.23 | 2.02 | 4.99 | 2.62 | 5.28 | 2.26 | 3.90 | 4.85 | 7.00 | 4.85 | 5.63 | 4.05 | 4.72 | 3.83 | 1.45 | 41.31 |
| C0_DH032 | 0.34 | 4.18 | 1.67 | 2.62 | 4.94 | 2.66 | 4.04 | 5.66 | 7.34 | 8.15 | 5.07 | 4.30 | 5.12 | 6.43 | 1.99 | 35.48 |
| C0_DH033 | 0.79 | 3.20 | 6.06 | 2.44 | 4.42 | 1.95 | 4.22 | 4.65 | 5.41 | 5.94 | 4.24 | 4.50 | 4.39 | 4.54 | 1.74 | 41.49 |
| C0_DH034 | 0.61 | 2.05 | 5.48 | 3.87 | 2.10 | 2.22 | 6.34 | 3.07 | 11.20 | 7.00 | 1.93 | 5.60 | 4.66 | 3.80 | 1.76 | 38.29 |
| C0_DH035 | 0.65 | 3.41 | 4.01 | 2.23 | 4.17 | 1.84 | 6.80 | 3.45 | 2.75 | 3.68 | 3.92 | 4.63 | 2.82 | 2.44 | 1.94 | 51.24 |
| C0_DH036 | 0.81 | 3.15 | 4.48 | 2.97 | 3.18 | 2.08 | 7.40 | 2.99 | 5.75 | 8.91 | 3.23 | 3.20 | 3.37 | 5.55 | 1.62 | 41.32 |
| C0_DH037 | 0.96 | 3.88 | 3.92 | 2.18 | 4.97 | 2.79 | 3.34 | 4.44 | 6.66 | 5.78 | 4.76 | 5.05 | 3.72 | 5.22 | 1.98 | 40.36 |
| C0_DH038 | 1.03 | 4.12 | 5.82 | 3.17 | 2.55 | 2.21 | 9.57 | 7.16 | 5.70 | 4.57 | 2.30 | 4.15 | 2.81 | 5.71 | 1.95 | 37.17 |

Table S2.1. Continued

| DH Line | A3G-3-3-1-3 | CI 540 | Fe (Parent of F1B1) | I-159 | IL1 2E | B2 (Parent of F1B1) | Oh 3167 B | Os 420 | Tr 9-1-1-6 | WD 456 | I224 | LE 23 | 461 | Hy | AH 83 | Non-IBD |
|---|---|---|---|---|---|---|---|---|---|---|---|---|---|---|---|---|
| C0_DH039 | 0.94 | 4.08 | 4.36 | 3.13 | 2.85 | 2.82 | 3.64 | 3.97 | 4.02 | 5.45 | 2.81 | 5.71 | 4.08 | 6.11 | 2.49 | 43.56 |
| C0_DH040 | 0.45 | 2.18 | 2.73 | 1.75 | 4.19 | 2.64 | 2.70 | 5.38 | 5.19 | 7.99 | 4.46 | 4.52 | 2.95 | 6.51 | 1.65 | 44.70 |
| C0_DH041 | 0.82 | 3.13 | 4.02 | 2.08 | 2.84 | 2.86 | 6.50 | 3.55 | 7.39 | 7.68 | 2.94 | 5.02 | 4.89 | 4.95 | 2.31 | 39.02 |
| C0_DH042 | 0.88 | 2.43 | 4.98 | 2.27 | 3.90 | 1.99 | 8.34 | 2.82 | 6.64 | 5.82 | 3.67 | 5.28 | 2.46 | 7.78 | 1.68 | 39.06 |
| C0_DH043 | 0.57 | 3.52 | 4.09 | 2.65 | 3.87 | 2.84 | 7.37 | 4.05 | 5.30 | 4.85 | 3.70 | 5.63 | 3.52 | 5.61 | 1.71 | 40.73 |
| C0_DH044 | 0.81 | 5.48 | 4.33 | 3.11 | 6.48 | 2.03 | 4.82 | 3.01 | 4.93 | 4.77 | 6.04 | 4.46 | 4.11 | 6.27 | 2.25 | 37.09 |
| C0_DH045 | 1.31 | 5.98 | 4.57 | 3.48 | 4.00 | 2.86 | 6.76 | 3.37 | 5.15 | 4.37 | 4.10 | 3.81 | 2.51 | 6.37 | 1.65 | 39.71 |
| C0_DH046 | 0.43 | 3.59 | 3.97 | 2.74 | 4.06 | 2.80 | 7.22 | 4.20 | 5.29 | 4.52 | 3.82 | 5.36 | 3.18 | 5.62 | 1.65 | 41.55 |
| C0_DH047 | 0.88 | 2.63 | 2.58 | 2.78 | 2.58 | 3.12 | 7.44 | 7.71 | 5.60 | 7.11 | 2.84 | 4.48 | 4.36 | 7.81 | 1.93 | 36.15 |
| C0_DH048 | 0.92 | 3.60 | 2.98 | 2.60 | 4.37 | 1.82 | 6.60 | 3.55 | 5.77 | 5.63 | 4.33 | 3.04 | 4.84 | 3.98 | 2.12 | 43.84 |
| C0_DH049 | 1.02 | 3.82 | 3.84 | 2.49 | 3.88 | 2.51 | 4.96 | 3.95 | 5.74 | 4.40 | 4.41 | 7.18 | 3.96 | 2.85 | 2.21 | 42.78 |
| C0_DH050 | 0.65 | 4.02 | 4.09 | 1.74 | 4.42 | 2.56 | 6.05 | 4.92 | 5.68 | 4.92 | 4.60 | 5.09 | 2.27 | 4.03 | 1.74 | 43.21 |
| C0_DH051 | 1.10 | 5.03 | 3.46 | 2.28 | 3.61 | 3.33 | 3.85 | 7.09 | 3.75 | 6.35 | 3.67 | 4.20 | 4.59 | 5.16 | 2.20 | 40.35 |
| C0_DH052 | 1.13 | 2.41 | 4.74 | 2.58 | 4.38 | 2.29 | 6.51 | 6.02 | 4.92 | 4.30 | 4.07 | 3.76 | 2.44 | 5.40 | 2.33 | 42.73 |
| C0_DH053 | 1.06 | 5.76 | 3.84 | 2.84 | 4.00 | 2.49 | 4.67 | 5.54 | 3.15 | 3.96 | 3.79 | 4.32 | 4.09 | 6.80 | 2.26 | 41.42 |
| C0_DH054 | 1.06 | 2.06 | 3.51 | 1.56 | 4.40 | 1.87 | 9.66 | 2.44 | 7.17 | 6.78 | 4.66 | 4.15 | 3.63 | 4.28 | 1.37 | 41.40 |
| C0_DH055 | 0.86 | 4.78 | 7.40 | 2.86 | 4.36 | 1.73 | 4.09 | 4.31 | 6.67 | 3.85 | 4.18 | 5.67 | 5.07 | 3.44 | 2.29 | 38.42 |
| C0_DH056 | 1.09 | 2.96 | 5.15 | 2.33 | 3.86 | 2.34 | 7.46 | 5.60 | 5.66 | 4.21 | 4.27 | 5.03 | 4.10 | 5.92 | 1.79 | 38.23 |
| C0_DH058 | 0.57 | 5.49 | 4.40 | 2.85 | 2.14 | 1.34 | 7.86 | 3.45 | 6.55 | 3.78 | 2.38 | 5.55 | 4.96 | 3.91 | 2.22 | 42.56 |
| C0_DH059 | 0.40 | 2.89 | 5.49 | 2.37 | 4.23 | 2.43 | 10.33 | 5.16 | 4.75 | 4.37 | 3.74 | 3.75 | 2.55 | 4.51 | 1.57 | 41.45 |
| C0_DH060 | 0.76 | 3.92 | 5.86 | 3.62 | 3.64 | 2.58 | 3.09 | 2.97 | 8.46 | 7.70 | 4.02 | 6.04 | 3.34 | 4.47 | 1.89 | 37.65 |
| C0_DH061 | 0.96 | 6.51 | 4.43 | 4.07 | 3.15 | 2.22 | 3.69 | 3.84 | 4.00 | 6.65 | 2.97 | 6.69 | 4.24 | 3.85 | 2.36 | 40.37 |
| C0_DH062 | 1.27 | 5.24 | 4.08 | 2.23 | 3.90 | 2.10 | 5.86 | 7.24 | 5.81 | 9.03 | 4.24 | 6.65 | 2.92 | 3.18 | 2.14 | 34.12 |
| C0_DH063 | 1.25 | 2.78 | 4.10 | 3.11 | 4.69 | 3.45 | 4.21 | 4.15 | 7.55 | 4.49 | 4.90 | 3.92 | 4.29 | 6.66 | 1.94 | 38.49 |
| C0_DH064 | 1.15 | 2.33 | 4.60 | 2.24 | 4.13 | 2.42 | 3.17 | 7.75 | 4.41 | 5.18 | 4.05 | 4.20 | 3.66 | 6.14 | 2.48 | 42.07 |
| C0_DH065 | 1.05 | 4.58 | 3.99 | 4.25 | 6.65 | 1.99 | 6.83 | 4.10 | 6.38 | 3.58 | 6.64 | 3.14 | 4.43 | 5.11 | 1.58 | 35.72 |
| C0_DH066 | 0.96 | 3.98 | 4.29 | 3.22 | 3.86 | 2.62 | 4.27 | 4.22 | 4.67 | 3.79 | 3.56 | 7.09 | 2.69 | 3.64 | 2.30 | 44.84 |
| C0_DH067 | 1.00 | 2.36 | 6.38 | 3.10 | 5.30 | 2.55 | 5.69 | 3.35 | 8.13 | 7.94 | 5.16 | 3.22 | 2.04 | 4.00 | 1.16 | 38.63 |
| C0_DH068 | 0.52 | 4.60 | 2.61 | 3.59 | 3.03 | 1.91 | 7.97 | 4.43 | 4.21 | 4.90 | 2.70 | 3.54 | 3.31 | 4.45 | 2.20 | 46.05 |
| C0_DH069 | 1.08 | 3.34 | 7.39 | 3.61 | 3.23 | 3.91 | 6.36 | 4.86 | 3.82 | 5.99 | 3.75 | 4.52 | 4.04 | 5.66 | 2.28 | 36.15 |
| C0_DH071 | 1.25 | 2.99 | 5.65 | 2.71 | 4.53 | 2.64 | 3.46 | 6.86 | 3.51 | 5.73 | 4.56 | 7.11 | 3.86 | 4.82 | 2.47 | 37.86 |
| C0_DH072 | 0.70 | 5.75 | 4.65 | 3.72 | 3.65 | 2.89 | 3.49 | 2.05 | 3.66 | 4.39 | 3.54 | 5.95 | 3.59 | 8.71 | 2.27 | 40.99 |
| C0_DH073 | 1.00 | 4.43 | 8.24 | 3.97 | 3.00 | 2.36 | 8.76 | 4.63 | 4.08 | 4.85 | 2.99 | 4.01 | 4.43 | 2.51 | 2.20 | 38.55 |
| C0_DH075 | 1.04 | 2.88 | 5.10 | 3.15 | 4.26 | 2.99 | 8.22 | 3.60 | 4.78 | 5.55 | 4.43 | 3.37 | 4.21 | 4.37 | 2.16 | 39.90 |
| C0_DH076 | 0.89 | 1.63 | 6.10 | 2.87 | 4.51 | 1.66 | 4.83 | 4.29 | 6.93 | 6.22 | 4.14 | 5.89 | 6.09 | 3.55 | 1.74 | 38.66 |

Table S2.1. Continued

| DH Line | A3G-3-3-1-3 | CI 540 | Fe (Parent of F1B1) | I-159 | IL1 2E | B2 (Parent of F1B1) | Oh 3167 B | Os 420 | Tr 9-1-1-6 | WD 456 | I224 | LE 23 | 461 | Hy | AH 83 | Non-IBD |
|---|---|---|---|---|---|---|---|---|---|---|---|---|---|---|---|---|
| C0_DH077 | 1.06 | 3.15 | 7.09 | 2.83 | 4.19 | 2.54 | 5.50 | 2.96 | 7.75 | 7.14 | 3.95 | 3.98 | 3.98 | 4.12 | 1.99 | 37.78 |
| C0_DH078 | 0.52 | 5.75 | 5.59 | 4.34 | 2.94 | 2.38 | 6.17 | 3.53 | 6.64 | 4.31 | 2.93 | 3.91 | 2.16 | 4.59 | 2.10 | 42.12 |
| C0_DH080 | 0.53 | 4.33 | 4.64 | 3.11 | 5.42 | 2.36 | 4.61 | 4.18 | 2.13 | 4.57 | 5.04 | 6.79 | 3.56 | 3.29 | 2.44 | 42.99 |
| C0_DH081 | 1.43 | 5.62 | 3.38 | 2.45 | 3.51 | 1.73 | 6.97 | 3.26 | 3.42 | 6.44 | 3.51 | 5.30 | 3.42 | 4.82 | 2.61 | 42.14 |
| C0_DH082 | 0.98 | 3.65 | 3.57 | 2.87 | 3.98 | 2.92 | 4.84 | 3.69 | 5.82 | 6.58 | 3.99 | 3.90 | 2.89 | 6.17 | 1.93 | 42.22 |
| C0_DH083 | 0.81 | 2.59 | 6.46 | 2.43 | 4.23 | 2.15 | 9.17 | 2.66 | 6.94 | 6.19 | 4.40 | 4.38 | 3.17 | 3.53 | 2.07 | 38.82 |
| C0_DH085 | 1.11 | 3.61 | 5.34 | 3.54 | 3.09 | 2.84 | 3.59 | 5.57 | 5.12 | 4.82 | 3.38 | 4.28 | 2.47 | 7.95 | 2.24 | 41.05 |
| C0_DH086 | 0.77 | 3.53 | 5.47 | 2.36 | 2.52 | 1.99 | 5.04 | 4.77 | 8.55 | 7.75 | 2.80 | 3.84 | 4.29 | 6.51 | 2.30 | 37.50 |
| C0_DH087 | 0.80 | 5.65 | 4.66 | 2.71 | 4.43 | 3.18 | 6.88 | 3.60 | 3.94 | 4.92 | 4.75 | 4.05 | 2.65 | 4.25 | 1.86 | 41.65 |
| C0_DH088 | 0.96 | 1.85 | 3.90 | 3.40 | 3.96 | 2.00 | 6.37 | 6.06 | 3.71 | 9.57 | 4.42 | 6.29 | 3.59 | 4.17 | 1.98 | 37.77 |
| C0_DH089 | 1.36 | 3.25 | 4.97 | 4.46 | 4.42 | 2.67 | 4.34 | 3.63 | 9.26 | 7.42 | 4.38 | 2.78 | 2.84 | 5.60 | 1.66 | 36.96 |
| C0_DH090 | 1.00 | 2.66 | 5.90 | 3.02 | 5.21 | 1.94 | 5.94 | 3.56 | 3.47 | 3.97 | 4.74 | 5.27 | 2.66 | 7.17 | 2.33 | 41.16 |
| C0_DH091 | 0.83 | 4.02 | 4.52 | 2.84 | 2.91 | 2.32 | 7.00 | 4.70 | 6.92 | 7.24 | 3.05 | 5.55 | 3.53 | 6.39 | 1.38 | 36.79 |
| C0_DH092 | 1.10 | 2.88 | 4.09 | 2.88 | 4.32 | 2.53 | 4.42 | 6.85 | 5.58 | 4.99 | 4.52 | 4.01 | 3.80 | 5.96 | 2.12 | 39.95 |
| C0_DH093 | 0.80 | 3.42 | 5.94 | 3.16 | 4.25 | 2.64 | 6.17 | 3.88 | 5.86 | 5.19 | 4.26 | 3.76 | 3.01 | 4.88 | 1.61 | 41.19 |
| C0_DH094 | 0.75 | 3.34 | 5.74 | 3.35 | 4.44 | 2.62 | 5.83 | 3.89 | 5.84 | 5.80 | 4.36 | 3.45 | 3.16 | 4.96 | 1.55 | 40.93 |
| C0_DH095 | 1.05 | 3.22 | 3.87 | 3.04 | 3.83 | 2.34 | 7.68 | 5.72 | 6.93 | 7.28 | 4.42 | 2.86 | 3.53 | 3.93 | 2.64 | 37.65 |
| C0_DH096 | 1.16 | 4.52 | 4.50 | 4.17 | 4.30 | 1.69 | 7.01 | 3.38 | 4.94 | 7.36 | 4.51 | 6.56 | 4.00 | 4.34 | 1.84 | 35.73 |
| C0_DH098 | 0.79 | 3.02 | 3.80 | 2.55 | 5.18 | 1.81 | 6.53 | 3.27 | 4.64 | 4.07 | 5.01 | 5.24 | 3.24 | 5.26 | 2.80 | 42.79 |
| C0_DH099 | 0.69 | 4.46 | 3.23 | 2.44 | 5.42 | 1.85 | 5.59 | 7.63 | 4.75 | 6.76 | 4.79 | 4.08 | 4.97 | 6.25 | 2.26 | 34.82 |
| C0_DH100 | 0.87 | 2.40 | 3.99 | 3.14 | 3.45 | 3.73 | 7.43 | 6.40 | 6.88 | 7.41 | 3.71 | 2.90 | 4.05 | 4.07 | 1.85 | 37.72 |
| C0_DH102 | 1.06 | 3.19 | 4.84 | 2.19 | 4.61 | 2.42 | 4.16 | 6.42 | 3.42 | 5.02 | 4.01 | 3.85 | 3.25 | 7.10 | 1.58 | 42.87 |
| C0_DH103 | 1.10 | 1.92 | 5.20 | 3.48 | 3.71 | 3.68 | 3.56 | 4.36 | 6.52 | 8.40 | 3.31 | 4.20 | 3.22 | 6.83 | 1.67 | 38.84 |
| C0_DH104 | 0.61 | 3.55 | 5.44 | 4.13 | 3.92 | 2.39 | 4.32 | 4.34 | 5.99 | 8.86 | 3.27 | 7.62 | 3.45 | 3.70 | 2.13 | 36.27 |
| C0_DH106 | 0.76 | 2.69 | 4.09 | 2.77 | 3.89 | 2.16 | 6.41 | 5.61 | 5.15 | 6.18 | 3.82 | 4.49 | 3.45 | 5.19 | 1.49 | 41.85 |
| C0_DH107 | 0.76 | 2.98 | 2.48 | 3.40 | 3.76 | 2.51 | 5.56 | 9.38 | 4.44 | 8.38 | 4.27 | 3.74 | 5.76 | 8.14 | 1.89 | 32.56 |
| C0_DH108 | 1.18 | 1.60 | 4.42 | 2.97 | 4.20 | 2.91 | 3.16 | 5.80 | 4.76 | 6.03 | 3.94 | 3.66 | 2.74 | 8.22 | 2.21 | 42.20 |
| C0_DH109 | 1.07 | 2.11 | 5.10 | 2.18 | 2.89 | 1.75 | 7.05 | 6.00 | 5.19 | 11.20 | 3.15 | 4.62 | 4.57 | 3.97 | 1.57 | 37.58 |
| C0_DH110 | 0.73 | 1.82 | 5.27 | 3.88 | 3.26 | 3.25 | 5.50 | 4.40 | 4.69 | 3.62 | 3.41 | 3.97 | 2.39 | 7.50 | 1.88 | 44.42 |
| C0_DH111 | 1.34 | 5.31 | 2.32 | 4.07 | 3.33 | 2.44 | 5.25 | 3.40 | 6.15 | 8.26 | 3.12 | 7.57 | 4.12 | 4.97 | 1.93 | 36.43 |
| C0_DH112 | 0.82 | 3.54 | 3.73 | 3.46 | 4.98 | 1.82 | 7.12 | 6.26 | 7.63 | 4.22 | 5.07 | 2.55 | 5.23 | 3.99 | 2.14 | 37.44 |
| C0_DH114 | 0.29 | 2.58 | 6.11 | 2.45 | 2.96 | 2.72 | 5.98 | 3.33 | 4.29 | 8.90 | 3.40 | 7.87 | 2.99 | 7.03 | 2.71 | 36.40 |
| C0_DH115 | 0.70 | 1.82 | 6.23 | 3.32 | 3.51 | 3.16 | 3.60 | 3.94 | 7.70 | 7.99 | 3.68 | 2.94 | 2.69 | 6.15 | 2.61 | 39.95 |
| C0_DH116 | 1.02 | 3.29 | 5.93 | 1.81 | 4.40 | 2.42 | 5.33 | 4.34 | 3.26 | 5.17 | 4.08 | 4.99 | 3.09 | 2.04 | 1.62 | 47.22 |
| C0_DH117 | 0.61 | 2.06 | 3.57 | 2.69 | 2.37 | 2.37 | 2.57 | 6.46 | 6.27 | 5.41 | 2.14 | 7.28 | 3.67 | 5.02 | 1.73 | 45.78 |

Table S2.1. Continued

| DH Line | A3G-3-3-1-3 | CI 540 | Fe (Parent of F1B1) | I-159 | IL1 2E | B2 (Parent of F1B1) | Oh 3167 B | Os 420 | Tr 9-1-1-6 | WD 456 | I224 | LE 23 | 461 | Hy | AH 83 | Non-IBD |
|---|---|---|---|---|---|---|---|---|---|---|---|---|---|---|---|---|
| C0_DH118 | 0.59 | 2.88 | 4.67 | 3.21 | 2.79 | 2.56 | 5.27 | 7.79 | 9.63 | 2.85 | 3.02 | 5.70 | 4.00 | 7.37 | 2.26 | 35.41 |
| C0_DH119 | 0.40 | 5.90 | 6.41 | 3.86 | 4.18 | 2.17 | 4.15 | 4.84 | 2.83 | 4.09 | 3.74 | 8.00 | 3.71 | 3.35 | 1.76 | 40.61 |
| C0_DH120 | 0.56 | 1.38 | 5.76 | 2.09 | 3.25 | 2.63 | 7.38 | 4.36 | 2.88 | 7.63 | 3.33 | 6.85 | 2.28 | 6.34 | 2.50 | 40.79 |
| C0_DH121 | 1.04 | 2.21 | 2.56 | 2.29 | 4.47 | 3.47 | 6.21 | 4.99 | 3.19 | 4.69 | 4.35 | 4.91 | 4.21 | 6.82 | 2.34 | 42.27 |
| C0_DH122 | 1.15 | 3.79 | 5.70 | 3.98 | 3.75 | 2.63 | 4.65 | 3.12 | 5.88 | 7.43 | 3.67 | 6.22 | 4.03 | 5.22 | 2.15 | 36.63 |
| C0_DH123 | 0.92 | 5.56 | 3.09 | 2.53 | 5.58 | 2.24 | 4.15 | 5.28 | 6.87 | 4.77 | 5.57 | 3.30 | 3.63 | 5.75 | 1.77 | 39.00 |
| C0_DH124 | 0.76 | 2.55 | 5.03 | 2.27 | 5.17 | 2.38 | 3.41 | 4.19 | 4.35 | 4.88 | 5.79 | 3.86 | 2.06 | 5.34 | 1.49 | 46.47 |
| C0_DH125 | 1.09 | 2.76 | 5.11 | 2.61 | 3.42 | 2.83 | 7.09 | 6.85 | 6.15 | 6.03 | 3.69 | 2.31 | 4.61 | 6.25 | 2.47 | 36.73 |
| C0_DH127 | 0.83 | 2.70 | 3.55 | 2.06 | 3.71 | 2.11 | 3.20 | 4.90 | 6.56 | 4.24 | 4.36 | 3.83 | 3.16 | 8.48 | 1.85 | 44.46 |
| C0_DH128 | 1.58 | 4.29 | 6.03 | 2.06 | 3.16 | 3.34 | 6.98 | 2.67 | 6.20 | 4.41 | 3.02 | 4.19 | 3.95 | 6.35 | 2.35 | 39.43 |
| C0_DH130 | 0.96 | 2.09 | 4.16 | 2.87 | 4.53 | 3.11 | 3.09 | 2.48 | 5.25 | 6.20 | 4.79 | 7.31 | 3.10 | 8.72 | 2.33 | 39.01 |
| C0_DH131 | 0.98 | 6.42 | 4.70 | 2.68 | 4.38 | 2.09 | 6.60 | 3.63 | 5.99 | 3.27 | 5.06 | 5.93 | 3.93 | 5.39 | 2.62 | 36.33 |
| C0_DH132 | 0.74 | 2.13 | 1.97 | 1.92 | 5.39 | 1.84 | 12.78 | 5.23 | 5.61 | 6.31 | 5.60 | 3.73 | 1.84 | 4.70 | 1.88 | 38.34 |
| C0_DH133 | 1.02 | 2.91 | 2.17 | 3.20 | 3.37 | 1.84 | 6.38 | 3.72 | 5.30 | 6.65 | 3.23 | 4.53 | 3.72 | 6.45 | 1.36 | 44.15 |
| C0_DH134 | 1.06 | 2.28 | 7.31 | 3.22 | 3.49 | 3.12 | 3.66 | 3.24 | 7.03 | 3.51 | 3.63 | 3.53 | 3.04 | 7.56 | 1.75 | 42.57 |
| C0_DH135 | 1.36 | 7.27 | 8.72 | 2.42 | 3.32 | 2.33 | 2.51 | 5.40 | 7.41 | 5.03 | 3.47 | 2.95 | 3.94 | 5.52 | 1.63 | 36.72 |
| C0_DH136 | 0.61 | 4.13 | 4.65 | 4.48 | 3.84 | 3.22 | 7.93 | 6.02 | 5.11 | 4.16 | 4.45 | 3.82 | 1.96 | 8.33 | 2.05 | 35.27 |
| C0_DH137 | 0.44 | 3.70 | 4.39 | 2.83 | 3.95 | 1.97 | 11.48 | 4.48 | 4.74 | 6.61 | 4.03 | 3.27 | 3.32 | 5.74 | 1.38 | 37.67 |
| C0_DH138 | 1.22 | 4.71 | 5.67 | 3.43 | 2.75 | 1.71 | 4.44 | 6.03 | 3.98 | 4.44 | 2.84 | 3.72 | 4.24 | 3.69 | 1.62 | 45.50 |
| C0_DH139 | 1.02 | 3.24 | 4.46 | 2.07 | 3.10 | 2.60 | 7.44 | 4.23 | 6.33 | 5.65 | 3.00 | 6.65 | 2.48 | 7.44 | 2.31 | 37.99 |
| C0_DH140 | 0.70 | 2.84 | 2.40 | 3.52 | 3.11 | 2.14 | 7.01 | 6.01 | 5.25 | 8.14 | 3.21 | 3.80 | 5.46 | 7.20 | 2.02 | 37.21 |
| C0_DH141 | 1.08 | 2.93 | 6.78 | 3.97 | 2.43 | 1.95 | 6.51 | 5.06 | 5.80 | 5.72 | 2.86 | 4.59 | 3.71 | 4.51 | 2.12 | 39.97 |
| C0_DH143 | 0.89 | 3.35 | 5.24 | 2.17 | 2.92 | 3.07 | 4.38 | 5.09 | 7.64 | 7.06 | 2.73 | 5.93 | 1.81 | 4.03 | 2.00 | 41.70 |
| C0_DH144 | 1.19 | 3.42 | 3.35 | 1.89 | 2.80 | 1.67 | 7.70 | 6.57 | 5.17 | 4.20 | 2.89 | 5.92 | 3.89 | 8.37 | 1.60 | 39.38 |
| C0_DH145 | 0.95 | 1.50 | 8.28 | 3.37 | 3.51 | 1.26 | 7.90 | 3.65 | 7.31 | 4.22 | 3.40 | 3.01 | 2.29 | 5.07 | 1.43 | 42.88 |
| C0_DH146 | 1.04 | 2.78 | 4.26 | 2.14 | 4.12 | 2.24 | 4.71 | 6.47 | 6.30 | 4.13 | 4.60 | 5.84 | 4.11 | 7.39 | 2.37 | 37.50 |
| C0_DH147 | 0.79 | 3.97 | 5.07 | 2.28 | 4.73 | 2.04 | 5.12 | 5.78 | 3.23 | 4.81 | 4.19 | 3.44 | 3.17 | 5.41 | 2.15 | 43.80 |
| C0_DH148 | 1.14 | 4.55 | 4.00 | 4.38 | 4.40 | 2.86 | 5.49 | 3.48 | 7.38 | 5.29 | 4.40 | 7.37 | 5.13 | 4.19 | 1.50 | 34.45 |
| C0_DH149 | 0.77 | 3.22 | 7.31 | 3.37 | 3.42 | 2.36 | 4.97 | 5.72 | 9.00 | 9.25 | 3.32 | 3.18 | 4.82 | 3.97 | 2.10 | 33.23 |
| C0C17_DH001 | 1.15 | 2.33 | 3.54 | 1.18 | 4.43 | 1.47 | 5.17 | 3.17 | 4.14 | 4.03 | 4.38 | 3.57 | 2.71 | 2.67 | 1.49 | 54.56 |
| C0C17_DH002 | 0.51 | 5.28 | 4.28 | 1.91 | 3.44 | 0.91 | 4.51 | 4.14 | 5.01 | 3.30 | 3.58 | 4.05 | 1.98 | 4.57 | 1.50 | 51.02 |
| C0C17_DH003 | 0.79 | 3.29 | 2.69 | 3.08 | 2.56 | 2.06 | 2.73 | 5.36 | 6.16 | 4.05 | 3.07 | 3.54 | 2.72 | 3.79 | 1.51 | 52.61 |
| C0C17_DH005 | 0.68 | 2.05 | 3.95 | 1.69 | 2.82 | 1.34 | 3.81 | 3.95 | 5.69 | 4.52 | 2.68 | 3.19 | 3.23 | 4.42 | 1.10 | 54.86 |
| C0C17_DH007 | 0.96 | 4.91 | 2.34 | 3.00 | 3.74 | 2.07 | 4.39 | 3.56 | 5.98 | 5.05 | 3.51 | 3.30 | 2.94 | 3.94 | 1.35 | 48.96 |
| C0C17_DH008 | 0.51 | 3.16 | 4.63 | 2.63 | 2.16 | 1.41 | 4.62 | 2.96 | 5.37 | 3.67 | 2.15 | 2.79 | 2.49 | 2.76 | 1.40 | 57.29 |

Table S2.1. Continued

| DH Line | A3G-3-3-1-3 | CI 540 | Fe (Parent of F1B1) | I-159 | IL1 2E | B2 (Parent of F1B1) | Oh 3167 B | Os 420 | Tr 9-1-1-6 | WD 456 | I224 | LE 23 | 461 | Hy | AH 83 | Non-IBD |
|---|---|---|---|---|---|---|---|---|---|---|---|---|---|---|---|---|
| C0C17_DH010 | 0.70 | 4.48 | 4.89 | 1.54 | 2.82 | 2.12 | 3.90 | 3.12 | 6.28 | 7.44 | 2.86 | 4.25 | 4.60 | 3.80 | 1.46 | 45.76 |
| C0C17_DH012 | 0.59 | 2.97 | 3.21 | 2.02 | 3.15 | 1.93 | 4.15 | 3.58 | 5.14 | 5.43 | 3.77 | 2.36 | 3.06 | 5.55 | 1.79 | 51.30 |
| C0C17_DH013 | 0.62 | 5.38 | 4.08 | 2.77 | 3.78 | 2.05 | 5.65 | 2.94 | 4.53 | 4.63 | 3.97 | 3.48 | 2.93 | 5.07 | 1.45 | 46.66 |
| C0C17_DH014 | 0.87 | 1.98 | 5.20 | 1.11 | 4.64 | 1.76 | 5.16 | 5.37 | 6.77 | 5.72 | 4.73 | 1.75 | 3.36 | 5.61 | 1.63 | 44.34 |
| C0C17_DH015 | 1.13 | 2.43 | 3.84 | 2.42 | 2.88 | 2.14 | 3.61 | 3.00 | 6.88 | 4.24 | 3.14 | 2.91 | 2.92 | 5.53 | 1.97 | 50.97 |
| C0C17_DH016 | 1.23 | 3.33 | 3.54 | 1.39 | 3.27 | 1.62 | 6.24 | 3.10 | 3.89 | 4.88 | 3.08 | 1.65 | 3.07 | 6.23 | 1.82 | 51.66 |
| C0C17_DH017 | 0.89 | 4.05 | 3.81 | 2.56 | 3.54 | 2.08 | 6.08 | 4.12 | 2.85 | 5.19 | 3.27 | 2.19 | 2.82 | 3.73 | 1.31 | 51.51 |
| C0C17_DH018 | 0.96 | 4.02 | 2.01 | 1.57 | 2.18 | 2.76 | 2.83 | 2.76 | 4.82 | 5.84 | 2.38 | 5.91 | 2.27 | 6.76 | 1.54 | 51.38 |
| C0C17_DH019 | 1.19 | 3.44 | 4.33 | 1.83 | 2.75 | 1.89 | 3.25 | 6.20 | 3.04 | 3.69 | 2.59 | 4.40 | 2.29 | 3.25 | 1.73 | 54.14 |
| C0C17_DH020 | 0.61 | 2.86 | 5.80 | 1.40 | 5.04 | 2.79 | 4.91 | 3.14 | 4.39 | 4.24 | 4.85 | 4.62 | 2.98 | 4.94 | 1.78 | 45.67 |
| C0C17_DH021 | 0.90 | 5.15 | 2.78 | 1.89 | 2.47 | 1.87 | 5.30 | 4.90 | 2.83 | 5.26 | 2.48 | 3.86 | 2.08 | 4.09 | 1.79 | 52.36 |
| C0C17_DH024 | 0.51 | 2.43 | 3.58 | 2.66 | 3.15 | 2.69 | 6.77 | 5.31 | 3.54 | 3.61 | 2.97 | 2.96 | 2.37 | 7.70 | 1.54 | 48.20 |
| C0C17_DH025 | 0.50 | 2.99 | 6.61 | 3.01 | 3.58 | 1.59 | 4.52 | 4.60 | 3.80 | 4.90 | 3.66 | 4.61 | 2.68 | 5.53 | 2.14 | 45.27 |
| C0C17_DH027 | 1.12 | 3.04 | 4.20 | 1.88 | 2.74 | 2.27 | 5.69 | 3.26 | 6.07 | 4.02 | 2.91 | 5.83 | 2.10 | 2.95 | 2.13 | 49.79 |
| C0C17_DH030 | 0.26 | 2.62 | 5.24 | 2.57 | 3.83 | 1.61 | 4.03 | 5.33 | 5.17 | 5.47 | 3.62 | 2.69 | 3.08 | 2.07 | 1.46 | 50.96 |
| C0C17_DH033 | 0.75 | 1.42 | 2.52 | 1.45 | 3.39 | 2.20 | 5.07 | 4.17 | 4.69 | 4.24 | 3.40 | 3.28 | 3.20 | 4.22 | 1.44 | 54.55 |
| C0C17_DH035 | 1.20 | 3.08 | 5.24 | 2.71 | 3.75 | 2.74 | 4.48 | 3.79 | 3.41 | 9.21 | 3.93 | 3.42 | 4.27 | 4.06 | 1.25 | 43.46 |
| C0C17_DH037 | 0.90 | 3.19 | 3.05 | 2.72 | 2.54 | 1.92 | 4.76 | 5.93 | 6.99 | 4.47 | 2.22 | 4.48 | 3.19 | 5.13 | 1.48 | 47.03 |
| C0C17_DH038 | 0.62 | 1.26 | 3.58 | 1.62 | 2.56 | 1.83 | 4.25 | 5.93 | 3.09 | 3.20 | 2.35 | 4.30 | 3.31 | 4.25 | 1.39 | 56.48 |
| C0C17_DH040 | 0.66 | 4.36 | 4.07 | 2.33 | 2.48 | 1.27 | 3.22 | 6.70 | 4.77 | 3.68 | 2.65 | 2.99 | 3.05 | 3.97 | 2.25 | 51.56 |
| C0C17_DH041 | 0.57 | 3.49 | 3.83 | 1.17 | 3.14 | 2.31 | 4.55 | 4.26 | 4.59 | 3.34 | 3.29 | 2.41 | 3.31 | 6.68 | 1.62 | 51.47 |
| C0C17_DH042 | 0.74 | 4.22 | 3.59 | 2.03 | 3.12 | 2.07 | 2.42 | 5.45 | 5.16 | 5.78 | 2.87 | 1.49 | 3.08 | 5.00 | 0.95 | 52.03 |
| C0C17_DH043 | 1.00 | 3.42 | 3.09 | 2.06 | 2.66 | 1.97 | 4.10 | 7.54 | 3.47 | 3.45 | 2.43 | 4.32 | 3.47 | 4.36 | 1.93 | 50.73 |
| C0C17_DH044 | 0.88 | 4.57 | 3.97 | 1.63 | 3.25 | 1.54 | 7.42 | 3.53 | 4.03 | 5.34 | 3.51 | 2.94 | 3.07 | 4.62 | 1.40 | 48.29 |
| C0C17_DH045 | 0.73 | 2.65 | 4.66 | 2.35 | 3.96 | 1.94 | 3.53 | 4.31 | 4.87 | 4.06 | 3.79 | 4.29 | 4.28 | 6.01 | 1.43 | 47.13 |
| C0C17_DH047 | 0.89 | 3.50 | 4.24 | 2.39 | 2.58 | 1.83 | 5.79 | 3.61 | 6.86 | 4.71 | 2.58 | 4.75 | 3.84 | 5.46 | 1.67 | 45.30 |
| C0C17_DH048 | 0.30 | 5.75 | 2.58 | 3.01 | 2.42 | 1.86 | 2.29 | 4.27 | 5.72 | 3.19 | 2.22 | 3.67 | 3.17 | 5.16 | 2.53 | 51.84 |
| C0C17_DH049 | 1.12 | 6.75 | 3.10 | 1.85 | 3.99 | 1.74 | 2.23 | 4.60 | 3.19 | 6.40 | 4.02 | 3.15 | 3.95 | 3.97 | 1.60 | 48.36 |
| C0C17_DH051 | 1.09 | 1.76 | 2.43 | 1.74 | 2.67 | 1.86 | 4.59 | 4.73 | 3.51 | 8.18 | 2.70 | 2.63 | 2.68 | 3.17 | 1.15 | 55.12 |
| C0C17_DH052 | 1.05 | 3.65 | 3.53 | 1.38 | 1.94 | 1.59 | 6.14 | 3.83 | 6.54 | 5.39 | 1.95 | 3.19 | 2.09 | 4.26 | 1.16 | 52.30 |
| C0C17_DH053 | 0.71 | 3.31 | 3.11 | 2.12 | 2.88 | 1.77 | 4.38 | 7.83 | 3.55 | 3.59 | 2.39 | 4.56 | 3.57 | 4.34 | 2.02 | 49.87 |
| C0C17_DH056 | 0.67 | 3.64 | 2.53 | 1.67 | 3.41 | 1.89 | 4.90 | 4.09 | 4.52 | 5.87 | 3.12 | 4.73 | 3.18 | 3.53 | 2.14 | 50.12 |
| C0C17_DH058 | 1.02 | 3.67 | 3.76 | 2.40 | 2.99 | 2.11 | 4.46 | 4.49 | 3.24 | 3.88 | 3.19 | 3.15 | 3.02 | 6.03 | 2.32 | 50.25 |
| C0C17_DH059 | 0.49 | 2.57 | 7.87 | 3.19 | 2.07 | 2.16 | 6.06 | 4.61 | 4.72 | 4.51 | 2.29 | 3.87 | 3.24 | 5.65 | 1.21 | 45.49 |
| C0C17_DH060 | 0.94 | 2.92 | 4.22 | 1.74 | 3.03 | 1.66 | 4.98 | 4.00 | 5.76 | 7.48 | 2.94 | 2.74 | 2.28 | 5.33 | 1.52 | 48.47 |

Table S2.1. Continued

| DH Line | A3G-3-3-1-3 | CI 540 | Fe (Parent of F1B1) | I-159 | IL1 2E | B2 (Parent of F1B1) | Oh 3167 B | Os 420 | Tr 9-1-1-6 | WD 456 | I224 | LE 23 | 461 | Hy | AH 83 | Non-IBD |
|---|---|---|---|---|---|---|---|---|---|---|---|---|---|---|---|---|
| C0C17_DH061 | 1.18 | 4.40 | 2.88 | 3.14 | 2.76 | 2.12 | 6.00 | 3.62 | 3.64 | 7.68 | 2.16 | 2.44 | 3.09 | 4.05 | 1.68 | 49.15 |
| C0C17_DH062 | 0.72 | 2.89 | 3.70 | 1.10 | 3.91 | 2.13 | 3.54 | 4.46 | 4.96 | 3.75 | 3.84 | 3.79 | 2.64 | 6.38 | 1.14 | 51.04 |
| C0C17_DH064 | 1.31 | 1.92 | 3.93 | 2.19 | 2.16 | 1.42 | 5.90 | 3.60 | 5.86 | 3.99 | 2.47 | 4.42 | 2.42 | 3.99 | 1.93 | 52.48 |
| C0C17_DH066 | 1.05 | 3.53 | 2.58 | 1.99 | 3.20 | 2.54 | 6.34 | 4.97 | 3.54 | 4.07 | 3.39 | 2.80 | 2.83 | 5.03 | 1.99 | 50.15 |
| C0C17_DH068 | 0.59 | 3.03 | 2.79 | 1.61 | 3.89 | 2.72 | 5.21 | 3.26 | 3.43 | 3.49 | 3.22 | 3.37 | 2.54 | 5.02 | 1.39 | 54.43 |
| C0C17_DH069 | 0.63 | 2.69 | 3.79 | 3.05 | 3.35 | 2.73 | 4.51 | 5.01 | 3.92 | 6.85 | 2.88 | 2.41 | 2.88 | 5.35 | 1.54 | 48.40 |
| C0C17_DH070 | 1.03 | 2.64 | 6.13 | 1.14 | 3.31 | 1.66 | 4.51 | 6.73 | 4.38 | 3.36 | 3.40 | 5.08 | 2.91 | 3.69 | 1.23 | 48.82 |
| C0C17_DH071 | 0.82 | 3.11 | 3.88 | 2.92 | 2.45 | 1.75 | 2.11 | 4.64 | 4.11 | 5.54 | 2.44 | 3.07 | 2.55 | 5.93 | 1.22 | 53.46 |
| C0C17_DH072 | 1.12 | 2.22 | 3.07 | 2.35 | 2.59 | 2.17 | 3.82 | 4.35 | 5.75 | 3.84 | 2.76 | 2.73 | 1.95 | 6.85 | 1.31 | 53.13 |
| C0C17_DH073 | 0.58 | 3.53 | 4.16 | 1.57 | 3.17 | 3.29 | 5.35 | 4.58 | 4.65 | 6.70 | 2.92 | 4.34 | 2.69 | 4.00 | 1.43 | 47.06 |
| C0C17_DH074 | 0.58 | 2.88 | 5.19 | 2.02 | 3.86 | 1.84 | 3.16 | 3.43 | 6.56 | 7.23 | 4.20 | 4.38 | 2.43 | 3.05 | 1.75 | 47.44 |
| C0C17_DH076 | 0.72 | 4.94 | 5.66 | 2.11 | 4.57 | 1.70 | 6.54 | 2.90 | 3.25 | 4.28 | 4.44 | 4.03 | 2.49 | 4.58 | 1.73 | 46.05 |
| C0C17_DH078 | 0.87 | 3.63 | 3.90 | 2.89 | 2.62 | 1.92 | 3.39 | 4.18 | 4.56 | 5.58 | 2.13 | 3.08 | 3.26 | 5.92 | 1.22 | 50.85 |
| C0C17_DH079 | 0.51 | 2.85 | 4.25 | 2.07 | 3.90 | 2.21 | 3.45 | 5.21 | 5.73 | 4.71 | 3.39 | 2.96 | 3.76 | 6.22 | 1.61 | 47.20 |
| C0C17_DH080 | 1.44 | 3.74 | 3.19 | 1.36 | 2.61 | 2.12 | 5.64 | 3.97 | 5.07 | 3.29 | 2.76 | 3.91 | 2.95 | 4.64 | 1.01 | 52.29 |
| C0C17_DH081 | 0.92 | 2.29 | 3.50 | 1.17 | 3.34 | 2.46 | 5.45 | 7.20 | 2.69 | 3.40 | 3.21 | 5.99 | 1.98 | 5.35 | 1.71 | 49.33 |
| C0C17_DH082 | 0.74 | 2.03 | 3.37 | 1.37 | 3.62 | 2.05 | 6.53 | 3.92 | 5.50 | 5.71 | 3.80 | 2.57 | 2.75 | 1.69 | 1.02 | 53.33 |
| C0C17_DH083 | 1.29 | 4.31 | 3.81 | 1.07 | 3.29 | 1.65 | 6.78 | 5.52 | 3.31 | 4.15 | 3.41 | 1.31 | 3.14 | 3.20 | 2.40 | 51.34 |
| C0C17_DH084 | 0.53 | 3.21 | 3.38 | 1.82 | 4.10 | 2.72 | 5.93 | 4.61 | 5.49 | 4.83 | 4.22 | 3.46 | 2.76 | 5.27 | 1.48 | 46.18 |
| C0C17_DH085 | 1.01 | 2.83 | 5.05 | 1.68 | 3.05 | 2.05 | 7.04 | 2.47 | 4.81 | 4.72 | 2.96 | 3.40 | 2.35 | 4.18 | 1.57 | 50.82 |
| C0C17_DH086 | 0.94 | 4.36 | 2.39 | 1.13 | 4.63 | 2.18 | 4.21 | 4.83 | 4.06 | 4.64 | 4.61 | 1.52 | 2.38 | 4.95 | 1.44 | 51.72 |
| C0C17_DH087 | 0.53 | 2.80 | 5.08 | 2.35 | 3.23 | 2.47 | 5.79 | 5.29 | 4.69 | 4.23 | 3.33 | 3.39 | 2.20 | 6.39 | 1.82 | 46.40 |
| C0C17_DH088 | 1.80 | 4.08 | 2.95 | 1.47 | 2.98 | 1.62 | 5.30 | 3.60 | 5.13 | 5.09 | 2.71 | 3.20 | 2.51 | 5.14 | 1.60 | 50.81 |
| C0C17_DH089 | 0.83 | 2.57 | 5.18 | 2.84 | 2.45 | 1.26 | 5.61 | 2.92 | 4.75 | 3.90 | 2.28 | 4.11 | 3.05 | 2.60 | 1.85 | 53.79 |
| C0C17_DH090 | 1.11 | 4.17 | 4.93 | 2.27 | 2.60 | 2.10 | 2.44 | 3.57 | 4.04 | 5.11 | 2.66 | 4.24 | 3.04 | 3.95 | 1.94 | 51.84 |
| C0C17_DH091 | 0.87 | 3.30 | 4.17 | 2.49 | 3.18 | 2.47 | 3.40 | 4.27 | 5.66 | 3.75 | 2.96 | 1.92 | 2.22 | 6.81 | 1.07 | 51.46 |
| C0C17_DH092 | 0.91 | 4.86 | 5.65 | 1.10 | 4.39 | 1.98 | 3.55 | 3.89 | 3.96 | 6.15 | 4.11 | 3.67 | 2.99 | 2.32 | 1.07 | 49.40 |
| C0C17_DH094 | 0.80 | 3.77 | 3.66 | 1.79 | 3.29 | 2.32 | 5.76 | 5.12 | 4.16 | 4.73 | 3.54 | 3.74 | 3.25 | 6.04 | 1.62 | 46.41 |
| C0C17_DH095 | 1.37 | 3.60 | 3.28 | 1.30 | 3.57 | 2.26 | 3.04 | 5.32 | 4.44 | 6.42 | 3.69 | 4.69 | 2.44 | 4.31 | 1.86 | 48.40 |
| C0C17_DH096 | 0.65 | 2.42 | 2.60 | 1.91 | 4.56 | 2.14 | 6.52 | 3.33 | 4.18 | 3.78 | 4.76 | 2.39 | 2.72 | 7.23 | 1.56 | 49.26 |
| C0C17_DH097 | 1.07 | 4.41 | 4.22 | 1.67 | 4.24 | 1.84 | 4.64 | 3.95 | 5.15 | 2.92 | 4.26 | 3.40 | 2.51 | 4.59 | 1.38 | 49.76 |
| C0C17_DH100 | 0.95 | 3.05 | 3.23 | 1.05 | 4.28 | 1.35 | 7.27 | 4.15 | 4.37 | 4.92 | 3.99 | 2.84 | 2.86 | 4.73 | 0.94 | 50.03 |
| C0C17_DH103 | 0.87 | 3.23 | 3.85 | 2.15 | 3.49 | 1.46 | 5.13 | 3.61 | 4.13 | 5.45 | 3.45 | 3.20 | 1.76 | 3.97 | 1.59 | 52.65 |
| C0C17_DH104 | 0.54 | 2.44 | 5.37 | 2.37 | 3.20 | 1.61 | 5.20 | 6.47 | 5.47 | 3.77 | 2.82 | 3.94 | 2.44 | 3.31 | 0.89 | 50.16 |
| C0C17_DH105 | 1.71 | 4.62 | 3.26 | 1.79 | 3.65 | 1.89 | 4.74 | 6.16 | 4.38 | 5.14 | 3.23 | 3.44 | 2.14 | 4.13 | 1.34 | 48.38 |

Table S2.1. Continued

| DH Line | A3G-3-3-1-3 | CI 540 | Fe (Parent of F1B1) | I-159 | IL1 2E | B2 (Parent of F1B1) | Oh 3167 B | Os 420 | Tr 9-1-1-6 | WD 456 | I224 | LE 23 | 461 | Hy | AH 83 | Non-IBD |
|---|---|---|---|---|---|---|---|---|---|---|---|---|---|---|---|---|
| C0C17_DH106 | 0.55 | 2.96 | 5.11 | 2.45 | 2.21 | 1.50 | 5.04 | 2.67 | 4.53 | 4.68 | 2.32 | 2.34 | 2.64 | 2.47 | 1.53 | 57.00 |
| C0C17_DH107 | 1.42 | 2.92 | 3.01 | 1.91 | 5.30 | 2.22 | 3.26 | 7.32 | 5.14 | 5.29 | 4.86 | 3.42 | 3.53 | 3.54 | 1.26 | 45.60 |
| C0C17_DH108 | 0.81 | 2.37 | 1.59 | 1.25 | 1.85 | 1.40 | 5.66 | 4.54 | 4.40 | 3.72 | 1.80 | 5.15 | 3.02 | 5.13 | 1.77 | 55.54 |
| C0C17_DH109 | 0.25 | 4.57 | 4.21 | 1.86 | 3.92 | 2.04 | 6.18 | 4.08 | 4.84 | 4.54 | 3.49 | 2.51 | 3.26 | 5.72 | 1.71 | 46.81 |
| C0C17_DH112 | 0.90 | 3.59 | 3.16 | 1.90 | 3.37 | 2.23 | 4.68 | 3.59 | 4.26 | 5.87 | 3.69 | 3.00 | 2.63 | 7.43 | 1.39 | 48.30 |
| C0C17_DH114 | 1.22 | 4.77 | 4.46 | 1.30 | 3.31 | 1.24 | 2.99 | 5.53 | 2.78 | 7.84 | 3.45 | 4.26 | 3.12 | 4.19 | 1.28 | 48.26 |
| C0C17_DH117 | 0.68 | 3.70 | 2.60 | 2.37 | 2.96 | 1.58 | 6.92 | 4.59 | 5.57 | 4.75 | 2.64 | 3.57 | 4.00 | 4.83 | 1.22 | 48.04 |
| C0C17_DH118 | 0.60 | 2.97 | 2.15 | 1.83 | 3.12 | 2.02 | 4.45 | 3.09 | 3.86 | 3.95 | 2.89 | 4.05 | 2.94 | 5.39 | 1.35 | 55.35 |
| C0C17_DH121 | 0.42 | 3.99 | 2.78 | 2.06 | 4.36 | 1.73 | 7.80 | 2.16 | 5.80 | 6.22 | 4.06 | 3.29 | 3.18 | 2.59 | 1.48 | 48.09 |
| C0C17_DH122 | 0.75 | 3.04 | 4.18 | 1.56 | 3.03 | 2.28 | 9.36 | 5.21 | 4.35 | 6.43 | 2.81 | 2.63 | 2.02 | 4.54 | 1.84 | 45.96 |
| C0C17_DH125 | 1.12 | 2.24 | 4.67 | 2.08 | 3.90 | 2.81 | 4.83 | 5.52 | 3.41 | 5.89 | 3.70 | 1.95 | 2.64 | 4.98 | 1.97 | 48.30 |
| C0C17_DH126 | 0.91 | 1.78 | 4.78 | 1.46 | 4.59 | 2.40 | 3.70 | 3.91 | 5.31 | 4.84 | 3.74 | 5.03 | 2.37 | 5.16 | 1.12 | 48.91 |
| C0C17_DH129 | 0.85 | 1.58 | 4.37 | 1.83 | 2.44 | 2.58 | 4.22 | 4.08 | 5.38 | 5.36 | 2.72 | 2.46 | 3.80 | 6.77 | 1.39 | 50.15 |
| C0C17_DH130 | 0.97 | 3.53 | 4.31 | 1.55 | 1.85 | 1.88 | 4.82 | 3.99 | 4.02 | 5.01 | 1.96 | 5.37 | 2.96 | 4.58 | 1.71 | 51.47 |
| C0C17_DH132 | 0.32 | 0.87 | 3.93 | 2.36 | 4.94 | 1.87 | 4.62 | 5.87 | 6.31 | 6.77 | 4.38 | 3.75 | 3.99 | 6.52 | 1.64 | 41.86 |
| C0C17_DH136 | 1.29 | 3.36 | 3.60 | 2.48 | 5.16 | 1.37 | 4.22 | 3.28 | 4.14 | 4.54 | 5.17 | 2.76 | 4.01 | 3.70 | 1.91 | 49.01 |
| C0C17_DH137 | 0.85 | 1.93 | 3.39 | 2.27 | 3.72 | 2.74 | 3.54 | 4.36 | 4.60 | 3.08 | 3.74 | 4.64 | 2.37 | 5.46 | 0.85 | 52.46 |
| C0C17_DH139 | 1.02 | 4.01 | 4.06 | 1.51 | 2.46 | 1.56 | 3.04 | 4.14 | 4.55 | 6.99 | 2.28 | 4.45 | 2.28 | 4.76 | 1.57 | 51.31 |
| C0C17_DH140 | 1.00 | 2.03 | 7.37 | 1.80 | 3.25 | 2.00 | 6.22 | 2.72 | 3.38 | 5.83 | 3.55 | 1.61 | 2.26 | 3.64 | 1.81 | 51.54 |
| C0C17_DH141 | 0.81 | 2.36 | 4.33 | 1.68 | 2.58 | 2.21 | 4.62 | 5.65 | 4.27 | 2.90 | 2.61 | 3.29 | 3.58 | 4.16 | 2.25 | 52.71 |
| C0C17_DH142 | 0.65 | 4.23 | 6.68 | 2.09 | 4.19 | 2.13 | 4.07 | 2.58 | 3.22 | 7.81 | 4.11 | 4.63 | 2.64 | 3.50 | 1.66 | 45.80 |
| C0C17_DH146 | 1.13 | 4.18 | 3.60 | 1.97 | 2.37 | 1.30 | 2.22 | 6.52 | 3.76 | 4.12 | 2.82 | 2.63 | 3.09 | 2.77 | 2.10 | 55.42 |
| C0C17_DH147 | 0.54 | 3.53 | 3.33 | 1.97 | 4.55 | 3.13 | 5.67 | 4.40 | 5.15 | 3.97 | 4.02 | 3.76 | 4.20 | 5.26 | 1.83 | 44.69 |
| C0C17_DH148 | 1.28 | 3.41 | 3.76 | 2.08 | 4.07 | 2.83 | 3.78 | 5.65 | 3.44 | 5.58 | 4.14 | 4.31 | 2.70 | 6.33 | 1.84 | 44.79 |
| C0C17_DH149 | 1.09 | 3.12 | 3.98 | 2.08 | 3.22 | 2.21 | 4.00 | 3.27 | 3.23 | 5.58 | 3.29 | 3.05 | 2.24 | 4.50 | 1.66 | 53.48 |
| C0C17_DH150 | 0.84 | 2.83 | 3.91 | 2.20 | 2.87 | 2.37 | 5.03 | 6.27 | 4.94 | 2.90 | 2.91 | 6.28 | 4.29 | 5.40 | 1.82 | 45.15 |
| C0C17_DH152 | 0.78 | 3.69 | 3.39 | 2.27 | 3.96 | 2.65 | 4.10 | 3.73 | 5.27 | 5.76 | 3.66 | 3.38 | 2.83 | 3.78 | 1.66 | 49.09 |
| C0C17_DH153 | 0.72 | 3.67 | 4.34 | 2.04 | 4.27 | 2.07 | 6.87 | 3.61 | 4.96 | 3.30 | 4.54 | 3.52 | 2.72 | 5.49 | 1.55 | 46.35 |
| C0C17_DH154 | 0.57 | 5.45 | 3.56 | 1.90 | 3.41 | 1.76 | 4.41 | 3.87 | 4.64 | 4.55 | 3.10 | 2.17 | 3.79 | 6.12 | 1.33 | 49.36 |
| C0C17_DH155 | 0.99 | 3.10 | 4.41 | 1.48 | 5.45 | 1.75 | 3.39 | 4.96 | 5.16 | 5.77 | 4.99 | 2.91 | 2.83 | 3.55 | 1.26 | 48.02 |
| C0C17_DH156 | 0.77 | 3.69 | 5.19 | 1.76 | 3.49 | 2.02 | 3.17 | 3.76 | 5.87 | 5.63 | 3.19 | 1.89 | 3.29 | 5.79 | 1.48 | 49.01 |
| C0C17_DH157 | 0.78 | 1.78 | 4.12 | 1.75 | 3.52 | 2.36 | 4.46 | 4.42 | 5.08 | 4.40 | 3.12 | 4.07 | 1.24 | 3.01 | 1.17 | 54.71 |
| C0C17_DH158 | 1.16 | 2.36 | 3.14 | 2.05 | 3.93 | 1.54 | 3.94 | 5.35 | 6.50 | 4.24 | 4.04 | 2.53 | 2.27 | 7.31 | 1.79 | 47.84 |
| C0C17_DH159 | 0.53 | 1.81 | 5.99 | 1.44 | 3.11 | 2.30 | 6.01 | 4.96 | 3.53 | 4.10 | 3.49 | 3.32 | 3.09 | 4.78 | 1.36 | 50.16 |
| C0C17_DH160 | 1.10 | 4.56 | 4.43 | 1.56 | 3.34 | 1.59 | 3.96 | 3.39 | 3.10 | 4.85 | 3.79 | 2.96 | 3.01 | 4.43 | 2.31 | 51.63 |

Table S2.1. Continued

| DH Line | A3G-3-3-1-3 | CI 540 | Fe (Parent of F1B1) | I-159 | IL1 2E | B2 (Parent of F1B1) | Oh 3167 B | Os 420 | Tr 9-1-1-6 | WD 456 | I224 | LE 23 | 461 | Hy | AH 83 | Non-IBD |
|---|---|---|---|---|---|---|---|---|---|---|---|---|---|---|---|---|
| C0C17_DH161 | 0.74 | 3.19 | 3.78 | 2.64 | 2.85 | 2.41 | 4.11 | 3.13 | 4.94 | 6.96 | 3.27 | 4.30 | 3.24 | 6.42 | 1.87 | 46.15 |
| C0C17_DH162 | 0.49 | 2.05 | 5.69 | 2.84 | 3.54 | 2.09 | 4.67 | 3.54 | 5.77 | 5.32 | 3.01 | 4.25 | 3.00 | 4.21 | 1.68 | 47.85 |
| C0C17_DH163 | 0.92 | 3.13 | 4.87 | 2.96 | 3.43 | 1.66 | 6.30 | 4.86 | 4.54 | 3.16 | 3.68 | 3.29 | 3.62 | 5.22 | 1.28 | 47.08 |
| C0C17_DH164 | 1.01 | 4.63 | 3.36 | 3.95 | 3.17 | 1.91 | 8.27 | 3.79 | 4.19 | 4.62 | 2.79 | 3.22 | 2.86 | 3.51 | 1.73 | 47.01 |
| C0C17_DH165 | 1.07 | 3.77 | 2.42 | 2.26 | 2.90 | 1.66 | 7.10 | 4.95 | 6.26 | 5.73 | 2.24 | 3.00 | 3.38 | 4.39 | 1.71 | 47.16 |
| C0C17_DH166 | 1.09 | 3.98 | 4.13 | 2.04 | 4.70 | 3.08 | 5.14 | 4.56 | 3.49 | 5.36 | 4.39 | 2.67 | 3.99 | 5.25 | 1.08 | 45.04 |
| C0C17_DH168 | 1.11 | 3.65 | 4.06 | 2.62 | 3.60 | 2.82 | 2.40 | 4.75 | 5.56 | 5.97 | 3.78 | 4.79 | 3.28 | 3.83 | 1.65 | 46.12 |
| C0C17_DH169 | 0.62 | 2.43 | 4.31 | 1.98 | 3.60 | 3.50 | 3.08 | 4.23 | 5.68 | 6.18 | 3.87 | 6.32 | 2.68 | 3.52 | 1.51 | 46.47 |
| C0C17_DH172 | 0.72 | 1.61 | 3.00 | 2.04 | 3.52 | 2.74 | 7.19 | 3.14 | 4.04 | 4.30 | 3.85 | 4.56 | 3.22 | 4.65 | 1.57 | 49.85 |
| C0C17_DH174 | 0.42 | 2.43 | 3.02 | 1.32 | 3.43 | 2.33 | 4.70 | 3.78 | 4.84 | 5.61 | 3.52 | 3.10 | 2.87 | 3.03 | 1.73 | 53.87 |
| C0C17_DH177 | 0.67 | 1.72 | 2.96 | 1.67 | 2.98 | 1.34 | 5.80 | 3.16 | 5.81 | 6.58 | 2.88 | 3.15 | 2.35 | 5.61 | 1.60 | 51.74 |
| C0C17_DH178 | 0.99 | 2.74 | 3.53 | 3.08 | 3.76 | 1.61 | 4.71 | 3.36 | 4.16 | 5.88 | 3.59 | 3.15 | 3.08 | 6.28 | 2.30 | 47.78 |
| C0C17_DH183 | 0.64 | 2.23 | 2.93 | 2.31 | 4.14 | 1.74 | 4.89 | 2.29 | 4.30 | 3.88 | 3.72 | 4.11 | 3.70 | 5.83 | 1.41 | 51.89 |
| C0C17_DH184 | 0.76 | 2.41 | 5.71 | 1.51 | 2.83 | 2.22 | 4.65 | 6.42 | 4.75 | 4.80 | 2.70 | 5.82 | 3.31 | 3.36 | 1.92 | 46.81 |
| C0C17_DH185 | 1.18 | 3.07 | 4.19 | 1.66 | 2.92 | 1.65 | 2.88 | 4.75 | 3.13 | 3.27 | 2.45 | 3.63 | 3.80 | 3.95 | 1.27 | 56.21 |
| C0C17_DH187 | 1.10 | 2.27 | 3.67 | 2.46 | 2.89 | 1.95 | 5.15 | 4.63 | 4.88 | 4.45 | 2.80 | 5.23 | 3.15 | 4.89 | 1.53 | 48.95 |
| C0C17_DH188 | 0.98 | 5.22 | 3.93 | 2.14 | 3.46 | 2.53 | 5.56 | 4.24 | 3.71 | 4.10 | 2.89 | 2.39 | 3.06 | 6.25 | 1.87 | 47.65 |
| C0C17_DH189 | 0.79 | 1.37 | 6.10 | 1.98 | 3.68 | 2.08 | 3.15 | 3.83 | 5.19 | 4.27 | 4.17 | 5.70 | 2.90 | 5.23 | 0.97 | 48.59 |
| C0C17_DH190 | 0.73 | 1.40 | 5.22 | 1.26 | 3.05 | 1.61 | 3.00 | 4.04 | 4.08 | 4.58 | 2.76 | 3.62 | 2.05 | 3.53 | 0.83 | 58.24 |
| C0C17_DH191 | 1.06 | 4.12 | 2.36 | 1.88 | 4.09 | 1.41 | 4.43 | 5.82 | 3.75 | 3.80 | 3.86 | 3.50 | 3.01 | 4.35 | 1.51 | 51.03 |
| C0C17_DH192 | 0.46 | 4.06 | 4.03 | 2.16 | 2.67 | 1.09 | 5.08 | 6.45 | 4.45 | 4.56 | 2.72 | 2.56 | 3.55 | 5.41 | 1.45 | 49.30 |
| C0C17_DH193 | 0.89 | 3.85 | 2.74 | 1.30 | 2.73 | 1.20 | 5.12 | 5.85 | 3.26 | 4.04 | 2.32 | 2.00 | 2.91 | 3.24 | 1.24 | 57.33 |
| C0C17_DH195 | 0.51 | 2.70 | 3.10 | 1.07 | 3.64 | 2.27 | 4.26 | 4.40 | 5.00 | 4.85 | 4.04 | 2.25 | 2.69 | 7.88 | 1.73 | 49.62 |
| C0C17_DH196 | 1.06 | 2.72 | 2.28 | 1.87 | 1.88 | 1.57 | 6.12 | 4.01 | 4.30 | 3.67 | 2.05 | 3.77 | 4.45 | 5.57 | 1.87 | 52.81 |
| C0C17_DH197 | 0.85 | 1.52 | 4.09 | 1.60 | 3.76 | 1.49 | 5.06 | 4.80 | 5.07 | 3.80 | 3.77 | 4.09 | 2.87 | 4.60 | 1.23 | 51.39 |
| C0C17_DH198 | 0.30 | 5.26 | 2.76 | 2.48 | 2.94 | 1.68 | 3.96 | 3.57 | 5.58 | 4.42 | 2.77 | 4.21 | 4.57 | 2.90 | 2.07 | 50.53 |
| C0C17_DH199 | 0.70 | 1.92 | 4.20 | 1.54 | 3.62 | 1.56 | 4.98 | 4.92 | 4.97 | 3.74 | 3.65 | 3.91 | 3.04 | 4.68 | 0.90 | 51.68 |
| C0C17_DH200 | 1.33 | 2.67 | 5.17 | 2.14 | 2.31 | 1.69 | 5.48 | 6.41 | 4.28 | 3.64 | 2.40 | 3.07 | 2.66 | 4.10 | 1.41 | 51.24 |
| C0C17_DH201 | 0.79 | 1.76 | 4.38 | 1.52 | 3.72 | 1.51 | 4.49 | 4.91 | 4.88 | 3.67 | 3.69 | 3.91 | 2.52 | 4.64 | 1.26 | 52.35 |
| C0C17_DH202 | 1.19 | 3.69 | 2.23 | 2.88 | 3.32 | 2.74 | 5.40 | 4.37 | 5.33 | 5.67 | 3.18 | 2.65 | 3.92 | 4.00 | 1.97 | 47.47 |
| C0C17_DH203 | 0.69 | 3.46 | 2.78 | 1.09 | 3.93 | 1.60 | 4.13 | 6.41 | 2.95 | 3.59 | 4.15 | 1.99 | 1.48 | 2.27 | 1.24 | 58.22 |
| C0C17_DH204 | 1.30 | 4.03 | 2.23 | 3.44 | 3.33 | 2.72 | 5.41 | 4.61 | 4.46 | 5.59 | 3.11 | 2.57 | 3.84 | 3.81 | 2.11 | 47.43 |
| C0C17_DH205 | 0.56 | 3.70 | 3.30 | 2.04 | 2.88 | 1.79 | 5.33 | 5.45 | 3.79 | 4.05 | 2.57 | 4.82 | 3.59 | 3.48 | 1.21 | 51.46 |
| C0C17_DH206 | 0.51 | 2.14 | 5.10 | 1.36 | 3.72 | 1.74 | 2.82 | 6.87 | 4.91 | 4.91 | 3.20 | 4.33 | 3.56 | 3.46 | 1.42 | 49.96 |
| C0C17_DH207 | 0.97 | 5.27 | 2.70 | 2.31 | 3.49 | 1.56 | 5.61 | 5.93 | 5.00 | 4.79 | 3.46 | 3.11 | 1.96 | 4.40 | 1.64 | 47.81 |

Table S2.1. Continued

| DH Line | A3G-3-3-1-3 | CI 540 | Fe (Parent of F1B1) | I-159 | IL1 2E | B2 (Parent of F1B1) | Oh 3167 B | Os 420 | Tr 9-1-1-6 | WD 456 | I224 | LE 23 | 461 | Hy | AH 83 | Non-IBD |
|---|---|---|---|---|---|---|---|---|---|---|---|---|---|---|---|---|
| C0C17_DH208 | 1.22 | 5.20 | 5.35 | 2.32 | 2.91 | 1.83 | 3.66 | 2.98 | 4.06 | 5.58 | 2.81 | 3.84 | 2.57 | 3.88 | 1.09 | 50.69 |
| C0C17_DH209 | 1.42 | 3.64 | 4.24 | 2.09 | 3.39 | 1.68 | 3.69 | 5.21 | 6.28 | 4.26 | 3.50 | 4.53 | 1.84 | 6.85 | 1.99 | 45.39 |
| C0C17_DH212 | 1.14 | 2.44 | 2.69 | 1.74 | 2.61 | 1.50 | 3.79 | 4.69 | 4.97 | 4.95 | 2.76 | 2.56 | 2.38 | 6.01 | 1.80 | 53.96 |
| C0C17_DH213 | 0.88 | 2.36 | 4.12 | 1.84 | 3.90 | 1.76 | 4.27 | 3.26 | 5.55 | 6.46 | 4.06 | 4.94 | 3.82 | 2.95 | 2.27 | 47.55 |
| C0C17_DH214 | 0.92 | 2.35 | 4.11 | 1.85 | 3.75 | 1.75 | 4.17 | 3.30 | 5.67 | 6.54 | 4.05 | 4.99 | 3.95 | 3.05 | 2.25 | 47.29 |
| C0C17_DH215 | 0.41 | 2.64 | 4.18 | 1.27 | 2.79 | 1.62 | 5.01 | 5.20 | 4.27 | 4.14 | 2.45 | 2.29 | 2.51 | 5.28 | 1.31 | 54.62 |
| C0C17_DH216 | 0.85 | 3.46 | 3.02 | 1.40 | 2.23 | 2.24 | 4.91 | 5.00 | 3.72 | 5.35 | 2.38 | 4.03 | 3.71 | 5.01 | 1.25 | 51.43 |
| C0C17_DH217 | 1.10 | 2.61 | 5.39 | 2.01 | 4.00 | 1.88 | 5.60 | 4.77 | 3.34 | 5.24 | 4.57 | 2.03 | 2.88 | 4.78 | 0.96 | 48.83 |
| C0C17_DH220 | 0.68 | 2.87 | 5.99 | 1.54 | 2.98 | 2.49 | 3.92 | 4.22 | 4.88 | 8.08 | 2.96 | 2.26 | 3.12 | 5.36 | 1.41 | 47.25 |
| C0C17_DH221 | 0.88 | 3.03 | 4.41 | 2.63 | 4.27 | 2.35 | 6.45 | 5.90 | 3.61 | 6.16 | 4.58 | 3.55 | 2.76 | 4.79 | 2.31 | 42.32 |
| C0C17_DH222 | 0.80 | 3.66 | 4.66 | 2.09 | 2.03 | 1.29 | 5.02 | 5.34 | 3.79 | 4.94 | 2.03 | 1.88 | 3.95 | 3.06 | 1.62 | 53.84 |
| C0C17_DH224 | 1.17 | 1.79 | 3.96 | 1.63 | 4.52 | 2.20 | 3.95 | 4.73 | 6.63 | 5.88 | 4.48 | 2.93 | 4.01 | 2.86 | 1.00 | 48.27 |
| C0C17_DH225 | 0.83 | 2.96 | 2.91 | 1.79 | 3.81 | 2.27 | 5.77 | 3.67 | 3.69 | 4.17 | 3.98 | 2.40 | 2.92 | 5.24 | 1.19 | 52.40 |
| C0C17_DH226 | 0.86 | 4.07 | 3.21 | 1.28 | 3.97 | 1.44 | 5.95 | 4.95 | 3.43 | 4.62 | 3.34 | 3.37 | 3.40 | 4.86 | 1.71 | 49.55 |
| C0C17_DH228 | 0.91 | 3.10 | 4.64 | 1.92 | 3.02 | 1.07 | 2.88 | 3.43 | 6.22 | 7.01 | 2.43 | 3.05 | 3.90 | 4.39 | 1.42 | 50.60 |
| C0C17_DH230 | 0.63 | 3.33 | 4.10 | 1.15 | 4.13 | 2.47 | 7.19 | 4.28 | 3.14 | 4.39 | 4.08 | 3.20 | 2.72 | 4.50 | 1.56 | 49.14 |
| C0C17_DH231 | 0.99 | 2.24 | 2.06 | 2.62 | 3.97 | 2.08 | 4.53 | 3.40 | 2.86 | 4.84 | 3.61 | 3.01 | 3.43 | 5.54 | 1.59 | 53.24 |
| C0C17_DH232 | 0.80 | 2.99 | 2.50 | 1.44 | 3.41 | 1.62 | 7.00 | 3.00 | 3.68 | 4.99 | 3.29 | 3.69 | 3.01 | 4.01 | 2.14 | 52.47 |
| C0C17_DH234 | 1.08 | 2.85 | 3.83 | 2.04 | 3.94 | 1.73 | 5.92 | 4.84 | 4.82 | 3.36 | 4.10 | 2.98 | 4.09 | 3.96 | 1.30 | 49.16 |
| C0C17_DH235 | 1.00 | 3.86 | 4.25 | 1.42 | 2.21 | 1.34 | 5.46 | 6.81 | 3.53 | 3.68 | 2.42 | 3.31 | 1.63 | 6.01 | 1.91 | 51.16 |
| C0C17_DH236 | 0.61 | 1.59 | 5.98 | 1.64 | 2.86 | 1.68 | 4.53 | 3.07 | 5.07 | 6.78 | 2.98 | 4.65 | 2.35 | 3.70 | 1.64 | 50.85 |
| C0C17_DH238 | 1.65 | 2.43 | 4.86 | 2.46 | 2.77 | 1.35 | 4.97 | 2.92 | 4.48 | 4.43 | 2.49 | 4.94 | 3.70 | 4.00 | 1.65 | 50.90 |
| C0C17_DH242 | 0.98 | 1.62 | 4.22 | 2.22 | 2.97 | 2.66 | 4.38 | 5.81 | 5.19 | 6.64 | 3.34 | 4.59 | 3.08 | 3.71 | 1.55 | 47.05 |
| C0C17_DH244 | 0.94 | 2.14 | 2.31 | 1.99 | 5.10 | 2.00 | 3.95 | 5.42 | 3.78 | 4.09 | 4.79 | 3.33 | 3.47 | 5.79 | 2.29 | 48.61 |
| C17_DH001 | 0.46 | 3.76 | 2.87 | 1.40 | 3.48 | 0.76 | 2.94 | 4.34 | 4.68 | 4.32 | 3.41 | 2.47 | 2.74 | 4.10 | 1.13 | 57.14 |
| C17_DH003 | 0.35 | 2.87 | 2.32 | 1.14 | 2.52 | 1.79 | 4.14 | 4.38 | 3.83 | 3.93 | 2.16 | 2.81 | 2.34 | 4.72 | 1.20 | 59.50 |
| C17_DH004 | 0.87 | 3.51 | 2.17 | 1.10 | 3.27 | 1.43 | 3.54 | 3.99 | 2.81 | 2.88 | 3.57 | 1.30 | 2.46 | 3.94 | 0.88 | 62.30 |
| C17_DH005 | 0.71 | 3.52 | 3.73 | 1.40 | 1.88 | 1.48 | 3.18 | 3.89 | 3.75 | 4.61 | 2.22 | 2.81 | 3.09 | 4.05 | 1.18 | 58.48 |
| C17_DH006 | 0.61 | 3.11 | 2.95 | 0.83 | 2.97 | 1.90 | 3.08 | 5.03 | 4.80 | 3.75 | 2.76 | 2.65 | 3.64 | 3.60 | 1.41 | 56.91 |
| C17_DH010 | 0.56 | 3.69 | 2.28 | 1.12 | 2.63 | 0.99 | 3.88 | 6.20 | 3.35 | 4.26 | 2.81 | 2.13 | 3.05 | 3.60 | 0.83 | 58.61 |
| C17_DH011 | 0.62 | 2.91 | 2.78 | 1.24 | 3.07 | 1.35 | 3.08 | 6.19 | 4.68 | 3.91 | 3.35 | 1.41 | 2.71 | 4.14 | 0.87 | 57.71 |
| C17_DH013 | 0.82 | 3.96 | 4.24 | 1.13 | 2.92 | 0.96 | 4.63 | 4.10 | 4.43 | 3.92 | 2.91 | 2.56 | 1.99 | 3.43 | 1.04 | 56.97 |
| C17_DH014 | 0.49 | 4.92 | 2.91 | 0.78 | 2.95 | 1.19 | 3.33 | 4.14 | 3.82 | 4.27 | 2.84 | 2.54 | 2.37 | 4.81 | 0.83 | 57.81 |
| C17_DH018 | 0.35 | 3.32 | 2.84 | 1.54 | 2.65 | 1.66 | 3.43 | 3.82 | 3.70 | 4.16 | 2.48 | 2.29 | 1.97 | 3.14 | 1.06 | 61.61 |
| C17_DH019 | 0.82 | 3.25 | 2.96 | 1.39 | 3.41 | 1.36 | 3.10 | 5.41 | 2.67 | 4.28 | 3.02 | 4.34 | 2.78 | 3.79 | 1.25 | 56.19 |

Table S2.1. Continued

| DH Line | A3G-3-3-1-3 | CI 540 | Fe (Parent of F1B1) | I-159 | IL1 2E | B2 (Parent of F1B1) | Oh 3167 B | Os 420 | Tr 9-1-1-6 | WD 456 | I224 | LE 23 | 461 | Hy | AH 83 | Non-IBD |
|---|---|---|---|---|---|---|---|---|---|---|---|---|---|---|---|---|
| C17_DH020 | 0.77 | 1.76 | 2.44 | 1.24 | 3.39 | 1.84 | 3.85 | 5.87 | 5.30 | 3.91 | 3.24 | 2.17 | 3.09 | 4.20 | 1.30 | 55.64 |
| C17_DH021 | 0.80 | 3.88 | 3.49 | 1.62 | 2.98 | 1.54 | 3.56 | 6.34 | 2.41 | 4.36 | 2.62 | 2.71 | 1.73 | 4.00 | 1.46 | 56.50 |
| C17_DH022 | 0.36 | 2.67 | 2.91 | 0.80 | 4.02 | 1.38 | 4.70 | 3.49 | 2.77 | 4.58 | 3.93 | 1.90 | 2.48 | 4.64 | 1.42 | 57.94 |
| C17_DH024 | 0.84 | 3.36 | 1.96 | 0.85 | 3.70 | 1.18 | 2.50 | 5.77 | 2.00 | 4.20 | 3.69 | 2.77 | 2.01 | 5.11 | 1.54 | 58.54 |
| C17_DH026 | 0.70 | 3.35 | 3.59 | 0.99 | 3.38 | 1.21 | 3.59 | 3.97 | 2.54 | 3.65 | 2.79 | 2.12 | 2.42 | 3.35 | 1.39 | 60.97 |
| C17_DH029 | 0.69 | 3.07 | 3.24 | 0.47 | 3.39 | 1.16 | 4.60 | 5.10 | 5.00 | 4.67 | 3.54 | 1.91 | 1.89 | 3.16 | 1.41 | 56.70 |
| C17_DH031 | 0.53 | 4.28 | 3.70 | 1.17 | 2.68 | 1.41 | 4.12 | 4.85 | 4.22 | 3.81 | 2.36 | 2.57 | 2.94 | 4.50 | 0.91 | 55.95 |
| C17_DH034 | 0.69 | 4.29 | 3.86 | 0.96 | 3.55 | 1.20 | 3.36 | 3.53 | 4.26 | 4.61 | 3.01 | 2.69 | 2.25 | 3.14 | 0.99 | 57.62 |
| C17_DH035 | 0.39 | 3.98 | 3.80 | 1.12 | 2.83 | 1.03 | 2.31 | 3.14 | 4.13 | 3.94 | 2.98 | 2.51 | 2.57 | 4.85 | 1.30 | 59.13 |
| C17_DH036 | 0.81 | 3.14 | 5.06 | 0.50 | 2.93 | 1.37 | 4.21 | 4.39 | 3.17 | 4.72 | 2.36 | 2.56 | 1.48 | 4.41 | 0.77 | 58.12 |
| C17_DH038 | 0.42 | 3.69 | 3.55 | 0.97 | 3.26 | 0.88 | 3.22 | 3.54 | 3.98 | 3.98 | 3.07 | 2.75 | 2.98 | 4.37 | 1.59 | 57.75 |
| C17_DH041 | 0.16 | 3.53 | 3.46 | 0.73 | 1.99 | 1.18 | 4.14 | 4.08 | 3.17 | 4.09 | 1.86 | 2.71 | 1.46 | 4.17 | 0.77 | 62.50 |
| C17_DH043 | 0.12 | 2.88 | 3.21 | 0.91 | 2.09 | 2.11 | 3.96 | 3.60 | 2.94 | 3.86 | 1.94 | 2.77 | 2.12 | 5.45 | 1.01 | 61.03 |
| C17_DH044 | 0.46 | 3.46 | 2.94 | 0.96 | 3.58 | 0.71 | 4.83 | 4.81 | 4.93 | 5.03 | 3.39 | 2.73 | 2.49 | 4.34 | 1.09 | 54.25 |
| C17_DH045 | 0.65 | 4.06 | 2.73 | 1.54 | 3.12 | 1.38 | 5.14 | 4.20 | 3.93 | 3.91 | 2.84 | 2.13 | 2.37 | 4.03 | 0.71 | 57.26 |
| C17_DH046 | 0.75 | 3.83 | 3.61 | 1.15 | 2.71 | 1.63 | 3.71 | 4.75 | 3.56 | 4.37 | 2.44 | 2.28 | 1.94 | 4.54 | 1.45 | 57.27 |
| C17_DH050 | 0.71 | 3.51 | 3.45 | 0.91 | 2.94 | 1.45 | 2.97 | 4.76 | 4.01 | 5.32 | 2.59 | 2.45 | 2.11 | 3.87 | 1.15 | 57.81 |
| C17_DH052 | 0.80 | 3.23 | 2.93 | 1.60 | 2.20 | 1.59 | 5.32 | 6.87 | 3.57 | 4.42 | 2.21 | 1.68 | 2.74 | 3.79 | 1.42 | 55.64 |
| C17_DH053 | 0.37 | 3.49 | 2.91 | 0.87 | 2.75 | 1.84 | 3.71 | 4.89 | 2.74 | 5.93 | 2.33 | 1.84 | 2.89 | 3.93 | 0.95 | 58.55 |
| C17_DH054 | 0.53 | 4.24 | 2.75 | 1.13 | 2.58 | 0.96 | 3.71 | 4.29 | 3.82 | 3.46 | 2.49 | 2.63 | 2.27 | 3.13 | 1.33 | 60.70 |
| C17_DH055 | 0.55 | 3.76 | 4.31 | 0.85 | 2.82 | 1.08 | 3.35 | 4.42 | 2.81 | 4.65 | 2.72 | 1.40 | 3.07 | 4.94 | 1.60 | 57.69 |
| C17_DH056 | 0.51 | 3.18 | 2.95 | 1.16 | 3.25 | 1.10 | 4.42 | 4.83 | 2.64 | 4.99 | 3.24 | 2.03 | 3.17 | 4.39 | 0.87 | 57.27 |
| C17_DH058 | 0.45 | 3.10 | 3.61 | 0.97 | 2.89 | 1.48 | 4.61 | 3.92 | 3.06 | 4.07 | 2.71 | 2.48 | 1.82 | 4.90 | 1.28 | 58.64 |
| C17_DH061 | 0.64 | 4.77 | 2.57 | 1.12 | 3.42 | 0.99 | 4.35 | 4.68 | 1.66 | 4.82 | 2.94 | 2.23 | 2.92 | 3.90 | 1.00 | 57.97 |
| C17_DH062 | 0.64 | 3.99 | 4.04 | 0.84 | 2.33 | 1.05 | 3.57 | 4.78 | 4.15 | 4.86 | 2.18 | 2.05 | 2.26 | 4.39 | 0.93 | 57.93 |
| C17_DH064 | 0.94 | 3.47 | 2.84 | 1.46 | 2.92 | 1.48 | 3.60 | 4.01 | 3.73 | 4.33 | 2.66 | 2.57 | 2.79 | 3.38 | 1.52 | 58.31 |
| C17_DH066 | 0.81 | 2.90 | 2.02 | 1.58 | 2.64 | 1.79 | 4.23 | 4.92 | 3.41 | 3.68 | 2.58 | 2.60 | 2.00 | 3.18 | 1.31 | 60.34 |
| C17_DH067 | 0.66 | 3.61 | 3.75 | 1.09 | 2.89 | 1.08 | 3.51 | 5.65 | 2.92 | 5.22 | 2.59 | 2.00 | 2.79 | 3.83 | 1.30 | 57.12 |
| C17_DH071 | 0.83 | 4.42 | 3.17 | 1.06 | 3.01 | 1.26 | 3.75 | 2.56 | 1.42 | 4.35 | 3.29 | 2.47 | 2.58 | 3.76 | 0.89 | 61.19 |
| C17_DH072 | 0.91 | 3.04 | 4.52 | 1.24 | 1.97 | 1.29 | 3.62 | 4.44 | 3.75 | 4.35 | 2.04 | 2.53 | 3.26 | 4.10 | 1.13 | 57.81 |
| C17_DH074 | 0.85 | 3.26 | 3.87 | 1.41 | 2.54 | 1.09 | 3.12 | 5.78 | 3.76 | 3.62 | 2.55 | 2.96 | 3.04 | 4.29 | 1.20 | 56.66 |
| C17_DH077 | 0.66 | 3.91 | 2.29 | 1.40 | 3.08 | 1.58 | 3.76 | 4.63 | 3.76 | 4.10 | 2.75 | 1.83 | 1.97 | 4.83 | 1.01 | 58.45 |
| C17_DH078 | 0.62 | 3.80 | 2.01 | 1.46 | 2.85 | 1.71 | 3.07 | 5.02 | 4.39 | 4.29 | 2.52 | 2.34 | 2.65 | 4.37 | 0.94 | 57.97 |
| C17_DH079 | 0.64 | 3.21 | 2.85 | 0.68 | 2.77 | 1.44 | 3.20 | 4.77 | 4.51 | 3.54 | 2.98 | 1.97 | 3.05 | 4.46 | 0.75 | 59.16 |
| C17_DH080 | 0.82 | 3.58 | 4.04 | 1.13 | 3.39 | 1.43 | 4.22 | 5.09 | 4.34 | 4.65 | 2.52 | 1.88 | 2.89 | 3.41 | 1.38 | 55.21 |

Table S2.1. Continued

| DH Line | A3G-3-3-1-3 | CI 540 | Fe (Parent of F1B1) | I-159 | IL1 2E | B2 (Parent of F1B1) | Oh 3167 B | Os 420 | Tr 9-1-1-6 | WD 456 | I224 | LE 23 | 461 | Hy | AH 83 | Non-IBD |
|---|---|---|---|---|---|---|---|---|---|---|---|---|---|---|---|---|
| C17_DH082 | 0.49 | 3.43 | 3.32 | 0.68 | 3.08 | 1.05 | 3.58 | 3.76 | 4.15 | 4.26 | 2.84 | 2.96 | 2.98 | 4.42 | 1.51 | 57.48 |
| C17_DH087 | 0.60 | 3.52 | 3.98 | 1.18 | 2.26 | 1.18 | 4.54 | 3.75 | 2.82 | 3.53 | 2.14 | 1.98 | 4.07 | 4.17 | 1.19 | 59.09 |
| C17_DH089 | 0.92 | 4.64 | 4.11 | 1.19 | 2.86 | 0.83 | 3.04 | 3.28 | 5.05 | 3.08 | 2.98 | 3.12 | 2.25 | 3.21 | 0.95 | 58.48 |
| C17_DH090 | 0.65 | 3.28 | 3.87 | 0.96 | 3.06 | 1.29 | 3.79 | 5.16 | 3.35 | 3.71 | 3.53 | 2.50 | 2.45 | 5.93 | 1.21 | 55.26 |
| C17_DH091 | 1.08 | 4.15 | 2.47 | 0.89 | 2.89 | 1.89 | 4.23 | 3.40 | 4.70 | 2.62 | 2.82 | 2.75 | 2.10 | 5.18 | 2.01 | 56.80 |
| C17_DH093 | 0.64 | 4.03 | 2.74 | 1.10 | 2.87 | 1.19 | 4.45 | 3.83 | 3.37 | 5.76 | 2.69 | 1.93 | 2.35 | 4.16 | 0.80 | 58.07 |
| C17_DH098 | 0.63 | 3.04 | 4.52 | 1.66 | 1.91 | 1.41 | 3.97 | 5.13 | 2.54 | 5.73 | 1.59 | 2.79 | 2.47 | 4.67 | 1.27 | 56.68 |
| C17_DH102 | 1.14 | 4.00 | 4.52 | 1.05 | 2.52 | 1.31 | 4.63 | 3.78 | 3.74 | 5.75 | 2.35 | 1.36 | 2.53 | 4.17 | 0.82 | 56.33 |
| C17_DH103 | 0.51 | 3.29 | 4.06 | 1.03 | 2.54 | 1.05 | 3.93 | 5.25 | 2.12 | 4.16 | 2.62 | 1.87 | 1.99 | 4.85 | 0.93 | 59.78 |
| C17_DH105 | 0.47 | 2.12 | 2.16 | 1.39 | 2.63 | 1.73 | 4.45 | 6.33 | 5.54 | 3.59 | 2.24 | 2.46 | 3.78 | 5.28 | 0.98 | 54.85 |
| C17_DH106 | 0.95 | 4.18 | 4.89 | 1.33 | 2.37 | 1.14 | 3.81 | 4.40 | 4.25 | 5.27 | 2.02 | 1.71 | 3.04 | 3.91 | 1.18 | 55.57 |
| C17_DH107 | 0.55 | 3.53 | 2.68 | 0.80 | 3.28 | 1.14 | 3.51 | 3.86 | 1.59 | 4.97 | 2.64 | 1.85 | 2.21 | 4.37 | 1.21 | 61.81 |
| C17_DH108 | 0.39 | 3.04 | 3.67 | 1.01 | 2.22 | 0.91 | 4.17 | 3.97 | 4.04 | 3.86 | 2.10 | 3.57 | 2.61 | 3.58 | 1.25 | 59.60 |
| C17_DH109 | 0.08 | 2.52 | 2.99 | 1.21 | 2.22 | 1.69 | 4.14 | 5.69 | 3.26 | 5.31 | 2.35 | 3.01 | 2.16 | 2.83 | 1.10 | 59.44 |
| C17_DH110 | 0.85 | 2.78 | 2.66 | 1.02 | 2.57 | 1.55 | 3.76 | 4.35 | 4.65 | 5.06 | 2.68 | 3.46 | 1.97 | 4.21 | 1.37 | 57.06 |
| C17_DH111 | 0.76 | 3.99 | 3.92 | 0.92 | 2.79 | 1.39 | 3.01 | 6.43 | 3.35 | 4.21 | 2.44 | 2.70 | 2.08 | 3.84 | 1.27 | 56.89 |
| C17_DH113 | 1.12 | 3.43 | 4.27 | 0.98 | 2.92 | 1.41 | 4.22 | 4.42 | 1.79 | 4.85 | 2.89 | 3.12 | 2.30 | 3.32 | 0.97 | 58.00 |
| C17_DH115 | 0.49 | 4.43 | 3.00 | 0.92 | 2.17 | 1.67 | 2.82 | 5.07 | 3.62 | 3.15 | 1.97 | 3.29 | 3.30 | 3.98 | 1.00 | 59.13 |
| C17_DH116 | 0.54 | 2.69 | 2.53 | 1.00 | 2.81 | 0.75 | 3.85 | 6.05 | 3.83 | 3.59 | 3.05 | 2.06 | 2.35 | 3.65 | 1.04 | 60.23 |
| C17_DH118 | 0.46 | 2.73 | 3.74 | 1.14 | 2.58 | 1.02 | 4.18 | 3.93 | 3.14 | 3.98 | 2.54 | 2.93 | 2.69 | 3.61 | 1.19 | 60.14 |
| C17_DH119 | 0.68 | 3.96 | 3.83 | 0.86 | 3.07 | 1.04 | 4.29 | 3.25 | 3.88 | 3.95 | 2.96 | 3.06 | 2.22 | 4.18 | 0.74 | 58.01 |
| C17_DH120 | 0.43 | 3.52 | 3.43 | 0.93 | 2.95 | 1.51 | 2.71 | 4.00 | 2.63 | 4.27 | 2.92 | 1.85 | 1.91 | 4.37 | 1.04 | 61.52 |
| C17_DH121 | 0.64 | 4.63 | 3.48 | 1.26 | 2.86 | 1.32 | 3.56 | 4.67 | 2.97 | 4.57 | 2.63 | 2.60 | 3.28 | 4.03 | 1.24 | 56.25 |
| C17_DH124 | 0.67 | 3.59 | 2.65 | 1.44 | 2.25 | 1.45 | 4.04 | 4.55 | 2.72 | 4.39 | 2.43 | 2.04 | 3.28 | 4.33 | 1.21 | 58.95 |
| C17_DH126 | 0.92 | 4.16 | 3.18 | 1.01 | 3.07 | 1.48 | 3.75 | 3.43 | 3.38 | 4.43 | 2.47 | 2.57 | 3.27 | 3.85 | 1.19 | 57.85 |
| C17_DH127 | 0.53 | 2.68 | 4.34 | 0.61 | 2.46 | 1.06 | 3.01 | 6.05 | 2.68 | 4.80 | 2.31 | 2.59 | 2.59 | 3.46 | 0.87 | 59.96 |
| C17_DH128 | 0.49 | 2.56 | 3.49 | 1.24 | 2.88 | 1.41 | 4.21 | 3.37 | 2.40 | 3.41 | 2.60 | 3.64 | 2.33 | 3.24 | 1.01 | 61.73 |
| C17_DH129 | 0.64 | 3.20 | 3.10 | 1.24 | 2.78 | 1.29 | 4.02 | 6.68 | 2.19 | 3.93 | 2.73 | 2.82 | 2.47 | 4.16 | 1.35 | 57.41 |
| C17_DH132 | 0.41 | 2.42 | 2.37 | 1.27 | 3.01 | 1.42 | 3.93 | 4.39 | 3.32 | 4.03 | 3.20 | 1.93 | 3.42 | 4.05 | 1.05 | 59.78 |
| C17_DH134 | 0.61 | 2.73 | 2.61 | 1.39 | 2.92 | 1.69 | 3.65 | 5.74 | 2.87 | 3.59 | 2.90 | 1.83 | 3.22 | 4.37 | 1.22 | 58.66 |
| C17_DH135 | 0.76 | 4.14 | 4.44 | 1.11 | 2.91 | 1.35 | 3.54 | 5.02 | 3.33 | 5.71 | 2.80 | 2.72 | 2.17 | 2.57 | 1.39 | 56.05 |
| C17_DH136 | 0.48 | 4.08 | 2.68 | 0.63 | 3.09 | 1.83 | 3.72 | 4.96 | 2.89 | 4.98 | 2.80 | 2.09 | 1.99 | 4.84 | 1.26 | 57.68 |
| C17_DH138 | 0.67 | 3.68 | 2.63 | 1.28 | 2.89 | 1.61 | 3.40 | 4.50 | 3.25 | 4.11 | 2.96 | 2.28 | 3.36 | 3.36 | 1.46 | 58.56 |
| C17_DH139 | 0.69 | 3.72 | 3.53 | 1.17 | 3.65 | 0.83 | 3.58 | 4.37 | 4.86 | 3.54 | 3.46 | 3.12 | 1.98 | 4.07 | 1.10 | 56.30 |
| C17_DH140 | 0.83 | 2.68 | 2.39 | 0.63 | 3.32 | 1.07 | 4.04 | 3.84 | 3.34 | 5.04 | 2.91 | 2.88 | 1.57 | 3.94 | 1.45 | 60.06 |

Table S2.1. Continued

| DH Line | A3G-3-3-1-3 | CI 540 | Fe (Parent of F1B1) | I-159 | IL1 2E | B2 (Parent of F1B1) | Oh 3167 B | Os 420 | Tr 9-1-1-6 | WD 456 | I224 | LE 23 | 461 | Hy | AH 83 | Non-IBD |
|---|---|---|---|---|---|---|---|---|---|---|---|---|---|---|---|---|
| C17_DH142 | 0.50 | 3.71 | 3.41 | 1.01 | 3.37 | 0.93 | 4.35 | 4.71 | 3.95 | 5.08 | 2.79 | 1.46 | 2.01 | 4.09 | 1.09 | 57.52 |
| C17_DH143 | 0.55 | 4.13 | 4.43 | 1.40 | 3.75 | 1.17 | 4.44 | 4.12 | 4.14 | 3.53 | 3.64 | 2.57 | 2.09 | 4.03 | 1.65 | 54.37 |
| C17_DH144 | 0.54 | 3.87 | 2.66 | 1.08 | 3.72 | 0.93 | 2.39 | 7.28 | 3.07 | 4.26 | 3.47 | 2.17 | 3.32 | 4.32 | 1.22 | 55.67 |
| C17_DH146 | 0.37 | 2.70 | 4.02 | 0.91 | 2.22 | 1.19 | 4.96 | 4.86 | 2.70 | 4.32 | 1.78 | 2.05 | 2.07 | 3.45 | 0.91 | 61.50 |
| C17_DH147 | 0.66 | 3.93 | 3.41 | 1.20 | 3.06 | 0.92 | 3.54 | 4.70 | 4.15 | 4.76 | 2.78 | 2.88 | 2.58 | 4.24 | 1.16 | 56.02 |
| C17_DH150 | 0.92 | 2.35 | 3.58 | 0.84 | 2.41 | 1.62 | 3.03 | 4.50 | 3.42 | 3.51 | 2.51 | 3.12 | 2.79 | 3.06 | 1.42 | 60.91 |
| C17_DH152 | 0.76 | 2.64 | 2.74 | 1.17 | 2.59 | 1.71 | 4.13 | 5.28 | 4.72 | 4.24 | 2.41 | 2.38 | 2.91 | 4.56 | 1.58 | 56.17 |
| C17_DH153 | 0.80 | 2.83 | 3.38 | 1.32 | 3.02 | 1.90 | 2.47 | 5.89 | 4.26 | 2.98 | 3.43 | 3.13 | 1.64 | 4.00 | 1.12 | 57.83 |
| C17_DH154 | 0.58 | 3.46 | 3.23 | 0.93 | 2.18 | 1.31 | 3.02 | 6.17 | 4.49 | 3.50 | 2.42 | 1.94 | 2.96 | 5.18 | 1.12 | 57.49 |
| C17_DH155 | 0.52 | 4.00 | 1.96 | 0.50 | 3.12 | 1.64 | 4.26 | 4.19 | 3.27 | 5.59 | 3.26 | 2.44 | 2.49 | 4.34 | 1.15 | 57.26 |
| C17_DH158 | 0.50 | 2.62 | 3.33 | 1.57 | 2.13 | 1.93 | 2.70 | 5.14 | 2.33 | 3.64 | 2.32 | 3.40 | 3.25 | 4.15 | 1.30 | 59.69 |
| C17_DH160 | 0.61 | 3.03 | 1.89 | 1.20 | 3.14 | 1.54 | 3.72 | 3.49 | 4.65 | 3.12 | 3.10 | 1.82 | 1.90 | 4.39 | 1.27 | 61.15 |
| C17_DH161 | 0.59 | 2.14 | 2.01 | 0.88 | 2.04 | 2.09 | 3.82 | 5.29 | 4.01 | 3.65 | 1.91 | 2.95 | 2.21 | 4.20 | 1.40 | 60.80 |
| C17_DH162 | 0.34 | 2.63 | 2.90 | 1.23 | 2.65 | 1.59 | 4.54 | 4.47 | 3.42 | 4.08 | 2.77 | 2.08 | 3.51 | 4.07 | 0.97 | 58.75 |
| C17_DH163 | 0.90 | 3.21 | 2.43 | 1.13 | 3.07 | 1.73 | 3.00 | 5.27 | 1.91 | 3.73 | 3.29 | 2.91 | 2.43 | 4.64 | 1.67 | 58.67 |
| C17_DH165 | 0.59 | 4.13 | 2.81 | 1.12 | 2.70 | 0.84 | 3.27 | 3.94 | 3.01 | 4.88 | 2.41 | 1.76 | 2.92 | 4.48 | 1.02 | 60.12 |
| C17_DH166 | 0.71 | 2.92 | 3.36 | 1.24 | 2.35 | 0.83 | 4.53 | 4.47 | 2.82 | 4.62 | 2.13 | 2.60 | 2.59 | 2.64 | 0.93 | 61.27 |
| C17_DH167 | 0.93 | 3.07 | 3.04 | 1.25 | 2.74 | 1.67 | 4.41 | 4.09 | 4.08 | 3.57 | 2.86 | 3.90 | 2.14 | 5.48 | 1.68 | 55.11 |
| C17_DH169 | 0.38 | 3.36 | 3.56 | 1.26 | 2.43 | 1.62 | 3.92 | 4.73 | 4.50 | 3.11 | 2.29 | 1.94 | 2.72 | 4.31 | 1.36 | 58.52 |
| C17_DH170 | 0.32 | 3.15 | 3.76 | 1.10 | 2.78 | 1.07 | 3.90 | 3.40 | 4.23 | 3.92 | 2.74 | 2.12 | 2.96 | 3.10 | 1.78 | 59.68 |
| C17_DH172 | 0.61 | 3.57 | 3.27 | 1.12 | 2.97 | 1.46 | 4.56 | 3.83 | 2.16 | 4.15 | 2.60 | 2.93 | 2.62 | 3.63 | 1.10 | 59.42 |
| C17_DH174 | 0.55 | 3.46 | 2.53 | 1.25 | 3.03 | 1.31 | 4.49 | 5.25 | 2.62 | 4.37 | 2.87 | 2.13 | 2.10 | 2.92 | 1.13 | 60.00 |
| C17_DH175 | 0.75 | 4.41 | 3.20 | 1.21 | 3.16 | 1.18 | 2.84 | 4.21 | 4.11 | 5.05 | 2.75 | 2.90 | 2.73 | 4.06 | 0.95 | 56.49 |
| C17_DH177 | 0.82 | 3.54 | 2.69 | 1.28 | 3.19 | 1.20 | 2.15 | 5.81 | 3.41 | 3.77 | 3.11 | 1.60 | 2.85 | 4.53 | 1.23 | 58.82 |
| C17_DH179 | 0.66 | 4.24 | 2.91 | 1.09 | 2.88 | 1.07 | 3.99 | 4.12 | 4.02 | 3.43 | 3.01 | 2.07 | 3.00 | 3.51 | 1.20 | 58.80 |
| C17_DH180 | 0.85 | 2.84 | 4.04 | 0.75 | 3.44 | 0.92 | 4.12 | 4.07 | 5.09 | 3.61 | 2.85 | 1.82 | 2.31 | 3.79 | 1.49 | 58.00 |
| C17_DH181 | 0.24 | 3.67 | 3.34 | 1.43 | 3.56 | 0.82 | 3.86 | 4.12 | 3.99 | 3.58 | 3.03 | 2.46 | 2.23 | 4.26 | 0.85 | 58.56 |
| C17_DH184 | 1.02 | 4.49 | 4.08 | 1.03 | 2.92 | 0.99 | 3.51 | 2.95 | 3.28 | 3.29 | 2.61 | 3.40 | 2.55 | 3.06 | 1.22 | 59.59 |
| C17_DH188 | 0.49 | 3.22 | 1.81 | 1.03 | 3.17 | 1.15 | 2.92 | 2.88 | 3.77 | 4.42 | 3.10 | 3.71 | 3.14 | 4.32 | 1.17 | 59.72 |
| C17_DH189 | 0.59 | 4.42 | 2.73 | 1.41 | 2.59 | 0.99 | 2.99 | 3.54 | 4.02 | 3.27 | 3.09 | 2.66 | 2.29 | 3.59 | 0.57 | 61.25 |
| C17_DH190 | 0.24 | 2.93 | 2.64 | 1.41 | 2.17 | 1.31 | 2.70 | 3.77 | 4.75 | 3.28 | 2.26 | 2.61 | 3.72 | 4.30 | 1.03 | 60.88 |
| C17_DH191 | 0.68 | 3.53 | 2.50 | 1.13 | 2.48 | 1.13 | 4.43 | 3.40 | 3.49 | 4.17 | 2.49 | 3.40 | 1.93 | 4.86 | 1.15 | 59.23 |
| C17_DH195 | 0.58 | 4.18 | 4.25 | 1.26 | 2.57 | 1.35 | 2.54 | 3.58 | 5.68 | 3.23 | 2.20 | 3.75 | 2.03 | 3.07 | 1.26 | 58.48 |
| C17_DH196 | 0.52 | 3.15 | 3.35 | 1.68 | 2.63 | 1.56 | 3.18 | 4.05 | 4.28 | 4.18 | 2.26 | 2.28 | 2.13 | 4.71 | 1.63 | 58.42 |
| C17_DH202 | 0.93 | 2.79 | 2.89 | 1.27 | 2.98 | 1.11 | 4.50 | 3.29 | 3.31 | 5.24 | 2.71 | 2.88 | 2.58 | 4.02 | 1.36 | 58.14 |

Table S2.1. Continued

| DH Line | A3G-3-3-1-3 | CI 540 | Fe (Parent of F1B1) | I-159 | IL1 2E | B2 (Parent of F1B1) | Oh 3167 B | Os 420 | Tr 9-1-1-6 | WD 456 | I224 | LE 23 | 461 | Hy | AH 83 | Non-IBD |
|---|---|---|---|---|---|---|---|---|---|---|---|---|---|---|---|---|
| C17_DH205 | 0.51 | 3.08 | 3.00 | 1.22 | 3.06 | 1.27 | 3.09 | 4.76 | 4.39 | 4.77 | 2.96 | 2.73 | 1.64 | 4.99 | 1.15 | 57.38 |
| C17_DH210 | 0.64 | 2.19 | 4.10 | 1.11 | 2.67 | 1.27 | 3.94 | 5.03 | 4.92 | 4.22 | 2.77 | 2.94 | 2.05 | 3.57 | 0.90 | 57.68 |
| C17_DH216 | 0.54 | 3.55 | 4.01 | 1.20 | 2.43 | 1.54 | 4.47 | 5.50 | 3.39 | 3.02 | 2.66 | 2.97 | 2.57 | 4.47 | 1.30 | 56.37 |
| C17_DH217 | 0.71 | 3.38 | 3.28 | 1.43 | 3.53 | 1.51 | 3.40 | 4.27 | 3.32 | 2.90 | 3.42 | 2.49 | 2.58 | 4.73 | 1.24 | 57.82 |
| C17_DH218 | 0.49 | 3.24 | 4.92 | 0.85 | 2.39 | 1.03 | 3.87 | 4.05 | 4.46 | 3.57 | 2.26 | 2.09 | 1.66 | 3.44 | 1.00 | 60.67 |
| C17_DH219 | 0.51 | 3.54 | 3.11 | 1.51 | 2.97 | 1.56 | 2.36 | 7.20 | 2.55 | 3.80 | 2.90 | 2.52 | 2.85 | 3.84 | 0.85 | 57.94 |
| C17_DH220 | 0.89 | 3.86 | 3.93 | 1.15 | 1.86 | 1.16 | 4.35 | 4.20 | 3.25 | 3.27 | 1.96 | 2.88 | 2.38 | 4.22 | 0.92 | 59.73 |
| C17_DH221 | 0.83 | 2.90 | 3.47 | 1.69 | 2.63 | 1.16 | 4.88 | 5.37 | 3.67 | 3.10 | 2.50 | 2.35 | 2.47 | 3.24 | 1.32 | 58.41 |
| C17_DH223 | 1.01 | 3.89 | 3.70 | 0.87 | 3.31 | 1.07 | 5.45 | 4.10 | 2.20 | 3.03 | 3.19 | 2.18 | 3.73 | 4.38 | 1.50 | 56.40 |
| C17_DH224 | 0.69 | 3.98 | 2.90 | 1.18 | 3.39 | 1.10 | 3.15 | 3.03 | 2.23 | 3.57 | 3.00 | 2.31 | 2.13 | 3.10 | 1.12 | 63.11 |
| C17_DH225 | 0.43 | 3.09 | 3.26 | 0.87 | 3.12 | 1.22 | 3.26 | 4.37 | 3.86 | 5.01 | 2.56 | 2.90 | 2.94 | 3.59 | 0.78 | 58.73 |
| C17_DH226 | 0.48 | 4.25 | 3.16 | 0.76 | 3.10 | 1.34 | 4.24 | 4.55 | 3.93 | 3.93 | 2.75 | 2.45 | 2.71 | 4.34 | 1.39 | 56.62 |
| C17_DH228 | 0.59 | 2.55 | 3.64 | 0.99 | 3.92 | 1.29 | 4.66 | 2.77 | 2.30 | 3.84 | 3.47 | 4.57 | 3.39 | 4.15 | 0.94 | 56.94 |
| C17_DH232 | 0.74 | 3.14 | 2.77 | 1.07 | 2.51 | 1.63 | 3.52 | 4.95 | 3.92 | 4.86 | 2.76 | 2.76 | 2.61 | 5.07 | 0.90 | 56.78 |
| C17_DH233 | 0.75 | 4.06 | 4.17 | 0.92 | 2.79 | 1.46 | 2.99 | 6.20 | 3.17 | 4.48 | 2.44 | 2.68 | 2.15 | 3.79 | 1.13 | 56.82 |
| C17_DH236 | 0.19 | 3.08 | 2.11 | 1.34 | 3.11 | 1.20 | 4.40 | 4.36 | 4.73 | 3.77 | 3.07 | 3.04 | 2.63 | 4.19 | 0.94 | 57.85 |
| C17_DH238 | 0.70 | 3.47 | 3.50 | 0.96 | 2.19 | 1.32 | 3.89 | 4.87 | 3.62 | 4.41 | 2.19 | 2.79 | 2.47 | 3.23 | 1.24 | 59.15 |
| C17_DH239 | 0.70 | 3.86 | 2.76 | 1.29 | 2.78 | 1.19 | 3.41 | 4.59 | 4.63 | 2.97 | 2.62 | 2.55 | 3.32 | 3.90 | 1.04 | 58.39 |
| C17_DH240 | 0.69 | 2.77 | 1.76 | 1.58 | 2.91 | 1.46 | 3.55 | 5.22 | 3.76 | 3.81 | 3.01 | 2.79 | 3.17 | 3.89 | 1.33 | 58.29 |
| C17_DH241 | 0.46 | 4.91 | 3.42 | 0.86 | 2.03 | 1.27 | 3.43 | 5.85 | 2.59 | 4.96 | 2.05 | 1.74 | 1.77 | 2.72 | 1.01 | 60.92 |
| C17_DH243 | 0.64 | 3.57 | 3.40 | 1.21 | 2.73 | 1.18 | 3.69 | 5.07 | 5.06 | 3.84 | 2.27 | 3.15 | 2.58 | 3.46 | 0.97 | 57.18 |
| C17_DH244 | 1.04 | 4.16 | 3.50 | 1.34 | 3.31 | 1.43 | 4.49 | 5.37 | 4.10 | 3.61 | 2.74 | 1.35 | 2.35 | 3.21 | 1.34 | 56.64 |
| C17_DH247 | 0.69 | 2.77 | 2.41 | 1.05 | 2.91 | 1.77 | 2.69 | 5.47 | 3.73 | 3.53 | 3.00 | 2.72 | 2.27 | 4.42 | 0.96 | 59.61 |
| C17_DH248 | 0.90 | 2.04 | 2.41 | 1.39 | 3.23 | 1.84 | 4.58 | 3.96 | 4.43 | 3.99 | 2.96 | 2.39 | 3.89 | 2.73 | 1.35 | 57.93 |
| C17_DH252 | 0.42 | 4.62 | 3.77 | 0.99 | 3.06 | 1.41 | 3.46 | 4.85 | 2.89 | 5.33 | 2.84 | 2.60 | 2.23 | 3.97 | 1.07 | 56.48 |
| C17_DH253 | 1.10 | 4.13 | 2.82 | 0.73 | 2.38 | 1.65 | 4.21 | 4.42 | 4.61 | 4.51 | 2.31 | 1.44 | 2.84 | 3.81 | 1.53 | 57.54 |
| C17_DH255 | 1.02 | 3.05 | 3.00 | 0.60 | 2.97 | 1.55 | 3.87 | 4.58 | 2.56 | 3.84 | 2.87 | 1.59 | 2.97 | 4.33 | 1.05 | 60.15 |
| C17_DH258 | 1.06 | 3.21 | 3.82 | 0.93 | 2.97 | 1.82 | 3.74 | 3.78 | 3.39 | 4.77 | 2.67 | 2.41 | 2.78 | 3.25 | 1.09 | 58.30 |
| C17_DH259 | 0.71 | 5.03 | 3.93 | 0.61 | 2.39 | 1.46 | 3.43 | 4.12 | 3.82 | 5.51 | 2.50 | 2.10 | 2.26 | 3.60 | 1.14 | 57.40 |
| C17_DH262 | 0.75 | 4.10 | 3.43 | 1.12 | 2.54 | 1.18 | 3.46 | 5.57 | 2.76 | 3.38 | 2.32 | 2.38 | 2.25 | 3.52 | 1.68 | 59.56 |
| C17_DH264 | 0.34 | 3.56 | 3.50 | 0.67 | 2.99 | 1.27 | 2.58 | 4.59 | 3.52 | 4.79 | 2.76 | 2.02 | 3.52 | 3.68 | 1.11 | 59.11 |
| C17_DH265 | 0.55 | 4.30 | 3.13 | 1.28 | 2.88 | 1.22 | 3.49 | 5.16 | 3.68 | 4.10 | 2.86 | 2.47 | 2.40 | 3.80 | 1.46 | 57.24 |
| C17_DH267 | 0.90 | 3.35 | 3.76 | 0.85 | 2.54 | 1.26 | 2.73 | 5.20 | 3.33 | 3.77 | 2.18 | 2.91 | 2.14 | 2.90 | 1.66 | 60.51 |
| C17_DH268 | 0.70 | 3.70 | 3.88 | 0.78 | 2.60 | 1.48 | 3.66 | 5.93 | 4.21 | 4.74 | 2.46 | 2.64 | 2.82 | 3.57 | 1.45 | 55.38 |
| C17_DH270 | 0.30 | 4.10 | 3.93 | 0.99 | 2.80 | 1.29 | 3.21 | 4.85 | 3.14 | 5.11 | 2.54 | 1.77 | 3.38 | 4.29 | 1.37 | 56.93 |

Table S2.1. Continued

| DH Line | A3G-3-3-1-3 | CI 540 | Fe (Parent of F1B1) | I-159 | IL1 2E | B2 (Parent of F1B1) | Oh 3167 B | Os 420 | Tr 9-1-1-6 | WD 456 | I224 | LE 23 | 461 | Hy | AH 83 | Non-IBD |
|---|---|---|---|---|---|---|---|---|---|---|---|---|---|---|---|---|
| C17_DH271 | 0.80 | 4.15 | 4.69 | 1.04 | 2.44 | 1.54 | 3.95 | 5.66 | 2.36 | 3.54 | 2.48 | 3.23 | 2.81 | 5.16 | 1.33 | 54.81 |
| C17_DH273 | 0.60 | 3.35 | 3.95 | 1.69 | 1.85 | 1.74 | 3.06 | 4.72 | 3.73 | 3.48 | 1.65 | 2.45 | 3.03 | 4.93 | 1.27 | 58.50 |
| C17_DH280 | 0.68 | 3.37 | 2.95 | 1.18 | 2.63 | 1.19 | 3.95 | 5.90 | 2.73 | 3.92 | 2.33 | 1.90 | 2.67 | 4.31 | 0.98 | 59.33 |
| C17_DH282 | 0.51 | 3.38 | 3.15 | 0.89 | 3.86 | 1.68 | 3.17 | 5.27 | 3.01 | 5.11 | 2.94 | 2.04 | 2.92 | 3.53 | 1.70 | 56.84 |
| C17_DH283 | 0.33 | 3.16 | 2.93 | 0.98 | 2.89 | 1.83 | 3.56 | 6.80 | 3.77 | 3.72 | 3.10 | 1.99 | 2.80 | 5.75 | 1.00 | 55.38 |
| C17_DH284 | 0.77 | 3.57 | 4.12 | 1.17 | 1.88 | 1.49 | 2.32 | 5.41 | 2.23 | 4.22 | 1.88 | 4.30 | 1.80 | 4.38 | 1.06 | 59.42 |
| C17_DH286 | 0.68 | 3.41 | 2.98 | 0.92 | 2.98 | 1.50 | 3.43 | 5.83 | 3.01 | 3.66 | 2.51 | 2.53 | 2.07 | 4.53 | 0.83 | 59.14 |
| C17_DH287 | 0.78 | 3.62 | 4.00 | 1.31 | 2.91 | 1.14 | 3.98 | 3.16 | 3.53 | 4.48 | 2.48 | 2.76 | 3.07 | 3.14 | 1.78 | 57.85 |
| C17_DH290 | 0.46 | 4.66 | 3.10 | 1.22 | 3.01 | 1.34 | 4.49 | 3.56 | 4.52 | 4.09 | 3.02 | 3.02 | 2.13 | 4.94 | 1.40 | 55.05 |
| C17_DH294 | 0.43 | 2.56 | 2.67 | 1.19 | 3.38 | 0.84 | 5.13 | 2.70 | 4.39 | 3.50 | 3.06 | 2.83 | 1.71 | 3.92 | 0.59 | 61.12 |
| C17_DH296 | 0.39 | 2.33 | 2.42 | 1.11 | 2.35 | 1.34 | 4.41 | 4.82 | 3.13 | 3.03 | 2.23 | 2.94 | 3.31 | 4.93 | 1.15 | 60.10 |
| C17_DH297 | 0.58 | 3.89 | 3.66 | 0.93 | 2.22 | 1.29 | 3.93 | 5.73 | 2.15 | 4.00 | 2.34 | 2.08 | 2.46 | 3.37 | 1.51 | 59.87 |
| C17_DH298 | 0.55 | 3.39 | 4.18 | 1.34 | 2.36 | 0.92 | 3.78 | 3.00 | 3.32 | 4.40 | 2.44 | 1.95 | 3.06 | 5.36 | 1.13 | 58.83 |
| C17_DH299 | 0.65 | 4.08 | 1.57 | 1.08 | 2.64 | 1.65 | 3.23 | 4.32 | 1.92 | 3.59 | 2.68 | 1.79 | 2.30 | 4.54 | 1.03 | 62.93 |
| C17_DH301 | 0.42 | 2.62 | 5.33 | 1.46 | 2.63 | 1.97 | 3.67 | 4.45 | 2.97 | 3.52 | 1.95 | 3.25 | 3.40 | 3.70 | 1.59 | 57.07 |
| C17_DH304 | 0.51 | 3.96 | 3.84 | 0.96 | 2.91 | 1.43 | 4.28 | 4.50 | 3.09 | 3.96 | 2.55 | 2.94 | 3.30 | 4.41 | 1.20 | 56.17 |
| C17_DH305 | 0.35 | 3.04 | 4.08 | 1.09 | 2.58 | 1.12 | 3.77 | 3.64 | 2.11 | 3.38 | 2.27 | 3.69 | 1.47 | 3.67 | 1.24 | 62.49 |
| C17_DH307 | 0.87 | 3.18 | 2.53 | 0.97 | 2.46 | 1.32 | 2.65 | 6.19 | 4.07 | 3.70 | 2.65 | 1.79 | 2.40 | 3.64 | 1.27 | 60.29 |
| C17_DH308 | 0.46 | 3.33 | 3.13 | 1.30 | 2.22 | 1.20 | 3.84 | 4.38 | 3.84 | 5.02 | 2.13 | 1.64 | 2.20 | 3.02 | 1.15 | 61.15 |
| C17_DH309 | 0.80 | 4.38 | 2.88 | 1.14 | 2.58 | 1.34 | 3.63 | 4.24 | 2.88 | 4.27 | 2.32 | 3.14 | 2.38 | 2.53 | 0.98 | 60.50 |
| C17_DH310 | 0.91 | 2.32 | 2.50 | 1.12 | 2.88 | 1.54 | 3.73 | 5.58 | 4.02 | 3.84 | 2.69 | 2.67 | 3.45 | 2.53 | 1.26 | 58.96 |
| C17_DH311 | 0.78 | 3.87 | 1.93 | 0.91 | 3.31 | 1.67 | 3.95 | 4.04 | 5.16 | 3.98 | 3.31 | 2.39 | 2.24 | 3.86 | 0.88 | 57.73 |
| C17_DH312 | 0.26 | 2.18 | 4.51 | 0.66 | 2.60 | 1.07 | 2.91 | 5.89 | 2.51 | 4.08 | 2.85 | 2.94 | 2.98 | 4.71 | 1.20 | 58.65 |
| C17_DH313 | 0.35 | 3.42 | 3.58 | 1.30 | 3.17 | 1.12 | 2.65 | 4.78 | 2.85 | 3.98 | 2.45 | 3.44 | 3.49 | 3.73 | 1.32 | 58.37 |
| C17_DH315 | 0.50 | 3.20 | 3.67 | 1.06 | 2.05 | 1.01 | 3.25 | 5.20 | 2.42 | 4.06 | 2.23 | 1.82 | 2.55 | 5.46 | 1.10 | 60.44 |
| C17_DH316 | 0.63 | 2.87 | 3.66 | 0.51 | 2.47 | 1.21 | 2.74 | 5.57 | 5.17 | 4.04 | 2.48 | 2.89 | 1.25 | 4.43 | 0.63 | 59.45 |
| C17_DH317 | 0.33 | 4.71 | 4.79 | 1.05 | 2.23 | 1.21 | 4.21 | 4.57 | 3.20 | 4.55 | 2.33 | 1.20 | 2.32 | 4.35 | 1.12 | 57.81 |
| C17_DH319 | 0.39 | 3.05 | 4.48 | 0.81 | 3.17 | 1.69 | 4.16 | 3.25 | 3.50 | 4.24 | 3.07 | 1.83 | 1.75 | 4.39 | 0.88 | 59.35 |
| C17_DH321 | 0.45 | 4.10 | 2.20 | 0.94 | 2.48 | 0.99 | 4.49 | 3.92 | 4.55 | 5.30 | 2.46 | 2.20 | 2.94 | 3.52 | 1.07 | 58.40 |
| C17_DH323 | 0.90 | 3.78 | 2.88 | 0.62 | 2.46 | 1.73 | 3.24 | 4.58 | 3.83 | 3.90 | 2.27 | 2.36 | 3.82 | 4.04 | 1.71 | 57.88 |
| C17_DH324 | 0.53 | 4.27 | 2.40 | 0.93 | 2.92 | 1.17 | 3.65 | 4.45 | 4.52 | 3.75 | 2.51 | 3.20 | 2.15 | 3.11 | 1.26 | 59.17 |
| C17_DH326 | 0.69 | 3.43 | 3.65 | 1.07 | 2.48 | 1.31 | 2.75 | 5.04 | 4.55 | 4.75 | 2.32 | 2.27 | 3.41 | 5.03 | 0.94 | 56.30 |
| C17_DH327 | 0.62 | 4.31 | 2.92 | 1.17 | 2.41 | 1.38 | 3.24 | 3.85 | 3.26 | 3.63 | 2.03 | 3.01 | 2.83 | 4.27 | 1.14 | 59.94 |
| C17_DH332 | 0.97 | 3.68 | 3.23 | 1.12 | 2.96 | 1.01 | 4.20 | 3.47 | 3.85 | 4.64 | 2.81 | 1.79 | 2.24 | 4.12 | 0.83 | 59.07 |

# CHAPTER 3. GENOME-WIDE ASSOCIATION ANALYSIS OF PLANT ARCHITECTURE TRAITS USING DOUBLED HAPLOID LINES DERIVED FROM DIFFERENT CYCLES OF THE IOWA STIFF STALK SYNTHETIC MAIZE POPULATION

Alejandro Ledesma[1], Fernando S. Aguilar[1], Jode Edwards[2], Ursula Frei[1], and Thomas Lübberstedt[1]

[1]Department of Agronomy, Iowa State University, Ames, IA 50011, USA.

[2]USDA-ARS Corn Insects and Crop Genetics Research Unit, Ames, IA 50011, USA.

Modified from a manuscript to be submitted to *Theoretical and Applied Genetics*

## Abstract

Selection in the Iowa Stiff Stalk Synthetic (BSSS) maize population for high yield, grain moisture, and root and stalk lodging has indirectly modified plant architecture traits that are important for adaptation to high plant density. In this study, we developed Doubled Haploid (DH) lines from the BSSS maize population in the earlier cycle "C0" (BSSS(R)C0), the later cycle "C17" (BSSS(R)17), and the cross between the two cycles "C0/C17" (BSSS(R)C0/BSSS(R)C17). The DH lines developed plus the 16 progenitors were evaluated in a *per se* evaluation trial and phenotypic data were collected on an individual plot basis for male flowering, female flowering, anthesis-silking interval, plant height, ear height, flag leaf angle, tassel length, and the number of primary tassel branches to compare C0, C17, and C0/C17 derived DH lines for plant architecture traits and identify DH lines with both significant C0 background and in addition modern plant architecture traits conferring adaptation to high plant density, that could be used as genetic resources. Using the genotypic and phenotypic information of the BSSS DH lines, we performed Genome-Wide Association Studies (GWAS) to identify regions in the genome associated with these plant architecture changes. Descriptive statistical analysis confirmed trait variability in the different groups of DH lines. Considerable variation

between populations was observed for all traits except for plant height. As expected, phenotypic differences ($P \leq 0.001$) were found between different groups of DH lines, indicating a wide range of variability present. DH lines within the C0_DHL group had the highest mean values for flowering time, ear height, flag leaf angle, and the number of primary tassel branches and were statistically different ($P \leq 0.001$) between the groups of DH lines. Using GWAS analysis, significant SNP markers-trait associations were found in flowering and plant architecture traits using different GWAS analysis models. 38 SNP markers were found associated with different evaluated traits across more than one method tested and among the groups of DH lines. The genome regions with the highest significance were found on chromosome 2 and 7 for the traits number of primary tassel branches and flag leaf angles. By searching for candidate genes up and downstream of the 38 in common significant SNP markers, 55 candidate genes were associated with flowering time and different plant architecture traits. DH lines developed from the BSSS maize population are useful for association analysis, identifying candidate genes controlling plant architecture traits. This study may help to elucidate the genetic basis of these plant architecture traits.

Keywords: Characterization, doubled haploid, genetic resources, performance, *Zea mays*

## Introduction

Genetic variability is essential in plant breeding programs. Plant breeders typically focus on short-term breeding goals, mainly because of the need to deliver new varieties. This may result in a narrow genetic base of elite maize germplasm (Andorf et al. 2019; Smith 1988) and could lead to a yield plateau, increasing vulnerability to pests, and make it difficult to meet new market demands (Pollak 2003). Assessment of the genetic variability that exists in available germplasm is fundamental for crop improvement. Genetic improvement of important agronomic traits while maintaining genetic variability long-term is desirable in maize breeding programs

(Hallauer and Darrah 1985). Genetic variability will be preserved if an adequate number of lines are intermated for the synthesis of the next cycle of selection. Recurrent selection procedures in maize have proven to be an effective way of increasing the frequency of superior lines for grain yield and other agronomic traits while maintaining genetic variability (Hallauer & Darrah 1985).

Recurrent selection is the systematic selection of desirable individuals from a population followed by the selected individuals' recombination to form a new cycle of the population. It was suggested by (Jenkins 1940) as a method of intrapopulation improvement and later described for population improvement using a tester (Hull 1945). The most significant advantage of this method is the increase in populations' mean performance for one or more characters by increasing the frequency of favourable alleles while maintaining genetic variability for continued genetic improvement (Hull 1945; Jenkins 1940).

The Iowa Stiff Stalk Synthetic (BSSS) maize population (Sprague 1946) has undergone recurrent selection since 1939. This population was developed by intermating 16 inbred lines selected by various corn breeders for superior stalk quality. Of these progenitors, 10 were derived from multiple strains of the 'Reid Yellow Dent' open-pollinated population, 4 had miscellaneous origins, and the genetic background of 2 is unknown (Sprague 1946). The base population cycle 0 (BSSS(R)C0) was submitted to multiple recurrent selection cycles. Currently, cycle 19 is available. The BSSS maize population has been under recurrent selection for increasing grain yield, low grain moisture at harvest, and increased resistance to root and stalk lodging. Several inbreeds lines have been developed from the BSSS population (B14, B37, B73). They have made significant contributions to the maize industry in the U.S., especially B73 (Coffman et al. 2019), one of the most successful maize inbred lines developed in the public sector and benefited industry and farmers substantially.

Agronomic and plant architecture changes have been reported for different selection cycles in the BSSS maize population; plant height, anthesis-silking interval (ASI), leaf angle, number of tassel branches have experienced changes (Brekke et al. 2011; Edwards 2011). Changes in plant architecture traits over continuous selection cycles, driven by testing under higher population densities, have increased throughout the hybrid era achieving maximum grain yields (Brekke et al. 2011). Consequently, inbred lines or plants from later cycles had more erect leaves, reduced ASI, and fewer tassel branches as an indirectly improved adaptation to high plant density. Identifying genomic regions associated with plant architecture changes would help to unlock genetic resources not adapted yet to high plant densities, either by selecting for such regions in genetic resource populations like early cycles of recurrent selection programs or after introgressing them into respective materials.

Genome-wide association studies (GWAS) are a useful tool for analyzing allelic diversity to identify superior alleles and dissect the genetic architecture related to traits, which furthers genetic improvement in crops (Atwell et al. 2010). The Increasing application of association mapping is due to the rapid development of sequencing and DNA marker techniques, which resulted in cost-effective high-throughput genotyping technologies. Genomic regions and candidate genes conferring adaptation to high plant density identified by GWAS could help to speed up genetic resource utilization.

The aim of this study is to observe whether we have potentially lost diversity from C0 to C17 in the BSSS maize population (caused by selection or drift) and whether DH lines from C17 are better accessible as a genetic resource closely related to elite germplasm. Understanding which regions control plant architecture traits and converting early recurrent selection cycles germplasm to modern plant types, particularly with plant architecture traits, adapted to higher

plant density. In this study, we conducted a phenotypic characterization of DH lines developed from the base population C0 (BSSS(R)C0), C17 (BSSS(R)C17), and the cross C0/C17 (BSSS(R)C0/BSSS(R)C17) populations to i) compare C0 and C17 derived DH lines for plant architecture traits, ii) identify DH lines with both significant C0 background and in addition modern plant architecture traits conferring adaptation to high plant density, that could be used as genetic resources, iii) evaluate how to best use DH lines from the three subpopulations (C0, C17, C0/C17) to identify regions affecting plant architecture traits, and iv) determine the inheritance of those regions, in particular, whether major genes are involved that may facilitate introgression of other genetic resources.

## Materials and Methods

### Breeding Populations

Three synthetic populations BSSS(R)C0, BSSS(R)C17, and BSSS(R)C0/BSSS(R)C17 representing different stages of cycle advancement in the recurrent selection program of the Iowa Stiff Stalk maize population [BSSS(R)] were used to develop DH lines. The synthetic BSSS(R)C0 corresponds to the unselected base population (C0) formed by intermating 16 inbred lines selected for above average stalk quality in 1934 (Sprague 1946). The C0 seed used came from subsequent cycles of seed multiplication in C0 for maintenance over time. The BSSS(R)C17 population corresponds to the most advanced cycle (C17) available of the reciprocal recurrent selection program. Finally, the BSSS(R)C0/BSSS(R)C17 population was created by intermating plants from BSSS(R)C0 and BSSS(R)C17 to create the BSSS(R)C0/C17 population (C0/C17).

### Doubled Haploid Line Development

Plants from BSSS(R)C0, BSSS(R)C17, and BSSS(R)C0/BSSS(R)C17 were pollinated with a maternal haploid inducer BHI301 (Almeida et al. 2020) in an isolation field to generate

the haploid seed. Seed produced from these plants was screened and kernels expressing the *R-nj* marker gene in the endosperm but not in the embryo were classified as haploid kernels. The haploid seed was then germinated in plug trays in a greenhouse at the Department of Agronomy, Iowa State University (ISU). Once seedlings developed 2-3 leaves, a colchicine treatment was applied following the protocol used by the DH Facility at ISU (Vanous et al. 2017). Two days after the colchicine treatment, haploid seedlings were transplanted in the field at the Agricultural Engineering and Agronomy Research Farm, Boone, IA, in 2017. At the flowering stage, putative $DH_0$ plants shedding pollen were self-pollinated to produce $DH_1$ generation seed. Seed multiplication was performed during subsequent generations, and lines were screened for uniformity and discarded if segregating or variable. In total, 135 DH lines from BSSS (C0_DHL), 194 DH lines from BSSS(R)17 (C17_ DHL), and 187 DH lines from BSSS/BSSS(R)17 (C0C17_DHL) were obtained. The DH Facility developed these DH lines at Iowa State University (http://www.plantbreeding.iastate.edu/DHF/DHF.htm).

**Experimental Design and Phenotypic Data Collection**

The 516 DH lines plus 16 progenitors of the BSSS population (A3G-3-3-1-3, CI 540, Fe (Parent of F1B1), I-159, IL12E, B2 (Parent of F1B1), Oh 3167B, Os 420, Tr 9-1-1-6, WD 456, I224, LE 23, 461, Hy, AH83, CI 187-2) and the inbred line B73 were planted during summer 2019 near Ames, IA, in three locations: Plant Introduction Station (PI) at Ames, IA, Johnson Farm (JSN) near Kelly, IA and Burkey (BRK) at Agronomy Farm, Boone, IA. The inbred line B73 was used as a check and replicated 14 times within each replicate block in each location to have 546 experimental units per replicate. B73 was randomly distributed across the three populations, while the progenitors were included in the BSSS population due to its phenotypic resemblance. The experiment was planted in each location using a modified split-plot design with two replications, where the DH lines for the breeding populations (BSSS(R)C0,

BSSS(R)C17, and BSSS(R)C0/BSSS(R)C17) constitutes the whole plot treatment factor and the DH lines within each population as the subplot treatment factor. This design differs from a classical split-plot because the subplot factor (DH lines) was not cross-classified with the whole-plot factor and because the whole plot was assigned to more than one experimental unit in the field. The subplot experimental unit consisted of a single row plot, spaced at 0.76 m, 3.8 m long with 15 plants. The whole-plot factor experimental unit was a block containing 39 subplots arranged side by side. Each replicate, containing 546 subplots, was divided into three whole plots, separated into 4, 5, and 5 blocks for C0_DHL, C17_DHL, and C0/C17_DHL, respectively. Each block of the whole plot was randomly assigned to a range in the field.

Phenotypic data were collected on an individual plot basis for male flowering, female flowering, anthesis-silking interval, plant height, ear height, flag leaf angle, tassel length, and the number of primary tassel branches. Male flowering and female flowering were recorded as the date when 50% of the plants in the row were shedding pollen and had visible silks, respectively. Plants were recorded as shedding pollen when a single anther could be seen, and plants were recorded as silking when one or more silks were visible. Anthesis-Silking interval was calculated as the difference in days between male flowering and female flowering. Plant and ear height were recorded two weeks after pollination, plant height as the height (cm) between the base of a plant to the insertion of the flag leaf collar (this measure excluded any variation in tassel size from the flag leaf to the top of the plant) and ear height as height (cm) between the base of a plant to the top ear of the same plant. The flag leaf angle was recorded using a protractor. The protractor was placed against the portion of stalk beneath the flag leaf. The protractor was held underneath the flag leaf's midrib to record the angle of attachment of the flag leaf at the point of attachment to the stalk. Tassel length was measured two weeks after pollination as the length

(cm) between the flag leaf node up to the tassel tip. The number of primary tassel branches was recorded simultaneously as tassel length by counting the number of primary tassel branches that branch directly off the main branch.

**Statistical Data Analysis**

Data analysis was carried out fitting the following full linear model to the data collected:

$$Y_{ijklm} = \mu + E_i + R(E)_{li} + G_j + GE_{ij} + D(G)_{jk} + ED(G)_{ijk} + P(ER)_{mil} + A(ER)_{nil} + \varepsilon_{ijklmn}$$

where: $Y_{ijklm}$ is the response in the environment *i*, group *j*, DH line *k*, replicate block *l*, pass *m*, range *n*; μ is the overall mean. $E_i$ the effect of environment *i*, $R(E)_{li}$ the effect of replicate block *l* within environment *i*, $G_j$ the effect of the group of DH line *j*, $GE_{ij}$ the effect of the interaction between group *j* and environment *i*, $D(G)_{jk}$ the effect of the DH line *k* within the group *j*, $ED(G)_{ijk}$ the effect of the interaction of environment *i* and DH line *k* within the group of DH line *j*, $P(ER)_{mil}$ the effect of the pass *m* within the environment *i* and replication *l*, $A(ER)_{nil}$ the effect of the range *n* within the environment *i* and replication *l* and $\varepsilon_{ijklm}$ the effect of the residual error of the range *n*, pass *m*, block *l*, individual DH line *k*, group of DH line *j* and environment *i*. The effects of the environment, replicate block *l* within environment *i*, and the effect of the group of DH line *j* was considered as fixed effects. In contrast, the other effects were considered as random. All phenotypic data analyses were conducted using the MIXED procedure of SAS 9.4 software (SAS Institute, Cary, NC). After fitting the full linear model to all traits, data were checked for outliers by computing the probability of studentized residuals using the t-distribution and adjusted with a Bonferroni correction for the number of residuals. Observations were considered outliers if the Bonferroni corrected p-value on the residuals were less than 2%. Then, a model containing all fixed effects but with different combinations of the random effects and homogeneity/heterogeneity in the residual variance across environments was tested. Based on the smallest Bayesian Information Criteria (BIC), we decided which random effects to retain in the

model. Least square means were obtained for the environments and group effects, while the best linear unbiased predictors (BLUPs) for DH lines nested within the group were estimated.

Repeatability on an entry-means basis was calculated with the formula:

$$Repeatability = \frac{\sigma_g^2}{\sigma_g^2 + \frac{\sigma_{gxe}^2}{e} + \frac{\sigma_e^2}{re}}$$

where $\sigma_g^2$ corresponds to the genotypic variance, $\sigma_{gxe}^2$ to genotype by environment interaction variance, $\sigma_e^2$ to the residual variance and *r* and *e* to the number of replications and environments, respectively (Carena et al. 2010).

Trait correlations were calculated using the BLUPs of each trait to obtain the phenotypic correlation matrix, using Pearson's correlation coefficient implemented in R (R Core Team 2019).

**Genotyping and Quality Control**

Genomic DNA was extracted from DH line seedlings established in the greenhouse at the Agronomy Department of Iowa State University. Leaf tissue samples from three plants per DH line were collected at the 3-4 leaf developmental stage, and the DNA extraction was done using the standard CIMMYT laboratory protocol (CIMMYT 2005). Genotyping was carried out using the Diversity Arrays Technology sequencing (DArT-seq) method (Kilian et al. 2012) provided by the Genetic Analysis Service for Agriculture (SAGA) at CIMMYT. DArT-seq is a high-throughput, robust, reproducible, and cost-effective marker system based on genome complexity reduction using a combination of restriction enzymes, followed by hybridization to microarrays to simultaneously assay hundreds to thousands of markers across the genome (Kilian et al. 2012).

A total of 51,418 SNP markers were generated, but only 32,929 unimputed SNP markers were successfully called within the B73 RefGen_v4 (Jiao et al. 2017). The 32,929 SNP markers were filtered according to the following criteria: 1) minimum call rate; 2) Minor Allele

Frequency (MAF), 3) duplicate and monomorphic markers, and 4) heterozygosity. We used a threshold of ≥ 50% to remove poorly genotyped SNP markers, for which information was missing for more than half of the lines. SNP markers with low MAF ≤ 1 % were excluded. Duplicate and monomorphic SNP markers were removed using the conditional formatting highlight in Excel. Finally, genotypes with significant heterozygosity (not expected in DH or inbred lines) were excluded. We kept genotypes with ≤ 3.5 % heterozygosity for further analysis. Additionally, the inbred line B73 was used as technical control and was repeated in seven separate plates to verify assay reproducibility.

After the filtering process and quality control of the data, the resulting SNP core set consisted of 15,891 SNP markers corresponding to 487 DH lines (132 DH lines from BSSS (C0_DHL), 170 DH lines from BSSS/BSSS(R)17 (C0C17_DHL), and 185 DH lines from BSSS(R)17 (C17_ DHL) and were used for further analysis. 29 DH lines (3 in C0_DHL, 17 in C0/C17_DHL, and 9 in C17_DHL) were discarded from the GWAS analysis due to obvious phenotypic segregation observed in field trials, missing genotypic data, or levels of heterozygosity in the genotypic data above 3.5 %. The software TASSEL v.5.2.52 (Bradbury et al. 2007) was used for the imputation of missing data using the LDkNNi (linkage disequilibrium k-nearest neighbors imputation) method (Money et al. 2016). LDkNNi process considers the linkage disequilibrium (LD) between SNPs when choosing the nearest neighbors. It exploits the fact that markers useful for imputation are often not physically close to the missing genotype rather distributed throughout the genome (Money et al. 2016).

**Linkage Disequilibrium and Population Structure**

The average linkage disequilibrium (LD) between SNP markers on each chromosome was measured using the squared value of the Pearson correlation coefficient ($r^2$) in each group of DH lines and the entire panel of DH lines to assess the level of LD decay on each chromosome.

The average LD decay distance across the genome was estimated using the software TASSEL v.5.2.52 (Bradbury et al. 2007). A 50 kb sliding window was used to estimate the width of the window on one side of the start site. The resulting data were imported into R (R Core Team 2019) to create LD decay plots and to fit a smooth line using Hill and Weir expectations of $r^2$ between adjacent sites (Hill and Weir 1988).

The selected 487 DH lines were known to belong to the three populations (BSSS, BSSS/BSSS(R)17, and BSSS(R)17. However, to exemplify, we run a principal component analysis (PCA) to identify the origin's population for each DH line. The incorporation of population structure through principal components analysis (PCA) as a covariate in the fixed effects model increases the power to detect associations, and it has the advantage of eliminating false positives due to non-genetic effects associated with the structure of the population. PCA was performed using the software GAPIT v.3 (Lipka et al. 2012). Bayesian Information Criterion (BIC) (Schwarz 1978) was used to identify the optimal number of principal components by selecting the lowest BIC model. The principal components results were used to display the first two principal components in R software (R Core Team 2019).

**Genome-Wide Association Studies**

A GWAS was performed using the filtered SNP dataset and trait BLUPs estimated in the *per se* evaluation trials for each subpopulation separately (C0_DHL, C0/C17_DHL, and C17_DHL, respectively). Additionally, we run the GWAS analysis using the entire panel (487 DH lines) to observe the differences in a more significant population size.

The analytical software GAPIT (Lipka et al. 2012) was used in the GWAS analysis. Three statistical methods implemented in GAPIT were used to reduce the chance of performing type 1 and type 2 errors: 1) general linear model (GLM) approach, which also included PCA results for population structure as fixed effect covariate (Lipka et al. 2012) to account for

population structure; 2) fixed and random model circulating probability unification (FarmCPU), which includes PCA results as a covariate, kinship to account for the relatedness among individuals as an additional covariate (VanRaden 2008), and additional algorithms that aid in solving the confounding problem between testing markers and covariates (Liu et al. 2016); 3) SUPER (Settlement of MLM Under Progressively Exclusive Relationship) (Wang et al. 2014), which extracts a small subset of SNPs and uses them in Fast-LMM (Factored Spectrally Transformed Linear Mixed Model) retaining the computational advantage and also increasing the statistical power.

For GWAS analysis, we used the traits that we found consistent changes in at least four phenotypic traits that are known to be associated with adaptation to high plant density and have changed through the recurrent selection program (male and female flowering, flag leaf angle, and the number of primary tassel branches). Manhattan plots were used to visualize the genome-wide association significance level by chromosome location of each trait. The X-axis plot each SNP marker's genomic position, and the numbers shown correspond to chromosome numbers. The Y-axis represents the negative logarithm of the p-value obtained from the GWAS model. The solid horizontal line indicates the significance threshold. The SimpleM (Gao et al. 2008, 2009) script was used in the R software (R Core team 2019) to determine a significance threshold to account for multiple testing. Simple M uses composite LD to capture the correlation between markers and employs PCA to calculate the effective number of independent tests (Meff_G). The desired alpha level is then divided by Meff_G to obtain the threshold that accounts for multiple testing, which was determined to be $6.82 \times 10^{-6}$ in C0_DHL, $5.97 \times 10^{-6}$ in C0/C17_DHL, $9.17 \times 10^{-6}$ in C17_DHL, and $4.63 \times 10^{-6}$ in the entire panel of DH lines.

### Candidate Gene Mining

The available maize genome sequence (B73) was used as the reference genome for candidate gene identification. Candidate genes were identified using the Ensembl Biomart tool (Kinsella et al. 2011) to obtain information on genes present. Candidate genes were considered if significantly associated SNP markers fell within regions of candidate genes or if they were within the range of LD decay, observed for each chromosome (upstream and downstream) corresponding to the associated SNPs. Candidate genes corresponding to each SNP were checked according to the SNP marker's physical position in the MaizeGDB molecular marker database (http://www.maizegdb.org/) (Portwood et al. 2019). Functional annotations of candidate genes were predicted in NCBI (http://www.ncbi.nlm.nih.gov/gene).

## Results

### Phenotypic Data Analysis and Trait Correlations

With the BIC-based model selection procedure, a final model was identified as having the best fit for each evaluated trait. The model with the smallest BIC value chosen as the final model is shown in Appendix: Supplemental Table S3.1. After fitting the correct model, least-square means were obtained for the environment and group effects, while the BLUPs for the DH lines nested within groups were estimated. The trait BLUPs of flowering time and plant architecture traits for each DH line are listed in Appendix: Supplemental Table S3.2. Descriptive statistical analysis confirmed trait variability in the different groups of DH lines. Considerable variation between populations was observed for all traits except for plant height. As expected, phenotypic differences ($P \leq 0.001$) were found between different groups of DH lines, indicating a wide range of variability present. DH lines within the C0_DHL group had the highest mean values for flowering time, ear height, flag leaf angle, and the number of primary tassel branches and were statistically different ($P \leq 0.001$) between the groups of DH lines. Moreover, DH lines within

C17 had the lowest values for these traits (Table 3.1). Male flowering and female flowering were reduced about four and six days from C0_DHL to C17_DHL groups. The C17_DHL group had a smaller anthesis-silking interval of 0.1, meaning that plants showed silks and pollen shed almost simultaneously. The C0/C17_DHL group had an anthesis-silking interval of -0.9, which increased to -1.7 days in the C0_DHL group being statistically different ($P \leq 0.001$). Synchronization of pollen and silk availability in the C17_DHL group indicates that plants have a larger chance of successful pollination. For plant height, no statistical differences ($P = 0.05$) were detected among the different groups. Ear height of the C17_DHL group was lower (69 cm) and significantly different ($P \leq 0.001$) from C0_DHL (84 cm) and C0/C17_DHL groups (79 cm). The C17_DHL group had a significantly ($P \leq 0.001$) more upright flag leaf angle (14°) than the other two groups (C0/C17_DHL with 30° and C0_DHL with 42°). Tassel length was also significant ($P \leq 0.001$) different among the groups of DH lines with 37, 39, and 42 cm in C0, C0/C17, and C17_DHL groups, respectively. However, fewer primary tassel branches were found in the C17_DHL group with seven compared to the C0/C17_DHL group with 11 and C0_DHL with 15. These results are in agreement with (Brekke et al. 2011), where changes in plant architecture traits such as more upright flag leaf angle, reduction on the number of tassel branches, and plant stature were found as the cycles of selection advance in the BSSS maize population.

Repeatabilities calculated for the complete set of DH lines across the three locations were found to be high across all traits. They ranged from 0.90 to 0.94, with flag leaf angle and tassel length slightly lower (0.90 and 0.91, respectively) and male flowering, female flowering, plant height, and the number of primary tassel branches showing the highest repeatability (0.94). Mean, minimum, maximum, range, and the standard deviation (SD) are listed in Table 3.1. In

general, we observed a tendency to have wider ranges in the C0_DHL group for all traits except for tassel length, where C0/C17 had a wider range. In contrast, C17_DHL had a tighter range in almost all evaluated traits except in flowering time, where the C0/C17 DHL group had the lowest range (Table 3.1). Additionally, the SD of the data confirms the variation showed in the different groups of DH lines, where C0_DHL had a bigger SD in all traits except in tassel length, where the C0/C17 DHL group had the most significant SD. In contrast, the C17_DHL group showed a lower SD for all the traits (Table 3.1). This tendency to have wider ranges and SD in the C0_DHL and tighter range and SD in the C17_DHL group could indicate the loss of phenotypic variability in the C17_DHL group. Additionally, the C0/C17_DHL group would likely be the population to identify lines with the right architecture traits, with significant C0 contribution.

Trait correlations were explored to determine relationships among evaluated traits. The closest positive correlation ($r = 0.88$) was observed between male flowering and female flowering and was statistically significant ($P < 0.001$). Also, plant and ear height were significantly ($P < 0.001$) and positively correlated (0.76). Plant and ear height were significantly and positively correlated with almost all other studied traits, except for the number of primary tassel branches. Table 3.2 shows all of Pearson's product-moment correlations coefficients (r) between flowering and plant architecture traits evaluated. We found consistent changes in at least four phenotypic traits that are known to be associated with adaptation to high plant density: male and female flowering, flag leaf angle, and tassel branch number. However, improving these plant architecture traits comes with a penalty of reducing phenotypic variation when advancing cycles of selection.

**Linkage Disequilibrium and Population Structure**

Linkage Disequilibrium (LD) decay varied across the ten chromosomes and different genetic regions within chromosomes. The C17_DHL group showed the largest LD decay

distance ranging from 1,348 to 2,817 kb on chromosomes 5 and 4, respectively. In contrast, the C0/C17_DHL group displayed the smallest LD decay distance (255 kb on chromosome 10 to 627 kb on chromosome 3). For C0_DHL, the LD decay varied from 319 to 788 kb for chromosomes 7 and 3, respectively (Table 3.3). The genome-wide LD decay distance was 494 kb, 420 kb, and 2,016 kb for the C0_DHL, C0/C17_DHL, and C17_DHL groups, respectively. The genome-wide LD decay distance over all ten chromosomes in the entire DH line panel with an $r^2 = 0.2$ threshold was 381 kb (Figure 3.1).

Based on PCA, population structure analysis suggested that the DH lines developed from BSSS can be divided into three subgroups. The principal components, plotted in a two-dimensional plot using discriminant analysis of principal components (DAPC), showed a clear grouping of the DH lines into the C0_DHL, C17_DHL, C0C17_DHL. The first two principal components explained 14.3 % of the total SNP variation in the entire panel. Also, the C0C17_DH lines group was scattered over a broader range, similar to the C0_DHL group.

**Genome-Wide Association Studies**

The genome-wide association results from each combination model, in each set of DH lines, and the entire panel is displayed in Table 3.4 and Manhattan plots Figures 3.2-3.5. Multiple testing correction was done using simpleM (Gao et al. 2010), resulting in the following significance thresholds ($p = 6.63 \times 10^{-6}$, $p = 5.97 \times 10^{-6}$, $p = 9.17 \times 10^{-6}$, $p = 4.63 \times 10^{-6}$ threshold for C0_DHL, C0/C17_DHL, C17_DHL, and entire panel of DH lines, respectively).

Significant SNP markers-trait associations surpassing the simple M significance threshold were found in flowering and plant architecture traits using different GWAS analysis models. In the C0_DHL group, 17 significant SNP markers were associated with different traits (3 for male flowering, 1 for female flowering, 13 for flag leaf angle. For the number of primary tassel branches, no significant SNP marker was found to be significantly associated. In the

C0/C17_DHL group, ten significant SNP markers were significantly associated, 4 in male flowering and 6 in the number of primary tassel branches. Additionally, in the C17_DHL group, only 10 SNP markers were associated with the number of primary tassel branches. When the entire panel of DH lines was combined and used for GWAS, 159 SNP markers were found to be associated with the different traits: 32, 17, 51, and 59 for male flowering, female flowering, flag leaf angle, and the number of primary tassel branches, respectively (Table 3.4). Using the entire panel of DH lines (487 DH lines) seems to be the most meaningful approach when conducting a GWAS and identifying the most significant SNP markers associated with traits of interest. This could be due to incorporating more phenotypic variation or the increasing population size when analyzing the three groups of DH lines as a whole set.

From the different models used, the GLM method identified 67 significant SNP markers in different traits among the groups of DH lines (10 for male flowering, 7 for female flowering, 35 for flag leaf angle, and 15 for the number of primary tassel branches), FarmCPU identified 27 significant SNP markers (7 for male flowering, 2 for female flowering, 6 for flag leaf angle and 12 for the number of primary tassel branches), and SUPER identified 102 SNP markers associated with different traits (22 for male flowering, 9 for female flowering, 23 for flag leaf angle and 48 for the number of primary tassel branches) evaluated and among the DH lines groups (Table 3.4). Across the GWAS methods used in this study, SUPER was the best method for identifying associated SNPs to the different evaluated traits.

Only 38 SNP markers were found associated with different evaluated traits across more than one method tested and among the groups of DH lines. C0_DHL group had 2 SNP markers that were found with different models tested: 1 SNP for male flowering (S2_223717633) found with GLM and FarmCPU methods and 1 SNP for flag leaf angle (S7_143116333) found with

GLM, FarmCPU, and SUPER methods. The method GLM + SUPER identified 28 associated SNP marker in common (8, 9, and 11 for male flowering, number of primary tassel branches, and flag leaf angle, respectively) in the entire panel of DH lines, GLM + FarmCPU + SUPER identified four associated SNP marker in common (1 and 3 for male flowering and the number of primary tassel branches respectively) in the entire panel of DH lines. The models FarmCPU + SUPER identified four associated SNP markers (2, 1, and 1 for male flowering, female flowering, and the number of primary tassel branches, respectively). In groups C17_DHL and C0/C17_DHL, no SNP markers were found associated in common with the different methods tested (Table 3.5).

The magnitude of p-values and the number of markers that surpassed the significance threshold varied across the ten chromosomes depending on the group and the model evaluated. For the 38 SNP markers associated with more than one method tested, chromosomes 7 and 2 had the highest number associated SNP markers that surpassed the threshold with (13 and 11 SNP markers, respectively). In contrast, chromosomes 4 and 8 only had 1 SNP markers, respectively (Table 3.5). For the number of primary tassel branches, 13 SNP markers (9 2, 1, and 1 in chromosome 2, 7, 4, and 9, respectively) surpassed the significance threshold. For male flowering, 12 associated SNP markers (2, 8, and 2 in chromosomes 2, 3, and 10, respectively) were found. For the trait flag leaf angle, 12 SNP markers (11 on chromosome 7 and 1 on chromosome 8) were associated. Finally, only 1 SNP marker on chromosome 9 was found to be associated with female flowering

No SNP markers were found in common between flowering and flag leaf angle and the number of primary tassel branches. Only the SNP markers S3_159544248, S3_159544337, S3_161013994, and S3_161169145, were found to be associated with male flowering and female

flowering traits in the entire panel of DH lines. Due to the entire panel of DH lines showed the most numbers of associated SNP markers and agreed with the three methods tested, the Manhattan plots for male flowering, female flowering, flag leaf angle, and the number of primary tassel branches are displayed in this paper Figure 3.2-3.5 respectively. The genome regions with the highest significance were found on chromosome 2 and 7 for the traits number of primary tassel branches and flag leaf angle, respectively. Finding candidate genes on these limited genome regions could help to alter plant architecture dramatically. Additionally, the fewer regions with larger effect could be a better source for gene introgression

**Candidate Gene Mining**

By searching for candidate genes up and downstream of the 38 in common significant SNP markers being in LD with the corresponding chromosome based on the B73 RefGen_v4 (Jiao et al. 2017), 55 candidate genes were found into the boundaries of the SNP markers associated with flowering time and different plant architecture traits (18, 2, 14 and 22 for male flowering, female flowering, flag leaf angle and the number of primary tassel branches, respectively). The candidate gene *sbp22* (Zm00001d042319) was the only candidate gen found to be affecting male flowering and female flowering. Flowering, flag leaf angle, and the number of primary tassel branches candidate genes are listed in Table 3.6. Significantly associated SNP markers were also compared to previously published candidate genes.

## Discussion

**Plant Architecture Traits Adapting to High Plant Density**

The breeding potential of the BSSS maize population DH lines is reflected by the distribution of the traits that have been modified in this population, and these plant architecture traits are involved in the adaptation to high plant densities as was observed by (Duncan 1971; Duncan et al. 1967; Edwards, 2011; Mock and Pearce 1975). C17_DHL group presented the

most favorable characteristics when adapting germplasm to higher plant densities, reducing flowering time, ear height, tassel length, and the number of primary tassel branches additionally showed more upright flag leaf angles. The phenotypic data used in this study showed high values of repeatability from 0.90 to 0.94. These repeatabilities agree with other studies (Buckler et al. 2009; Peiffer et al. 2014; Romay et al. 2013; Vanous et al. 2018). The traits that were evaluated at *per se* level were parent-ability traits or traits strongly correlated to hybrid performance. In this study, we found changes in plant architecture traits among different groups of DH lines, even when the purpose of the recurrent selection method was to improve the mean performance of the population for one or more characters while maintaining genetic variability (Comstock et al. 1949; Hull 1945; Jenkins 1940). In previous studies on the BSSS maize population, Gerke et al. 2015 found that reduction in diversity in the BSSS reciprocal recurrent selection program was not different from what was expected by genetic drift alone with almost not signature of selection. These authors suggested that most of the genome was carried along during the selection program with no impact on selection. In this scenario, likely, favorable alleles related to yield or other traits that were present in C0 were lost, given a substantially reduced genetic diversity in C17 compared to C0. Flowering time showed a reduction of four days to anthesis and six days to silking from C0_DHL to C17_DHL groups. However, all DH lines flowered within a timeframe expected for the central U.S. Corn Belt. Reduction in flag leaf angle has been reported in hybrids through the selection process and adaptation to high plant density (Brekke et al. 2011; Duvick 2005; Edwards 2011), as we found in this study. C17_DHL group could be a source of favorable alleles that impact more erect flag leaf angles.

We found a reduction in the number of primary tassel branches from an average of 15 in C0_DHL to 7 in the C17_DHL groups. These results confirmed a reduction in the number of

primary tassel branches found by Edwards (2011) in the BSSS maize population's recurrent selection program. Changes observed across selection programs were for traits that increase light penetration into the canopy, including tassel branch number. Plant height and ear height are closely correlated traits ($r = 0.76$), but plant height did not differ among groups of DH lines. However, ear heigh for the C17_DHL group was significantly lower than for C0_DHLs. Plant and ear height are traits of interest when adapting germplasm as they are closely associated with flowering time, lodging resistance, biomass production, and grain yield (Durand et al. 2012; Teng et al. 2013). During selection for industrial agriculture, adaptation to height traits increases harvest uniformity, favorably partition carbon and nutrients between grain and non-grain biomass, and enhance fertilizer, pesticide, and water use efficiency (Khush 2001).

C17_DHL group was altered in traits important for high plant density tolerance compared to the C0_DHL group. In general, the C17_DHL group showed a better performance in important agronomic traits than the C0_DHL group. These differences demonstrate that 17 cycles of recurrent selection have been effective. At the same time, the C0/C17 DHL group showed the most considerable variation and could be used as a source of new alleles for important agronomic traits. These results suggest that we can develop DH lines and hybrids to be adapted to high planting densities. Developing DH lines in more advanced cycles of selection lead to an improved agronomic trait: flowering time, flag leaf angle, and the number of primary tassel branches. If there were few major loci available in early selection cycles, they probably got fixed during the selection process. Therefore, the extraction of DH lines out of the BSSS maize population was effective, as indicated by plant architecture traits conferring adaptation to high plant density. Some correlations between the traits evaluated were significant, indicating that

adaptation based on plant architecture traits is viable in altering other important adaptation-related traits.

**The Exploitation of Early Cycle of BSSS DH Lines**

A method to exploit maize's genetic diversity is introducing exotic germplasm and/or using landraces as a source of new alleles. However, several cycles of inbreeding are required. Additionally, inbreeding from landraces results in a high load of recessive alleles, mutations, and deleterious alleles that needs to be selected against by conventional breeding methods (Strigens et al. 2013). Thus, to have a sufficient number of lines to be evaluated for testcross performance from exotic germplasm, it is necessary to start the breeding program with a large number of plants. This laborious effort is the main reason why exotic germplasm is limited used in modern breeding programs (Goodman 2005). DH technology enables more effective access to landraces' genetic diversity (Chaikam et al. 2019; Strigens et al. 2013). Deleterious alleles from landraces are expressed in the haploid stage and can be purged through selection. Hence, DH technology is a useful tool to access the genetic diversity present in landraces and to expand the genetic diversity of the elite germplasm (Böhm et al. 2017; Chaikam et al. 2019; Strigens et al. 2013; Wilde et al. 2010).

An alternative approach to exploring genetic diversity in maize is using early cycles of recurrent selection programs. In this study, we developed DH lines from the earlier cycle of the BSSS maize population to explore the phenotypic variation that has left behind when advancing cycles of recurrent selection. Significant phenotypic variation was observed between the groups of DH lines for all traits evaluated, except for plant height. C17_DHL group presented the most favorable characteristics when adapting germplasm to higher plant densities, reducing flowering time, ear height, tassel length, and the number of primary tassel branches additionally showed more upright flag leaf angles. However, the genetic variability presented among the C0_DH lines

and the C0/C17_DHL allowed the identification of DH lines with desirable plant architecture traits that confers adaptation to high plant density. Some of these DH lines are a promising source of favorable alleles for plant density response, thus selected DH lines could be introgressed into current germplasm to improve the adaptation to high plan density. The large genetic distances (data not shown) of the C0_DHL compared to the C17_DHL demonstrated the potential of the C0_DHL group to broaden the genetic base of the Stiff Stalk (SS) germplasm. However, more studies need to be conducted at the testcross level to know the hybrid combinations' performance. The use of early selected cycles and DH technology opens new opportunities for exploring genetic diversity.

**Linkage Disequilibrium and GWAS Analysis**

Linkage disequilibrium (LD) refers to the nonrandom association of alleles at different loci in a breeding population (Flint-Garcia et al. 2003). It can be estimated using the correlation between SNP markers. The magnitude of LD and its decay with the genetic distance is important to determine the resolution of association mapping because LD's extent determines the required number of SNP markers and the mapping resolution (Vos et al. 2017). In our panel of BSSS DH lines, we found that the LD decayed over a distance of 381 kb across the genome at the r2 = 0.2 threshold (Figure 3.1). However, LD decay varied across the ten chromosomes and different genetic regions within chromosomes ranging from 244 kb for chromosome 10 to 614 kb in chromosome 3 (Figure 3.1D). These results agree with Vanous et al. 2018. They investigated a diverse panel consisting of exotic derived DH lines and found that LD decayed over a distance greater than 500 kb for all chromosomes. The LD within the C17_DHL group is quite more extensive than in C0_DHL and C0/C17_DHL. The larger LD decay distance observed in the C17_DHL group may be due to the breeding history of the population (e.g., the occurrence of bottlenecks) and the lower genetic diversity represented by this population. The C17_DH lines

come from a population that was gone through 17 cycles of recurrent selection, which probably have caused some genetic drift, or a small effective population size, resulting in the larger decay distances since LD decay more rapid in pools with higher genetic diversity (Romay et al. 2013; Wu et al. 2016). The rapid LD decay, together with high genotypic variances and absence of population structure within populations, enables good resolution association mapping in some germplasm (Strigens et al. 2013). In our study, when we analyzed every group of DH lines (C0_DHL, C17_DHL, and C0/C17 DHL respectively, the number of SNP markers associated was low (17, 10, 10, respectively). However, when we used the entire DH lines panel, we found 159 SNP markers associated with the different evaluated traits. These results could be due to the lower variation presented in each DH line group or the smaller population size that affects the power to detect SNP associated. Another possible reason for having a little power to identify associated SNP markers to plant architecture traits when we performed the analysis by each group of DH lines could be due to the fixation of alleles. In the C17_DHL group, if there are major genes affecting plant architecture traits and respective alleles are present at a low frequency in the C0_DHL group. Still, then enriched in subsequent cycles and fixed in C17_DHLs, this could be a scenario of having little power to detect those genes associated with C0_DHL and are unable to identify those in the C17_DHL group because of fixation.

**Candidate Genes for Plant Architecture Traits Adapting to High Plant Density**

Since we found consistent changes in at least four traits that are known to be associated with adaptation to high plant density and trends for reducing male and female flowering time, the number of primary tassel branches, and more upright flag leaf angles in C17_DHL compared with the C0_DHL, we focused our discussion on candidate genes for these traits. Additionally, these trends have been reported for parental inbred lines of hybrids previously released (Duvick

2005; Lauer et al. 2012). This could reflect a correlated response of modern breeding germplasm to selection for grain yield under higher plant densities (Duvick 2005; Edwards 2011).

Male flowering and female flowering are close and positive correlated traits that are important when adapting germplasm. Flowering time is essential in determining local adaptation and is one of the most significant issues that must be overcome when locally adapting new maize germplasm. In this study, we identified 20 candidate genes that affect male flowering and female flowering (18 and 2, respectively). These candidate genes were found on chromosomes 2, 3, 9, and 10 (Table 3.6). The Squamosa promoter-binding-like protein (*sbp22)* candidate gene was identified in common, affecting male and female flowering. This gene was found in previous studies where the presence of candidate genes controlling flowering pathway in *Arabidopsis thaliana* where a Squamosa promoter-binding-like protein (*sbp22*) have been related with the activation of genes that execute the switch from vegetative to reproductive development and also define a separate endogenous flowering pathway where high levels of this promoter in young plants prevent precocious flowering (Wang et al. 2009). Additionally, Chardon et al. (2004), studying the genetic architecture of flowering time in maize as inferred from QTL Meta-analysis, found a QTL on chromosome 3 influencing silking date, leaf number, and plant height traits. These results are in agreement with the region that we saw in chromosome 3 affecting male and female flowering.

The number of primary tassel branches is considered the principal component of maize tassel inflorescence architecture and is a typical quantitative trait controlled by multiple genes (Chen et al. 2017). Reductions in tassel size and tassel branch number have continuously been decreased over time (Duvick 2005). Previous studies in the BSSS maize population have revealed changes through advancing cycles in the recurrent selection program. A reduction from

20 branches in the BSSS to just seven branches in BSSS(R)17 was observed (Brekke et al. 2011). Similar results were found in this study where C0_DHL had 15 and C17_DHL, just seven primary tassel branches. According to Duncan et al. (1967), tassels could block enough sunlight to reduce photosynthesis by 19 %, being small tassel size a more desirable trait. We identified 22 candidates genes (17, 3, 1, and 1 in chromosome 2, 4, 7, and 9, respectively). Chen et al. (2017) identified 11 QTL located in chromosomes 2, 3, 5, and 7 demonstrating that tassel branch number variation was mainly caused by alleles with a major effect, minor effect, and slightly modified by epistatic effects. These results are in agreement with what we found in chromosomes 2 and 7.

Flag leaf angles have also experienced changes when advancing cycles in the recurrent selection program. In this study, we found that C17_DHL had more upright FLA than the other two groups of DH lines. These results are in agreement with different hybrids studies were a trend toward vertical flag leaf angle had been observed in recent decades. More vertical upper leaves are the desired trait since permit more light to penetrate the canopy, improving the photosynthetic efficiency and allowed farmers to plant maize at higher densities (Edwards 2011). In this study, we identified a region with ten candidate genes on chromosome 7, and they have located between the region 135.2 to 146.6 Mb according to the B73 RefGen_v4 (Jiao et al. 2017). This suggests that the surrounding genomic region has a strong association with the trait. Multiple studies have found candidate genes on chromosome 7 impacting a leaf development transcription factor controls abaxial cell fate, delineation of leaf margins, initiation of vascular and photosynthetic tissues (Candela et al. 2008).

DH lines developed in this study could be sources of new germplasm for broadening the genetic variation compared to elite germplasm to develop varieties or hybrids adapted to the U.S.

corn belt. Thus, individual lines with superior performance for agronomic and morphological traits can be selected and introgressed into elite materials. However, the testcross performance of the DH lines remains to be evaluated to test their yield potential in hybrid combinations. Additionally, in this study, we found that the entire panel of DH lines could be used for association analysis for flowering and plant architecture traits. Instead of using each DH line group individually, since the power of detecting associated SNP increased when we used the entire panel of DH lines. However, the slow LD decay distance found could be a limitation because the evidence that we can obtain for candidate genes is limited since we are searching at large genome regions rather than individual genes or polymorphism since the magnitude of LD and its decay with genetic distance determine the resolution of association mapping. Additionally, identifying QTL or regions for plant architecture traits in this study may help to elucidate the genetic basis of these traits and facilitate future work about marker-assisted selection or map-based cloning in maize breeding programs.

## Tables and Figures

Table 3.1 Summary statistics of flowering and plant architecture traits in different groups of DH lines derived from the BSSS maize population. Means with the same letter in column are not statistically different from each other (P > 0.05).

| Trait | Group* | Mean | Min | Max | Range | SD |
|---|---|---|---|---|---|---|
| Male flowering (days) | C0_DHL | 67 a | 60 | 74 | 14 | 2.5 |
| | C0/C17_DHL | 65 b | 61 | 71 | 10 | 2.2 |
| | C17_DHL | 63 c | 59 | 69 | 10 | 2.0 |
| Female flowering (days) | C0_DHL | 69 a | 61 | 75 | 14 | 2.8 |
| | C0/C17_DHL | 66 b | 61 | 72 | 11 | 2.7 |
| | C17_DHL | 63 c | 58 | 70 | 12 | 2.1 |
| Anthesis-silking interval (days) | C0_DHL | -1.7 a | -4.5 | 1.5 | 6.0 | 1.2 |
| | C0/C17_DHL | -0.9 b | -4.4 | 1.6 | 6.0 | 1.1 |
| | C17_DHL | 0.1 c | -1.9 | 2.4 | 4.3 | 0.8 |

Table 3.1 Continued

| Trait | Group* | Mean | Min | Max | Range | SD |
|---|---|---|---|---|---|---|
| Plant height (cm) | C0_DHL | 170 a | 116 | 210 | 94 | 16.1 |
| | C0/C17_DHL | 171 a | 130 | 221 | 91 | 15.5 |
| | C17_DHL | 170 a | 127 | 207 | 80 | 13.4 |
| Ear height (cm) | C0_DHL | 84 a | 48 | 137 | 89 | 14.4 |
| | C0/C17_DHL | 79 b | 44 | 122 | 78 | 14.3 |
| | C17_DHL | 69 c | 41 | 99 | 58 | 10.8 |
| Flag leaf angle (Degrees from vertical) | C0_DHL | 42 a | 15 | 90 | 75 | 12.3 |
| | C0/C17_DHL | 30 b | 7 | 73 | 66 | 11.6 |
| | C17_DHL | 14 c | 5 | 38 | 33 | 6.5 |
| Tassel length (cm) | C0_DHL | 37 a | 28 | 47 | 19 | 3.9 |
| | C0/C17_DHL | 39 b | 27 | 52 | 25 | 4.3 |
| | C17_DHL | 42 c | 35 | 53 | 18 | 3.6 |
| Primary tassel branches (number) | C0_DHL | 15 a | 3 | 30 | 27 | 4.7 |
| | C0/C17_DHL | 11 b | 3 | 22 | 19 | 3.7 |
| | C17_DHL | 7 c | 3 | 16 | 13 | 2.3 |

* Group, C0_DHL corresponds to the 132 derived DH lines from cycle 0, C0/C17_DHL corresponds to the 170 derived DH lines from C0/C17, and C17 corresponds to the 187 derived DH lines from cycle 17. Values are estimated from trait BLUPs of n lines within each group: SD, standard deviation.

Table 3.2 Pearson's correlation coefficients ($r^2$) of flowering and plant architecture traits of DH lines developed from the BSSS maize population.

| | MAFL | FEFL | ASI | PLHE | EAHE | FLA | TALE | NPTB |
|---|---|---|---|---|---|---|---|---|
| **MAFL** | 1 | | | | | | | |
| **FEFL** | 0.88** | 1 | | | | | | |
| **ASI** | -0.02 | -0.48 | 1 | | | | | |
| **PLHE** | 0.20** | 0.14** | 0.06 | 1 | | | | |
| **EAHE** | 0.36** | 0.27** | 0.10* | 0.76** | 1 | | | |
| **FLA** | -0.04 | -0.05 | 0.02 | 0.10* | 0.15* | 1 | | |
| **TALE** | -0.05 | 0.01* | -0.11 | 0.24** | 0.13* | -0.07 | 1 | |
| **NPTB** | 0.02 | 0.08* | -0.12 | -0.02 | 0.07 | 0.10* | -0.04 | 1 |

** Significant at $P \leq 0.001$, * Significant at $P \leq 0.05$

MAFL - male flowering, FEFL - female flowering, ASI - anthesis–silking interval, PLHE - plant height, EAHE - ear height, FLA - flag leaf angle, TALE - tassel length, NPTB - number of primary tassel branches.

Table 3.3 Linkage disequilibrium decay distance per chromosome in the different groups of DH lines and the entire panel.

| | LD decay distance (kb) | | | |
|---|---|---|---|---|
| **Chromosome** | **C0_DHL** | **C0/C17_DHL** | **C17_DHL** | **Entire panel** |
| 1 | 665 | 535 | 2815 | 524 |
| 2 | 576 | 443 | 2345 | 399 |
| 3 | 788 | 627 | 1535 | 614 |
| 4 | 487 | 525 | 2817 | 445 |
| 5 | 356 | 303 | 1348 | 263 |
| 6 | 455 | 416 | 1702 | 371 |
| 7 | 319 | 324 | 2426 | 288 |
| 8 | 662 | 463 | 1690 | 419 |
| 9 | 359 | 317 | 1718 | 282 |
| 10 | 321 | 255 | 2195 | 244 |
| Genome-wide | 494 | 420 | 2016 | 381 |

Table 3.4 The number of significant SNP markers associated with flowering and plant architecture traits in different groups of DH lines and the entire panel.

| **Population** | **Model** | **Phenotypic traits** | | | | Total |
|---|---|---|---|---|---|---|
| | | Male flowering | Female flowering | Flag leaf angle | Number of Primary branches | |
| C0_DHL | GLM | 1 | 1 | 2 | 0 | 4 |
| | FarmCPU | 2 | 0 | 4 | 0 | 6 |
| | SUPER | 0 | 0 | 7 | 0 | 7 |
| C0/C17_DHL | GLM | 0 | 0 | 0 | 0 | 0 |
| | FarmCPU | 0 | 0 | 0 | 0 | 0 |
| | SUPER | 4 | 0 | 0 | 6 | 10 |
| C17_DHL | GLM | 0 | 0 | 0 | 0 | 0 |
| | FarmCPU | 0 | 0 | 0 | 0 | 0 |
| | SUPER | 0 | 0 | 0 | 10 | 10 |
| Entire_panel | GLM | 9 | 6 | 33 | 15 | 63 |
| | FarmCPU | 5 | 2 | 2 | 12 | 21 |
| | SUPER | 18 | 9 | 16 | 32 | 75 |

Table 3.5 SNP markers associated with flowering and plant architecture traits using different models.

| Trait | Group | Method | SNP | Chr. | Position | MAF |
|---|---|---|---|---|---|---|
| NPTB | All_DHL | GLM + SUPER | S2_29243584 | 2 | 29243584 | 0.119 |
| NPTB | All_DHL | GLM + SUPER | S2_37816138 | 2 | 37816138 | 0.461 |
| NPTB | All_DHL | GLM + SUPER | S2_38563731 | 2 | 38563731 | 0.295 |
| NPTB | All_DHL | GLM + SUPER | S2_39114494 | 2 | 39114494 | 0.289 |
| NPTB | All_DHL | GLM + SUPER | S2_39228908 | 2 | 39228908 | 0.377 |
| NPTB | All_DHL | GLM + SUPER | S2_39235771 | 2 | 39235771 | 0.373 |
| NPTB | All_DHL | GLM + SUPER | S2_39702179 | 2 | 39702179 | 0.283 |
| NPTB | All_DHL | GLM + SUPER | S2_43281298 | 2 | 43281298 | 0.168 |
| NPTB | All_DHL | GLM + SUPER | S7_53234559 | 7 | 53234559 | 0.264 |
| MAFL | All_DHL | GLM + SUPER | S2_53592492 | 2 | 53592492 | 0.436 |
| MAFL | All_DHL | GLM + SUPER | S3_159544248 | 3 | 159544248 | 0.362 |
| MAFL | All_DHL | GLM + SUPER | S3_159544337 | 3 | 159544337 | 0.368 |
| MAFL | All_DHL | GLM + SUPER | S3_159924271 | 3 | 159924271 | 0.393 |
| MAFL | All_DHL | GLM + SUPER | S3_160402290 | 3 | 160402290 | 0.433 |
| MAFL | All_DHL | GLM + SUPER | S3_161013994 | 3 | 161013994 | 0.432 |
| MAFL | All_DHL | GLM + SUPER | S3_55090098 | 3 | 55090098 | 0.241 |
| MAFL | All_DHL | GLM + SUPER | S10_138884892 | 10 | 138884892 | 0.355 |
| FLA | All_DHL | GLM + SUPER | S7_135266011 | 7 | 135266011 | 0.080 |
| FLA | All_DHL | GLM + SUPER | S7_135316507 | 7 | 135316507 | 0.097 |
| FLA | All_DHL | GLM + SUPER | S7_135687915 | 7 | 135687915 | 0.077 |
| FLA | All_DHL | GLM + SUPER | S7_135843534 | 7 | 135843534 | 0.080 |
| FLA | All_DHL | GLM + SUPER | S7_136481483 | 7 | 136481483 | 0.079 |
| FLA | All_DHL | GLM + SUPER | S7_137992358 | 7 | 137992358 | 0.105 |
| FLA | All_DHL | GLM + SUPER | S7_142500815 | 7 | 142500815 | 0.074 |
| FLA | All_DHL | GLM + SUPER | S7_143116184 | 7 | 143116184 | 0.084 |
| FLA | All_DHL | GLM + SUPER | S7_145446635 | 7 | 145446635 | 0.127 |
| FLA | All_DHL | GLM + SUPER | S7_146343585 | 7 | 146343585 | 0.088 |
| FLA | All_DHL | GLM + SUPER | S8_113271449 | 8 | 113271449 | 0.006 |
| NPTB | All_DHL | GLM + FarmCPU + SUPER | S4_18124463 | 4 | 18124463 | 0.131 |
| NPTB | All_DHL | GLM + FarmCPU + SUPER | S7_44973843 | 7 | 44973843 | 0.262 |
| NPTB | All_DHL | GLM + FarmCPU + SUPER | S9_114409650 | 9 | 114409650 | 0.189 |
| MAFL | All_DHL | GLM + FarmCPU + SUPER | S3_161169145 | 3 | 161169145 | 0.435 |
| FLA | C0_DHL | GLM + FarmCPU + SUPER | S7_143116333 | 7 | 143116333 | 0.163 |
| MAFL | C0_DHL | GLM + FarmCPU | S2_223717633 | 2 | 223717633 | 0.348 |
| NPTB | All_DHL | FarmCPU + SUPER | S2_29243534 | 2 | 29243534 | 0.123 |
| MAFL | All_DHL | FarmCPU + SUPER | S3_157316324 | 3 | 157316324 | 0.035 |
| MAFL | All_DHL | FarmCPU + SUPER | S10_76631220 | 10 | 76631220 | 0.169 |
| FEFL | All_DHL | FarmCPU + SUPER | S9_19217823 | 9 | 19217823 | 0.351 |

MAFL - male flowering, FEFL - female flowering, FLA - flag leaf angle, NPTB - number of primary tassel branches.

Table 3.6 Candidate genes associated with plant architecture traits in the BSSS DH lines.

| Trait | Chr. | Gene start (Mb) | Gene ID MaizeGDB | Gene ID Gramene | Gene name | Gene description |
|---|---|---|---|---|---|---|
| Male flowering | 2 | 224.1 | Zm00001d007188 | GRMZM2G003558 | eil2 | transcription factor 2 |
| | 2 | 53.9 | Zm00001d003679 | GRMZM2G147619 | sdg102 | set domain gene102 |
| | 2 | 53.8 | Zm00001d003677 | GRMZM2G147685 | o11 | opaque endosperm11 |
| | 2 | 223.8 | Zm00001d007173 | GRMZM2G172621 | abi39 | ABI3-VP1-transcription factor 39 |
| | 2 | 224.2 | Zm00001d007191 | GRMZM2G176327 | myb110 | MYB-transcription factor 110 |
| | 2 | 223.7 | Zm00001d007168 | GRMZM2G359116 | ofp12 | OVATE-transcription factor 12 |
| | 3 | 157.0 | Zm00001d042231 | GRMZM2G091445 | betl10 | basal endosperm transfer layer10 |
| | 3 | 160.0 | Zm00001d042303 | GRMZM2G092112 | atg6a | autophagy6a |
| | 3 | 160.0 | Zm00001d042305 | GRMZM2G092214 | tcptf8 | TCP-transcription factor 8 |
| | 3 | 160.5 | Zm00001d042313 | GRMZM2G171600 | camta3 | CAMTA-transcription factor 3 |
| | 3 | 160.6 | Zm00001d042315 | GRMZM2G171650 | mads69 | MADS-transcription factor 69 |
| | 3 | 160.5 | Zm00001d042312 | GRMZM2G471529 | hk2 | hk2 - histidine kinase2 |
| | 3 | 161.0 | Zm00001d042319 | GRMZM5G878561 | sbp22 | SBP-transcription factor 22 |
| | 10 | 76.7 | Zm00001d024532 | GRMZM2G123308 | glk55 | G2-like-transcription factor 55 |
| | 10 | 139.1 | Zm00001d026126 | GRMZM2G142832 | umc1045 | umc1045 - |
| | 10 | 76.8 | Zm00001d024534 | GRMZM2G305582 | c3h31 | C3H-transcription factor 331 |
| | 10 | 138.7 | Zm00001d026111 | GRMZM2G702579 | ago1b | argonaute1b |
| | 10 | 138.7 | Zm00001d026113 | GRMZM5G884137 | nkd2 | naked endosperm2 |
| Female flowering | 9 | 18.9 | Zm00001d045323 | GRMZM2G028594 | dbb11 | double B-box zinc finger protein11 |
| | 3 | 161.0 | Zm00001d042319 | GRMZM5G878561 | sbp22 | SBP-transcription factor 22 |
| Flag leaf angle | 7 | 138.2 | Zm00001d020971 | GRMZM2G004583 | ij1 | iojap striping1 |
| | 7 | 138.2 | Zm00001d020970 | GRMZM2G004683 | dfr1 | dihydroflavonoid reductase1 |
| | 7 | 146.3 | Zm00001d021214 | GRMZM2G018138 | ereb88 | AP2-EREBP-transcription factor 88 |
| | 7 | 145.4 | Zm00001d021191 | GRMZM2G043600 | bzip22 | bZIP-transcription factor 22 |
| | 7 | 142.5 | Zm00001d021087 | GRMZM2G059225 | dsc3 | Discolored-paralog3 |
| | 7 | 146.6 | Zm00001d021226 | GRMZM2G073377 | nthr3 | anther-specific protein 3 |
| | 7 | 135.2 | Zm00001d020874 | GRMZM2G078691 | ca5p16 | CCAAT-HAP5-transcription factor 516 |
| | 7 | 135.2 | Zm00001d020875 | GRMZM2G078779 | burp4 | BURP domain-containing protein-RD22-like4 |
| | 7 | 142.5 | Zm00001d021089 | GRMZM2G131281 | ereb116 | AP2-EREBP-transcription factor 116 |
| | 7 | 135.3 | Zm00001d020881 | GRMZM2G151407 | wrky52 | WRKY-transcription factor 52 |
| | 8 | 113.2 | Zm00001d010406 | GRMZM2G021069 | mcm6 | minichromosome maintenance6 |
| | 8 | 113.5 | Zm00001d010411 | GRMZM2G035465 | iaa38 | Aux/IAA-transcription factor 38 |
| | 8 | 113.4 | Zm00001d010410 | GRMZM2G108273 | tip4b | tonoplast intrinsic protein4 |
| | 8 | 112.9 | Zm00001d010399 | GRMZM2G449681 | wrky92 | WRKY-transcription factor 92 |
| Number of primary tassel branches | 2 | 29.2 | Zm00001d002999 | GRMZM2G006964 | ga2ox2 | gibberellin 2-oxidase2 |
| | 2 | 28.9 | Zm00001d002989 | GRMZM2G008792 | ckx12 | cytokinin oxidase12 |
| | 2 | 43.6 | Zm00001d003412 | GRMZM2G032655 | myb49 | MYB-transcription factor 49 |
| | 2 | 43.6 | Zm00001d003409 | GRMZM2G032905 | mads63 | MADS-transcription factor 63 |
| | 2 | 28.9 | Zm00001d002982 | GRMZM2G035688 | abph1 | aberrant phyllotaxy1 |

Table 3.6 Continued

| Trait | Chr. | Gene start (Mb) | Gene ID MaizeGDB | Gene ID Gramene | Gene name | Gene description |
|---|---|---|---|---|---|---|
| | 2 | 39.0 | Zm00001d003291 | GRMZM2G045005 | tgz21 | transglutaminase21 |
| | 2 | 43.0 | Zm00001d003398 | GRMZM2G094532 | fl1 | floury endosperm1 |
| | 2 | 38.1 | Zm00001d003258 | GRMZM2G100872 | hag103a | histone acetyl transferase GNAT/MYST103a |
| | 2 | 37.8 | Zm00001d003247 | GRMZM2G102183 | mas1 | mas1 - malate synthase1 |
| | 2 | 43.1 | Zm00001d003401 | GRMZM2G102499 | grf1 | general regulatory factor1 |
| | 2 | 29.4 | Zm00001d003011 | GRMZM2G122614 | arftf6 | ARF-transcription factor 6 |
| | 2 | 38.0 | Zm00001d003252 | GRMZM2G130230 | gpdh1 | glucose-6-phosphate dehydrogenase1 |
| | 2 | 38.7 | Zm00001d003284 | GRMZM2G135396 | mybr93 | MYB-related-transcription factor 93 |
| | 2 | 39.4 | Zm00001d003300 | GRMZM2G139846 | nbr1b | next to brca1b |
| | 2 | 29.3 | Zm00001d003006 | GRMZM2G178693 | pip2a | plasma membrane intrinsic protein2 |
| | 2 | 29.5 | Zm00001d003016 | GRMZM2G441347 | pal2 | phenylalanine ammonia lyase2 |
| | 2 | 39.1 | Zm00001d003293 | GRMZM2G450445 | nactf111 | NAC-transcription factor 111 |
| | 4 | 17.9 | Zm00001d049152 | GRMZM2G079452 | prda1 | pep-related development arrested1 homolog |
| | 4 | 18.4 | Zm00001d049158 | GRMZM2G080168 | bhlh141 | bHLH-transcription factor 141 |
| | 4 | 18.5 | Zm00001d049160 | GRMZM2G143392 | sig2A | sigma factor sig2A |
| | 7 | 53.2 | Zm00001d019712 | GRMZM2G050550 | myb153 | MYB-transcription factor 153 |
| | 9 | 114.2 | Zm00001d046981 | GRMZM2G454449 | glk32 | G2-like-transcription factor 32 |

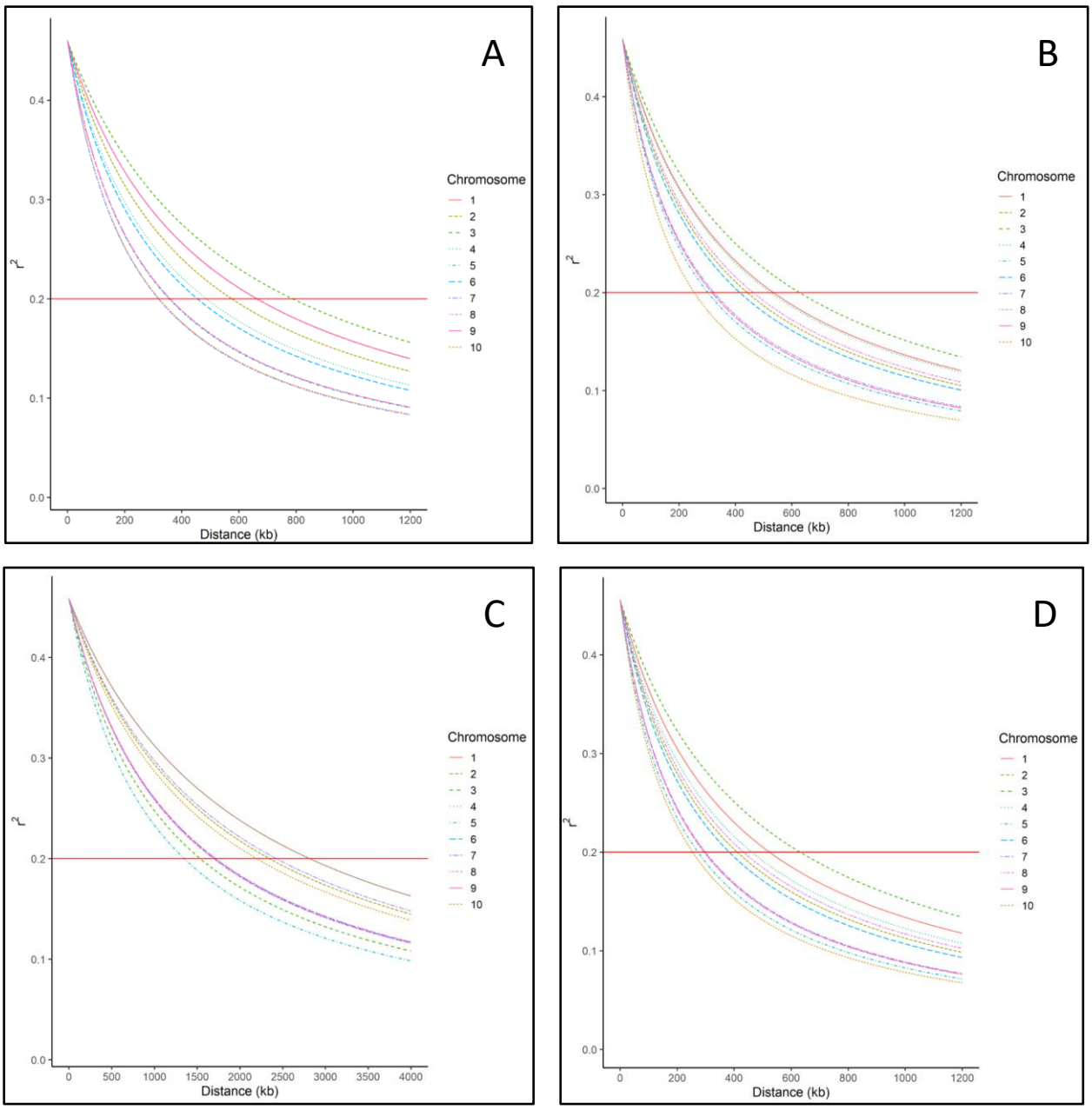


Figure 3.1 Genome-wide LD decay distance in A) C0_DHL group, B) C0/C17_DHL group, C) C17_DHL group, and D) Entire panel of 487 DH lines.

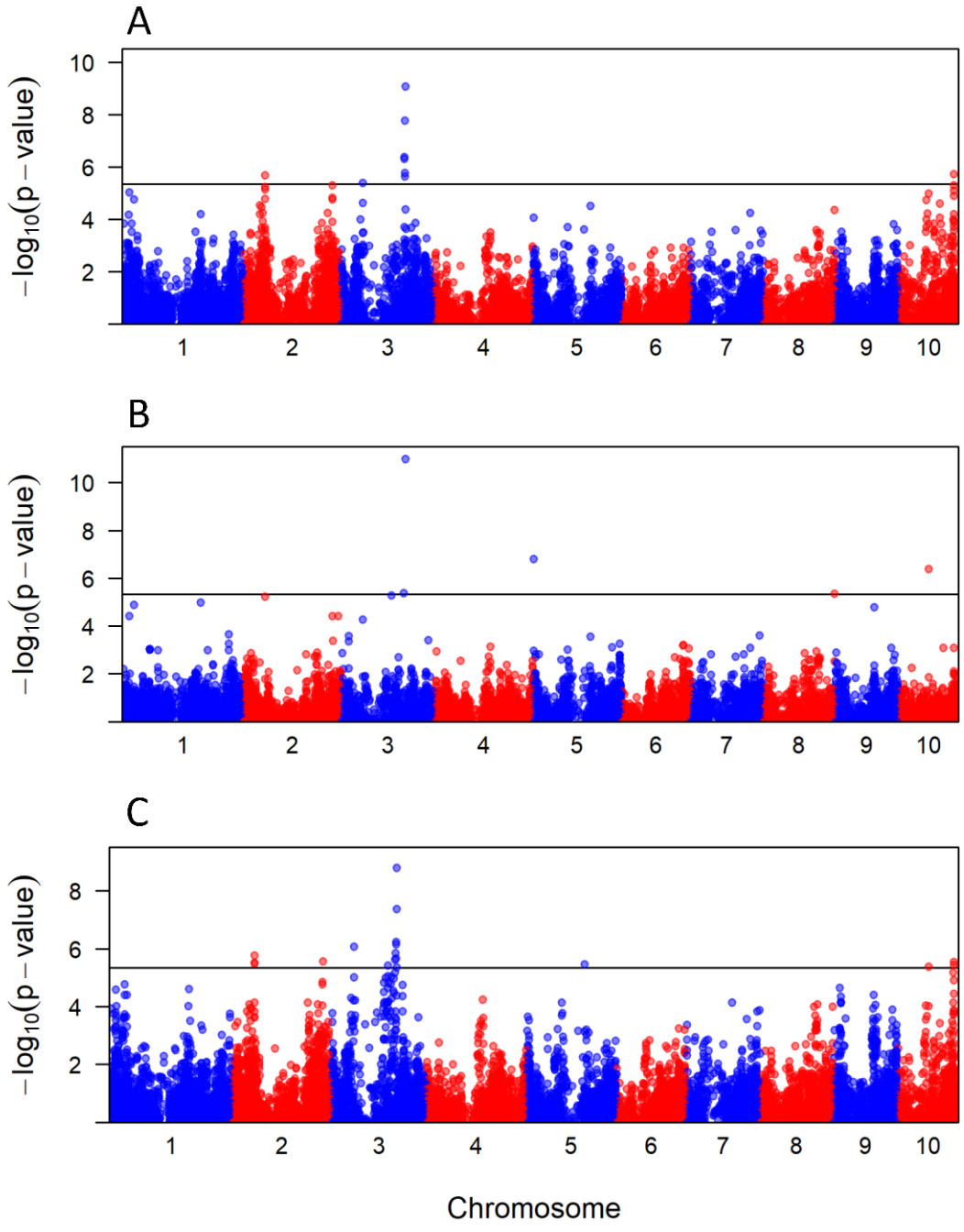


Figure 3.2 Manhattan plot results showing significant SNP markers associated with **male flowering** in the entire panel of DH lines using different methods. A) GLM, B) FarmCPU, and C) SUPER. The X-axis represents the genomic position of the SNPs per chromosome, and the Y-axis is the negative log base 10.

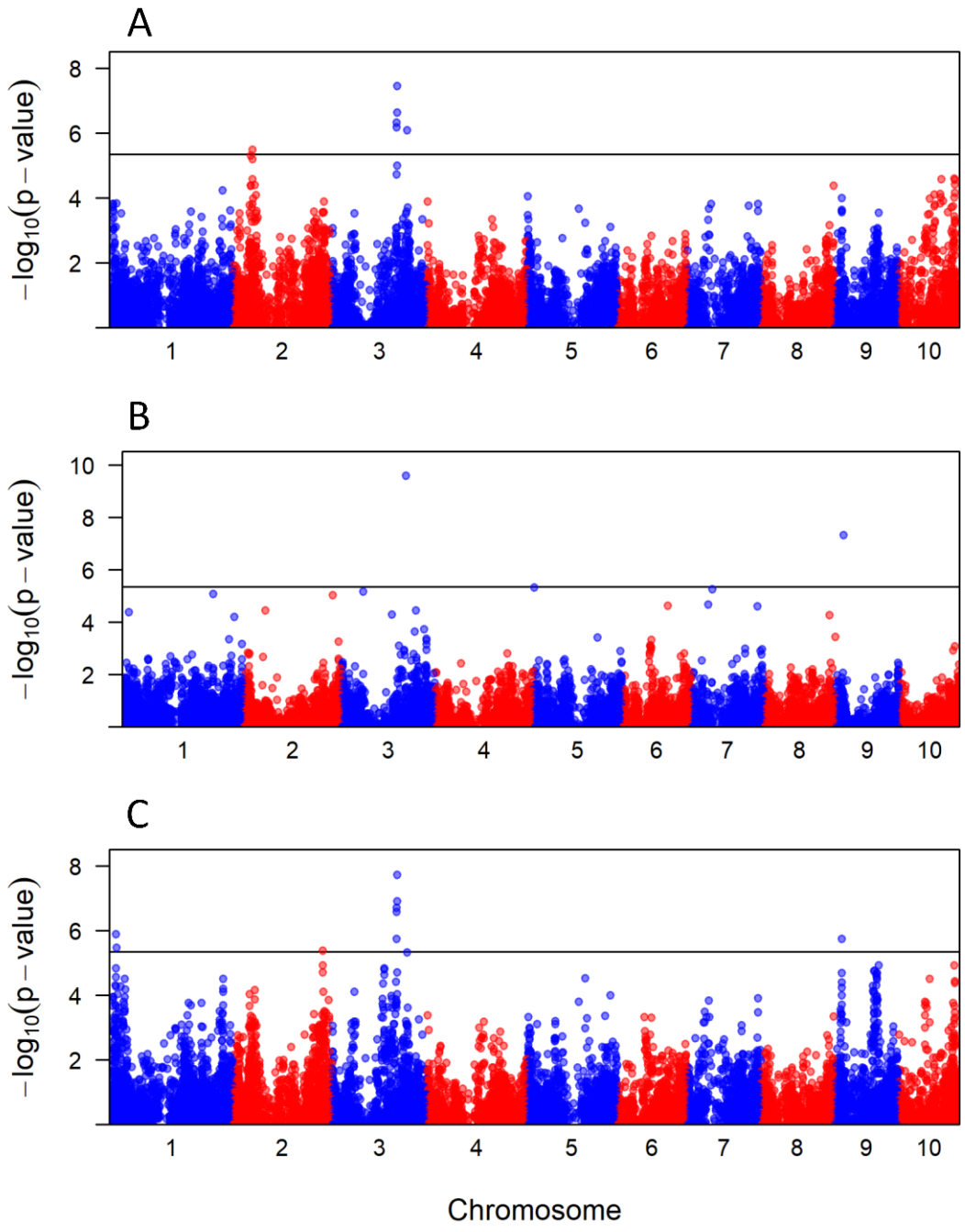


Figure 3.3 Manhattan plot results showing significant SNP markers associated with **female flowering** in the entire panel of DH lines using different methods. A) GLM, B) FarmCPU, and C) SUPER. The X-axis represents the genomic position of the SNPs per chromosome, and the Y-axis is the negative log base 10.

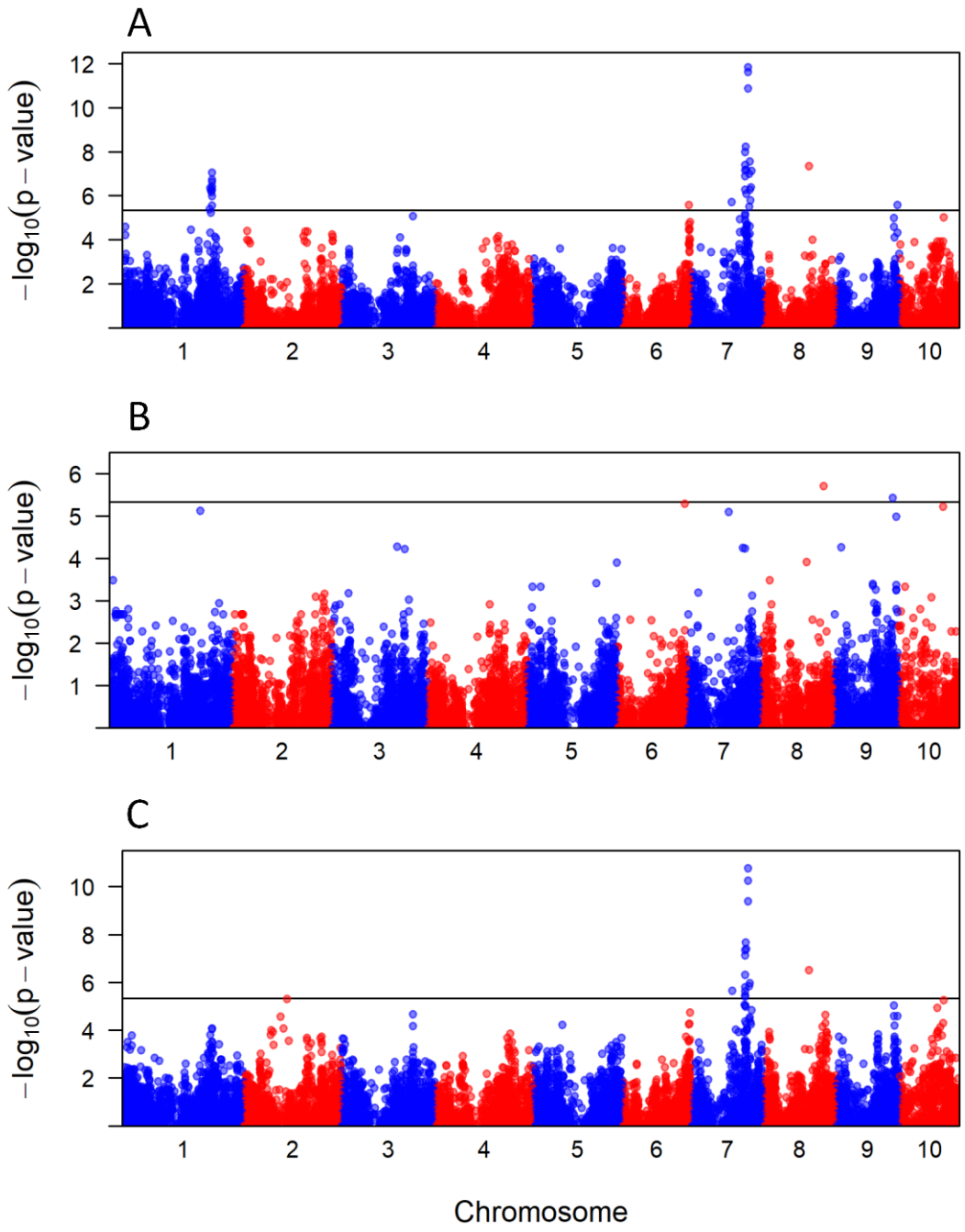


Figure 3.4 Manhattan plot results showing significant SNP markers associated with **flag leaf angle** in the entire panel of DH lines using different methods. A) GLM, B) FarmCPU, and C) SUPER. The X-axis represents the SNPs' genomic position per chromosome, and the Y-axis is the negative log base 10.

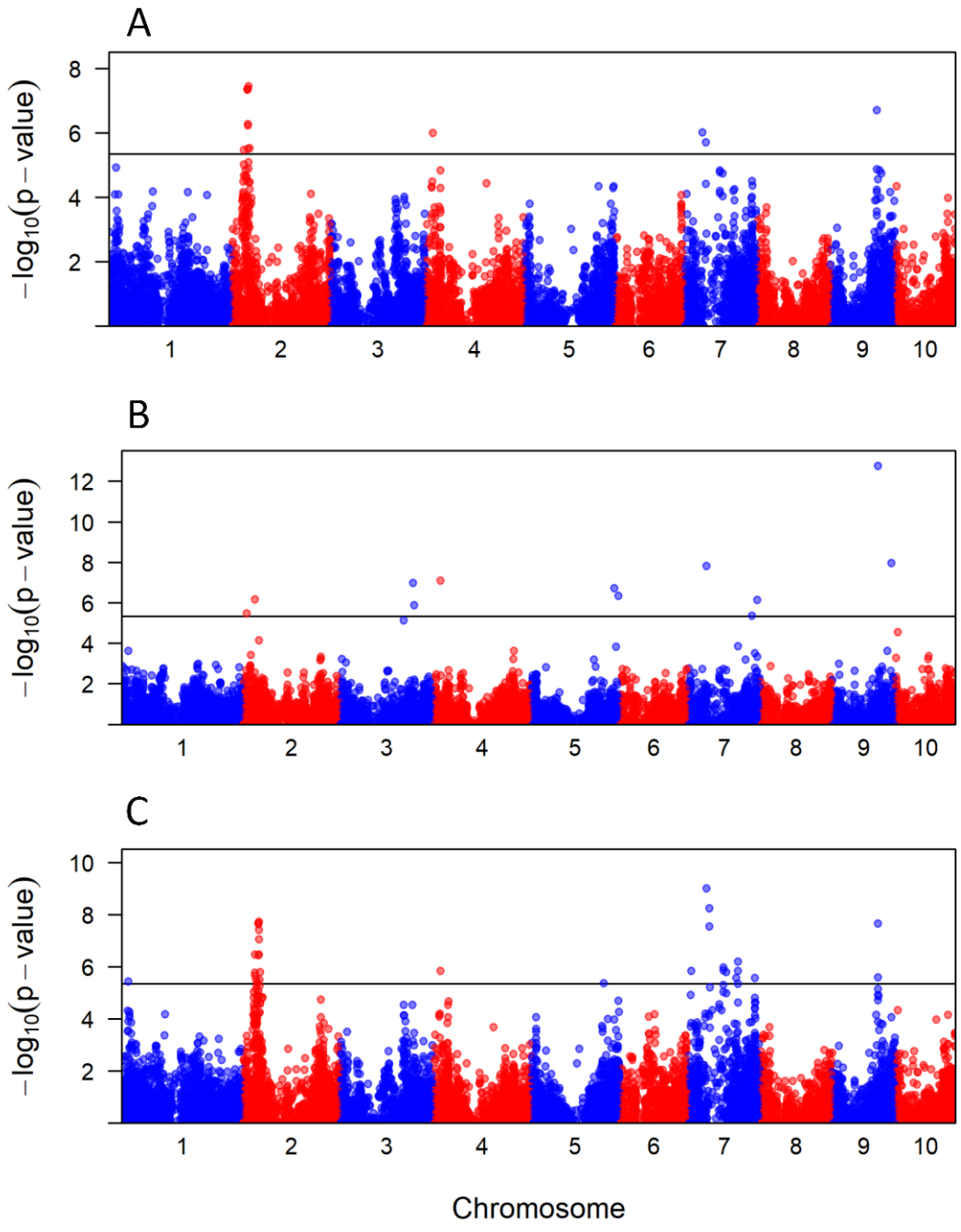


Figure 3.5 Manhattan plot results showing significant SNP markers associated with the **number of primary tassel branches** in the entire panel of DH lines using different methods. A) GLM, B) FarmCPU, and C) SUPER. The X-axis represents the SNPs' genomic position per chromosome, and the Y-axis is the negative log base 10.

## References

Almeida, V. C., Trentin, H. U., Frei, U. K., & Lübberstedt, T. (2020). Genomic prediction of maternal haploid induction rate in maize. Plant Genome, 13(1). https://doi.org/10.1002/tpg2.20014

Andorf, C., Beavis, W. D., Hufford, M., Smith, S., Suza, W. P., Wang, K., … Lübberstedt, T. (2019). Technological advances in maize breeding: past, present and future. Theoretical and Applied Genetics. https://doi.org/10.1007/s00122-019-03306-3

Atwell, S., Huang, Y. S., Vilhjálmsson, B. J., Willems, G., Horton, M., Li, Y., … Nordborg, M. (2010). Genome-wide association study of 107 phenotypes in Arabidopsis thaliana inbred lines. Nature, 465(7298), 627–631. https://doi.org/10.1038/nature08800

Böhm, J., Schipprack, W., Utz, H. F., & Melchinger, A. E. (2017). Tapping the genetic diversity of landraces in allogamous crops with doubled haploid lines: a case study from European flint maize. Theoretical and Applied Genetics, 130(5), 861–873. https://doi.org/10.1007/s00122-017-2856-x

Bradbury, P. J., Zhang, Z., Kroon, D. E., Casstevens, T. M., Ramdoss, Y., & Buckler, E. S. (2007). TASSEL: Software for association mapping of complex traits in diverse samples. Bioinformatics, 23(19), 2633–2635. https://doi.org/10.1093/bioinformatics/btm308

Brekke, B., Edwards, J., & Knapp, A. (2011). Selection and adaptation to high plant density in the Iowa StiffStalk Synthetic maize (Zea mays L.) population: II. plant morphology. Crop Science, 51(6), 2344–2351. https://doi.org/10.2135/cropsci2010.09.0562

Buckler, E. S., Holland, J. B., Bradbury, P. J., Acharya, C. B., Brown, P. J., Browne, C., … McMullen, M. D. (2009). The genetic architecture of maize flowering time. Science, 325(5941), 714–718. https://doi.org/10.1126/science.1174276

Candela, H., Johnston, R., Gerhold, A., Foster, T., & Hake, S. (2008). The milkweed pod1 gene encodes a KANADI protein that is required for abaxial/adaxial patterning in maize leaves. Plant Cell, 20(8), 2073–2087. https://doi.org/10.1105/tpc.108.059709

Carena, M. J., Hallauer, A. R., & Miranda Filho, J. B. (2010). Quantitative Genetics in Maize Breeding. New York, NY: Springer New York. https://doi.org/10.1007/978-1-4419-0766-0

Chaikam, V., Molenaar, W., Melchinger, A. E., & Boddupalli, P. M. (2019). Doubled haploid technology for line development in maize : technical advances and prospects. Theoretical and Applied Genetics, 132(12), 3227–3243. https://doi.org/10.1007/s00122-019-03433-x

Chardon, F., Virlon, B., Moreau, L., Falque, M., Joets, J., Decousset, L., … Charcosset, A. (2004). Genetic architecture of flowering time in maize as inferred from quantitative trait loci meta-analysis and synteny conservation with the rice genome. Genetics, 168(4), 2169–2185. https://doi.org/10.1534/genetics.104.032375

Chen, Z., Yang, C., Tang, D., Zhang, L., Zhang, L., Qu, J., & Liu, J. (2017). Dissection of the genetic architecture for tassel branch number by QTL analysis in two related populations in maize. Journal of Integrative Agriculture, 16(7), 1432–1442. https://doi.org/10.1016/S2095-3119(16)61538-1

Coffman, S. M., Hufford, M. B., Andorf, C. M., & Lübberstedt, T. (2019). Haplotype structure in commercial maize breeding programs in relation to key founder lines. Theoretical and Applied Genetics. https://doi.org/10.1007/s00122-019-03486-y

Comstock, R. E., Robinson, H. F., & Harvey, P. H. (1949). A Breeding Procedure Designed To Make Maximum Use of Both General and Specific Combining Ability 1. Agronomy Journal, 41(8), 360–367. https://doi.org/10.2134/agronj1949.00021962004100080006x

Duncan, W. G. (1971). Leaf Angles, Leaf Area, and Canopy Photosynthesis, (4), 2–5.

Duncan, W. G., Loomis, R. S., Williams, W. A., & Hanau, R. (1967). A model for simulating photosynthesis in plant communities. Hilgardia, 38(4), 181–205. https://doi.org/10.3733/hilg.v38n04p181

Durand, E., Bouchet, S., Bertin, P., Ressayre, A., Jamin, P., Charcosset, A., … Tenaillon, M. I. (2012). Flowering time in maize: Linkage and epistasis at a major effect locus. Genetics, 190(4), 1547–1562. https://doi.org/10.1534/genetics.111.136903

Duvick, D. N. (2005). The Contribution of Breeding to Yield Advances in maize (Zea mays L.). Advances in Agronomy. https://doi.org/10.1016/S0065-2113(05)86002-X

Edwards, J. (2011). Changes in plant morphology in response to recurrent selection in the Iowa Stiff Stalk Synthetic maize population. Crop Science, 51(6), 2352–2361. https://doi.org/10.2135/cropsci2010.09.0564

Flint-Garcia, S. A., Thornsberry, J. M., & Edward IV, S. B. (2003). Structure of Linkage Disequilibrium in Plants. Annual Review of Plant Biology, 54, 357–374. https://doi.org/10.1146/annurev.arplant.54.031902.134907

Gao, X., Becker, L. C., Becker, D. M., Starmer, J. D., & Province, M. A. (2010). Avoiding the high Bonferroni penalty in genome-wide association studies. Genetic Epidemiology, 34(1), 100–105. https://doi.org/10.1002/gepi.20430

Gao, X., Becker, L. C., Becker, D. M., Starmer, J. D., Province, M. A., & Martin, E. R. (2008). A multiple testing correction method for genetic association studies using correlated single nucleotide polymorphisms. Genetic Epidemiology, 32(4), 361–369. https://doi.org/10.1002/gepi.20310

Gerke, J. P., Edwards, J. W., Guill, K. E., Ross-Ibarra, J., & McMullen, M. D. (2015). The genomic impacts of drift and selection for hybrid performance in maize. Genetics, 201(3), 1201–1211. https://doi.org/10.1534/genetics.115.182410

Goodman, M. M. (2005). Broadening the U.S. maize germplasm base. Maydica, 50(3), 203–214.

Hallauer, A. R., & Darrah, L. L. (1985). Compendium of recurrent selection methods and their application. Critical Reviews in Plant Sciences, 3(1), 1–33. https://doi.org/10.1080/07352688509382202

Hill, W. G., & Weir, B. S. (1988). Variances and covariances of squared linkage disequilibria in finite populations. Theoretical Population Biology, 33(1), 54–78. https://doi.org/10.1016/0040-5809(88)90004-4

Hull, F. H. (1945). Recurrent Selection for Specific Combining Ability in Corn 1. Agronomy Journal, 37(2), 134–145. https://doi.org/10.2134/agronj1945.00021962003700020006x

Jenkins, M. T. (1940). The Segregation of Genes Affecting Yield of Grain in Maize 1. Agronomy Journal, 32(1), 55–63. https://doi.org/10.2134/agronj1940.00021962003200010008x

Jiao, Y., Peluso, P., Shi, J., Liang, T., Stitzer, M. C., Wang, B., … Ware, D. (2017). Improved maize reference genome with single-molecule technologies. Nature, 546(7659), 524–527. https://doi.org/10.1038/nature22971

Khush, G. S. (2001). Green revolution: The way forward. Nature Reviews Genetics, 2, 815–822.

Kilian, A., Wenzl, P., Huttner, E., Carling, J., Xia, L., Blois, H., … Uszynski, G. (2012). Diversity Arrays Technology: A Generic Genome Profiling Technology on Open Platforms (pp. 67–89). https://doi.org/10.1007/978-1-61779-870-2_5

Kinsella, R. J., Kahari, A., Haider, S., Zamora, J., Proctor, G., Spudich, G., … Flicek, P. (2011). Ensembl BioMarts: a hub for data retrieval across taxonomic space. Database, 2011, bar030–bar030. https://doi.org/10.1093/database/bar030

Lauer, S., Hall, B. D., Mulaosmanovic, E., Anderson, S. R., Nelson, B., & Smith, S. (2012). Morphological changes in parental lines of Pioneer brand maize hybrids in the U.S. central Corn Belt. Crop Science, 52(3), 1033–1043. https://doi.org/10.2135/cropsci2011.05.0274

Lipka, A. E., Tian, F., Wang, Q., Peiffer, J., Li, M., Bradbury, P. J., … Zhang, Z. (2012). GAPIT: genome association and prediction integrated tool. Bioinformatics, 28(18), 2397–2399. https://doi.org/10.1093/bioinformatics/bts444

Liu, X., Huang, M., Fan, B., Buckler, E. S., & Zhang, Z. (2016). Iterative Usage of Fixed and Random Effect Models for Powerful and Efficient Genome-Wide Association Studies. PLOS Genetics, 12(2), e1005767. https://doi.org/10.1371/journal.pgen.1005767

Mock, J. J., & Pearce, R. B. (1975). An ideotype of maize. Euphytica, 24(3), 613–623. https://doi.org/10.1007/BF00132898

Money, D., Gardner, K., Migicovsky, Z., Schwaninger, H., Zhong, G., & Myles, S. (2016). LinkImpute : Fast and Accurate Genotype Imputation for Non-Model LinkImpute : Fast and Accurate Genotype Imputation for Nonmodel Organisms, (January). https://doi.org/10.1534/g3.115.021667

Peiffer, J. A., Romay, M. C., Gore, M. A., Flint-Garcia, S. A., Zhang, Z., Millard, M. J., … Buckler, E. S. (2014). The genetic architecture of maize height. Genetics, 196(4), 1337–1356. https://doi.org/10.1534/genetics.113.159152

Pollak, L. M. (2003). The History and Success of the public–private project on germplasm enhancement of maize (GEM) (pp. 45–87). https://doi.org/10.1016/S0065-2113(02)78002-4

Portwood, J. L., Woodhouse, M. R., Cannon, E. K., Gardiner, J. M., Harper, L. C., Schaeffer, M. L., … Andorf, C. M. (2019). MaizeGDB 2018: the maize multi-genome genetics and genomics database. Nucleic Acids Research, 47(D1), D1146–D1154. https://doi.org/10.1093/nar/gky1046

R Core Team. (2019). R: A language and environment for statistical computing. R Foundation for Statistical Computing.

Romay, M. C., Flint-Garcia, S. A., Casstevens, T. M., Glaubitz, J. C., McMullen, M. D., Holland, J. B., … Buckler, E. S. (2013). Comprehensive genotyping of the USA national maize inbred seed bank. Genome Biology, 14(6). https://doi.org/10.1186/gb-2013-14-6-r55

SAS Institute. SAS 9.4 Statements: Reference. Cary, NC: SAS Institute Inc.

Schwarz, G. (1978). Estimating the Dimension of a Model. *The Annals of Statistics*, *6*(2), 461–464.

Smith, J. S. C. (1988). Diversity of United States Hybrid Maize Germplasm; Isozymic and Chromatographic Evidence. Crop Science, 28(1), 63–69. https://doi.org/10.2135/cropsci1988.0011183x002800010016x

Sprague, G. F. (1946). Early Testing of Inbred Lines of Corn. Journal of the American Society of Agronomy.

Strigens, A., Schipprack, W., Reif, J. C., & Melchinger, A. E. (2013). Unlocking the Genetic Diversity of Maize Landraces with Doubled Haploids Opens New Avenues for Breeding. PLoS ONE, 8(2), 7–9. https://doi.org/10.1371/journal.pone.0057234

Teng, F., Zhai, L., Liu, R., Bai, W., Wang, L., Huo, D., … Zhang, Z. (2013). ZmGA3ox2 , a candidate gene for a major QTL, qPH3.1, for plant height in maize. The Plant Journal, 73(3), 405–416. https://doi.org/10.1111/tpj.12038

Vanous, K., Vanous, A., Frei, U. K., & Lübberstedt, T. (2017). Generation of Maize ( Zea mays ) Doubled Haploids via Traditional Methods. *Current Protocols in Plant Biology*, 147–157. https://doi.org/10.1002/cppb.20050

Vanous, A., Gardner, C., Blanco, M., Martin-Schwarze, A., Lipka, A. E., Flint-Garcia, S., … Lübberstedt, T. (2018). Association Mapping of Flowering and Height Traits in Germplasm Enhancement of Maize Doubled Haploid (GEM-DH) Lines. The Plant Genome, 11(2), 0. https://doi.org/10.3835/plantgenome2017.09.0083

VanRaden, P. M. (2008). Efficient Methods to Compute Genomic Predictions. Journal of Dairy Science, 91(11), 4414–4423. https://doi.org/10.3168/jds.2007-0980

Vos, P. G., Paulo, M. J., Voorrips, R. E., Visser, R. G. F., van Eck, H. J., & van Eeuwijk, F. A. (2017). Evaluation of LD decay and various LD-decay estimators in simulated and SNP-array data of tetraploid potato. Theoretical and Applied Genetics, 130(1), 123–135. https://doi.org/10.1007/s00122-016-2798-8

Wang, J. W., Czech, B., & Weigel, D. (2009). miR156-Regulated SPL Transcription Factors Define an Endogenous Flowering Pathway in Arabidopsis thaliana. Cell, 138(4), 738–749. https://doi.org/10.1016/j.cell.2009.06.014

Wang, Q., Tian, F., Pan, Y., Buckler, E. S., & Zhang, Z. (2014). A SUPER powerful method for genome wide association study. PLoS ONE, 9(9). https://doi.org/10.1371/journal.pone.0107684

Wilde, K., Burger, H., Prigge, V., Presterl, T., Schmidt, W., Ouzunova, M., & Geiger, H. H. (2010). Testcross performance of doubled-haploid lines developed from European flint maize landraces. Plant Breeding, 129(2), 181–185. https://doi.org/10.1111/j.1439-0523.2009.01677.x

Wu, Y., San Vicente, F., Huang, K., Dhliwayo, T., Costich, D. E., Semagn, K., … Babu, R. (2016). Molecular characterization of CIMMYT maize inbred lines with genotyping-by-sequencing SNPs. Theoretical and Applied Genetics, 129(4), 753–765. https://doi.org/10.1007/s00122-016-2664-8

## Appendix: Supplemental Tables

Table S3.1. Combination of random effects with the lowest Bayesian Information Criterion (BIC) values used in the final model to analyze the phenotypic data.

| | Random effects | | | | | | Traits evaluated | | | | | | | |
|---|---|---|---|---|---|---|---|---|---|---|---|---|---|---|
| **Model** | **$G_j$** | **$GE_{ij}$** | **$ED(G)_{ijk}$** | **$A(ER)_{nil}$** | **$P(ER)_{mil}$** | **Homoscedasticity** | **MAFL** | **FEFL** | **ASI** | **PLHE** | **EAHE** | **FLA** | **TALE** | **NPTB** |
| 1 | x | x | x | x | x | No | 6124 | 7007 | 4867 | 19432 | 19076 | 18811 | 11992 | 10140 |
| 1 | x | x | x | x | x | Yes | 6191 | 7029 | 4951 | 19419 | 19073 | 18804 | 11982 | 10140 |
| 2 | x | x | x | x | | No | 6357 | 7160 | 4861 | 19620 | 19111 | 18803 | 11985 | 10132 |
| 2 | x | x | x | x | | Yes | 6492 | 7238 | 4951 | 19613 | 19113 | 18796 | 11975 | 10132 |
| 3 | x | x | x | | x | No | 6337 | 7147 | 4866 | 19627 | 19111 | 18806 | 12017 | 10165 |
| 3 | x | x | x | | x | Yes | 6379 | 7165 | 4950 | 19612 | 19108 | 18800 | 12006 | 10166 |
| 4 | x | x | | x | x | No | 6314 | 7180 | 5012 | 19493 | 19091 | 18805 | 12031 | 10159 |
| 4 | x | x | | x | x | Yes | 6388 | 7210 | 5098 | 19479 | 19090 | 18798 | 12017 | 10160 |
| 5 | x | x | x | | | No | 6538 | 7281 | 4860 | 19770 | 19140 | 18798 | 12009 | 10157 |
| 5 | x | x | x | | | Yes | 6619 | 7334 | 4950 | 19760 | 19141 | 18792 | 11998 | 10158 |
| 6 | x | x | | x | | No | 6490 | 7301 | 5006 | 19675 | 19127 | 18797 | 12024 | 10152 |
| 6 | x | x | | x | | Yes | 6628 | 7384 | 5096 | 19667 | 19130 | 18790 | 12011 | 10152 |
| 7 | x | x | | | x | No | 6488 | 7299 | 5015 | 19671 | 19124 | 18800 | 12056 | 10183 |
| 7 | x | x | | | x | Yes | 6539 | 7324 | 5100 | 19655 | 19124 | 18794 | 12043 | 10185 |
| 8 | x | x | | | | No | 6644 | 7409 | 5008 | 19813 | 19154 | 18792 | 12049 | 10175 |
| 8 | x | x | | | | Yes | 6735 | 7470 | 5098 | 19800 | 19158 | 18786 | 12035 | 10177 |
| 9 | x | | x | | | No | 6650 | 7322 | 4919 | 19765 | 19133 | 18865 | 12026 | 10149 |
| 9 | x | | x | | | Yes | 6716 | 7376 | 5014 | 19754 | 19134 | 18857 | 12015 | 10150 |
| 10 | x | | | x | | No | 6502 | 7302 | 5034 | 19667 | 19119 | 18823 | 12023 | 10144 |
| 10 | x | | | x | | Yes | 6641 | 7387 | 5126 | 19659 | 19122 | 18816 | 12010 | 10144 |
| 11 | x | | | | x | No | 6701 | 7387 | 5097 | 19668 | 19118 | 18873 | 12081 | 10175 |
| 11 | x | | | | x | Yes | 6718 | 7407 | 5203 | 19653 | 19117 | 18865 | 12066 | 10177 |
| 12 | x | | | | | No | 6833 | 7477 | 5089 | 19810 | 19147 | 18865 | 12073 | 10167 |
| 12 | x | | | | | Yes | 6883 | 7538 | 5198 | 19797 | 19151 | 18857 | 12058 | 10169 |

MAFL - male flowering, FEFL - female flowering, ASI - anthesis–silking interval, PLHE - plant height, EAHE - ear height, FLA - flag leaf angle, TALE - tassel length, NPTB - number of primary tassel branches.

$G_j$ = the effect of the group of DH line *j;* $GE_{ij}$ = the effect of the interaction between group *j* and environment *i;* $ED(G)_{ijk}$ = the effect of the interaction of environment *i* and DH line *k* within the group of DH line *j;* $A(ER)_{nil}$ = the effect of the range *n* within the environment *i* and replication *l;* $P(ER)_{mil}$ = the effect of the pass *m* within the environment *i* and replication *l*.

Supplemental Table S3.2. Trait BLUPs of flowering and plant architecture traits for 487 BSSS DH lines.

| No | Group | DH line | MAFL | FEFL | ASI | PLHE | EAHE | FLA | TALE | NPTB |
|---|---|---|---|---|---|---|---|---|---|---|
| 1 | C0 | C0_DH001 | 65.6 | 68.4 | -2.8 | 158.9 | 95.1 | 37.2 | 43.8 | 22.9 |
| 2 | C0 | C0_DH002 | 65.4 | 65.5 | -0.1 | 160.4 | 76.1 | 24.4 | 36.6 | 13.3 |
| 3 | C0 | C0_DH004 | 69.4 | 71.2 | -1.7 | 180.3 | 96.9 | 34.9 | 30.5 | 17.5 |
| 4 | C0 | C0_DH005 | 66.7 | 68.4 | -1.6 | 192.0 | 103.0 | 68.0 | 41.6 | 22.8 |
| 5 | C0 | C0_DH006 | 72.1 | 72.6 | -0.6 | 199.5 | 81.1 | 47.7 | 39.0 | 2.5 |
| 6 | C0 | C0_DH007 | 64.8 | 65.1 | -0.4 | 179.6 | 94.4 | 62.7 | 39.1 | 20.0 |
| 7 | C0 | C0_DH008 | 66.1 | 67.0 | -0.8 | 176.5 | 67.0 | 61.2 | 37.9 | 17.9 |
| 8 | C0 | C0_DH010 | 64.8 | 67.1 | -2.1 | 158.5 | 64.7 | 45.4 | 42.5 | 16.6 |
| 9 | C0 | C0_DH011 | 67.0 | 67.8 | -0.9 | 148.5 | 76.5 | 39.4 | 37.9 | 9.9 |
| 10 | C0 | C0_DH013 | 70.0 | 72.1 | -2.0 | 156.1 | 71.5 | 34.9 | 40.6 | 17.9 |
| 11 | C0 | C0_DH014 | 71.1 | 70.5 | 0.3 | 185.1 | 94.8 | 43.2 | 43.3 | 14.1 |
| 12 | C0 | C0_DH015 | 69.7 | 69.8 | -0.6 | 190.5 | 93.9 | 50.3 | 39.0 | 21.9 |
| 13 | C0 | C0_DH016 | 67.7 | 66.4 | 0.9 | 145.4 | 67.9 | 43.9 | 35.2 | 15.2 |
| 14 | C0 | C0_DH017 | 68.4 | 71.6 | -3.2 | 178.7 | 80.6 | 60.5 | 37.7 | 6.3 |
| 15 | C0 | C0_DH018 | 67.1 | 71.8 | -4.4 | 175.7 | 50.4 | 34.9 | 39.4 | 22.8 |
| 16 | C0 | C0_DH019 | 65.5 | 66.9 | -1.4 | 165.7 | 70.6 | 28.1 | 37.6 | 11.8 |
| 17 | C0 | C0_DH020 | 68.4 | 71.0 | -2.6 | 188.7 | 93.6 | 25.1 | 33.6 | 14.0 |
| 18 | C0 | C0_DH021 | 64.7 | 69.3 | -4.2 | 181.2 | 96.3 | 30.4 | 41.7 | 13.9 |
| 19 | C0 | C0_DH022 | 69.9 | 71.0 | -1.5 | 172.8 | 87.4 | 31.9 | 38.2 | 12.4 |
| 20 | C0 | C0_DH023 | 67.0 | 64.9 | 1.5 | 176.7 | 90.7 | 27.4 | 41.2 | 16.0 |
| 21 | C0 | C0_DH024 | 67.6 | 67.8 | -0.5 | 163.4 | 76.5 | 28.1 | 30.7 | 10.7 |
| 22 | C0 | C0_DH025 | 66.7 | 68.6 | -1.8 | 172.4 | 83.6 | 35.7 | 33.4 | 10.8 |
| 23 | C0 | C0_DH026 | 66.7 | 67.5 | -1.0 | 168.6 | 74.9 | 21.2 | 35.7 | 21.4 |
| 24 | C0 | C0_DH027 | 68.1 | 71.8 | -3.4 | 159.3 | 84.6 | 28.9 | 42.1 | 23.9 |
| 25 | C0 | C0_DH028 | 66.2 | 67.5 | -1.3 | 157.1 | 65.0 | 42.4 | 40.1 | 23.6 |
| 26 | C0 | C0_DH029 | 67.9 | 69.5 | -1.7 | 174.8 | 84.2 | 34.9 | 33.8 | 21.5 |
| 27 | C0 | C0_DH032 | 70.5 | 71.0 | -0.7 | 164.8 | 98.9 | 42.4 | 30.7 | 21.1 |
| 28 | C0 | C0_DH033 | 64.6 | 63.9 | 0.4 | 156.0 | 70.6 | 22.9 | 36.3 | 21.3 |
| 29 | C0 | C0_DH034 | 68.3 | 70.1 | -1.8 | 199.0 | 99.3 | 31.9 | 33.9 | 17.1 |
| 30 | C0 | C0_DH035 | 67.4 | 68.1 | -0.9 | 149.6 | 70.3 | 34.2 | 30.5 | 13.6 |
| 31 | C0 | C0_DH036 | 65.6 | 64.0 | 1.2 | 168.8 | 85.0 | 56.7 | 40.4 | 16.4 |
| 32 | C0 | C0_DH037 | 69.5 | 71.7 | -2.2 | 174.8 | 93.0 | 53.0 | 37.0 | 16.5 |
| 33 | C0 | C0_DH038 | 64.5 | 65.6 | -1.2 | 142.7 | 60.0 | 36.9 | 36.9 | 10.2 |
| 34 | C0 | C0_DH039 | 68.6 | 70.6 | -1.9 | 168.8 | 82.4 | 53.0 | 39.4 | 13.7 |
| 35 | C0 | C0_DH040 | 70.4 | 73.1 | -2.7 | 190.9 | 102.4 | 46.9 | 33.7 | 13.0 |
| 36 | C0 | C0_DH041 | 65.8 | 65.5 | 0.2 | 157.9 | 76.7 | 44.7 | 30.0 | 14.5 |
| 37 | C0 | C0_DH042 | 67.5 | 69.7 | -2.0 | 163.7 | 76.8 | 56.7 | 38.5 | 19.3 |
| 38 | C0 | C0_DH043 | 70.8 | 72.5 | -1.6 | 161.7 | 98.9 | 39.4 | 36.0 | 14.8 |
| 39 | C0 | C0_DH044 | 67.3 | 69.0 | -1.7 | 163.0 | 91.4 | 59.0 | 32.8 | 22.2 |
| 40 | C0 | C0_DH045 | 67.5 | 70.1 | -2.5 | 182.7 | 98.8 | 51.5 | 39.8 | 12.4 |
| 41 | C0 | C0_DH046 | 70.6 | 72.5 | -1.9 | 165.4 | 100.0 | 37.2 | 35.8 | 14.1 |
| 42 | C0 | C0_DH047 | 60.3 | 63.3 | -3.0 | 149.7 | 62.8 | 33.4 | 38.4 | 18.2 |
| 43 | C0 | C0_DH048 | 65.8 | 68.4 | -2.3 | 173.4 | 76.4 | 44.7 | 36.4 | 18.3 |
| 44 | C0 | C0_DH049 | 70.9 | 72.3 | -1.3 | 178.4 | 97.4 | 52.2 | 42.4 | 13.9 |
| 45 | C0 | C0_DH050 | 72.2 | 72.2 | -0.1 | 147.4 | 71.0 | 35.7 | 29.8 | 7.2 |
| 46 | C0 | C0_DH051 | 64.0 | 65.5 | -1.5 | 173.4 | 87.7 | 89.7 | 38.5 | 17.7 |
| 47 | C0 | C0_DH052 | 64.0 | 66.7 | -2.6 | 161.1 | 71.4 | 39.4 | 38.8 | 22.2 |
| 48 | C0 | C0_DH053 | 67.3 | 70.3 | -2.8 | 177.3 | 89.3 | 42.4 | 35.0 | 8.6 |
| 49 | C0 | C0_DH054 | 62.5 | 64.9 | -2.1 | 185.8 | 105.5 | 43.9 | 40.5 | 13.1 |
| 50 | C0 | C0_DH055 | 66.8 | 67.3 | -0.4 | 164.7 | 74.7 | 35.7 | 34.7 | 10.8 |
| 51 | C0 | C0_DH056 | 63.9 | 64.3 | -0.4 | 184.6 | 84.8 | 40.9 | 43.7 | 12.9 |
| 52 | C0 | C0_DH058 | 67.6 | 69.6 | -1.8 | 159.5 | 71.2 | 25.9 | 36.2 | 16.3 |

Table S3.2. Continued

| No | Group | DH line | MAFL | FEFL | ASI | PLHE | EAHE | FLA | TALE | NPTB |
|---|---|---|---|---|---|---|---|---|---|---|
| 53 | C0 | C0_DH059 | 70.8 | 72.2 | -1.5 | 174.6 | 87.7 | 26.6 | 39.0 | 11.0 |
| 54 | C0 | C0_DH060 | 66.4 | 67.3 | -0.9 | 186.5 | 87.8 | 64.2 | 40.3 | 7.6 |
| 55 | C0 | C0_DH061 | 70.0 | 73.4 | -3.2 | 181.2 | 89.6 | 38.7 | 36.6 | 14.5 |
| 56 | C0 | C0_DH062 | 72.3 | 73.6 | -1.4 | 162.7 | 91.0 | 39.4 | 33.9 | 15.3 |
| 57 | C0 | C0_DH063 | 68.4 | 70.9 | -2.5 | 184.2 | 100.3 | 53.0 | 27.9 | 19.2 |
| 58 | C0 | C0_DH064 | 60.8 | 60.6 | -0.2 | 148.6 | 67.8 | 88.8 | 33.2 | 14.1 |
| 59 | C0 | C0_DH065 | 65.1 | 68.7 | -3.2 | 180.9 | 112.5 | 47.7 | 37.8 | 24.7 |
| 60 | C0 | C0_DH066 | 68.1 | 70.0 | -1.9 | 185.0 | 87.6 | 34.9 | 36.3 | 11.8 |
| 61 | C0 | C0_DH067 | 71.2 | 72.1 | -0.9 | 190.1 | 101.3 | 55.2 | 38.1 | 19.5 |
| 62 | C0 | C0_DH068 | 66.0 | 67.1 | -1.2 | 177.4 | 95.9 | 33.4 | 44.6 | 12.3 |
| 63 | C0 | C0_DH069 | 64.7 | 64.4 | 0.0 | 132.1 | 58.3 | 50.0 | 32.8 | 13.7 |
| 64 | C0 | C0_DH071 | 66.6 | 68.6 | -1.9 | 191.9 | 106.4 | 42.4 | 34.9 | 11.5 |
| 65 | C0 | C0_DH072 | 67.2 | 68.6 | -1.4 | 116.4 | 61.4 | 37.2 | 38.8 | 23.1 |
| 66 | C0 | C0_DH073 | 66.7 | 67.7 | -1.0 | 163.4 | 75.2 | 27.4 | 44.9 | 14.8 |
| 67 | C0 | C0_DH075 | 68.1 | 69.3 | -1.1 | 189.9 | 92.3 | 42.4 | 39.0 | 21.4 |
| 68 | C0 | C0_DH076 | 65.5 | 67.0 | -1.5 | 164.8 | 74.2 | 33.4 | 34.3 | 9.5 |
| 69 | C0 | C0_DH077 | 72.1 | 73.6 | -1.4 | 194.5 | 108.9 | 41.7 | 31.0 | 11.1 |
| 70 | C0 | C0_DH078 | 68.4 | 72.3 | -3.8 | 185.6 | 61.9 | 33.4 | 36.2 | 20.4 |
| 71 | C0 | C0_DH080 | 67.8 | 70.4 | -2.5 | 178.2 | 94.1 | 37.9 | 38.5 | 17.8 |
| 72 | C0 | C0_DH081 | 65.2 | 68.5 | -3.0 | 152.9 | 76.6 | 31.9 | 38.5 | 14.1 |
| 73 | C0 | C0_DH082 | 64.6 | 67.9 | -3.0 | 180.0 | 96.1 | 59.0 | 35.8 | 16.5 |
| 74 | C0 | C0_DH083 | 69.9 | 73.8 | -3.8 | 182.4 | 90.8 | 52.2 | 38.1 | 18.5 |
| 75 | C0 | C0_DH085 | 66.1 | 66.2 | -0.3 | 197.8 | 102.1 | 37.9 | 40.8 | 15.4 |
| 76 | C0 | C0_DH086 | 68.2 | 70.0 | -1.6 | 150.1 | 71.0 | 42.4 | 33.6 | 15.9 |
| 77 | C0 | C0_DH087 | 70.3 | 71.4 | -1.1 | 177.3 | 103.8 | 39.4 | 37.1 | 18.0 |
| 78 | C0 | C0_DH088 | 71.3 | 73.9 | -2.7 | 172.5 | 102.7 | 34.9 | 32.1 | 11.3 |
| 79 | C0 | C0_DH089 | 69.4 | 71.8 | -2.4 | 209.7 | 136.6 | 35.7 | 37.1 | 14.6 |
| 80 | C0 | C0_DH090 | 67.8 | 70.1 | -2.4 | 150.3 | 65.2 | 37.9 | 39.9 | 17.7 |
| 81 | C0 | C0_DH091 | 68.7 | 69.9 | -1.2 | 181.3 | 85.7 | 51.5 | 37.7 | 14.6 |
| 82 | C0 | C0_DH092 | 68.6 | 70.2 | -1.5 | 183.1 | 103.0 | 59.7 | 37.4 | 18.9 |
| 83 | C0 | C0_DH093 | 70.6 | 71.4 | -0.9 | 158.0 | 75.6 | 50.7 | 36.4 | 9.4 |
| 84 | C0 | C0_DH094 | 70.0 | 72.7 | -2.3 | 159.8 | 81.3 | 37.2 | 36.5 | 10.6 |
| 85 | C0 | C0_DH095 | 67.1 | 68.7 | -1.6 | 181.4 | 90.4 | 56.0 | 43.4 | 11.9 |
| 86 | C0 | C0_DH096 | 66.9 | 70.8 | -3.7 | 150.0 | 69.8 | 32.7 | 42.1 | 19.7 |
| 87 | C0 | C0_DH098 | 67.0 | 69.6 | -2.5 | 166.2 | 74.7 | 15.2 | 31.7 | 15.4 |
| 88 | C0 | C0_DH099 | 67.8 | 70.5 | -2.7 | 168.6 | 93.8 | 39.4 | 33.6 | 15.6 |
| 89 | C0 | C0_DH100 | 63.2 | 63.9 | -0.6 | 134.1 | 52.0 | 37.2 | 32.5 | 22.8 |
| 90 | C0 | C0_DH102 | 62.6 | 66.3 | -3.4 | 181.2 | 70.4 | 40.2 | 35.1 | 29.8 |
| 91 | C0 | C0_DH103 | 66.8 | 68.2 | -1.6 | 151.8 | 80.7 | 39.4 | 27.7 | 18.9 |
| 92 | C0 | C0_DH104 | 65.6 | 67.0 | -1.5 | 175.4 | 82.4 | 43.9 | 37.8 | 6.9 |
| 93 | C0 | C0_DH106 | 67.5 | 67.9 | -0.5 | 153.2 | 73.6 | 31.9 | 32.1 | 14.9 |
| 94 | C0 | C0_DH107 | 63.4 | 67.0 | -3.3 | 143.4 | 48.1 | 38.7 | 33.3 | 17.3 |
| 95 | C0 | C0_DH108 | 66.1 | 67.5 | -1.6 | 149.4 | 67.9 | 43.9 | 29.7 | 10.1 |
| 96 | C0 | C0_DH109 | 67.3 | 68.6 | -1.5 | 161.2 | 76.0 | 47.7 | 35.4 | 12.0 |
| 97 | C0 | C0_DH110 | 69.0 | 71.0 | -1.8 | 148.9 | 71.2 | 40.9 | 37.3 | 26.1 |
| 98 | C0 | C0_DH111 | 69.8 | 73.2 | -3.2 | 168.6 | 80.5 | 52.2 | 40.0 | 14.5 |
| 99 | C0 | C0_DH112 | 65.4 | 69.8 | -4.0 | 158.7 | 84.9 | 41.7 | 35.8 | 18.1 |
| 100 | C0 | C0_DH114 | 69.4 | 71.4 | -2.1 | 160.6 | 70.7 | 59.0 | 39.0 | 11.5 |
| 101 | C0 | C0_DH115 | 67.9 | 71.1 | -3.3 | 171.0 | 79.6 | 41.7 | 46.5 | 17.9 |
| 102 | C0 | C0_DH116 | 64.6 | 64.7 | -0.4 | 165.4 | 79.4 | 23.6 | 32.1 | 16.4 |
| 103 | C0 | C0_DH117 | 66.0 | 67.3 | -1.5 | 179.1 | 92.2 | 43.2 | 43.6 | 10.9 |
| 104 | C0 | C0_DH118 | 70.0 | 73.0 | -3.0 | 151.7 | 66.0 | 41.7 | 39.3 | 23.1 |

Table S3.2. Continued

| No | Group | DH line | MAFL | FEFL | ASI | PLHE | EAHE | FLA | TALE | NPTB |
|---|---|---|---|---|---|---|---|---|---|---|
| 105 | C0 | C0_DH119 | 69.2 | 72.4 | -3.0 | 185.9 | 81.7 | 15.1 | 37.2 | 11.5 |
| 106 | C0 | C0_DH120 | 64.4 | 66.2 | -1.7 | 151.1 | 74.3 | 59.7 | 38.1 | 14.3 |
| 107 | C0 | C0_DH121 | 66.8 | 71.0 | -3.7 | 170.1 | 98.7 | 46.2 | 36.4 | 18.8 |
| 108 | C0 | C0_DH122 | 68.6 | 73.1 | -4.3 | 174.6 | 72.2 | 30.4 | 41.9 | 14.3 |
| 109 | C0 | C0_DH123 | 70.0 | 72.9 | -2.8 | 206.2 | 108.9 | 44.7 | 41.4 | 15.0 |
| 110 | C0 | C0_DH124 | 68.0 | 68.4 | -0.7 | 166.7 | 92.9 | 37.2 | 35.9 | 25.2 |
| 111 | C0 | C0_DH125 | 66.8 | 67.1 | -0.5 | 174.4 | 77.4 | 51.5 | 40.7 | 8.1 |
| 112 | C0 | C0_DH127 | 69.4 | 70.9 | -1.6 | 159.4 | 83.6 | 46.9 | 37.9 | 15.7 |
| 113 | C0 | C0_DH128 | 63.3 | 63.6 | -0.4 | 170.5 | 78.4 | 41.4 | 45.1 | 13.6 |
| 114 | C0 | C0_DH130 | 64.6 | 65.1 | -0.7 | 158.7 | 69.8 | 32.7 | 32.1 | 7.0 |
| 115 | C0 | C0_DH131 | 66.8 | 68.0 | -1.4 | 159.0 | 84.7 | 51.5 | 28.4 | 12.2 |
| 116 | C0 | C0_DH132 | 70.2 | 72.8 | -2.6 | 179.1 | 84.2 | 46.2 | 34.7 | 6.8 |
| 117 | C0 | C0_DH133 | 69.8 | 71.6 | -1.7 | 172.4 | 91.2 | 25.9 | 31.6 | 13.3 |
| 118 | C0 | C0_DH134 | 65.2 | 65.8 | -0.7 | 180.4 | 96.0 | 38.7 | 37.6 | 15.3 |
| 119 | C0 | C0_DH135 | 69.7 | 71.7 | -1.9 | 172.2 | 97.6 | 33.4 | 37.0 | 14.0 |
| 120 | C0 | C0_DH136 | 68.8 | 68.5 | 0.0 | 191.5 | 102.5 | 46.2 | 34.9 | 8.2 |
| 121 | C0 | C0_DH137 | 65.5 | 67.1 | -1.6 | 196.1 | 95.7 | 74.0 | 37.9 | 15.5 |
| 122 | C0 | C0_DH138 | 65.0 | 66.3 | -1.3 | 181.2 | 89.9 | 49.2 | 32.3 | 13.7 |
| 123 | C0 | C0_DH139 | 66.5 | 68.9 | -2.3 | 170.0 | 84.7 | 53.7 | 37.9 | 15.6 |
| 124 | C0 | C0_DH140 | 64.2 | 65.7 | -1.4 | 156.8 | 81.1 | 35.7 | 33.6 | 19.4 |
| 125 | C0 | C0_DH141 | 62.9 | 66.2 | -3.1 | 139.5 | 55.1 | 22.9 | 33.0 | 18.1 |
| 126 | C0 | C0_DH143 | 69.4 | 72.0 | -2.6 | 169.3 | 74.2 | 46.2 | 38.8 | 11.5 |
| 127 | C0 | C0_DH144 | 68.6 | 70.4 | -1.8 | 174.5 | 94.9 | 45.4 | 39.4 | 13.4 |
| 128 | C0 | C0_DH145 | 69.3 | 71.5 | -2.2 | 133.5 | 66.2 | 64.2 | 34.3 | 15.9 |
| 129 | C0 | C0_DH146 | 66.3 | 71.2 | -4.5 | 186.4 | 94.4 | 45.4 | 39.4 | 22.3 |
| 130 | C0 | C0_DH147 | 64.8 | 66.2 | -1.5 | 166.1 | 72.9 | 37.9 | 34.8 | 17.1 |
| 131 | C0 | C0_DH148 | 66.4 | 68.6 | -2.0 | 166.9 | 83.1 | 40.9 | 42.0 | 12.0 |
| 132 | C0 | C0_DH149 | 74.0 | 74.6 | -0.9 | 150.5 | 71.5 | 31.2 | 32.5 | 12.5 |
| 133 | C0C17 | C0C17_DH001 | 63.4 | 63.9 | -0.4 | 141.1 | 56.6 | 28.5 | 36.3 | 6.3 |
| 134 | C0C17 | C0C17_DH002 | 64.7 | 65.4 | -0.7 | 184.2 | 85.2 | 46.6 | 43.9 | 10.4 |
| 135 | C0C17 | C0C17_DH003 | 64.9 | 64.4 | 0.4 | 176.5 | 86.3 | 29.3 | 40.2 | 11.9 |
| 136 | C0C17 | C0C17_DH005 | 64.5 | 64.8 | -0.3 | 175.7 | 78.8 | 18.0 | 39.0 | 11.5 |
| 137 | C0C17 | C0C17_DH007 | 68.2 | 69.1 | -1.0 | 165.3 | 86.9 | 41.3 | 37.6 | 17.4 |
| 138 | C0C17 | C0C17_DH008 | 66.4 | 68.1 | -1.7 | 169.6 | 63.5 | 24.6 | 41.9 | 12.9 |
| 139 | C0C17 | C0C17_DH010 | 66.3 | 65.3 | 0.8 | 156.9 | 85.4 | 47.3 | 32.5 | 12.9 |
| 140 | C0C17 | C0C17_DH012 | 65.6 | 65.3 | 0.4 | 171.0 | 80.1 | 20.3 | 41.3 | 7.3 |
| 141 | C0C17 | C0C17_DH013 | 65.0 | 68.4 | -3.1 | 151.5 | 62.3 | 53.3 | 39.2 | 8.1 |
| 142 | C0C17 | C0C17_DH014 | 60.9 | 62.4 | -1.4 | 164.3 | 60.9 | 45.8 | 40.6 | 10.0 |
| 143 | C0C17 | C0C17_DH015 | 65.6 | 66.5 | -0.7 | 184.8 | 67.1 | 18.0 | 41.8 | 9.1 |
| 144 | C0C17 | C0C17_DH016 | 63.5 | 64.4 | -0.9 | 175.8 | 108.7 | 35.3 | 41.6 | 7.8 |
| 145 | C0C17 | C0C17_DH017 | 65.2 | 66.5 | -1.3 | 182.3 | 83.9 | 12.0 | 45.7 | 6.6 |
| 146 | C0C17 | C0C17_DH018 | 63.3 | 64.9 | -1.5 | 129.5 | 56.4 | 24.6 | 33.6 | 15.0 |
| 147 | C0C17 | C0C17_DH019 | 60.6 | 60.8 | -0.2 | 147.2 | 59.5 | 22.8 | 37.5 | 12.5 |
| 148 | C0C17 | C0C17_DH020 | 68.6 | 71.5 | -2.6 | 172.1 | 84.1 | 35.3 | 35.4 | 12.7 |
| 149 | C0C17 | C0C17_DH021 | 67.4 | 66.5 | 0.8 | 157.4 | 76.4 | 33.8 | 33.5 | 5.8 |
| 150 | C0C17 | C0C17_DH024 | 64.5 | 62.5 | 1.5 | 174.1 | 77.3 | 21.0 | 31.0 | 9.0 |
| 151 | C0C17 | C0C17_DH025 | 64.1 | 62.2 | 1.6 | 181.1 | 82.5 | 25.5 | 35.8 | 4.8 |
| 152 | C0C17 | C0C17_DH027 | 63.1 | 63.7 | -0.6 | 166.7 | 64.0 | 11.2 | 41.8 | 5.9 |
| 153 | C0C17 | C0C17_DH030 | 66.4 | 65.2 | 1.1 | 190.1 | 85.0 | 56.4 | 45.4 | 7.3 |
| 154 | C0C17 | C0C17_DH033 | 63.6 | 65.7 | -1.7 | 156.6 | 53.1 | 16.5 | 34.9 | 6.9 |
| 155 | C0C17 | C0C17_DH035 | 62.8 | 64.1 | -1.3 | 159.9 | 68.2 | 30.8 | 31.0 | 10.8 |
| 156 | C0C17 | C0C17_DH037 | 68.4 | 69.5 | -1.2 | 156.5 | 78.5 | 27.8 | 33.0 | 14.2 |

Table S3.2. Continued

| No | Group | DH line | MAFL | FEFL | ASI | PLHE | EAHE | FLA | TALE | NPTB |
|---|---|---|---|---|---|---|---|---|---|---|
| 157 | C0C17 | C0C17_DH038 | 63.5 | 64.5 | -1.0 | 180.0 | 76.6 | 17.8 | 46.8 | 5.4 |
| 158 | C0C17 | C0C17_DH040 | 68.4 | 70.2 | -1.5 | 198.2 | 111.8 | 15.7 | 44.3 | 8.4 |
| 159 | C0C17 | C0C17_DH041 | 61.4 | 61.9 | -0.6 | 167.4 | 75.4 | 18.0 | 38.8 | 8.5 |
| 160 | C0C17 | C0C17_DH042 | 66.5 | 67.1 | -0.5 | 161.5 | 73.3 | 36.8 | 36.7 | 11.0 |
| 161 | C0C17 | C0C17_DH043 | 71.1 | 71.7 | -0.8 | 185.6 | 94.7 | 37.6 | 41.5 | 18.9 |
| 162 | C0C17 | C0C17_DH044 | 62.4 | 63.1 | -0.7 | 171.9 | 55.8 | 20.1 | 44.1 | 10.0 |
| 163 | C0C17 | C0C17_DH045 | 67.1 | 68.4 | -1.2 | 148.4 | 66.4 | 24.8 | 32.5 | 11.9 |
| 164 | C0C17 | C0C17_DH047 | 65.6 | 66.2 | -0.8 | 189.9 | 108.9 | 26.3 | 47.3 | 10.0 |
| 165 | C0C17 | C0C17_DH048 | 66.3 | 66.8 | -0.6 | 170.2 | 89.2 | 38.3 | 34.7 | 13.0 |
| 166 | C0C17 | C0C17_DH049 | 63.5 | 64.6 | -1.0 | 149.5 | 72.7 | 31.5 | 34.5 | 10.7 |
| 167 | C0C17 | C0C17_DH051 | 65.5 | 69.2 | -3.3 | 158.3 | 74.8 | 36.8 | 39.4 | 8.2 |
| 168 | C0C17 | C0C17_DH052 | 62.9 | 62.6 | 0.1 | 188.0 | 93.3 | 54.4 | 36.0 | 11.1 |
| 169 | C0C17 | C0C17_DH053 | 69.8 | 71.6 | -1.6 | 187.2 | 87.7 | 35.3 | 42.0 | 19.1 |
| 170 | C0C17 | C0C17_DH056 | 61.7 | 63.1 | -1.3 | 168.8 | 80.4 | 32.3 | 30.7 | 10.4 |
| 171 | C0C17 | C0C17_DH058 | 70.7 | 68.1 | 1.2 | 162.8 | 76.2 | 16.5 | 39.1 | 10.1 |
| 172 | C0C17 | C0C17_DH059 | 66.6 | 69.9 | -3.0 | 191.7 | 90.3 | 34.5 | 39.3 | 9.4 |
| 173 | C0C17 | C0C17_DH060 | 64.7 | 64.4 | -0.1 | 209.3 | 95.2 | 47.3 | 42.4 | 12.5 |
| 174 | C0C17 | C0C17_DH061 | 70.1 | 70.5 | -0.6 | 188.8 | 86.2 | 25.5 | 28.4 | 12.6 |
| 175 | C0C17 | C0C17_DH062 | 62.4 | 63.6 | -1.3 | 187.7 | 95.9 | 32.3 | 43.8 | 7.3 |
| 176 | C0C17 | C0C17_DH064 | 65.0 | 66.5 | -1.5 | 149.4 | 62.0 | 30.8 | 38.6 | 20.5 |
| 177 | C0C17 | C0C17_DH066 | 62.0 | 60.6 | 1.0 | 168.6 | 80.9 | 39.8 | 34.8 | 10.1 |
| 178 | C0C17 | C0C17_DH068 | 66.7 | 69.6 | -2.6 | 175.2 | 89.4 | 20.3 | 32.1 | 9.6 |
| 179 | C0C17 | C0C17_DH069 | 66.1 | 66.8 | -0.5 | 169.1 | 77.6 | 22.5 | 38.3 | 10.9 |
| 180 | C0C17 | C0C17_DH070 | 68.3 | 68.8 | -0.4 | 172.7 | 103.5 | 33.8 | 34.5 | 20.4 |
| 181 | C0C17 | C0C17_DH071 | 66.5 | 68.1 | -1.4 | 178.8 | 87.6 | 27.0 | 44.8 | 12.7 |
| 182 | C0C17 | C0C17_DH072 | 64.3 | 65.7 | -1.4 | 179.8 | 88.4 | 43.6 | 36.7 | 15.0 |
| 183 | C0C17 | C0C17_DH073 | 62.3 | 62.3 | 0.1 | 189.1 | 65.0 | 25.5 | 36.7 | 8.1 |
| 184 | C0C17 | C0C17_DH074 | 67.1 | 67.1 | 0.0 | 176.0 | 74.3 | 27.8 | 38.5 | 14.9 |
| 185 | C0C17 | C0C17_DH076 | 61.2 | 62.7 | -1.4 | 180.8 | 71.8 | 24.0 | 44.4 | 5.9 |
| 186 | C0C17 | C0C17_DH078 | 64.0 | 63.9 | -0.1 | 175.5 | 67.5 | 23.3 | 35.6 | 11.2 |
| 187 | C0C17 | C0C17_DH079 | 64.3 | 64.8 | -0.6 | 190.3 | 94.0 | 47.3 | 39.8 | 12.8 |
| 188 | C0C17 | C0C17_DH080 | 60.6 | 60.9 | -0.4 | 183.7 | 67.9 | 43.6 | 42.4 | 5.3 |
| 189 | C0C17 | C0C17_DH081 | 63.1 | 65.5 | -2.2 | 161.7 | 78.1 | 20.1 | 43.4 | 10.5 |
| 190 | C0C17 | C0C17_DH082 | 66.1 | 65.2 | 0.9 | 171.9 | 65.4 | 21.6 | 36.5 | 5.9 |
| 191 | C0C17 | C0C17_DH083 | 70.7 | 70.7 | -0.2 | 169.3 | 77.6 | 16.3 | 44.5 | 6.4 |
| 192 | C0C17 | C0C17_DH084 | 66.3 | 69.1 | -2.8 | 152.7 | 47.9 | 36.0 | 37.0 | 9.9 |
| 193 | C0C17 | C0C17_DH085 | 66.1 | 68.1 | -1.9 | 163.8 | 82.5 | 34.5 | 46.9 | 9.4 |
| 194 | C0C17 | C0C17_DH086 | 64.2 | 64.0 | 0.1 | 179.2 | 78.9 | 24.0 | 38.2 | 13.3 |
| 195 | C0C17 | C0C17_DH087 | 64.7 | 64.7 | -0.2 | 166.3 | 81.0 | 38.3 | 42.3 | 6.3 |
| 196 | C0C17 | C0C17_DH088 | 66.5 | 69.4 | -3.0 | 163.8 | 65.7 | 12.7 | 42.2 | 6.1 |
| 197 | C0C17 | C0C17_DH089 | 64.9 | 66.4 | -1.5 | 185.8 | 91.2 | 15.0 | 36.2 | 11.4 |
| 198 | C0C17 | C0C17_DH090 | 67.8 | 69.9 | -2.0 | 164.3 | 97.9 | 35.3 | 27.1 | 12.0 |
| 199 | C0C17 | C0C17_DH091 | 67.0 | 68.0 | -1.0 | 164.9 | 77.0 | 8.5 | 40.3 | 6.5 |
| 200 | C0C17 | C0C17_DH092 | 61.8 | 64.0 | -2.2 | 184.5 | 73.7 | 17.2 | 40.1 | 10.5 |
| 201 | C0C17 | C0C17_DH094 | 63.6 | 64.3 | -0.8 | 144.7 | 50.3 | 23.3 | 35.4 | 16.0 |
| 202 | C0C17 | C0C17_DH095 | 65.1 | 69.1 | -3.8 | 160.5 | 73.2 | 36.0 | 44.4 | 11.9 |
| 203 | C0C17 | C0C17_DH096 | 65.2 | 66.6 | -1.2 | 158.4 | 78.6 | 37.6 | 36.9 | 14.6 |
| 204 | C0C17 | C0C17_DH097 | 67.7 | 69.9 | -2.0 | 184.9 | 96.2 | 33.8 | 41.9 | 12.1 |
| 205 | C0C17 | C0C17_DH100 | 67.6 | 66.7 | 0.7 | 184.0 | 91.0 | 27.8 | 37.4 | 8.2 |
| 206 | C0C17 | C0C17_DH103 | 66.3 | 66.8 | -0.6 | 168.8 | 75.3 | 23.9 | 36.6 | 9.5 |
| 207 | C0C17 | C0C17_DH104 | 67.0 | 68.6 | -1.5 | 193.4 | 88.2 | 30.8 | 42.9 | 9.6 |
| 208 | C0C17 | C0C17_DH105 | 63.0 | 64.9 | -1.7 | 163.3 | 84.3 | 39.8 | 35.9 | 4.9 |

Table S3.2. Continued

| No | Group | DH line | MAFL | FEFL | ASI | PLHE | EAHE | FLA | TALE | NPTB |
|---|---|---|---|---|---|---|---|---|---|---|
| 209 | C0C17 | C0C17_DH106 | 65.4 | 65.1 | 0.1 | 169.1 | 73.8 | 20.3 | 39.7 | 7.6 |
| 210 | C0C17 | C0C17_DH107 | 65.2 | 65.7 | -0.4 | 152.7 | 62.1 | 23.3 | 36.9 | 12.7 |
| 211 | C0C17 | C0C17_DH108 | 66.7 | 67.2 | -0.6 | 171.7 | 85.6 | 21.0 | 46.2 | 16.3 |
| 212 | C0C17 | C0C17_DH109 | 65.6 | 65.9 | -0.2 | 173.4 | 82.0 | 27.8 | 35.8 | 6.6 |
| 213 | C0C17 | C0C17_DH112 | 67.2 | 68.3 | -1.2 | 174.7 | 103.3 | 42.1 | 40.1 | 9.3 |
| 214 | C0C17 | C0C17_DH114 | 63.9 | 65.0 | -1.0 | 179.6 | 90.7 | 51.8 | 32.4 | 12.1 |
| 215 | C0C17 | C0C17_DH117 | 67.7 | 69.1 | -1.4 | 184.0 | 76.5 | 32.3 | 43.0 | 11.7 |
| 216 | C0C17 | C0C17_DH118 | 63.7 | 63.2 | 0.3 | 198.1 | 106.8 | 23.3 | 40.9 | 12.2 |
| 217 | C0C17 | C0C17_DH121 | 68.1 | 68.6 | -0.6 | 178.9 | 78.3 | 33.8 | 37.8 | 9.5 |
| 218 | C0C17 | C0C17_DH122 | 68.5 | 70.0 | -1.6 | 175.3 | 97.3 | 72.9 | 38.6 | 17.0 |
| 219 | C0C17 | C0C17_DH125 | 66.3 | 67.9 | -1.6 | 198.0 | 102.6 | 30.8 | 42.2 | 5.5 |
| 220 | C0C17 | C0C17_DH126 | 66.4 | 66.1 | 0.2 | 159.7 | 63.6 | 20.3 | 36.3 | 7.4 |
| 221 | C0C17 | C0C17_DH129 | 65.8 | 66.2 | -0.5 | 199.1 | 98.0 | 57.1 | 39.9 | 7.6 |
| 222 | C0C17 | C0C17_DH130 | 66.5 | 66.9 | -0.4 | 160.3 | 68.1 | 24.8 | 41.8 | 13.2 |
| 223 | C0C17 | C0C17_DH132 | 67.5 | 68.4 | -1.0 | 162.4 | 70.0 | 58.6 | 32.0 | 19.7 |
| 224 | C0C17 | C0C17_DH136 | 66.2 | 67.8 | -1.5 | 163.9 | 75.2 | 44.6 | 31.7 | 11.3 |
| 225 | C0C17 | C0C17_DH137 | 64.0 | 65.9 | -1.7 | 173.0 | 72.8 | 18.0 | 39.5 | 8.6 |
| 226 | C0C17 | C0C17_DH139 | 62.1 | 63.1 | -1.0 | 176.0 | 70.8 | 24.0 | 38.7 | 10.8 |
| 227 | C0C17 | C0C17_DH140 | 62.6 | 63.9 | -1.3 | 154.5 | 61.5 | 14.8 | 39.9 | 11.3 |
| 228 | C0C17 | C0C17_DH141 | 63.9 | 64.0 | -0.1 | 170.2 | 79.6 | 31.5 | 42.9 | 13.1 |
| 229 | C0C17 | C0C17_DH142 | 64.1 | 66.2 | -1.9 | 176.0 | 66.2 | 31.5 | 43.5 | 7.9 |
| 230 | C0C17 | C0C17_DH146 | 65.8 | 66.4 | -0.6 | 180.4 | 81.9 | 15.6 | 40.8 | 7.9 |
| 231 | C0C17 | C0C17_DH147 | 65.6 | 65.7 | -0.2 | 221.2 | 122.2 | 39.1 | 46.3 | 12.4 |
| 232 | C0C17 | C0C17_DH148 | 67.8 | 69.4 | -1.6 | 161.4 | 76.6 | 17.2 | 42.8 | 12.4 |
| 233 | C0C17 | C0C17_DH149 | 65.9 | 67.5 | -1.6 | 180.2 | 95.1 | 33.8 | 37.8 | 10.1 |
| 234 | C0C17 | C0C17_DH150 | 64.9 | 64.3 | 0.3 | 162.4 | 70.8 | 28.5 | 40.5 | 11.6 |
| 235 | C0C17 | C0C17_DH152 | 68.0 | 72.0 | -3.7 | 176.1 | 81.1 | 24.0 | 46.2 | 13.8 |
| 236 | C0C17 | C0C17_DH153 | 63.1 | 65.7 | -2.4 | 159.3 | 74.9 | 35.3 | 34.0 | 7.7 |
| 237 | C0C17 | C0C17_DH154 | 64.6 | 67.7 | -3.0 | 162.3 | 69.2 | 30.0 | 52.2 | 8.0 |
| 238 | C0C17 | C0C17_DH155 | 65.2 | 69.8 | -4.0 | 142.6 | 44.3 | 50.3 | 36.7 | 6.9 |
| 239 | C0C17 | C0C17_DH156 | 64.5 | 65.1 | -0.8 | 160.6 | 75.9 | 46.6 | 39.1 | 9.4 |
| 240 | C0C17 | C0C17_DH157 | 65.0 | 66.1 | -1.2 | 155.0 | 74.5 | 35.3 | 34.1 | 15.8 |
| 241 | C0C17 | C0C17_DH158 | 63.2 | 64.6 | -1.2 | 188.7 | 78.7 | 33.8 | 48.2 | 6.7 |
| 242 | C0C17 | C0C17_DH159 | 66.2 | 65.1 | 0.9 | 189.8 | 71.3 | 28.5 | 40.6 | 6.1 |
| 243 | C0C17 | C0C17_DH160 | 63.7 | 63.8 | -0.1 | 168.1 | 74.5 | 42.1 | 36.9 | 6.2 |
| 244 | C0C17 | C0C17_DH161 | 67.4 | 68.2 | -1.1 | 202.3 | 112.3 | 33.0 | 35.8 | 8.1 |
| 245 | C0C17 | C0C17_DH162 | 65.2 | 64.4 | 0.7 | 184.8 | 76.9 | 26.3 | 39.5 | 8.3 |
| 246 | C0C17 | C0C17_DH163 | 70.1 | 69.9 | 0.1 | 142.1 | 61.1 | 40.6 | 36.4 | 6.7 |
| 247 | C0C17 | C0C17_DH164 | 60.8 | 60.7 | 0.1 | 163.7 | 67.3 | 19.5 | 42.3 | 6.0 |
| 248 | C0C17 | C0C17_DH165 | 62.7 | 62.2 | 0.3 | 167.7 | 88.7 | 20.3 | 40.1 | 13.8 |
| 249 | C0C17 | C0C17_DH166 | 65.1 | 66.4 | -1.1 | 149.0 | 59.5 | 17.2 | 44.1 | 9.6 |
| 250 | C0C17 | C0C17_DH168 | 67.7 | 70.3 | -2.4 | 197.0 | 108.2 | 27.8 | 37.3 | 6.8 |
| 251 | C0C17 | C0C17_DH169 | 65.9 | 66.0 | -0.1 | 175.0 | 90.6 | 8.4 | 38.9 | 6.6 |
| 252 | C0C17 | C0C17_DH172 | 62.0 | 62.3 | -0.3 | 175.6 | 77.9 | 20.9 | 32.7 | 8.4 |
| 253 | C0C17 | C0C17_DH174 | 65.6 | 65.0 | 0.4 | 166.6 | 74.6 | 23.3 | 42.9 | 9.0 |
| 254 | C0C17 | C0C17_DH177 | 67.2 | 67.9 | -0.7 | 198.3 | 105.1 | 33.5 | 40.7 | 22.4 |
| 255 | C0C17 | C0C17_DH178 | 64.6 | 63.7 | 0.8 | 184.9 | 85.9 | 34.5 | 35.7 | 7.6 |
| 256 | C0C17 | C0C17_DH183 | 66.4 | 65.2 | 1.0 | 178.0 | 87.8 | 35.3 | 28.6 | 12.9 |
| 257 | C0C17 | C0C17_DH184 | 68.9 | 69.7 | -1.0 | 175.5 | 90.7 | 30.5 | 34.3 | 18.1 |
| 258 | C0C17 | C0C17_DH185 | 67.3 | 68.3 | -1.3 | 166.2 | 76.3 | 25.5 | 38.7 | 6.5 |
| 259 | C0C17 | C0C17_DH187 | 67.5 | 72.1 | -4.4 | 156.8 | 60.6 | 27.8 | 40.3 | 14.3 |
| 260 | C0C17 | C0C17_DH188 | 69.3 | 70.5 | -1.1 | 164.8 | 88.3 | 71.4 | 41.6 | 8.1 |

Table S3.2. Continued

| No | Group | DH line | MAFL | FEFL | ASI | PLHE | EAHE | FLA | TALE | NPTB |
|---|---|---|---|---|---|---|---|---|---|---|
| 261 | C0C17 | C0C17_DH189 | 66.4 | 67.0 | -0.8 | 181.9 | 76.3 | 10.2 | 36.8 | 4.5 |
| 262 | C0C17 | C0C17_DH190 | 66.5 | 69.0 | -2.3 | 154.0 | 77.8 | 32.3 | 31.6 | 6.8 |
| 263 | C0C17 | C0C17_DH191 | 66.3 | 67.5 | -1.1 | 146.3 | 54.3 | 21.8 | 41.7 | 18.5 |
| 264 | C0C17 | C0C17_DH192 | 64.3 | 64.9 | -0.5 | 170.8 | 82.0 | 25.5 | 38.9 | 10.4 |
| 265 | C0C17 | C0C17_DH193 | 63.9 | 64.9 | -0.9 | 164.4 | 72.8 | 20.3 | 45.8 | 7.9 |
| 266 | C0C17 | C0C17_DH195 | 68.5 | 68.7 | -0.5 | 199.4 | 115.5 | 33.8 | 40.2 | 10.5 |
| 267 | C0C17 | C0C17_DH196 | 65.9 | 66.1 | -0.4 | 187.4 | 99.3 | 36.8 | 44.3 | 11.5 |
| 268 | C0C17 | C0C17_DH197 | 62.9 | 62.6 | 0.2 | 191.8 | 87.0 | 45.7 | 44.0 | 11.8 |
| 269 | C0C17 | C0C17_DH198 | 66.3 | 67.0 | -0.7 | 170.8 | 70.2 | 45.8 | 38.8 | 9.5 |
| 270 | C0C17 | C0C17_DH199 | 62.3 | 62.1 | 0.0 | 189.3 | 89.2 | 54.1 | 39.2 | 13.3 |
| 271 | C0C17 | C0C17_DH200 | 63.9 | 66.0 | -2.0 | 154.4 | 54.6 | 30.0 | 40.4 | 15.1 |
| 272 | C0C17 | C0C17_DH201 | 61.5 | 62.1 | -0.6 | 202.0 | 94.2 | 48.1 | 44.1 | 12.3 |
| 273 | C0C17 | C0C17_DH202 | 65.6 | 65.1 | 0.4 | 183.7 | 87.1 | 30.0 | 43.2 | 9.2 |
| 274 | C0C17 | C0C17_DH203 | 65.9 | 66.7 | -1.0 | 199.1 | 98.4 | 46.6 | 38.9 | 12.3 |
| 275 | C0C17 | C0C17_DH204 | 65.2 | 64.3 | 0.6 | 184.1 | 85.9 | 39.8 | 42.7 | 8.3 |
| 276 | C0C17 | C0C17_DH205 | 68.3 | 69.2 | -0.8 | 165.0 | 92.9 | 40.6 | 36.6 | 6.5 |
| 277 | C0C17 | C0C17_DH206 | 67.2 | 68.3 | -1.1 | 171.3 | 99.7 | 29.3 | 35.2 | 22.0 |
| 278 | C0C17 | C0C17_DH207 | 64.9 | 65.8 | -0.7 | 147.1 | 60.8 | 18.8 | 40.2 | 11.5 |
| 279 | C0C17 | C0C17_DH208 | 65.5 | 69.8 | -3.9 | 169.8 | 69.8 | 34.5 | 38.7 | 15.8 |
| 280 | C0C17 | C0C17_DH209 | 61.8 | 61.6 | 0.0 | 182.4 | 71.6 | 18.0 | 46.4 | 4.9 |
| 281 | C0C17 | C0C17_DH212 | 64.3 | 65.9 | -1.3 | 148.4 | 55.0 | 34.5 | 37.3 | 10.6 |
| 282 | C0C17 | C0C17_DH213 | 67.8 | 69.5 | -1.6 | 151.6 | 65.5 | 10.5 | 35.2 | 2.9 |
| 283 | C0C17 | C0C17_DH214 | 68.0 | 68.7 | -0.7 | 154.3 | 68.7 | 6.6 | 36.3 | 2.9 |
| 284 | C0C17 | C0C17_DH215 | 68.8 | 69.2 | -0.5 | 193.9 | 91.6 | 18.0 | 38.1 | 11.8 |
| 285 | C0C17 | C0C17_DH216 | 63.9 | 64.1 | -0.4 | 164.8 | 63.4 | 36.8 | 37.2 | 10.8 |
| 286 | C0C17 | C0C17_DH217 | 68.4 | 70.3 | -1.6 | 180.2 | 93.7 | 35.3 | 40.1 | 8.5 |
| 287 | C0C17 | C0C17_DH220 | 64.4 | 63.9 | 0.2 | 181.1 | 69.5 | 30.8 | 33.5 | 8.1 |
| 288 | C0C17 | C0C17_DH221 | 65.9 | 64.9 | 0.9 | 182.4 | 86.0 | 35.3 | 38.0 | 10.9 |
| 289 | C0C17 | C0C17_DH222 | 61.1 | 61.6 | -0.5 | 139.6 | 61.3 | 33.0 | 36.1 | 15.4 |
| 290 | C0C17 | C0C17_DH224 | 69.7 | 71.4 | -1.7 | 178.4 | 90.2 | 26.6 | 36.0 | 12.3 |
| 291 | C0C17 | C0C17_DH225 | 65.9 | 65.4 | 0.5 | 156.2 | 73.8 | 27.0 | 32.0 | 7.3 |
| 292 | C0C17 | C0C17_DH226 | 66.5 | 67.3 | -0.8 | 158.5 | 69.9 | 36.8 | 35.3 | 9.9 |
| 293 | C0C17 | C0C17_DH228 | 64.0 | 66.6 | -2.4 | 147.2 | 66.8 | 25.5 | 34.7 | 5.3 |
| 294 | C0C17 | C0C17_DH230 | 66.2 | 66.9 | -0.6 | 152.4 | 61.0 | 27.0 | 38.4 | 9.2 |
| 295 | C0C17 | C0C17_DH231 | 63.9 | 64.1 | -0.3 | 177.6 | 74.4 | 27.0 | 35.9 | 7.3 |
| 296 | C0C17 | C0C17_DH232 | 63.8 | 63.5 | 0.1 | 163.9 | 85.1 | 45.1 | 41.5 | 10.1 |
| 297 | C0C17 | C0C17_DH234 | 67.5 | 70.6 | -2.9 | 144.4 | 70.3 | 27.8 | 33.2 | 11.6 |
| 298 | C0C17 | C0C17_DH235 | 66.2 | 66.8 | -0.4 | 192.3 | 102.6 | 23.3 | 41.4 | 15.0 |
| 299 | C0C17 | C0C17_DH236 | 62.0 | 62.6 | -0.5 | 176.7 | 71.7 | 20.3 | 39.1 | 7.0 |
| 300 | C0C17 | C0C17_DH238 | 63.7 | 64.6 | -0.9 | 178.2 | 77.9 | 27.8 | 40.5 | 10.3 |
| 301 | C0C17 | C0C17_DH242 | 67.0 | 69.1 | -1.9 | 159.6 | 85.2 | 33.0 | 29.0 | 10.0 |
| 302 | C0C17 | C0C17_DH244 | 62.8 | 65.1 | -2.2 | 169.6 | 71.0 | 27.8 | 36.9 | 9.3 |
| 303 | C17 | C17_DH001 | 63.6 | 64.1 | -0.4 | 183.5 | 85.6 | 12.7 | 43.3 | 5.5 |
| 304 | C17 | C17_DH003 | 67.6 | 65.5 | 1.8 | 198.4 | 96.3 | 25.4 | 37.2 | 8.6 |
| 305 | C17 | C17_DH004 | 63.3 | 61.8 | 1.3 | 134.1 | 58.8 | 13.3 | 37.2 | 5.1 |
| 306 | C17 | C17_DH005 | 61.6 | 60.4 | 0.9 | 171.7 | 71.8 | 13.1 | 40.2 | 7.6 |
| 307 | C17 | C17_DH006 | 61.8 | 61.7 | 0.1 | 190.6 | 76.7 | 14.2 | 43.9 | 11.0 |
| 308 | C17 | C17_DH010 | 62.9 | 61.6 | 1.1 | 165.4 | 74.4 | 6.9 | 41.4 | 7.2 |
| 309 | C17 | C17_DH011 | 60.5 | 60.1 | 0.2 | 170.9 | 72.7 | 23.2 | 47.0 | 5.2 |
| 310 | C17 | C17_DH013 | 64.3 | 65.5 | -1.0 | 163.4 | 66.8 | 35.2 | 44.6 | 8.4 |
| 311 | C17 | C17_DH014 | 60.0 | 59.3 | 0.5 | 170.8 | 65.7 | 16.3 | 38.3 | 7.9 |
| 312 | C17 | C17_DH018 | 63.5 | 62.2 | 1.2 | 178.4 | 82.0 | 8.6 | 42.2 | 5.7 |

Table S3.2. Continued

| No | Group | DH line | MAFL | FEFL | ASI | PLHE | EAHE | FLA | TALE | NPTB |
|---|---|---|---|---|---|---|---|---|---|---|
| 313 | C17 | C17_DH019 | 64.0 | 64.6 | -0.6 | 173.2 | 58.3 | 12.4 | 42.0 | 9.7 |
| 314 | C17 | C17_DH020 | 61.3 | 60.7 | 0.4 | 186.5 | 68.4 | 10.1 | 46.0 | 9.4 |
| 315 | C17 | C17_DH021 | 65.0 | 64.8 | 0.2 | 144.0 | 60.5 | 18.7 | 40.8 | 4.6 |
| 316 | C17 | C17_DH022 | 61.4 | 60.7 | 0.6 | 172.1 | 65.1 | 19.4 | 39.4 | 7.0 |
| 317 | C17 | C17_DH024 | 63.7 | 61.7 | 1.7 | 179.2 | 83.4 | 18.7 | 42.7 | 10.1 |
| 318 | C17 | C17_DH026 | 58.9 | 58.8 | 0.1 | 162.4 | 63.1 | 7.1 | 40.1 | 4.2 |
| 319 | C17 | C17_DH029 | 60.2 | 60.2 | -0.1 | 153.0 | 48.4 | 25.4 | 36.0 | 6.5 |
| 320 | C17 | C17_DH031 | 61.9 | 61.2 | 0.5 | 171.1 | 55.1 | 12.4 | 40.4 | 5.6 |
| 321 | C17 | C17_DH034 | 62.8 | 62.2 | 0.5 | 165.9 | 58.9 | 7.1 | 51.1 | 7.5 |
| 322 | C17 | C17_DH035 | 61.8 | 61.4 | 0.5 | 177.5 | 75.2 | 14.8 | 41.9 | 5.0 |
| 323 | C17 | C17_DH036 | 65.4 | 64.9 | 0.4 | 188.7 | 94.4 | 10.3 | 39.5 | 10.0 |
| 324 | C17 | C17_DH038 | 62.7 | 62.9 | -0.1 | 162.6 | 55.8 | 11.2 | 41.1 | 8.9 |
| 325 | C17 | C17_DH041 | 61.8 | 63.2 | -1.1 | 171.7 | 69.8 | 5.1 | 42.2 | 9.7 |
| 326 | C17 | C17_DH043 | 61.6 | 63.0 | -1.2 | 148.0 | 59.3 | 15.7 | 39.0 | 6.5 |
| 327 | C17 | C17_DH044 | 63.2 | 63.0 | 0.1 | 177.4 | 67.1 | 8.2 | 44.4 | 8.7 |
| 328 | C17 | C17_DH045 | 59.5 | 60.1 | -0.4 | 169.1 | 58.9 | 6.5 | 46.8 | 7.1 |
| 329 | C17 | C17_DH046 | 61.6 | 61.7 | 0.0 | 170.0 | 63.8 | 14.8 | 47.2 | 5.4 |
| 330 | C17 | C17_DH050 | 63.0 | 65.2 | -1.9 | 181.8 | 79.1 | 23.9 | 38.0 | 9.3 |
| 331 | C17 | C17_DH052 | 64.0 | 63.7 | 0.4 | 203.2 | 83.5 | 18.5 | 47.2 | 11.4 |
| 332 | C17 | C17_DH053 | 64.3 | 63.0 | 1.1 | 172.3 | 78.3 | 24.7 | 39.3 | 8.0 |
| 333 | C17 | C17_DH054 | 60.6 | 60.4 | 0.3 | 158.3 | 58.6 | 5.3 | 53.3 | 2.9 |
| 334 | C17 | C17_DH055 | 67.4 | 65.2 | 1.8 | 164.5 | 71.7 | 19.4 | 40.0 | 5.9 |
| 335 | C17 | C17_DH056 | 61.9 | 61.0 | 0.6 | 154.7 | 62.4 | 19.4 | 44.2 | 6.0 |
| 336 | C17 | C17_DH058 | 64.4 | 64.4 | 0.1 | 182.3 | 73.4 | 6.2 | 47.8 | 5.9 |
| 337 | C17 | C17_DH061 | 61.8 | 61.7 | 0.1 | 150.6 | 52.5 | 9.5 | 41.3 | 5.5 |
| 338 | C17 | C17_DH062 | 64.4 | 64.8 | -0.3 | 179.8 | 62.9 | 14.2 | 37.5 | 11.2 |
| 339 | C17 | C17_DH064 | 64.3 | 66.2 | -1.5 | 165.0 | 53.6 | 9.5 | 36.6 | 5.9 |
| 340 | C17 | C17_DH066 | 65.8 | 66.3 | -0.4 | 175.5 | 78.2 | 10.9 | 42.9 | 9.0 |
| 341 | C17 | C17_DH067 | 61.2 | 61.0 | 0.2 | 164.0 | 57.7 | 38.2 | 36.1 | 11.3 |
| 342 | C17 | C17_DH071 | 65.7 | 64.8 | 0.8 | 148.8 | 66.5 | 5.0 | 46.4 | 4.2 |
| 343 | C17 | C17_DH072 | 60.6 | 60.6 | 0.1 | 184.3 | 74.9 | 6.5 | 40.8 | 7.9 |
| 344 | C17 | C17_DH074 | 65.0 | 66.5 | -1.2 | 182.9 | 71.6 | 10.9 | 42.1 | 5.0 |
| 345 | C17 | C17_DH077 | 62.6 | 61.4 | 1.2 | 151.8 | 58.9 | 20.9 | 45.8 | 8.3 |
| 346 | C17 | C17_DH078 | 60.3 | 60.7 | -0.5 | 167.8 | 67.5 | 10.3 | 46.1 | 8.5 |
| 347 | C17 | C17_DH079 | 62.4 | 62.0 | 0.3 | 157.7 | 71.4 | 13.4 | 43.0 | 4.2 |
| 348 | C17 | C17_DH080 | 63.2 | 62.5 | 0.6 | 170.7 | 63.6 | 11.2 | 44.0 | 7.5 |
| 349 | C17 | C17_DH082 | 63.1 | 64.9 | -1.5 | 180.7 | 75.4 | 10.4 | 39.7 | 9.0 |
| 350 | C17 | C17_DH087 | 63.9 | 63.8 | 0.1 | 163.1 | 67.2 | 8.6 | 41.8 | 6.2 |
| 351 | C17 | C17_DH089 | 59.4 | 59.4 | -0.1 | 169.3 | 74.6 | 9.2 | 51.3 | 6.1 |
| 352 | C17 | C17_DH090 | 62.8 | 62.4 | 0.3 | 171.1 | 72.3 | 29.2 | 47.4 | 6.6 |
| 353 | C17 | C17_DH091 | 64.6 | 64.3 | 0.4 | 174.3 | 70.6 | 17.2 | 43.1 | 4.4 |
| 354 | C17 | C17_DH093 | 61.0 | 60.6 | 0.3 | 165.1 | 59.6 | 14.2 | 37.3 | 5.0 |
| 355 | C17 | C17_DH098 | 63.3 | 63.1 | 0.0 | 175.9 | 72.5 | 9.5 | 36.2 | 7.0 |
| 356 | C17 | C17_DH102 | 61.0 | 60.1 | 0.7 | 173.3 | 72.7 | 23.2 | 34.8 | 8.3 |
| 357 | C17 | C17_DH103 | 61.3 | 63.3 | -1.6 | 157.2 | 52.5 | 5.4 | 44.0 | 5.6 |
| 358 | C17 | C17_DH105 | 63.0 | 62.7 | 0.3 | 174.5 | 71.6 | 16.4 | 39.8 | 7.4 |
| 359 | C17 | C17_DH106 | 59.2 | 60.6 | -1.3 | 167.6 | 56.2 | 9.7 | 42.8 | 10.8 |
| 360 | C17 | C17_DH107 | 64.7 | 65.2 | -0.9 | 189.1 | 76.0 | 14.2 | 43.3 | 5.5 |
| 361 | C17 | C17_DH108 | 67.4 | 65.7 | 1.6 | 181.1 | 92.7 | 7.7 | 41.4 | 13.4 |
| 362 | C17 | C17_DH109 | 64.4 | 62.6 | 1.6 | 169.0 | 65.5 | 13.1 | 40.3 | 3.8 |
| 363 | C17 | C17_DH110 | 64.3 | 64.4 | 0.0 | 181.2 | 72.7 | 27.7 | 37.9 | 14.2 |
| 364 | C17 | C17_DH111 | 61.5 | 62.4 | -1.0 | 163.6 | 63.3 | 6.9 | 48.3 | 5.1 |

Table S3.2. Continued

| No | Group | DH line | MAFL | FEFL | ASI | PLHE | EAHE | FLA | TALE | NPTB |
|---|---|---|---|---|---|---|---|---|---|---|
| 365 | C17 | C17_DH113 | 60.6 | 60.6 | 0.0 | 174.3 | 73.5 | 23.2 | 42.8 | 7.6 |
| 366 | C17 | C17_DH115 | 65.8 | 62.9 | 2.4 | 182.3 | 95.6 | 8.6 | 46.5 | 7.5 |
| 367 | C17 | C17_DH116 | 62.6 | 63.6 | -0.9 | 170.3 | 66.9 | 18.4 | 43.0 | 12.6 |
| 368 | C17 | C17_DH118 | 64.0 | 63.3 | 0.5 | 179.5 | 77.9 | 10.3 | 46.0 | 7.4 |
| 369 | C17 | C17_DH119 | 64.1 | 63.9 | 0.1 | 171.7 | 67.5 | 6.0 | 43.3 | 8.6 |
| 370 | C17 | C17_DH120 | 63.9 | 64.0 | 0.1 | 151.5 | 59.5 | 17.2 | 41.6 | 10.7 |
| 371 | C17 | C17_DH121 | 62.7 | 61.3 | 1.3 | 157.0 | 64.2 | 13.1 | 43.0 | 6.3 |
| 372 | C17 | C17_DH124 | 59.8 | 59.7 | -0.1 | 170.9 | 67.5 | 10.1 | 42.0 | 8.0 |
| 373 | C17 | C17_DH126 | 65.4 | 65.0 | 0.4 | 201.2 | 86.9 | 15.7 | 39.3 | 6.9 |
| 374 | C17 | C17_DH127 | 62.8 | 63.7 | -0.8 | 167.8 | 68.5 | 10.4 | 46.0 | 8.0 |
| 375 | C17 | C17_DH128 | 63.0 | 64.2 | -0.9 | 163.9 | 62.2 | 14.9 | 46.1 | 6.7 |
| 376 | C17 | C17_DH129 | 64.5 | 65.1 | -0.4 | 158.9 | 70.8 | 12.7 | 39.2 | 7.5 |
| 377 | C17 | C17_DH132 | 63.1 | 62.2 | 0.7 | 166.9 | 68.8 | 11.9 | 44.8 | 4.6 |
| 378 | C17 | C17_DH134 | 62.0 | 62.9 | -0.8 | 161.4 | 58.9 | 6.9 | 40.8 | 5.5 |
| 379 | C17 | C17_DH135 | 60.8 | 61.7 | -0.7 | 126.6 | 44.2 | 12.5 | 39.5 | 7.5 |
| 380 | C17 | C17_DH136 | 64.7 | 64.9 | -0.2 | 196.9 | 72.2 | 14.8 | 46.8 | 5.0 |
| 381 | C17 | C17_DH138 | 61.3 | 60.2 | 0.8 | 183.1 | 67.3 | 8.2 | 41.9 | 5.7 |
| 382 | C17 | C17_DH139 | 64.9 | 64.4 | 0.4 | 165.5 | 71.9 | 12.7 | 47.2 | 4.3 |
| 383 | C17 | C17_DH140 | 66.4 | 64.9 | 1.4 | 186.0 | 69.6 | 11.0 | 42.6 | 7.9 |
| 384 | C17 | C17_DH142 | 61.5 | 60.6 | 0.9 | 149.9 | 53.8 | 14.2 | 38.3 | 8.3 |
| 385 | C17 | C17_DH143 | 60.5 | 61.0 | -0.6 | 138.2 | 40.6 | 11.2 | 45.3 | 7.9 |
| 386 | C17 | C17_DH144 | 65.4 | 65.6 | -0.1 | 162.8 | 58.8 | 6.2 | 40.8 | 7.8 |
| 387 | C17 | C17_DH146 | 62.6 | 63.4 | -0.8 | 174.9 | 71.2 | 11.0 | 38.9 | 7.9 |
| 388 | C17 | C17_DH147 | 62.4 | 62.7 | -0.2 | 169.9 | 65.0 | 14.9 | 45.0 | 9.3 |
| 389 | C17 | C17_DH150 | 62.2 | 62.6 | -0.2 | 176.7 | 67.8 | 24.7 | 37.0 | 9.6 |
| 390 | C17 | C17_DH152 | 64.5 | 63.2 | 1.1 | 164.1 | 69.6 | 8.6 | 45.4 | 7.2 |
| 391 | C17 | C17_DH153 | 65.6 | 66.6 | -1.0 | 175.2 | 74.2 | 11.9 | 43.2 | 6.6 |
| 392 | C17 | C17_DH154 | 61.8 | 61.3 | 0.3 | 168.4 | 69.5 | 17.8 | 39.5 | 8.3 |
| 393 | C17 | C17_DH155 | 65.5 | 64.9 | 0.5 | 193.3 | 92.5 | 21.7 | 40.1 | 10.5 |
| 394 | C17 | C17_DH158 | 63.7 | 64.7 | -0.9 | 178.0 | 76.9 | 12.0 | 43.5 | 8.5 |
| 395 | C17 | C17_DH160 | 61.7 | 61.1 | 0.6 | 142.2 | 49.2 | 12.7 | 38.9 | 7.6 |
| 396 | C17 | C17_DH161 | 63.8 | 63.1 | 0.6 | 156.4 | 60.7 | 17.9 | 42.8 | 6.2 |
| 397 | C17 | C17_DH162 | 61.7 | 63.2 | -1.2 | 182.9 | 67.5 | 5.3 | 38.2 | 4.4 |
| 398 | C17 | C17_DH163 | 63.9 | 64.1 | -0.2 | 167.2 | 78.3 | 10.3 | 43.3 | 8.1 |
| 399 | C17 | C17_DH165 | 60.1 | 60.3 | -0.1 | 158.9 | 62.4 | 25.4 | 48.4 | 7.4 |
| 400 | C17 | C17_DH166 | 64.3 | 66.3 | -1.5 | 188.7 | 82.8 | 5.4 | 42.1 | 8.1 |
| 401 | C17 | C17_DH167 | 65.9 | 65.7 | 0.2 | 193.6 | 89.5 | 17.2 | 39.7 | 5.2 |
| 402 | C17 | C17_DH169 | 63.1 | 63.9 | -0.6 | 182.9 | 81.8 | 9.5 | 42.5 | 4.6 |
| 403 | C17 | C17_DH170 | 58.6 | 58.9 | -0.1 | 141.7 | 51.3 | 12.5 | 41.9 | 5.5 |
| 404 | C17 | C17_DH172 | 66.7 | 65.3 | 1.2 | 176.5 | 72.6 | 8.0 | 42.7 | 4.9 |
| 405 | C17 | C17_DH174 | 61.2 | 61.2 | -0.1 | 175.8 | 64.4 | 18.7 | 41.0 | 5.6 |
| 406 | C17 | C17_DH175 | 60.2 | 59.6 | 0.7 | 153.2 | 58.2 | 35.2 | 35.9 | 5.8 |
| 407 | C17 | C17_DH177 | 62.7 | 64.0 | -0.5 | 171.6 | 66.3 | 11.6 | 43.6 | 5.1 |
| 408 | C17 | C17_DH179 | 62.2 | 62.7 | -0.2 | 179.7 | 72.4 | 15.7 | 45.9 | 8.8 |
| 409 | C17 | C17_DH180 | 62.1 | 62.8 | -0.6 | 180.5 | 67.9 | 7.7 | 39.2 | 9.0 |
| 410 | C17 | C17_DH181 | 66.4 | 65.4 | 1.0 | 182.9 | 75.7 | 8.6 | 39.7 | 5.8 |
| 411 | C17 | C17_DH184 | 63.5 | 63.4 | 0.1 | 155.2 | 74.2 | 10.1 | 45.0 | 5.0 |
| 412 | C17 | C17_DH188 | 63.5 | 62.3 | 1.0 | 183.5 | 70.4 | 13.4 | 44.4 | 5.5 |
| 413 | C17 | C17_DH189 | 60.2 | 58.9 | 1.2 | 184.9 | 84.5 | 12.5 | 45.9 | 4.5 |
| 414 | C17 | C17_DH190 | 60.5 | 60.1 | 0.4 | 151.2 | 54.7 | 6.2 | 47.7 | 5.2 |
| 415 | C17 | C17_DH191 | 60.1 | 58.9 | 1.0 | 166.4 | 68.2 | 23.9 | 38.2 | 11.7 |
| 416 | C17 | C17_DH195 | 60.8 | 60.6 | 0.1 | 172.9 | 61.0 | 6.8 | 39.5 | 5.4 |

Table S3.2. Continued

| No | Group | DH line | MAFL | FEFL | ASI | PLHE | EAHE | FLA | TALE | NPTB |
|---|---|---|---|---|---|---|---|---|---|---|
| 417 | C17 | C17_DH196 | 64.0 | 65.7 | -1.6 | 160.6 | 49.9 | 14.8 | 34.9 | 5.1 |
| 418 | C17 | C17_DH202 | 64.3 | 64.2 | 0.2 | 166.7 | 66.8 | 16.4 | 38.2 | 3.9 |
| 419 | C17 | C17_DH205 | 61.8 | 62.2 | -0.1 | 152.6 | 66.3 | 23.9 | 41.9 | 9.0 |
| 420 | C17 | C17_DH210 | 61.4 | 61.5 | -0.1 | 181.4 | 81.3 | 11.6 | 46.8 | 5.9 |
| 421 | C17 | C17_DH216 | 61.0 | 62.2 | -1.1 | 166.1 | 68.4 | 18.7 | 35.7 | 8.6 |
| 422 | C17 | C17_DH217 | 64.2 | 64.0 | 0.2 | 169.6 | 63.5 | 7.1 | 50.5 | 5.5 |
| 423 | C17 | C17_DH218 | 61.2 | 60.9 | 0.2 | 177.9 | 77.9 | 10.1 | 40.0 | 6.2 |
| 424 | C17 | C17_DH219 | 59.2 | 58.6 | 0.4 | 165.5 | 53.5 | 12.5 | 44.8 | 9.7 |
| 425 | C17 | C17_DH220 | 60.7 | 60.8 | -0.1 | 166.1 | 73.4 | 21.7 | 46.4 | 5.5 |
| 426 | C17 | C17_DH221 | 61.0 | 59.9 | 0.9 | 178.0 | 67.8 | 19.3 | 39.3 | 6.5 |
| 427 | C17 | C17_DH223 | 60.2 | 59.9 | 0.4 | 154.1 | 60.0 | 11.2 | 36.7 | 6.7 |
| 428 | C17 | C17_DH224 | 63.3 | 62.9 | 0.4 | 157.5 | 58.7 | 11.2 | 38.7 | 6.4 |
| 429 | C17 | C17_DH225 | 59.9 | 60.3 | -0.4 | 156.5 | 62.2 | 10.1 | 39.6 | 4.5 |
| 430 | C17 | C17_DH226 | 64.9 | 64.3 | 0.6 | 196.0 | 81.8 | 20.2 | 39.0 | 6.0 |
| 431 | C17 | C17_DH228 | 60.9 | 61.3 | -0.2 | 173.3 | 53.8 | 7.7 | 41.9 | 5.3 |
| 432 | C17 | C17_DH232 | 64.2 | 63.6 | 0.6 | 187.0 | 71.1 | 5.1 | 45.2 | 5.8 |
| 433 | C17 | C17_DH233 | 63.0 | 63.6 | -0.6 | 166.0 | 66.5 | 11.2 | 46.8 | 4.1 |
| 434 | C17 | C17_DH236 | 61.8 | 62.7 | -0.7 | 207.3 | 96.0 | 14.2 | 42.4 | 10.9 |
| 435 | C17 | C17_DH238 | 61.4 | 60.8 | 0.4 | 171.1 | 64.7 | 8.9 | 39.0 | 6.2 |
| 436 | C17 | C17_DH239 | 60.9 | 59.1 | 1.7 | 169.9 | 74.4 | 10.1 | 36.8 | 5.1 |
| 437 | C17 | C17_DH240 | 61.8 | 63.5 | -1.3 | 167.9 | 62.1 | 5.3 | 46.8 | 7.4 |
| 438 | C17 | C17_DH241 | 62.3 | 62.6 | -0.2 | 155.0 | 62.8 | 10.3 | 43.6 | 4.5 |
| 439 | C17 | C17_DH243 | 59.1 | 58.0 | 0.8 | 171.1 | 69.1 | 20.2 | 41.7 | 6.6 |
| 440 | C17 | C17_DH244 | 61.9 | 62.9 | -0.8 | 178.5 | 64.9 | 11.6 | 44.3 | 4.0 |
| 441 | C17 | C17_DH247 | 63.9 | 64.7 | -0.6 | 186.0 | 74.7 | 8.0 | 42.5 | 6.0 |
| 442 | C17 | C17_DH248 | 60.6 | 59.5 | 1.1 | 147.2 | 46.2 | 6.5 | 39.1 | 6.5 |
| 443 | C17 | C17_DH252 | 63.7 | 64.7 | -0.8 | 192.7 | 57.6 | 11.5 | 46.9 | 3.6 |
| 444 | C17 | C17_DH253 | 63.9 | 65.2 | -1.0 | 142.1 | 56.4 | 11.2 | 40.2 | 5.1 |
| 445 | C17 | C17_DH255 | 63.6 | 62.7 | 0.7 | 171.2 | 77.0 | 19.4 | 38.3 | 12.0 |
| 446 | C17 | C17_DH258 | 63.1 | 64.6 | -1.3 | 174.8 | 71.0 | 27.7 | 44.5 | 9.6 |
| 447 | C17 | C17_DH259 | 62.8 | 63.6 | -0.7 | 168.6 | 62.0 | 11.0 | 51.2 | 8.7 |
| 448 | C17 | C17_DH262 | 61.5 | 59.8 | 1.4 | 172.6 | 71.0 | 14.2 | 37.7 | 7.0 |
| 449 | C17 | C17_DH264 | 61.5 | 61.1 | 0.4 | 166.4 | 69.5 | 24.7 | 37.1 | 9.5 |
| 450 | C17 | C17_DH265 | 64.5 | 63.7 | 0.7 | 168.7 | 80.6 | 6.5 | 44.3 | 9.5 |
| 451 | C17 | C17_DH267 | 62.3 | 63.0 | -0.5 | 181.0 | 73.0 | 14.8 | 40.9 | 6.0 |
| 452 | C17 | C17_DH268 | 63.2 | 61.7 | 1.4 | 170.3 | 77.0 | 16.4 | 44.3 | 6.8 |
| 453 | C17 | C17_DH270 | 64.3 | 65.0 | -0.7 | 179.2 | 84.2 | 23.9 | 44.4 | 11.5 |
| 454 | C17 | C17_DH271 | 66.0 | 66.3 | -0.2 | 171.9 | 80.2 | 27.0 | 39.5 | 7.2 |
| 455 | C17 | C17_DH273 | 59.8 | 59.9 | 0.1 | 166.3 | 66.3 | 16.3 | 39.9 | 7.4 |
| 456 | C17 | C17_DH280 | 64.8 | 64.5 | 0.3 | 171.9 | 61.6 | 25.4 | 41.0 | 7.0 |
| 457 | C17 | C17_DH282 | 59.4 | 59.7 | -0.2 | 169.0 | 63.6 | 17.2 | 42.0 | 6.4 |
| 458 | C17 | C17_DH283 | 64.4 | 64.8 | -0.3 | 172.1 | 83.7 | 19.4 | 41.4 | 15.9 |
| 459 | C17 | C17_DH284 | 68.4 | 70.4 | -1.8 | 192.1 | 93.6 | 27.0 | 41.5 | 7.5 |
| 460 | C17 | C17_DH286 | 69.0 | 67.5 | 1.4 | 199.5 | 90.7 | 13.3 | 41.6 | 5.3 |
| 461 | C17 | C17_DH287 | 62.0 | 62.3 | -0.4 | 159.0 | 52.8 | 6.3 | 42.3 | 8.2 |
| 462 | C17 | C17_DH290 | 61.6 | 62.5 | -0.8 | 168.1 | 65.3 | 10.9 | 46.5 | 5.8 |
| 463 | C17 | C17_DH294 | 63.3 | 63.2 | 0.0 | 152.3 | 53.2 | 6.9 | 41.7 | 6.8 |
| 464 | C17 | C17_DH296 | 61.3 | 60.3 | 1.0 | 170.8 | 65.6 | 18.7 | 42.6 | 9.2 |
| 465 | C17 | C17_DH297 | 61.7 | 60.3 | 1.3 | 175.9 | 70.6 | 19.4 | 36.8 | 3.8 |
| 466 | C17 | C17_DH298 | 60.9 | 60.6 | 0.3 | 162.9 | 65.0 | 12.7 | 44.8 | 7.7 |
| 467 | C17 | C17_DH299 | 65.1 | 65.3 | 0.0 | 155.5 | 61.1 | 6.3 | 39.8 | 4.9 |
| 468 | C17 | C17_DH301 | 63.6 | 62.6 | 0.8 | 178.2 | 82.3 | 16.4 | 42.5 | 10.5 |

Table S3.2. Continued

| No | Group | DH line | MAFL | FEFL | ASI | PLHE | EAHE | FLA | TALE | NPTB |
|---|---|---|---|---|---|---|---|---|---|---|
| 469 | C17 | C17_DH304 | 60.7 | 59.8 | 0.6 | 169.5 | 56.4 | 26.2 | 35.5 | 6.1 |
| 470 | C17 | C17_DH305 | 62.7 | 63.1 | -0.3 | 162.4 | 55.6 | 8.8 | 38.0 | 6.2 |
| 471 | C17 | C17_DH307 | 66.2 | 65.9 | 0.3 | 197.2 | 98.7 | 8.0 | 49.3 | 12.0 |
| 472 | C17 | C17_DH308 | 61.6 | 62.2 | -0.6 | 166.8 | 57.6 | 20.2 | 41.6 | 7.9 |
| 473 | C17 | C17_DH309 | 63.2 | 65.0 | -1.6 | 179.2 | 68.3 | 11.2 | 46.0 | 6.0 |
| 474 | C17 | C17_DH310 | 62.7 | 63.0 | -0.4 | 163.9 | 54.7 | 17.2 | 38.4 | 12.3 |
| 475 | C17 | C17_DH311 | 63.6 | 63.5 | 0.1 | 165.8 | 71.4 | 7.1 | 50.1 | 5.0 |
| 476 | C17 | C17_DH312 | 65.2 | 65.4 | -0.1 | 184.0 | 81.1 | 20.9 | 39.2 | 9.6 |
| 477 | C17 | C17_DH313 | 62.1 | 62.1 | -0.1 | 162.3 | 68.9 | 11.2 | 44.3 | 9.4 |
| 478 | C17 | C17_DH315 | 63.5 | 63.1 | 0.3 | 169.0 | 71.8 | 11.9 | 40.7 | 7.6 |
| 479 | C17 | C17_DH316 | 60.7 | 61.9 | -0.9 | 183.0 | 77.7 | 11.2 | 44.4 | 9.3 |
| 480 | C17 | C17_DH317 | 63.7 | 64.1 | -0.3 | 161.1 | 73.8 | 11.0 | 45.8 | 6.6 |
| 481 | C17 | C17_DH319 | 65.1 | 66.5 | -1.1 | 161.9 | 57.6 | 14.9 | 47.0 | 6.1 |
| 482 | C17 | C17_DH321 | 60.3 | 59.6 | 0.6 | 163.6 | 64.5 | 17.2 | 40.6 | 6.9 |
| 483 | C17 | C17_DH323 | 63.2 | 62.7 | 0.5 | 161.2 | 46.8 | 18.7 | 43.2 | 6.9 |
| 484 | C17 | C17_DH324 | 63.1 | 62.6 | 0.4 | 154.7 | 65.9 | 15.5 | 36.5 | 5.0 |
| 485 | C17 | C17_DH326 | 61.1 | 61.3 | -0.1 | 167.8 | 70.8 | 10.1 | 45.5 | 8.1 |
| 486 | C17 | C17_DH327 | 62.9 | 61.5 | 1.0 | 168.6 | 64.1 | 17.9 | 40.2 | 8.6 |
| 487 | C17 | C17_DH332 | 61.8 | 62.1 | -0.1 | 189.9 | 76.9 | 8.2 | 39.3 | 11.1 |

MAFL - male flowering, FEFL - female flowering, ASI - anthesis–silking interval, PLHE - plant height, EAHE - ear height, FLA - flag leaf angle, TALE - tassel length, NPTB - number of primary tassel branches.

# CHAPTER 4. GENERAL CONCLUSION

Molecular characterization information and the understanding of the genetic diversity, genetic relationships, and genetic divergence of lines within a breeding program are essential for germplasm improvement and help maize breeders better understand how to utilize the current set of germplasm. The molecular characterization (CHAPTER 2) analysis revealed the population structure among the different sets of DH lines, the genetic variability still available among C0_DHLs and C0/C17_DHLs, the genetic relationships among the different group of DH lines, the apparent separation and the loss of genetic variability of the BSSS maize population through the recurrent selection process. The highest gene diversity values found in the C0_DHL group could be an indication of the presence of more rare alleles, which could be an important source to find new functional alleles of desirable traits that could be lost during the recurrent selection program and can be used to broaden the genetic base of maize breeding populations. The computation of dissimilarity coefficients or Euclidean genetic distance was broader between the progenitors and the C17_DHL group, and a lower genetic distance was observed between C17_DHLs and C0/C17_DHL. The lowest $F_{st}$ among the DH lines was observed between the progenitors and the C0_DHL group. The highest value was observed between progenitors and C17_DHL. The genetic differentiation among the different comparisons performed between the progenitors and the different groups of DH lines across the ten chromosomes, with similar patterns across chromosomes. $F_{ST}$ values of 1 and closer to 1 were observed between the progenitor group and the C17_DH lines group across the genome as expected, demonstrating a considerable differentiation degree. Although genetic drift can explain most of the genetic structure genome-wide, phenotypic data (CHAPTER 3) provide evidence that selection has altered favorable alleles frequencies in the BSSS maize population improving plant architecture

traits. Thus, exploring early BSSS cycles using DH technology may reveal natural and useful genetic diversity left behind in the recurrent selection process and could be an important resource to help drive future genetic gains in maize breeding program. The detection of long IBD segments in the different groups of DH lines showed that the progenitors had a higher genetic contribution in C0 compared with C0/C17 and C17 derived DH lines and some of the progenitors had a lower contribution in the C17_DHL. In addition, we performed a phenotypic characterization of the BSSS DH lines (CHAPTER 3) focused on plant architecture traits that have changed through the recurrent selection program and have been reported to have positive results when adapting plants to higher plant densities. Descriptive statistical analysis confirmed trait variability in the different groups of DH lines. Considerable variation between populations was observed for all traits except for plant height. As expected, phenotypic differences ($P \leq 0.001$) were found between different groups of DH lines, indicating a wide range of variability present. DH lines within the C0_DHL group had the highest mean values for flowering time, ear height, flag leaf angle, and the number of primary tassel branches and were statistically different ($P \leq 0.001$) between the groups of DH lines. Thus, DH lines developed in this study could be a source of new germplasm for broadening the genetic variation compared to elite germplasm to develop varieties or hybrids adapted to the U.S. corn belt. Thus, individual lines with superior performance for agronomic and morphological traits can be selected and introgressed into elite materials. However, the testcross performance of the DH lines remains to be evaluated to test their yield potential in hybrid combinations. We found that BSSS DH lines are useful for association analyses (CHAPTER 3) to identify genome regions associated with agronomic traits. Using GWAS analysis, significant SNP markers-trait associations were found in flowering and plant architecture traits using different GWAS analysis models. 38 SNP markers were found

associated with different evaluated traits across more than one method tested and among the groups of DH lines. The genome regions with the highest significance were found on chromosome 2 and 7 for the traits number of primary tassel branches and flag leaf angles. By searching for candidate genes up and downstream of the 38 in common significant SNP markers, 55 candidate genes were associated with flowering time and different plant architecture traits. Additionally, in this study, we found that the entire panel of DH lines could be used for association analysis for flowering and plant architecture traits. Instead of using each DH line group individually, since the power of detecting associated SNP increased when we used the entire panel of DH lines. Identifying candidate genes for plant architecture traits in this study may help to elucidate the genetic basis of these plant architecture traits. However, future work needs to be conducted, increasing the number of markers and/or genotypes to have a better resolution of the association analysis and to verify and validate the candidate genes identified. After the validation process, maize breeding programs could use these markers for selection to speed up the process of adapting plants to higher densities.